

**Carbonyl Compounds in Manuka Honey:  
Antibacterial Activity, Reactions and Metabolic  
Transit**

**DISSERTATION**

zur Erlangung des akademischen Grades

Doctor rerum naturalium  
(Dr. rer. nat.)

vorgelegt

dem Bereich Mathematik und Naturwissenschaften  
der Technischen Universität Dresden

von

**Diplom-Lebensmittelchemikerin Jana Rückriemen**

geboren am 24.09.1987 in Berlin

Eingereicht am 06.11.2017

Verteidigt am 08.02.2018

Die Dissertation wurde in der Zeit von Februar 2013 bis November 2017  
an der Professur für Lebensmittelchemie angefertigt.

Gutachter: Prof. Dr. rer. nat. Dr.-Ing. habil. Thomas Henle  
Prof. Dr. Sabine E. Kulling

---

# Table of contents

---

<b>Table of contents.....</b>	<b>I</b>
<b>List of figures .....</b>	<b>VII</b>
<b>List of tables .....</b>	<b>XV</b>
<b>List of equations .....</b>	<b>XVIII</b>
<b>List of abbreviations.....</b>	<b>XIX</b>
<b>Preface .....</b>	<b>1</b>
<b>1 Chapter A – The antibacterial effect of manuka honey .....</b>	<b>3</b>
1.1 Introduction.....	3
1.2 Background.....	4
1.2.1 Honey and its antibacterial properties.....	4
1.2.2. The mechanism of bacterial inhibition .....	6
1.2.3. Cyclodextrins .....	9
1.3. Aims.....	12
1.4. Methods .....	13
1.4.1. Chemicals.....	13
1.4.2. Materials .....	16
1.4.3. Devices.....	17
1.4.4. Honey samples .....	19
1.4.5. Quantification of methylglyoxal and dihydroxyacetone via RP-HPLC .....	20
1.4.6. Quantification of hydrogen peroxide .....	20
1.4.7. Bacterial assay .....	21
1.4.8. Hydrogen peroxide cleavage.....	25
1.4.9. Quantification of “growth delay” .....	25
1.4.10. Determination of bactericidal concentrations .....	26
1.4.11. Inhibition of <i>Helicobacter pylori</i> .....	26
1.4.12. Studies on the structure of cyclodextrin inclusion complexes.....	27
1.4.13. Enzyme inhibition with manuka honey .....	28

---

1.4.13.1. Urease activity assay .....	28
1.4.13.2. Urease inhibition assay.....	28
1.4.13.3. Inhibitory test compounds .....	29
1.4.13.4. Determination of Michaelis-Menten constant.....	29
1.4.13.5. Chromatographic quantification of ammonia.....	29
1.4.13.6. Further enzyme activity assays.....	30
<b>1.5. Results and discussion .....</b>	<b>32</b>
1.5.1. Antibacterial compounds in honey.....	32
1.5.1.1. Hydrogen peroxide formation in honeys.....	32
1.5.1.2. Influence of methylglyoxal on hydrogen peroxide formation in honey.....	35
1.5.1.3. Methylglyoxal .....	36
1.5.2. The antibacterial effect of honey.....	37
1.5.2.1. Bacterial growth curves.....	38
1.5.2.2. The antibacterial effect of hydrogen peroxide .....	39
1.5.2.3. The antibacterial effect of methylglyoxal .....	42
1.5.2.4. Comparison of hydrogen peroxide and methylglyoxal as antibacterial compounds.....	45
1.5.2.5. Comparison of bacteriostatic versus bactericidal effect.....	47
1.5.3. The antibacterial effect of manuka honey with cyclodextrin .....	49
1.5.4. The structure of inclusion complexes of manuka honey and cyclodextrin .....	52
1.5.5. Influence of manuka honey on urease activity .....	63
1.5.5.1. Development of a photometric method to measure urease activity .....	64
1.5.5.2. Inhibition of urease activity.....	67
<b>1.6. Summary of Chapter A – The antibacterial effect of manuka honey.....</b>	<b>73</b>
<b>2 Chapter B – Reactions of carbonyl compounds in honey .....</b>	<b>75</b>
2.1. Introduction.....	75
2.2. Background.....	76
2.2.1 Carbonyl compounds in food .....	76
2.2.2 Reactions of carbonyl compounds in food.....	79
2.2.3 Analysis of carbonyl reaction products .....	82
2.3. Aims.....	85
2.4. Methods.....	86

---

2.4.1	Chemicals.....	86
2.4.2	Materials .....	89
2.4.3	Devices.....	90
2.4.4	Honey samples .....	92
2.4.5	Quantification of methylglyoxal and dihydroxyacetone via RP-HPLC-UV ....	94
2.4.6	Quantification of hydroxymethylfurfural .....	94
2.4.7	Isolation and quantification of 2-acetyl-1-pyrroline .....	95
2.4.8	Protein isolation from honey.....	96
2.4.9	Protein determination.....	96
	Acid precipitates .....	96
	Dialysis retentates .....	97
2.4.10	Amino acid determination.....	97
	Free proline .....	97
	Protein-bound amino acids .....	97
2.4.11	Fluorescence measurement of honey proteins .....	98
2.4.12	Size exclusion chromatography of honey proteins .....	98
2.4.13	Enzymatic hydrolysis of proteins.....	98
2.4.14	Analysis of Maillard reaction products via HPLC-MS/MS.....	99
2.4.15	Model studies on 2-acetyl-1-pyrroline formation in honey .....	99
2.4.16	Model studies on protein reactions in honey .....	100
2.4.17	Model studies on Maillard reactions in honey.....	100
2.4.18	Rheological studies .....	100
	Thixotropy loop .....	100
	Creep recovery .....	101
2.5.	Results and discussion.....	102
2.5.1	Identification and quantification of 2-acetyl-1-pyrroline in manuka honey ...	102
2.5.2	Reactions of carbonyl compounds with honey proteins .....	107
2.5.2.1	Cross linking of honey proteins .....	107
2.5.2.2	Fluorescence properties of honey proteins .....	110
2.5.2.3	Maillard reaction products in honey proteins .....	114
2.6.	Summary of Chapter B - Reactions of carbonyl compounds in honey	121

<b>3</b>	<b>Chapter C – Metabolic transit of carbonyl compounds .....</b>	<b>123</b>
3.1.	Introduction.....	123
3.2.	Background.....	123
3.2.1	Carbonyl compounds in living organisms.....	123
	Formation of 3-deoxyglucosone.....	125
	Formation of methylglyoxal.....	126
	Dietary uptake of carbonyl compounds.....	127
3.2.2	Reactions of carbonyl compounds <i>in vivo</i> .....	129
	Metabolism of 3-DG .....	129
	Metabolism of MGO .....	130
	Metabolism of glucose and fructose.....	131
	Beyond metabolism: Reactions of carbonyl compounds <i>in vivo</i> .....	132
3.3.	Aims.....	134
3.4.	Methods.....	135
3.4.1.	Chemicals .....	135
3.4.2.	Materials.....	138
3.4.3.	Devices .....	139
3.4.4.	Honey samples .....	140
3.4.5.	Simulated gastrointestinal digestion.....	141
	Influence of the pH value on the simulated gastrointestinal digestion.....	143
	Influence of human saliva on MGO stability .....	143
3.4.6.	Quantification of methylglyoxal and dihydroxyacetone via RP-HPLC-UV..	144
3.4.7.	Sample preparation of simulated digestion samples for amino acid analysis	144
	Protein isolation.....	144
	Enzymatic hydrolysis .....	145
	Acid hydrolysis.....	145
3.4.8.	Amino acid determination .....	145
3.4.9.	Determination of carbonyl compounds via GC-MS.....	147
3.4.9.1.	In urine .....	147
	MGO.....	147
	3-Deoxyglucosone, 3-deoxyfructose and 3-deoxy-2-ketogluconic acid.....	148
3.4.9.2.	In blood.....	149

MGO .....	149
3-Deoxyglucosone, 3-deoxyfructose and 3-deoxy-2-ketogluconic acid .....	150
3.4.9.3. In saliva.....	151
3.4.10. Conception of nutrition studies.....	152
3.4.10.1. Metabolic transit in urine .....	152
3.4.10.2. Metabolic transit in blood .....	154
3.4.10.3. Metabolic transit in saliva.....	155
3.5. Results and discussion .....	156
3.5.1. Stability of carbonyl compounds during simulated digestion.....	156
Stability of MGO and DHA in manuka honey .....	156
Stability of MGO and DHA in cyclodextrin complexes.....	160
3.5.2. Amino acid modification during simulated digestion.....	162
3.5.3. Metabolic transit of carbonyl compounds.....	164
3.5.3.1. Metabolic transit in urine .....	164
Manuka honey.....	166
Multifloral honey .....	169
Cyclopower and $\alpha$ -cyclodextrin.....	171
Discussion of carbonyl transit to the urine .....	174
3.5.3.2. Metabolic transit in blood .....	179
Glucose .....	180
3-Deoxyglucosone .....	181
3-Deoxyfructose.....	182
3-Deoxy-2-ketogluconic acid.....	183
Methylglyoxal .....	183
Dihydroxyacetone phosphate.....	184
3.5.3.3. Discussion of the metabolic transit of carbonyl compounds .....	185
3.6. Summary of Chapter C - Metabolic transit of carbonyl compounds ...	188
<b>4 Further studies and outlook.....</b>	<b>190</b>
4.1. Antibacterial effect of manuka honey .....	190
4.1.1. The inhibition of <i>Helicobacter pylori</i> with manuka honey .....	190
4.1.2. The mechanism of bacterial inhibition with manuka honey.....	194
4.2. Reactions of carbonyl compounds in honey.....	194

---

4.2.1	Reaction sites for carbonyl compounds in honey.....	194
4.2.2	Functional consequences of carbonyl reactions with proteins .....	195
4.2.3	The origin of dihydroxyacetone in manuka nectar.....	201
4.3.	Metabolic transit of carbonyl compounds .....	203
5.3.1	Impact of the diet on carbonyl compounds in saliva.....	203
<b>5</b>	<b>Summary .....</b>	<b>208</b>
<b>6</b>	<b>Annex.....</b>	<b>211</b>
	ROESY-NMR data.....	211
	Dose-response curves.....	212
<b>7</b>	<b>References .....</b>	<b>213</b>
	<b>List of publications, posters and presentations .....</b>	<b>232</b>
	<b>Acknowledgment .....</b>	<b>235</b>
	<b>Affidavit.....</b>	<b>236</b>



---

**List of figures**

---

Figure 1: Non-enzymatic dehydration of dihydroxyacetone to methylglyoxal (based on PhD thesis of Julia Atrott: Methylglyoxal in Manuka-Honig: Bildung, Wirkung, Konsequenzen, 2013).....	5
Figure 2: Bacterial growth curve, solid line: stages of bacterial growth, dotted line: bacterial growth with lag time extension, OD stands for optical density (experimental data of <i>S. aureus</i> growth in minimal media) .....	6
Figure 3: Images are taken from Rabie et al. (2016), see next page for captions .....	8
Figure 4: Hydrogen peroxide production in artificial honeys with varying activity of glucose oxidase, single determination in 5 % (v/v) solutions.....	34
Figure 5: Concentration of methylglyoxal (MGO) and dihydroxyacetone (DHA) during 90 days storage at room temperature, results are expressed as mean values of duplicate measurement.....	37
Figure 6: Growth curve of <i>Escherichia coli</i> in media alone, with artificial honey or manuka honey MGO 250+. Samples were incubated for 17 h at 37 °C. ....	38
Figure 7: Dose-response curve of hydrogen peroxide towards <i>S. aureus</i> , <i>B. subtilis</i> , <i>E. coli</i> and <i>P. aeruginosa</i> before and after linearization. GD of hydrogen peroxide was referenced to 5 % (v/v) AH solution. Red stars indicate GD caused by 5 % (v/v) lime honey with 67 mg H <sub>2</sub> O <sub>2</sub> /kg*h.....	40
Figure 8: Dose-response curve of methylglyoxal towards <i>S. aureus</i> , <i>B. subtilis</i> , <i>E. coli</i> and <i>P. aeruginosa</i> before and after linearization. GD of MGO was referenced to 5 % (v/v) AH solution. ....	43
Figure 9: MGO stability in nutrient media. 5 % (v/v) solutions of manuka honey with 690 mg/kg MGO and of artificial honey with the same amount were incubated in nutrient media at 37 ° C for 30 h. Measurements were carried out in duplicate and error bars indicate standard deviation. ....	45
Figure 10: Antibacterial activity of manuka honey (non-peroxide effect) and lime honey (peroxide effect) on bacteria. Manuka honey contains MGO 488 mg/kg and lime honey contains H <sub>2</sub> O <sub>2</sub> 67 mg/kg*h. Both honeys were diluted to 5 % (v/v) and incubated with bacteria for 18 h at 37 °C. Growth delay of 9 indicates no growth during the entire incubation time. ....	46

Figure 11: Proliferation of <i>S. aureus</i> and <i>B. subtilis</i> after plating on fresh media after 16 h incubation with MGO in manuka honey. Plates were incubated for 24 h at 37 °C. ....	48
Figure 12: Dose-response curve of <i>B. subtilis</i> incubated with manuka honey and cyclopower. GD was referenced to 5 % (v/v) AH solution. ....	49
Figure 13: Dose-response curve of $\alpha$ -cyclodextrin towards <i>S. aureus</i> , <i>B. subtilis</i> , <i>E. coli</i> and <i>P. aeruginosa</i> GD was referenced to 5 % (v/v) AH solution. ....	50
Figure 14: Dose-response curve for cyclopower and sum of growth delay caused by MGO in manuka honey and $\alpha$ -cyclodextrin measured individually .....	51
Figure 15: Molecular structures and $^1\text{H-NMR}$ spectra of $\alpha$ -cyclodextrin, methylglyoxal and dihydroxyacetone with proton assignment .....	53
Figure 16: $^1\text{H-NMR}$ spectra of cyclopower, upper right corner: zoom spectrum of cyclopower with MGO and DHA signal assignment .....	54
Figure 17: $^1\text{H-NMR}$ spectra of the complex MGO-CD (black) and DHA-CD (red) with proton assignment.....	55
Figure 18: ROESY-NMR spectrum of model complex containing MGO and $\alpha$ -CD in equimolar ratio, protons are assigned to MGO and $\alpha$ -CD (protons 1-6), cross peaks of MGO and $\alpha$ -CD are marked with black circle .....	57
Figure 19: Structures of $\alpha$ -cyclodextrin and spatial orientation of protons .....	57
Figure 20: ROESY-NMR spectrum of model complex containing DHA and $\alpha$ -CD in equimolar ratio, protons are assigned to DHA and $\alpha$ -CD (protons 1-6), cross peak of DHA and $\alpha$ -CD is marked with black circle.....	58
Figure 21: ROESY-NMR spectrum of model complex containing MGO, DHA and $\alpha$ -CD in a 1:2:1 ratio, protons are assigned to DHA, MGO and $\alpha$ -CD (protons 1-6), cross peaks of MGO and $\alpha$ -CD are marked with black circle .....	59
Figure 22: Proposed 2-D models structures of inclusion complexes formed by $\alpha$ -CD and MGO (A), $\alpha$ -CD and DHA (B) and $\alpha$ -CD, MGO and DHA (C) .....	60
Figure 23: At top: ROESY-NMR spectrum of model complex containing 1-propanol (PrOH) and $\alpha$ -CD in a 2:1 ratio, protons are assigned to 1-propanol and $\alpha$ -CD (protons 1-6), cross peaks of 1-propanol and $\alpha$ -CD are marked with black circle; at bottom: zoomed ROESY-NMR spectrum of PrOH/ $\alpha$ -CD complex .....	61

- Figure 24: ROESY-NMR spectrum of model complex containing hydroxyacetone (HA) and  $\alpha$ -CD in a 2:1 ratio, protons are assigned to hydroxyacetone and  $\alpha$ -CD (protons 1-6), cross peak of hydroxyacetone and  $\alpha$ -CD are marked with black circle ..... 62
- Figure 25: (A) Berthelot reaction in the presence of water (control) or artificial honey after 30 min incubation time with 280 mM ammonia, zoom figure: Berthelot reaction in the presence of water (control) or fructose and glucose after 30 min incubation time with 280 mM ammonia; (B) Reaction of ammonia with ninhydrin in the presence of water (control) or artificial honey after 30 min incubation time with 270 mM ammonia..... 65
- Figure 26: Amino acid analysis via ion-exchange chromatography and post-column ninhydrin detection (a) Amino acid standard solution with ammonia, (b) ammonia cleaved by urease from urea, (c) ammonia cleaved by urease from urea in the presence of 400  $\mu$ M acetohydroxamic acid, (d) blank solvent..... 65
- Figure 27: (A) UV spectra after incubation of urea with urease and ninhydrin (■), urea with ammonia and ninhydrin (●), ninhydrin and ammonia (“Ruhemann purple”) (▼) and urea with ammonia (▲), (B) Correlation between ammonia, which was quantitated chromatographically and the UV absorbance of the photometric assay at 440 nm. .... 66
- Figure 28: Residual enzyme activity of urease, pepsin and angiotensin-converting enzyme (ACE) in the presence of 4 mM MGO (grey) or 7 mM DHA (dark grey)..... 68
- Figure 29: Urease inhibition caused by honeys. (A) Artificial honey (white) and non-manuka honeys, namely canola (light grey), lime (grey) and honeydew honey (black). (B) Manuka honeys, MH 1 (white), MH 2 (light grey), MH 3 (grey) and MH 4 (black). Results are expressed as mean values of three separate measurements and error bars indicate standard deviation. .... 69
- Figure 30: Urease inhibition caused by canola honey (sample S1), canola honey with added MGO and DHA (S2), a solution of MGO and DHA in water (S3), manuka honey MH 3 (S4) and manuka honey MH 3 after treatment with glyoxalase 1 and GSH (S5). All honeys were diluted to 5.5 % (w/v). MGO and DHA concentration was 33 mg/l and 87 mg/l, respectively, for the samples S2-S4. MGO and DHA concentration in S5 was not quantitated. Measurements were carried out in duplicate and error bars indicate standard deviation. Abbreviation: n.d., not detectable..... 71
- Figure 31: Molecular structures of 3-deoxyglucosone and methylglyoxal ..... 76

- Figure 32: Formation of 1-amino-1-deoxyketose (Amadori product) from glucose,  $R^2 = C_3O_3H_7$  ..... 77
- Figure 33: Formation of 3-deoxyglucosone from the Amadori product of glucose,  $R^2 = C_3O_3H_7$  ..... 77
- Figure 34: Formation of methylglyoxal from 3-DG,  $R^2 = C_3O_3H_7$  ..... 78
- Figure 35: GC-MS data for identification and quantitation of 2-AP. (A) synthetic standard solution, (B) manuka honey, (C) lime honey, (D) artificial honey spiked with proline and MGO (black line) and DHA (grey line) incubated for 20 weeks at 37 °C (D)..... 103
- Figure 36: (A) 2-AP concentration of commercial samples of non-manuka honey (n=8), manuka honey with MGO below 250 mg/kg (manuka 1) ( n=4) and above 250 mg/kg (manuka 2) ( n=7), stars indicate average value for each group, (B) correlation of 2-AP concentration and MGO content of manuka honeys (group 1 and 2)..... 104
- Figure 37: 2-AP formation in a non-manuka multifloral honey with (A) added MGO stored at 37 °C, (B) added MGO and DHA stored at 37°C and (C) added MGO and DHA stored at room temperature (n=2 for each time point and sample)..... 105
- Figure 38: (A) Size exclusion chromatography with UV detection at 220 nm of proteins isolated from manuka honey with high MGO content (MGO 900 mg/kg; black line), low MGO content (MGO 118 mg/kg; blue line) and canola honey (MGO 10 mg/kg; grey line). Calibration was achieved by analyzing natural proteins with defined molecular weights. Grey box indicates high molecular weight protein. (B) Relative amount of high molecular weight protein fraction in non-manuka honey (NMH) and manuka honey (MH) without addition of DTT (black) and after addition of DTT (grey). Stars indicate the average value of each group. .... 109
- Figure 39: (A) Fluorescence excitation spectrum of manuka honey protein (MH) and non-manuka honey protein (NMH), recorded at emission wavelength 440 nm with excitation wavelengths between 230 to 420 nm, (B) Fluorescence emission spectrum of manuka honey protein (MH) and non-manuka honey protein (NMH), recorded at excitation wavelength 350 nm with emission wavelength between 380 to 600 nm ..... 111
- Figure 40: Fluorescence intensities before (A) and after (B) enzymatic hydrolysis of non-manuka honey protein precipitate (■) and manuka honey protein precipitate (○) against honey MGO concentration. Fluorescence of the precipitates was recorded at an excitation

wavelength of 350 nm and an emission wavelength of 450 nm. MGO content was analyzed via RP-HPLC-UV.....	112
Figure 41: Fluorescence intensities of protein isolated from honey samples with added MGO and DHA stored at room temperature and 37 °C for 84 days. The label “low” corresponds to 100 and 200 mg/kg of MGO and DHA and “high” to 500 and 1000 mg/kg of MGO and DHA, respectively.....	113
Figure 42: Concentrations of protein-bound MRP MG-H1 and CEL in enzymatically hydrolyzed HMW fractions (dialysis retentates) of 8 non-Manuka honeys (NMH) and 12 Manuka honeys (MH). Dotted lines indicate the medians. Significance of differences between MH and NMH medians was assessed by the Mann-Whitney U test. Figure taken from Hellwig et al. (2017).....	115
Figure 43: (A) Correlation of MGO with protein-bound MG-H1 concentrations and (B) CEL concentrations in manuka honey (n=11). (C) Correlation of protein-bound MG-H1 and CEL in manuka honey (black squares) and in artificially spiked honey with MGO (500 mg/kg) and DHA (1000 mg/kg) (red stars) after storage at 30 °C. Number of storage days is given in red. Figures taken from Hellwig et al. (2017) and partly modified.....	116
Figure 44: Concentration of MGO (A), DHA (B) and HMF (C) in commercial manuka honey MGO30+ (■) and in manuka honey MGO30+ with added MGO and DHA (●) over 17 weeks of storage at 30 °C. Dotted line marks regulatory limit of HMF in commercial honey (40 mg/kg).....	118
Figure 45: Concentration of protein-bound MG-H1 (A) and CEL (B) in commercial manuka honey MGO30+ (■) and in manuka honey MGO30+ with added MGO and DHA (●) over 17 weeks of storage at 30 °C.....	119
Figure 46: Formation of 1,2-dicarbonyl compounds from enzymatic repair of glycated proteins.....	125
Figure 47: Formation of 3-DG from the polyol pathway.....	126
Figure 48: Formation of methylglyoxal <i>in vivo</i> (dashed arrows: non-enzymatic pathway)...	127
Figure 49: Metabolic degradation of 3-DG to 3-DF (reductive pathway) and 3-DGA (oxidative pathway), grey arrows represent approximate ratio of degradation.....	129
Figure 50: Metabolic degradation of MGO to D-lactate via the glyoxalase system, dashed arrow indicates non-enzymatic reaction.....	130

Figure 51: Stability of (A) MGO during simulated gastrointestinal digestion of MGO standard solution or manuka honey and (B) stability of DHA during simulated gastrointestinal digestion of manuka honey .....	157
Figure 52: Stability of MGO standard solution in gastric fluids (GF) and ileal fluids (IF) at pH 2 or pH 7.5 .....	159
Figure 53: Stability of (A) MGO during simulated gastrointestinal digestion of a MGO standard solution and CD complexes of manuka honey (cyclopower) or CD complexes of MGO in the ratio 175:1 (complex 1) and in the ratio 1:1 (complex 2) and (B) stability of DHA during simulated gastrointestinal digestion of the CD complex of manuka honey (cyclopower) .....	161
Figure 54: Urinary excretion in 24 h urine of 3-DG (A), 3-DF (B), 3-DGA (C) and MGO (D) during a mixed diet (day 1 and 7) and a raw-food diet (day 2-6) .....	165
Figure 55: Urinary excretion in 24 h urine of 3-DG (A), 3-DF (B), 3-DGA (C) and MGO (D) during a mixed diet (day 1 and 5) followed by a raw-food diet (day 2-4) and a dietary intervention on day 3 with 125 g manuka honey .....	167
Figure 56: Urinary excretion in 24 h urine of 3-DG (A), 3-DF (B), 3-DGA (C) and MGO (D) during a mixed diet (day 1 and 5) followed by a raw-food diet (day 2-4) and a dietary intervention on day 3 with 125 g multifloral honey.....	170
Figure 57: Urinary excretion in 24 h urine of 3-DG (A), 3-DF (B), 3-DGA (C) and MGO (D) during a mixed diet (day 1 and 5) followed by a raw-food diet (day 2-4) and a dietary intervention on day 3 with 2.7 g $\alpha$ -cyclodextrin powder .....	172
Figure 58: Urinary excretion in 24 h urine of 3-DG (A), 3-DF (B), 3-DGA (C) and MGO (D) during a mixed diet (day 1 and 5) followed by a raw-food diet (day 2-4) and a dietary intervention on day 3 with 12 cyclopower capsules .....	173
Figure 59: Urinary recovery of 3-DG, 3-DF and 3-DGA from the dietary 3-DG during manuka honey intervention (3-DG dose was 275 $\mu$ mol) and multifloral honey intervention (3-DG dose was 202 $\mu$ mol). Each pie chart stands for one participant. ....	177
Figure 60: Correlation of urinary 3-DF with 3-DGA .....	178
Figure 61: Correlation of urinary 3-DG level with urinary 3-DF (A), 3-DGA (B) and the sum of 3-DF and 3-DGA (C) of all participants.....	179

Figure 62: Progression of plasma glucose level after the consumption of 125 g of manuka honey or artificial honey.....	180
Figure 63: Progression of plasma 3-DG (A), 3-DF (B), 3-DGA (C) and MGO (D) level after the consumption of 125 g of manuka honey or artificial honey.....	182
Figure 64: Progression of plasma DHAP level after the consumption of 125 g of manuka honey or artificial honey.....	184
Figure 65: Schematic illustration of the metabolic routes for dietary glucose and 3-DG in cells .....	187
Figure 66: Microscopic picture of <i>H. pylori</i> cells prior to incubation (A) and after 48 h incubation (B).....	190
Figure 67: D- and L-Lactate concentration of cell supernatant. <i>H. pylori</i> cells were incubated for 48 h under microaerophilic conditions at pH 7 with the compounds mentioned above...	192
Figure 68: MGO concentration of cell supernatant. <i>H. pylori</i> cells were incubated for 48 h under microaerophilic conditions at pH 7 with the compounds mentioned in the diagram...	193
Figure 69: Chemical markers proposed by the Ministry of Primary Industries NZ for identifying manuka honey .....	195
Figure 70: Shear stress curves (“thixotropy loop”) of honeydew, polyfloral, heather and manuka honey.....	197
Figure 71: Viscosity curves of honeydew, polyfloral, heather and manuka honey.....	197
Figure 72: Creep recovery of rewarewa and manuka honey, samples were tested at 20 °C and under commercial conditions (no controlled humidity) .....	199
Figure 73: Difference of the initial viscosity and viscosity after shear stress ( $\Delta\eta$ ) of rewarewa and three manuka honey samples, which were stored at controlled humidity for two weeks	200
Figure 74: Salivary concentration of glucose (A) and fructose (B) prior (0 min) and after consumption of glucose, fructose, manuka honey, conventional honey or a glucose/fructose mix.....	204
Figure 75: Salivary concentration of 3-DG (A), 3-DF (B) and 3-DGA (C) prior (0 min) and after consumption of glucose, fructose, manuka honey, conventional honey or a glucose/fructose mix.....	205

Figure 76: Salivary concentration of MGO (A) and DHA (B) prior (0 min) and after consumption of glucose, fructose, manuka honey, conventional honey or a glucose/fructose mix ..... 206



---

**List of tables**

---

Table 1: List of chemicals used in chapter A .....	13
Table 2: List of materials used in chapter A.....	16
Table 3: List of devices used in chapter A .....	17
Table 4: List of commercial honey samples used in chapter A.....	19
Table 5: List of spiked honey samples used in chapter A .....	19
Table 6: List of bacteria used for the antibacterial studies .....	21
Table 7: List of weighed portions of manuka honey and final MGO concentration.....	22
Table 8: List of weighed portions of artificial honey with glucose oxidase and final hydrogen peroxide formation .....	23
Table 9: Model complexes .....	27
Table 10: Hydrogen peroxide formation of commercial honey samples, results are expressed as mean values of triplicate measurement with standard deviation.....	32
Table 11: Hydrogen peroxide formation of lime honey blends, results are expressed as mean values of triplicate measurement with standard deviation .....	35
Table 12: Slopes of dose-response curves when growth delay is plotted logarithmically against hydrogen peroxide formation in mg/kg*h.....	41
Table 13: Calculated hydrogen peroxide formation in honey, which would inhibit bacterial growth 5-fold stronger than a 5 % (v/v) sugar solution. n.d. stands for not determinable .....	42
Table 14: Slopes of dose-response curves when growth delay is plotted logarithmically against methylglyoxal concentration in mg/kg.....	43
Table 15: Calculated MGO levels in honey, which would inhibit bacterial growth 5-fold stronger than a 5 % (v/v) sugar solution. n.d. stands for not determinable .....	43
Table 16: Bactericidal concentrations (MBC) of MGO in manuka honey and hydrogen peroxide in artificial honey with GOX on <i>S. aureus</i> and <i>B. subtilis</i> (one determination per sample) .....	47
Table 17: MGO and DHA concentrations of manuka honeys MH1 to MH 4. Results are expressed as mean values of three separate measurements. ....	69

Table 18: Concentrations of 1,2-dicarbonyls in food and their cause of formation .....	78
Table 19: Structures and starting material of advanced glycation end-products .....	80
Table 20: Chemicals used for the studies presented in chapter B.....	86
Table 21: Materials used for the studies presented in chapter B .....	89
Table 22: Devices used for the studies presented in chapter B.....	90
Table 23: List of commercial honey samples, Chapter B .....	92
Table 24: List of spiked honey samples, Chapter B .....	93
Table 25: Concentrations of glucose, fructose, 3-deoxyglucosone and methylglyoxal in body fluids of healthy subjects before (F: fasting) and after (P: Postprandial) ingestion of compounds. ....	124
Table 26: Chemicals used for the studies presented in chapter C.....	135
Table 27: Materials used for the studies presented in chapter C .....	138
Table 28: Devices used for the studies presented in chapter C.....	139
Table 29: List of commercial honey samples, Chapter C .....	140
Table 30: List of food used for intervention studies (except honey), Chapter C.....	141
Table 31: Preparation of sample solutions for the simulated gastrointestinal digestion.....	142
Table 32: Preparation of model CD-complexes for the simulated gastrointestinal digestion	143
Table 33: Modifications of pH value during simulated gastrointestinal digestion.....	143
Table 34: Parameters of amino acid analysis.....	146
Table 35: SIM mode parameters for the GC-MS analysis of 3-DG, 3-DF and 3-DGA in urine and blood.....	149
Table 36: SIM mode parameters for the GC-MS analysis of MGO, DHA, DHAP, 3-DG, 3-DF, 3-DGA, fructose and glucose in saliva, *internal standard .....	151
Table 37: Dietary restrictions during the intervention study .....	153
Table 38: Characterisation of study subjects for metabolic transit in urine.....	154
Table 39: Characterisation of study subjects for metabolic transit in blood.....	154
Table 40: Characterisation of study subjects for metabolic transit in saliva .....	155

---

Table 41: Concentration of MGO after 5 min incubation in human saliva, based on initial MGO concentration .....	157
Table 42: Concentration of lysine, arginine and cystin based on the analysis of acidic hydrolysates by Zeitz (2013) in simulated ileal phase. MGO and DHA concentrations are calculated from the initial concentrations under consideration of the dilution factor .....	160
Table 43: Summary of the lysine and arginine recovery after enzymatic hydrolysis of the digestion samples with sample preparation via methanol precipitation or dialysis .....	163
Table 44: Concentrations of 3-DG, 3-DF, 3-DGA and MGO in 24 h urine of all subjects (n=23) during raw-food diet and mixed diet .....	175

---

**List of equations**

---

Equation 1: Calculation of volume of bacterial solution in the assay.....	24
Equation 2: Calculation of growth delay (GD) for inhibitor concentration x.....	25

---

**List of abbreviations**

---

1-D	One dimensional
2-AP	2-Acetyl-1-pyrroline
2-D	Two dimensional
3-DGH	3-Deoxyglucoson-derived hydroimidazolone
AH	Artificial honey
$a_w$	Water activity
CD	$\alpha$ -Cyclodextrin
CEL	N- $\epsilon$ -Carboxyethyllysine
CML	N- $\epsilon$ -Carboxymethyllysine
COSY	Homonuclear proton correlation spectroscopy
DCM	Dichloromethane
DHA	Dihydroxyacetone
DTT	Dithiothreitol
ESI	Electron spray ionization
GC	Gaschromatography
GD	Growth delay
GOLD	Glyoxal-derived lysine dimer
GOX	Glucose oxidase
HMBC	Heteronuclear multiple-bond correlation spectroscopy
HMF	5-Hydroxymethylfurfuraldehyd
HMW	High molecular weight
HPLC	High performance liquid chromatography
kDa	Kilo Dalton
MG-H1	Methylglyoxal-derived hydroimidazolone
MGO	Methylglyoxal
MH	Manuka honey
MOLD	Methylglyoxal-derived lysine dimer
MRP	Maillard reaction product
MS	Mass spectrometry
MWCO	Molecular weight cut off
NMR	Nuclear magnetic resonance
OD	Optical density
<i>o</i> PD	<i>ortho</i> -Phe nylenediamine
p.a.	Pro analysi

PBS	Phosphate buffered saline
ROESY	Rotating frame nuclear Overhauser effect spectroscopy
RP	Reversed phase
RT	Room temperature
SD	Standard deviation
SEC	Size exclusion chromatography
SPE	Solid phase extraction
TRIS	Tris(hydroxymethyl)-aminomethan
UV	Ultraviolet
VIS	Visible
$\lambda_{em}$	Emission wavelength
$\lambda_{ex}$	Excitation wavelength

---

## Preface

---

New Zealand is the world's third-largest honey exporter by value behind China and Argentina and honey accounts for up to 80 % of New Zealand's exports. However, it is only the 16<sup>th</sup> biggest global supplier by volume. Manuka honey from New Zealand is sold for premium prices and merchandised for its health benefits. Because of its exceptional antibacterial properties, there is a strong market demand and the price for a kilogram of manuka honey has tripled in recent years (Ministry for Primary Industries, 2015). When consumers are willing to pay prices up to 200 €/kg manuka honey, the risk of misleading advertisement and intended fraud increases. Until now, there is no consequent regulation of the requirements for labelling manuka honey. Labels to advertise certain health effects or claims like "active" and "doctor" are confusing to consumers and cannot be proven on a scientific basis. Moreover, a lot of research focused on the definition of "genuine" manuka honey during recent years. According to the Codex Alimentarius and the Codex standard for honey the origin of manuka honey should be "wholly or mainly" the manuka plant (Codex Alimentarius Commission, 2001). Up to now, a consent about the precise definition of "wholly or mainly" and reliable analytical methods to prove the manuka origin do not exist.

This thesis aims to further characterize manuka honey and contribute to the development of a manuka honey definition. The thesis is divided into three chapters. Chapter A deals with the antibacterial activity of manuka honey. The effect of manuka honey is mainly due to methylglyoxal, whereas the effect of non-manuka honeys is primarily caused by hydrogen peroxide. The objective is to develop a method to quantify the effect solely due to one of the respective chemical compounds and compare their effectiveness. Finally, an evaluation of the contribution of methylglyoxal and hydrogen peroxide to the inhibitory effect of honey should be given. In chapter B, chemical reactions of carbonyl compounds in honey will be discussed. Because of the reactive nature of carbonyl compounds, the formation of specific glycation compounds in honey is assumed. Since the carbonyl profile of manuka honey differs remarkably from non-manuka honeys, the reaction products are expected to vary widely. Specific compounds, solely present in manuka honey, could serve as quality control parameters to ensure manuka honey authenticity. Chapter C deals with the metabolism of food-derived carbonyl compounds. Carbonyl compounds, like methylglyoxal or 3-deoxyglucosone, are discussed to be potentially toxic to human tissues. Until now, only little is known about the impact of the diet on the physiological carbonyl-load and the metabolism

of carbonyl compounds. With the help of nutrition studies and the analysis of body fluids, the metabolic transit of carbonyl compounds shall be investigated.

Each chapter contains a separate theoretical background including a literature review of the current state of knowledge concerning the particular topic. The analytical methods used for the respective studies are presented in each of the chapters and the results are summarized separately. In the end of all chapters, the results will be presented in a comprehensive summary and an outlook for further studies will be given.

The structure of this thesis allows the reader to either gain an insight into each topic individually or gain an extensive view in the unique chemistry of manuka honey. The author holds the opinion that the results of this thesis are an important contribution to the last ten years of manuka honey science and the characterization of honey chemistry and its health benefits.



---

# 1 Chapter A – The antibacterial effect of manuka honey

---

## 1.1 Introduction

This chapter deals with the unique antibacterial properties of manuka honey compared to other conventional honeys. Since the discovery of penicillin in the 20<sup>th</sup> century, antibiotics have been a great resource to fight various bacterial infections. From 1935 to 1968, eleven classes of drugs had been introduced and approved in the American market. Since 1968, only two new classes of antibiotics have been identified and approved (Powers, 2004). Due to the lack of new classes, drug developers started to introduce “new generations” of an existing antibiotic by chemically modifying previously studied compounds. The increasing number of agents within classes and the lack of new classes slowed down the discovery of new drugs. In the meantime, antibiotic resistance became a growing problem. There are scientific claims that the golden era of antibiotics is over and we reached a “post-antibiotic” age (Alanis, 2005; Brown and Wright, 2016). This is due to increasing numbers of antibiotic-resistant bacteria leading to less effective antibiotic treatment of certain infections. In recent years, plenty of research concerning alternative treatments of bacterial infections has been conducted (Allen et al., 2013; Elshafie et al., 2016). The focus of research moved to natural, plant-based products and honey became an interesting candidate to fight superficial wound infections (Moore et al., 2001; Molan, 2006). Various scientific studies documented the exceptional effect of manuka honey on different bacterial species (Al Somal et al., 1994; Lusby et al., 2005; Cooper et al., 2010). The current chapter discusses the antibacterial activity of honey in general and aims to reveal the characteristic bioactivity of methylglyoxal in manuka honey. The objective is to develop a method to quantify and compare the antibacterial effect of methylglyoxal in manuka honey and hydrogen peroxide in conventional honeys. Moreover, the mode of action of honey compounds is not thoroughly studied yet. The second part of this chapter deals with the question, whether the inhibition of bacterial enzyme systems could be a cause for bacterial inhibition. This was studied using the enzyme urease from *Canavalia ensiformis*, which is also present in the bacterium *Helicobacter pylori*, and its inhibition by manuka honey. In conclusion, the results contribute to an evolved explanation of the antibacterial activity of manuka honey.

## 1.2 Background

### 1.2.1 Honey and its antibacterial properties

Manuka honey is endemic in New Zealand and its antibacterial properties are well known from the heritage of New Zealand's native inhabitants, the Māori. Long before the Europeans arrived in New Zealand in the 18<sup>th</sup> century, the Māori used local plants for medicinal purposes. This traditional medicine is called “Rongoā Māori”, which is still used by indigenous populations nowadays (Williams, 2008). Manuka honey was used to treat topical wounds and burns since ancient times. The reason for its exceptional antibacterial activity was long unknown. Mavric et al. (2008) discovered, that manuka honey contains up to 800 mg/kg of the chemical compound methylglyoxal (MGO). This amount is 100 times higher compared to conventional honeys and other food stuff. Methylglyoxal is a dicarbonyl compound which is normally formed as a by-product of glycolysis and can act cytotoxic. Mavric et al. (2008) were able to show, that methylglyoxal in manuka honey is directly responsible for its particular antibacterial activity. In general, manuka honeys are considered to exert a distinct amount of non-peroxide activity (NPA) due to methylglyoxal. In comparison to this, other conventional honeys can have a peroxide activity (PA). This activity is due to certain amounts of hydrogen peroxide, which is produced by the enzymatic reaction of glucose oxidase in the honey (White et al., 1963). Glucose oxidase catalyzes the reaction of glucose to gluconic acid and hydrogen peroxide. The bee-derived enzyme is secreted to the honey to decrease honey pH value, which enables better storage conditions. Additionally, in manuka honey MGO is formed non-enzymatically from dihydroxyacetone (DHA) (Adams et al., 2009; Atrott et al., 2012). The nectar of the manuka plant contains unusually high levels of DHA. The biochemical reason for the presence of high DHA concentrations in the manuka nectar is yet unknown. After collection of the nectar by the bees and honey storage in the hive, MGO is formed from DHA via non-enzymatic dehydration (see Figure 1) (Atrott, 2013). It was found, that MGO formation is a time-, pH- and temperature-dependent process. Moreover the presence of certain amino acids, namely alanine and glycine, is supposed to influence the DHA-to-MGO-conversion (Grainger et al., 2016b). In commercial manuka honeys, a good linear correlation between DHA and MGO values was observed, with a mean ratio of DHA:MGO of 2:1 (Atrott et al., 2012).

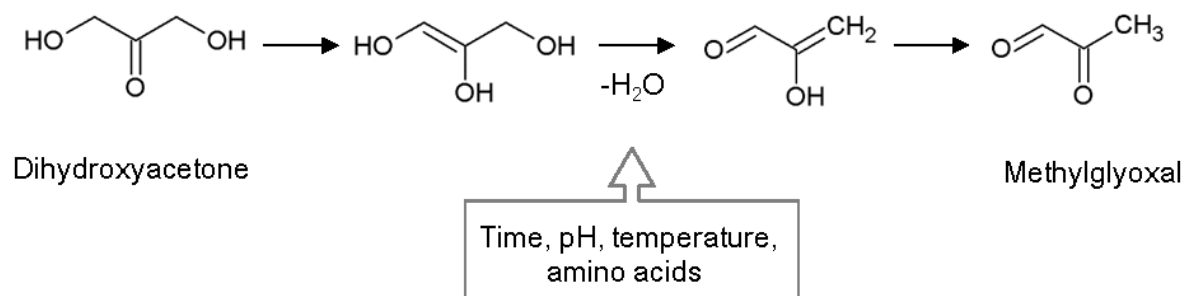


Figure 1: Non-enzymatic dehydration of dihydroxyacetone to methylglyoxal (based on PhD thesis of Julia Atrott: Methylglyoxal in Manuka-Honig: Bildung, Wirkung, Konsequenzen, 2013)

According to the Apiculture Monitoring Report by the New Zealand Ministry for Primary Industries, the total annual honey production increased from 12,500 t in 2010 to 19,700 t in 2015. Moreover in 2010 manuka honey cost was 7-38 NZ\$/kg, whereas in 2015 the price increased up to 10-117 NZ\$/kg (Ministry for Primary Industries, 2015). This clearly indicates the importance of manuka honey as one of the leading New Zealand Industries. The high market prices of manuka honey are justified by its unique antibacterial activities due to methylglyoxal. After the discovery of MGO in 2006, New Zealand honey producing companies started with labelling their products with its MGO content in 2007. Before that, it was generally recognized to characterise the bioactive effect of manuka honey with the “UMF” value. UMF stands for “Unique Manuka Factor”, which describes the antibacterial activity of honey compared to an equivalently effective concentration of a phenol solution. Besides that, a lot of manuka honey labels exist, which advertise a certain bioactive effect (e.g. “active 10+”, “Active AAH”). Since there is no governmental guideline concerning manuka honey labelling, the reliability of these labels is questionable. Until now, there exists no reliable method to compare and quantify the antibacterial effect due to hydrogen peroxide and the effect caused by MGO. To characterise an antibacterial effect, it is necessary to understand the mode of action of different antibacterial agents. The following section will discuss scientific studies of bacterial inhibition and the role of honey compounds in this context.

### 1.2.2. The mechanism of bacterial inhibition

Bacterial growth can be divided into four different stages. The first stage is the lag phase. During this stage, bacteria adapt to their environment and express specific genes, which code for enzymes, which are necessary for their metabolism. The length of a lag phase depends on the media and the adaptability of the bacterial species. The second stage is called log phase. This stage is characterised by cell doubling and exponential growth. If growth is not limited, doubling will continue at a constant rate. If media nutrients get depleted over time, bacteria will enter stage three, the stationary phase. During this stage, growth and death rate are equal. Finally, bacteria enter the death phase, which is characterised by cell lysis and thus, declining cell numbers (Novick, 1955; Zwietering et al., 1990). A common characterisation of bacterial growth can be achieved by measuring the optical density (OD). The OD, or turbidity, at 600 nm is a measure for the cell number of a specific kind of bacteria. Figure 2 depicts the classic growth phases of bacteria (solid line) and a growth curve of bacteria, treated with a bacteriostatic agent (dotted line).

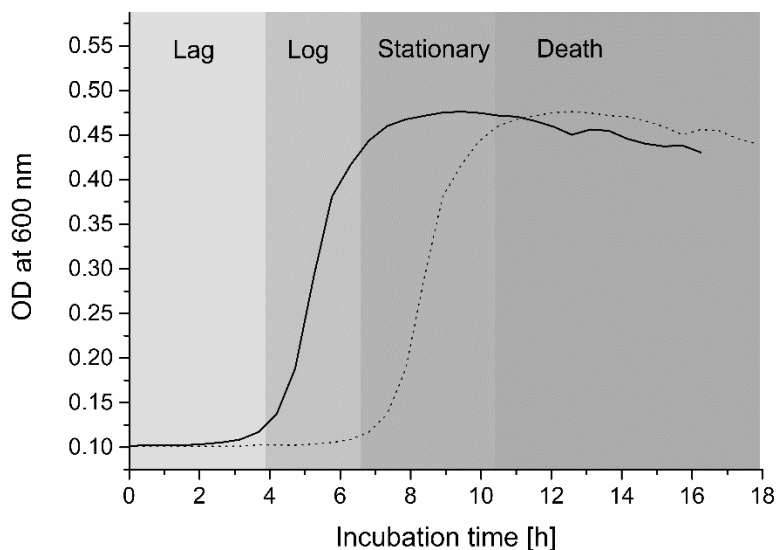


Figure 2: Bacterial growth curve, solid line: stages of bacterial growth, dotted line: bacterial growth with lag time extension, OD stands for optical density (experimental data of *S. aureus* growth in minimal media)

Antibacterial agents can intervene in the growth behaviour of bacteria. There are two different modes of action of antibacterial agents, which need to be differentiated: bacteriostatic and bactericidal. A bacteriostatic agent can inhibit bacterial growth for a certain time, but will not kill all bacterial cells. Thus, after prolonging the lag phase of bacterial growth, the bacteria

will equally enter the exponential growth phase and can rapidly multiply. In contrast bactericidal agents will cause complete cell death and thus prevent any further bacterial growth. Usually, it depends on the concentration of an antibacterial agent if it acts either bacteriostatic or bactericidal. The determination whether an antibacterial agent is considered to act bacteriostatic or bactericidal is markedly influenced by experimental conditions like media conditions, bacterial density and test duration (Pankey and Sabath, 2004). To quantify antibacterial activity, antibacterial agents are diluted in different concentrations in liquid media and incubated with a standard number of microorganisms. After incubation at 35-37°C for 18 to 24 h, the amount of antibacterial agent, which inhibited visible growth is called the minimal inhibitory concentration (MIC). The samples which did not show any growth are subcultured on fresh media (usually solid) and again incubated for 18 to 24 h. The minimal bactericidal concentration (MBC) represents the lowest concentration of an antibacterial agent that either totally prevents growth or results in a 99.9 % reduction of the initial inoculum (Pankey and Sabath, 2004). Several papers have been published on the comparison of MIC values for various food-derived antibacterial agents (Lin et al., 2011; Krauze-Baranowska et al., 2014; Elshafie et al., 2016). Although the MIC value gives a quantitative measure of antibacterial activity, it is not an accurate parameter to define bacterial inhibition. For example, MIC values of different studies can only be compared if testing conditions (incubation time, media and inoculum) are the same. In this context, an interpolation of inhibition data, in this case extension of the lag phase, could deliver a more precise measure of antibacterial activity. Moreover, the additional information if the tested antibacterial agent can also act bactericidal is of fundamental interest.

There are different mechanisms by which antibacterial agents interact with cells. The major targets of common antibacterial agents are cell wall synthesis (e.g. penicillin), cell membrane function (polymixin B), protein synthesis (chloramphenicol), nucleic acid synthesis (quinolones) or other metabolic processes (sulphonamides) (Kohanski et al., 2009). Especially the last mentioned target includes various processes like inhibition of folic acid biosynthesis (Ahmad et al., 1998) or acting as enzyme inhibitors (Andreu and Rivas, 1998). Since honey is a complex mixture of different bioactive agents, there cannot be made a clear statement on its mode of action. Nevertheless, when single honey compounds are studied individually, some conclusions about its antibacterial mechanisms can be made. Honey contains mainly fructose and glucose, which make up 85 % of its dry matter. The osmotic pressure caused by the highly saturated sugar solution and the low pH value of 3.5-4.0 caused by organic acids are responsible for the antibacterial effect of conventional honeys (Bogdanov, 1997; Mandal and

Mandal, 2011). Moreover, hydrogen peroxide, which originates from honey enzyme glucose oxidase, acts antibacterial by causing oxidative stress or even bactericidal by degrading bacterial DNA (Brudzynski et al., 2011). In contrast, very little is known about the antibacterial mechanism of MGO, which was identified as the main antibacterial factor in manuka honey (Mavric et al., 2008). With the exception of a few studies, which deal with either MGO or manuka honey, the increased antibacterial effect of manuka honey remains a secret. Henriques et al. (2010) studied the intracellular effect of manuka honey on *Staphylococcus aureus*. The authors studied MIC and MBC values of manuka honey and structural changes of the cells via scanning and transmission electron microscopy. They concluded that honey-treated cells (with 10 % (w/v) manuka honey) failed to progress normally through cell cycle and thus accumulate at the stage of cell division. The inclusion of a sugar-only control demonstrated, that honeys sugars are not involved in this process. In conclusion, the author hypothesized that manuka honey compounds target the cell division in *S. aureus*. No statements concerning the role of methylglyoxal in this process were made. Rabie et al. (2016) studied the morphological changes of *Escherichia coli* and *Bacillus subtilis* in the presence of methylglyoxal concentrations of 0.5 to 2 mM. The authors showed that with increasing MGO concentrations the fimbriae and flagella structures, which keep bacteria motile, disappear. At the highest concentration tested (2 mM) the structure of the membrane appeared shrunken and lost its integrity (see Figure 3). The authors concluded that the main reason for the antibacterial effect of MGO is the decrease of bacterial motility and the loss of its adherence capacity.

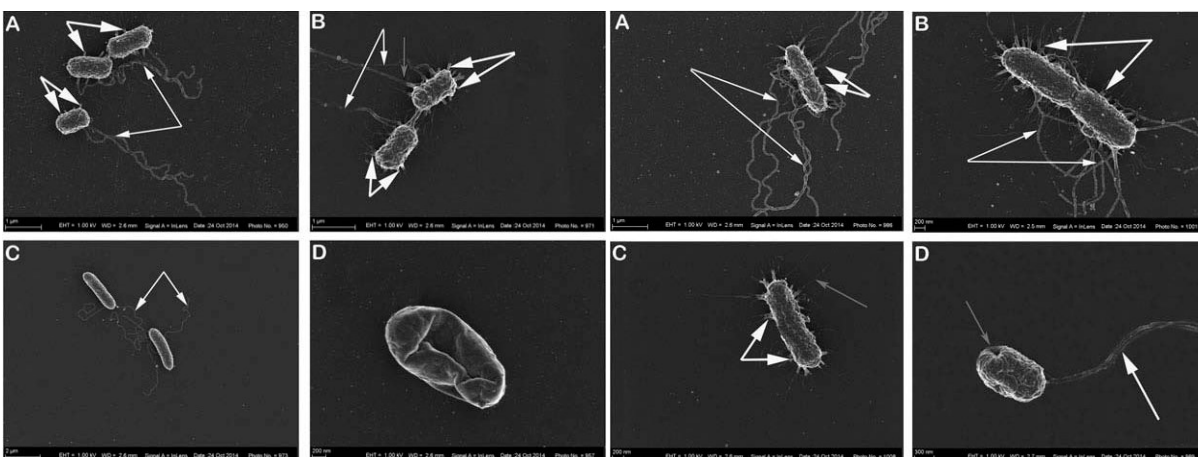


Figure 3: Images are taken from Rabie et al. (2016), see next page for captions

Left side: SEM micrographs of *B. subtilis* exposed to increasing concentrations of MGO. (A) Control; (B) 0.5 mM MGO; (C) 1.0 mM MGO; (D) 2.0 mM MGO. Thin white arrows indicate the flagella; thick white arrows indicate the fimbriae; the gray arrow in C shows a pilus; and the gray arrow in D indicates a hole in the cell.

Right side: SEM micrographs of *E. coli* exposed to increasing concentrations of MGO. (A) Control; (B) 0.5 mM MGO; (C) 1.0 mM MGO; (D) 2.0 mM MGO. Thin white arrows indicate the flagella; thick white arrows indicate the fimbriae; gray arrow in B shows a pilus.

The effects studied by Henriques et al. (2010) and Rabie et al. (2016) could be an explanation for the broad spectrum of bacterial species, which are influenced by manuka honey. Not only cell division but also motility is an essential feature for bacterial survival. A loss or restriction thereof can lead to decreased viability. Besides these universally effective mechanisms, it could be valuable to take a closer look at more bacteria-specific approaches. Over time, some bacteria developed a specialised metabolism as an evolutionary advantage, which could be a specific antibacterial target nowadays. For example, *Helicobacter pylori* is a gram-negative bacterium, which colonizes the human stomach and neutralizes the acidic pH value with continuous ammonia production. *Helicobacter pylori* infections are made responsible for gastric inflammation and ulcers (Marshall et al., 1987). Manuka honey was shown to exhibit an antibacterial effect against *H. pylori* (Al Somal et al., 1994). In the study, five clinical isolates of *H. pylori* were inoculated on agar plates, which contained 2.5 to 10.0 % manuka honey. A minimal inhibitory concentration (MIC) of 2.5 % of manuka honey was determined visually. A possible target of *Helicobacter pylori* inhibition is the enzyme urease (Ohta et al., 2001; Lin et al., 2005). The enzyme urease catalyses the formation of carbon dioxide and ammonia from urea. The activity of urease is essential for *Helicobacter pylori* survival. Until now, there is no study about the effect of individual honey compounds on the enzyme urease. To target specific enzymes or metabolic pathways in bacterial cells would be an interesting strategy for the development of new antibacterial agents or to research the mechanisms of existing antibiotics.

### 1.2.3. Cyclodextrins

Cyclodextrins (CD) are cyclic oligosaccharides, which consist of at least six  $\alpha$ -1,4-linked glucose units. CDs are naturally occurring, water soluble glycans, which are produced as a result of enzymatic starch degradation. The non-reducing oligosaccharides can consist of six, seven or eight glucopyranose units, referred to as  $\alpha$ -,  $\beta$ - or  $\gamma$ -cyclodextrins, respectively

(Szejtli, 1998; Singh et al., 2002). The hydroxyl groups of cyclodextrin are located on the outside of the molecule, whereas the inner part forms a hydrophobic cage-like structure. These structures can interact with hydrophobic molecules and form inclusion complexes of the “guest-host” type. The properties of the complexed material can change significantly, this is why CDs are widely applied in the industry sector, e.g. as drug and flavour carriers, in cosmetics or for separation processes. The modification can enhance the guest’s physicochemical properties by increasing solubility, stabilizing against degradation processes, trapping volatile compounds and controlling the release of bioactive compounds. The negligible toxicity of CDs make them good candidates for drug delivery systems. Especially  $\beta$ -CD is used in the development of delivery systems due to its optimal inner diameter for the molecular size of most drugs. Moreover CDs can be chemically modified (e.g. introduction of hydroxypropyl groups) to improve their complexation capacity. Cyclodextrin inclusion complexes are also described to interact with cellular membranes and thus increasing cellular uptake of the guest molecule. Since there are no physiologically relevant enzymes, which can degrade  $\alpha$ -cyclodextrin, it is characterized as a food fibre (Singh et al., 2002).

These advantages of cyclodextrin formulations were crucial for the development of the commercial product “Manuka Honey with CycloPower™” (CP). The company Manuka Health NZ Ltd. produces capsules, which contain 45 % manuka honey MGO 400+ and 55 %  $\alpha$ -cyclodextrin. The production of the inclusion complexes is described in section 1.4.12 (taken from the production protocol of Manuka Health NZ Ltd.). The bioactive effect of MGO in manuka honey is limited due to reactions with media compounds, mostly proteins or amino acids, and thus a decrease of the effective concentration can occur. Cyclopower was developed to increase the stability and bioavailability of MGO by slowly releasing MGO during digestion and exert a pronounced effect on digestive health. From a scientific point of view, it is not clear whether MGO and cyclodextrin form inclusion complexes and if so, how strong these interactions are. Moreover, the stability of potential MGO-CD complexes towards protein reactions was not studied before. Chepulis & Francis (2012) studied the anti-inflammatory effect of  $\alpha$ -cyclodextrin complexed manuka honey and found contradictory results. TNF-alpha secretion was both increased and decreased depending on MGO and other honey factors. Moreover, the authors showed a decrease of the antioxidant capacity, which was due to honey dilution with  $\alpha$ -cyclodextrin. Swift et al. (2014) were the first to show, that Manuka Honey with CycloPower™ had an increased antibacterial activity against *S. aureus*, *S. pyogenes* and *H. pylori* compared to manuka honey without cyclodextrin. The authors



concluded that manuka honey is an effective antibacterial agent which can be enhanced by complexing with  $\alpha$ -cyclodextrin. However, until now the functional consequences of manuka honey inclusion complexes with cyclodextrin are not profoundly studied yet.

### 1.3. Aims

The focus of this chapter is the comparison of the non-peroxide activity of manuka honey with the peroxide activity of conventional honeys. The aim was to quantify the inhibitory effect of honeys. This is normally achieved by comparing the minimal inhibitory concentration (MIC) of certain compounds. The validity of the MIC is limited due to different experimental settings. Moreover, the MIC value does not specify whether an inhibitory substance is acting bacteriostatic or bactericidal. The aim was to develop a method, which allows a characterization of the inhibitory effect of different concentrations and a kinetic prediction of the inhibition. The new method was supposed to compare the effect of non-peroxide vs. peroxide activity of honey and quantitative measures of their effectiveness on two gram-negative and two gram-positive bacteria species. In the end, an evaluation of the contribution of MGO and hydrogen peroxide to the inhibitory effect of honey should be made. Moreover, the effect of inclusion complexes formed from cyclodextrin and manuka honey on bacteria should be elucidated. Therefore, the molecular structure of model complexes formed by either MGO or DHA and  $\alpha$ -cyclodextrin was studied via NMR spectroscopy and the consequences for molecular interactions in Manuka Honey with CycloPower<sup>TM</sup> were deduced from the results. The antibacterial activity of CycloPower and CD alone was studied with the newly developed bacteria assay. Hence, functional consequences for manuka honey encapsulated with  $\alpha$ -cyclodextrin shall be presented. Furthermore, the mechanism of bacterial inhibition with manuka honey should be studied. Therefore, the influence of manuka honey compounds MGO and DHA on the enzyme urease, which is present in the bacterium *Helicobacter pylori*, will be studied. The results of the study are a contribution to mechanistically explain bacterial inhibition with manuka honey.

## 1.4. Methods

### 1.4.1. Chemicals

Table 1: List of chemicals used in chapter A

Chemical	Specification	Supplier
1,3-Dihydroxyacetone dimer	97 %	Sigma-Aldrich, Steinheim, Germany
1-propanol	> 99.5 %, p.a.	
2-Methylquinoxaline (2-MQ)	99.2 %	Sigma-Aldrich, Steinheim, Germany
Abz-FRK(Dnp)P-OH	≥ 95 % (HPLC)	Sigma-Aldrich, Steinheim, Germany
Acetic acid	100 %, p.a.	Carl Roth, Karlsruhe, Germany
Acetohydroxamic acid	98 %	Alfa Aesar, Karlsruhe, Germany
Ammonia	25 %	Merck, Darmstadt, Germany
Angiotensin- converting enzyme	from rabbit lung	Sigma-Aldrich, Steinheim, Germany
Blood agar	for microbiology	Carl Roth, Karlsruhe, Germany
Brain heart infusion broth	for microbiology	Carl Roth, Karlsruhe, Germany
Brucella broth base	for microbiology	Sigma-Aldrich, Steinheim, Germany
Catalase	from bovine liver, suspension in water, 15 000 000 U/15 ml	Merck, Darmstadt, Germany
D(-)Fructose	> 99,5 %, for biochemistry	Carl Roth, Karlsruhe, Germany
D(+)-Glucose	anhydrous, p.a.	Carl Roth, Karlsruhe, Germany
D(+)-Saccharose	≥ 99.5 %, p.a.	Carl Roth, Karlsruhe, Germany
D-/L-Lactic acid kit	for UV-method	R-Biopharm, Darmstadt,

		Germany
Deuterium oxide	99.9 atom % D	Sigma-Aldrich, Steinheim, Germany
Disodium hydrogenphosphate	99 %	Grüssing, Filsum, Germany
Ethanol	96 %, denatured with light petroleum	Berkel, Berlin, Germany
Glucose oxidase	from <i>Aspergillus niger</i> , G-6641 10 kU, 47200 U/g	Sigma-Aldrich, Steinheim, Germany
Glutathione (reduced)		Merck, Darmstadt, Germany
Glyoxalase 1	from <i>Saccharomyces cerevisiae</i>	Sigma-Aldrich, Steinheim, Germany
Haemoglobin	from bovine blood	Sigma-Aldrich, Steinheim, Germany
Horse serum		Sigma-Aldrich, Steinheim, Germany
Hydrochloric acid	37 %	Sigma-Aldrich, Steinheim, Germany
Hydrogen peroxide	30 %, p.a.	Sigma-Aldrich, Steinheim, Germany
Hydroxyacetone	90 %	Sigma-Aldrich, Steinheim, Germany
Lithium chloride	p.a.	Merck, Darmstadt, Germany
Lithium citrate buffer	0.12 N, pH 2.2	Sykam, Fuerstenfeldbruck, Germany
Lithium citrate buffer	0.12 N, pH 2.9	Sykam, Fuerstenfeldbruck, Germany
Lithium citrate buffer	0.3 N, pH 4.2	Sykam, Fuerstenfeldbruck, Germany
Lithium citrate-/ borate buffer	0.3 N, pH 8.0	Sykam, Fuerstenfeldbruck, Germany
Methanol	HPLC grade	VWR, Darmstadt, Germany
Methylglyoxal	~ 40 % (w/w), exact concentration was determined against 2-MQ	Sigma-Aldrich, Steinheim, Germany
Ninhydrin	p.a., min. 99 %	Serva Feinbiochemica,

		Heidelberg, Germany
ortho-Dianisidine		Sigma-Aldrich, Steinheim, Germany
ortho-Phenylenediamine (oPD)	≥98 %,	Sigma-Aldrich, Steinheim, Germany
Pepsin	from porcine gastric mucosa, 3555 U/mg protein	Sigma-Aldrich, Steinheim, Germany
Peroxidase	Type I from horseradish, 150 units/mg solid	Sigma-Aldrich, Steinheim, Germany
Sodium acetate	99.5 %; p.a	Grüssing, Filsum, Germany
Sodium chloride	99.7 %	VWR, Darmstadt, Germany
Sodium dihydrogenphosphate	99.5 %; p.a	Grüssing, Filsum, Germany
Sodium hydroxide	98.56 %	Fisher Scientific, Loughborough, UK Sigma-Aldrich,
Starch	soluble	Carl Roth, Karlsruhe, Germany
Sulphuric acid	95-97 %, p.a.	Merck, Darmstadt, Germany
Trichloroacetic acid	> 99 %; p.a.	Carl Roth, Karlsruhe, Germany
Tris(hydroxymethyl)-aminomethan (TRIS)	Buffer grade	Sigma-Aldrich, Steinheim, Germany
Urea	> 99.5 %	Fluka AG, Basel, Switzerland
Urease from <i>Canavalia ensiformis</i> (Jack bean)	Type III; 34310 U/g solid	Sigma-Aldrich, Steinheim, Germany
Yeast extract	Biochemika A 1552, 1000	AppliChem, Darmstadt, Germany
α-Cyclodextrin	≥98%, CAVAMAX® W6 FOOD	Wacker Chemicals AG, Supplied by Manuka Health NZ Ltd.

## 1.4.2. Materials

Table 2: List of materials used in chapter A

Name	Specification	Supplier
Amino acid analyser column	Cation exchange LCA K07/Li	Sykam, Fuerstenfeldbruck, Germany
Cuvette	Semi-micro, PMMA, 1,5 – 3,0 ml	Brand, Wertheim, Germany
Disposable inoculation loops		Carl Roth, Karlsruhe, Germany
Glass vessel	10-50 ml	VWR, Darmstadt, Germany
HPLC column	Eurospher 100 RP18 material (250mm x 4.6 mm, 5 µm particle size with integrated pre-column	Knauer, Berlin, Germany
HPLC vials with lit	1.5 ml, glass	VWR, Darmstadt, Germany
Incubation jar	2.5 l	Merck Millipore, Darmstadt, Germany
Membrane filter	Regenerated cellulose, 45 µm, 26 mm	Phenomenex, Aschaffenburg, Germany
Membrane filter for solvents	GH Polypro 0,45 µm, 47 mm hydrophilic polypropylene	Pall, Crailsheim, Germany
Microtiter plate	96 flat bottom, transparent, pureGrade, nonsterile	Brand, Wertheim, Germany
Microtiter plate	96 well plate, flat bottom, polystyrene, 0,34 cm <sup>2</sup> , steril, 162/cs	TPP Techno, Plastic Products AG, Switzerland
Microtiter plate	UV-star	Greiner Bio-One, Kremsmuenster, Austria
Multichannel pipette	10-100 µl	Brand, Wertheim, Germany
Oxoid™ CampyGen™ Sachet	2.5 l, produce gaseous atmosphere for growth of microaerophilic microorganisms	Thermo Scientific, Runcorn, UK
Parafilm	4 in x 125 ft	Bemis, Neenah, USA
Pasteur pipettes	230 mm, glass	VWR International, Leuven, Netherlands
Pipette tips	1-1000 µl	Brand, Wertheim, Germany

Self-adhesive sealing film	153x78mm, 25 µm, sterile, gas-permeable	Carl Roth, Karlsruhe, Germany
Septa for HPLC vials	8*0.4 mm, PTFE coated	VWR, Darmstadt, Germany
Sterile membrane filter	FP 30/0.2 CA-S, 0,2 µm	GE Healthcare Europe GmbH, Freiburg, Germany
Syringe	50 ml	Henke Sass Wolf, Tuttlingen, Germany
Syringe	1 ml	B. Braun, Melsungen, Germany
Tubes	1.5 ml, 2 ml	Eppendorf, Hamburg, Germany

### 1.4.3. Devices

Table 3: List of devices used in chapter A

Device	Specification	Supplier
Amino acid analyser	S 4300, Software: Chromstar 6.3 SCPA GmbH	Sykam, Fuerstenfeldbruck, Germany
Analytic balance	BP 121 S, accuracy: 0.0001 g, max. 120 g	Sartorius, Göttingen, Germany
Centrifuge	Eppendorf 5804-R	Eppendorf AG, Hamburg, Germany
Freeze dryer	Alpha 1 - 2	Martin Christ, Osterode, Germany
Freezer	Comfort	Liebherr, Bibrach an der Riss, Germany
Fridge	Econoic System, 5°C	Liebherr, Bibrach an der Riss, Germany
HPLC system 1	Äkta basic system pump P-900 auto sampler A-900 UV detector UV-900 online degasser K-5004	Amersham Pharmacia Biotech, Uppsala, Sweden  Knauer, Berlin, Germany
HPLC system 2	Smartline 1000 pump Dynamic mixing chamber	Knauer, Berlin, Germany

	solvent organizer K-1500 online degasser K-5004 Basic Marathon auto sampler Azura DAD detector 2.1 L	Knauer , Berlin, Germany Knauer , Berlin, Germany Sparks , Netherlands Knauer, Berlin, Germany
Incubator	BE 500	Memmert, Schwabach, Germany
Incubator	BE 400	Memmert, Schwabach, Germany
Incubator	ULM 500	Memmert, Schwabach, Germany
Incubator shaker	Multitron	INFORS AG, Bottmingen, Switzerland
Laboratory pipette	1-1000 $\mu$ l	Eppendorf AG, Hamburg, Germany
LabWater Purelab Plus water system	conductivity 0.055 $\mu$ S/cm	ELGA, Celle, Germany filter from USFilter, Ransbach-Baumbach, Germany
Laminar flow cabinet	HeraSafe	Heraeus, Hanau, Germany
Magnetic and heating stirrer	RH basic	IKA Labortechnik, Staufen, Germany
Multimode reader (one device: Institute for Microbiology, second device: Institute for Food Chemistry, TU Dresden)	Tecan infinite M200	Tecan, Mainz, Germany
NMR device	Bruker Avance III 600	Bruker, Billerica, USA
pH meter	InoLab Level 1, electrode: InLab Semi-Micro	Mettler-Toledo, Weilheim, Germany
Photometer	Spekol 1500	Analytik Jena, Jena, Germany
Ultrasonic bath	Sonorex RK 510 Super	Bandelin, Berlin, Germany
Vortex	Minishaker MS-1 IKA	IKA Labortechnik, Staufen, Germany



## 1.4.4. Honey samples

Table 4: List of commercial honey samples used in chapter A

Honey	Quantity	Manufacturer, Best before
Manuka honey MGO 30	1	Manuka Health NZ Ltd., 01/2018
Manuka honey MGO 250	2	Manuka Health NZ Ltd.
Manuka honey MGO 400	2	Manuka Health NZ Ltd.
Manuka honey MGO 550	3	Manuka Health NZ Ltd.
Manuka honey, fresh	1	Manuka Health NZ Ltd.
Honeydew honey		Biophar, Fürsten- Reform, Braunschweig, 04/2015
Canola honey	1	Bienen Wirtschaft Meißen, 06/2011
Polyfloral honey	1	Nektarquell, 04/2014
Lime honey	1	Imkerei R. Feldt, Eichede, 09/2015
Cyclopower, Manuka honey 400+ with $\alpha$ -cyclodextrin	1	Manuka Health NZ Ltd. Produced: 08/2012

Table 5: List of spiked honey samples used in chapter A

Honey	Specification	Active compound
AH	Artificial honey: 100g AH contain 46.5g fructose + 34g glucose + 1.5g sucrose + 18g ultrapure water	-
AH-GOX	Artificial honey spiked with glucose oxidase	H <sub>2</sub> O <sub>2</sub> : 115 mg/kg*h
AH-MGO	Artificial honey spiked with methylglyoxal	MGO: 873 mg/kg
Canola honey + MGO/DHA,	Canola honey spiked with	MGO: 600 mg/kg

S2	MGO and DHA	DHA: 1550 mg/kg
Manuka honey + glyoxalase/GSG, S5	Manuka honey MH 3 spiked with glyoxalase 1 and GSH	

#### 1.4.5. Quantification of methylglyoxal and dihydroxyacetone via RP-HPLC

The determination of MGO and DHA was performed according to (Atrott et al., 2012) with slight modifications. For quantification of MGO, 1 mL aliquots of 10% (w/v) honey solutions in 0.5 M phosphate buffer (pH 6.5) were mixed with 300  $\mu$ L phosphate buffer (pH 6.5) and 300  $\mu$ L *o*PD solution (1% in phosphate buffer pH 6.5). Samples were incubated in the dark at room temperature overnight and membrane filtered (0.45  $\mu$ m). For quantification of DHA, 1 mL aliquots of 10% honey solutions in 0.5 M acetate buffer (pH 4.0) were mixed with 300  $\mu$ L acetate buffer (pH 4.0) and 300  $\mu$ L *o*PD solution (1% in acetate buffer pH 4.0), followed by incubation for 16 h at 37 °C and membrane filtration (0.45  $\mu$ m).

HPLC analyses were performed using the HPLC system 1. Peak evaluation was managed using the software UNICORN 4.11. The separation of quinoxalines was realized on a stainless steel column filled with Eurospher 100 RP18 material (250mm x 4.6 mm, 5  $\mu$ m particle size with integrated pre-column; Knauer, Berlin, Germany). The mobile phase were 0.075 % acetic acid in water (solvent A) and a mixture of 80% methanol and 20% solvent A (solvent B). The gradient started with 40% solvent B for 1 min and was elevated linearly to 100% B over a period of 20 min, was changed back to 40% B in 4 min and was held there for 7 min. The flow rate was 0.9 mL/min, the separation was done at 30 °C, 20  $\mu$ L sample solution was injected and peaks were detected by measurement of UV absorbance at 312 nm. Quantification was achieved by external calibration with MGO standard solution or by standard addition method for DHA.

#### 1.4.6. Quantification of hydrogen peroxide

In honey the enzyme glucose oxidase catalyzes the formation of hydrogen peroxide and D-glucono- $\delta$ -lactone from glucose. In sulphuric acid solution in the presence of *o*-dianisidine and peroxidase, hydrogen peroxide forms a red complex, which absorbs at 540 nm.

All honey samples were diluted to 5 % (v/v) in 0.4 M phosphate buffer (pH 6.5). The peroxidase stock solution was prepared by diluting 50 mg peroxidase in 5 ml 0.01 M phosphate buffer (pH 6.5). The *o*-dianisidine stock solution was prepared by diluting 50 mg *o*-

dianisidine in 50 ml ultrapure water. The reaction mix was prepared by mixing 20  $\mu$ l of peroxidase stock solution and 500  $\mu$ l of o-dianisidine stock solution in 10 ml 0.01 M phosphate buffer (pH 6.5). 40  $\mu$ l of honey sample solutions were incubated for 1h at 37 °C in a microtiterplate (Greiner 96 flat bottom transparent). After 1h, 135  $\mu$ l of reaction mix were added and samples were incubated for exactly 5 min at room temperature. The reaction was stopped with the addition of 120  $\mu$ l sulphuric acid (6 M) and the absorbance at 540 nm was measured with a Tecan multimode reader after shaking for 15 s with 6 mm amplitude and 5 s waiting time. Evaluation was achieved by using the software Tecan i-control, version 1.10.4.0. The quantification of the formed amount of hydrogen peroxide was achieved with an external calibration. Therefore, six calibration standards with varying H<sub>2</sub>O<sub>2</sub> concentration from 0.1 to 8.0 mg/l were prepared in ultrapure water and treated like samples without incubation prior to derivatization. A blank containing 40  $\mu$ l calibration standard or sample solution and 135  $\mu$ l phosphate buffer (0.01 M) instead of reaction mix was included. The limit of detection (LOD) and the limit of quantification (LOQ) was measured based on standard deviation of the blank (Leiterer, 2008).

#### 1.4.7. Bacterial assay

The microbiological studies were performed at the Institute of Microbiology at the TU Dresden, Germany. The bacterial strains, which were kindly provided by the Institute of Microbiology (TU Dresden), are listed in Table 6. If there were no further information about the strains available, the corresponding columns are marked with “-“.

Table 6: List of bacteria used for the antibacterial studies

<b>Organism</b>	<i>Bacillus subtilis</i>	<i>Escherichia coli</i>	<i>Pseudomonas aeruginosa</i>	<i>Staphylococcus aureus</i>
Internal labeling	B04	B44	B12	B22
date	07.09.1995	28.05.1998	07.09.1995	19.05.1998
genotype	Wild type	-	-	-
Reference number	-	ATCC 25922	ATCC 27853	-

For all experiments, sterile ultrapure water, chemicals and consumables were used. The experimental work was performed at a laminar flow cabinet. Stock cultures stored at  $-80\text{ }^{\circ}\text{C}$  were cultured to produce single colonies on nutrient agar. The nutrient plate was incubated at  $37\text{ }^{\circ}\text{C}$  for at least 18 h. The liquid culturing media was prepared by mixing 1.5 ml yeast extract stock solution (300 g/l), 2.5 ml sodium chloride stock solution (100 g/l) and 2.5 ml glucose stock solution (200 g/l) and filling it up to 50 ml with sterile ultrapure water. All stock solutions were filter sterilized prior to use. In an Erlenmeyer flask, 10 ml of minimal media was inoculated with a single colony forming unit (cfu) of the corresponding bacteria, followed by subsequent incubation at  $37\text{ }^{\circ}\text{C}$  for 6 h in an incubator shaker at 220 rpm. The bacterial suspension, which was used for the growth experiments, was prepared by diluting the pre-culture 1:50 in minimal media.

To keep the osmotic effect of the sugar in all samples constant, the honeys were applied as 5 % (v/v) sugar solution. Therefore, 0.685 g of honey were weighed in and diluted in 5 ml minimal media. The resulting 10 % (v/v) solution is later diluted 1:1 in the assay with minimal media and bacteria to reach the final 5 %. To vary the amount of honey compounds in the assay, the desired quantity of honey was weighed in and the residual amount to reach 0.685 g was compensated with artificial honey. The solutions were used for antibacterial testing after sterile filtration. For manuka honey testing, two manuka honeys from Manuka Health NZ Ltd. were used. Both were labelled with “MGO 550+”, whereby one contained 663 mg MGO/kg and the other one contained 690 mg/kg. To test the effect of hydrogen peroxide on bacterial growth an artificial honey was spiked with glucose oxidase. The continuous formation of hydrogen peroxide from the reaction of glucose oxidase and glucose provides a honey matrix, which resembles natural levels of hydrogen peroxide in honeys. More detailed information about the honeys used for the tests are listed in Table 4 and Table 5. The weighed portions and the final MGO concentrations and hydrogen peroxide formation are listed in Table 7 and Table 8.

Table 7: List of weighed portions of manuka honey and final MGO concentration

	$m_{\text{MGO550+}}$ [g]	$m_{\text{AH}}$ [g]	$c_{\text{MGO}}$ [mg/kg]*	$c_{\text{MGO}}$ [mg/l]**
1	0.6850	0	690.00	47.27
2	0.652	0.0330	656.76	44.99
3	0.6000	0.0850	604.34	41.40
4	0.5072	0.1778	510.94	34.99

5	0.4500	0.2350	435.48	29.83
6	0.4000	0.2850	387.09	26.52
7	0.3000	0.3850	290.32	19.89
8	0.2500	0.4350	241.93	16.57
9	0.2000	0.4850	193.55	13.26
10	0.1500	0.5350	145.16	9.94
11	0.0450	0.6400	43.55	2.98
12	0.0045	0.6805	4.35	0.30

\* MGO content of the honey determined via RP-HPLC, see 1.4.5; \*\* in the final assay

Table 8: List of weighed portions of artificial honey with glucose oxidase and final hydrogen peroxide formation

	$m_{\text{AH-GOX}}$ [g]	$m_{\text{AH}}$ [g]	$c_{\text{H}_2\text{O}_2}$ [mg/kg*h] *	$c_{\text{H}_2\text{O}_2}$ [mg/l*h]**
1	0.600	0.085	114.4	7.8
2	0.500	0.185	104.8	7.2
3	0.400	0.285	89.0	6.1
4	0.300	0.385	62.9	4.3
5	0.200	0.485	36.6	2.5
6	0.150	0.535	16.6	1.1
7	0.100	0.585	8.2	0.6
8	0.075	0.610	3.9	0.3
9	0.050	0.635	1.8	0.1
10	0.025	0.660	0.2	0.01

\* photometric measurement, see 1.4.6; \*\* in the final assay

To test the antibacterial activity of  $\alpha$ -cyclodextrin alone (CD) and inclusion complexes formed by manuka honey and  $\alpha$ -cyclodextrin (CP), different concentrations of CD and CP were weighed in and solubilised in minimal media. To maintain a constant sugar concentration of 5 %, artificial honey was added to the assay. The sugar content of honey in CP was subtracted from the amount of added artificial honey. To the samples containing CD alone, always 685 mg artificial honey was added.

Tabelle 1: List of cyclopower and cyclodextrin weighed portions and final MGO concentration for antibacterial tests

	Cyclopower				$\alpha$ -Cyclodextrin		
	mCP [g]	mAH [g]	cMGO* [mg/l]	cCD* [mg/l]	mCD [g]	mKH [g]	cCD* [mg/l]
1	0.90	0.2835	19.26	49860	0.50	0.685	50000
2	0.80	0.3280	17.12	44320	0.42	0.685	42000
3	0.60	0.4175	12.84	33240	0.36	0.685	36000
4	0.50	0.4620	10.70	27700	0.28	0.685	28000
5	0.40	0.5065	8.56	22160	0.24	0.685	24000
6	0.30	0.5510	6.42	16620	0.20	0.685	20000
7	0.10	0.6405	2.14	5540	0.15	0.685	15000
8	0.01	0.6805	0.21	554	0.05	0.685	5000

\* in the final assay

The honey or cyclodextrin solutions, minimal media and bacterial suspension were mixed directly in the wells of a sterile 96-well microtiter plate. Every test was performed five times for each bacterium and test substance. The final volume of the incubation mix was 100  $\mu$ l. The starting optical density of the assay solution was 0.01 absorption units. The fixed starting OD ensured that every well contained the same number of bacteria cells and thus had identical starting conditions. The volume of bacterial solution, which needed to be added to the assay, was calculated from the OD of the pre-culture according to Equation 1. This needed to be calculated prior to every test, because the pre-culture did not always grow uniformly. The final assay consisted of the calculated amount of bacterial solution, 50  $\mu$ l diluted honey or cyclodextrin and the additional volume to fill up the 100  $\mu$ l was made up with minimal media. A bacteria control in minimal media only was included also five times for each fresh pre-culture.

$$V_{bacterial\ solution} = \frac{V_{total} * OD_{total}}{OD_{pre-culture\ 1:50}}$$

Equation 1: Calculation of volume of bacterial solution in the assay.

The microtiter plate was sealed with a sterile, gas-permeable membrane and incubated in multimode reader at 37 °C for 20 h. Every 30 min, the absorption at 600 nm was read. Between the readings, the microtiter plate was shaken with amplitude of 3 mm. The data evaluation was achieved with the software Tecan i-control, version 1.1.9.0.

#### 1.4.8. Hydrogen peroxide cleavage

To test whether the bacteria are able to cleave hydrogen peroxide to oxygen and water, bacterial cells were suspended in a 3 % hydrogen peroxide solution with a sterile toothpick. The formation of bubbles indicates the presence of enzymes, which are able to cleave H<sub>2</sub>O<sub>2</sub>. A catalase-positive *B. subtilis* strain served as a positive control and a catalase-negative *E. coli* strain served as a negative control. Both strains were kindly provided by Mrs. Buchwald from the strain bank of the Institute for Microbiology, TU Dresden.

#### 1.4.9. Quantification of “growth delay”

The growth curves, which were obtained with the bacterial assay, were analysed with the determination of the corresponding growth delay (GD) of each inhibitor compared to the control sample. In the presented thesis, bacterial growth was defined when the OD was  $\geq 0.05$ . The calculation of the start of bacterial growth was achieved by fitting the growth curves with the Boltzmann equation and calculating the x value (time) for y (OD) = 0.05. The corresponding growth delay for the inhibitor concentration x (GD<sub>x</sub>) was obtained by dividing the starting time of growth of the inhibited sample with the starting time of growth of the control sample (see Equation 2).

$$GD_x = \frac{t_{inhibitor (OD\ 0.05)}}{t_{control (OD\ 0.05)}}$$

Equation 2: Calculation of growth delay (GD) for inhibitor concentration x.

The GD of an inhibitor was plotted against the corresponding concentration and an exponential dose-response curve was obtained. Linearization of dose-response curves was achieved by plotting the logarithm of the GD against the inhibitor concentration. The inhibitors were compared with the help of the slope of their linear fitting curves. In contrast to

the determination of MIC values, an interpolation between the readings is possible now. In general, the higher the slope of a curve, the stronger is the bacteriostatic effect of an inhibitor.

#### 1.4.10. Determination of bactericidal concentrations

To test whether an antibacterial effect is of bacteriostatic or bactericidal nature, 70 µl of the assay solutions, which did not show any growth after the end of incubation, were incubated on fresh, solid nutrient agar plates at 37 °C for 24 h. The cells which were incubated with artificial honey only and grew well in the assay, were carried along as a negative control. Cells, which were incubated with the antibiotic ampicillin were tested as positive controls. The cfu were counted after 24 h and the corresponding honey concentrations of plates without any bacterial growth were characterised as bactericidal.

#### 1.4.11. Inhibition of *Helicobacter pylori*

The *H. pylori* pre-culture was obtained from the Deutsche Sammlung für Mikroorganismen und Zellkulturen (DSMZ). The DSM number was 21031 and a freeze-dried culture along with an active culture was ordered. The reactivation of the freeze-dried culture was achieved according to the manufacturer's information. To study the inhibition of *H. pylori* with honey, a pre-culture of *H. pylori* on a blood agar plate, which was incubated at 37 °C in a microaerophilic environment for 96 h was prepared. The cells of the pre-culture were re-suspended in brucella broth media, which was brought to pH 2 and pH 7 with HCl. The cell number in the inoculums was counted with Thoma cytometers und the microscope. For incubation, 60 µl of the cells were further diluted with 200 µl of either brucella broth media (serves as a control) or honey solutions (inhibition samples) in a microtiter plate. The plate was incubated at 37 °C and microaerophilic conditions and the optical density (OD) of the cells at 600 nm was read after 0, 24, 48 and 96 h. Honey was tested in concentrations ranging from 0.75 to 30 %, acetohydroxamic acid was tested in concentrations from 1 to 5 mg/l, MGO from 5 to 250 mg/l, DHA from 10 to 500 mg/l and cyclopower in concentrations from 0.75 to 10 %. Since the OD did not change during the incubation, samples were taken from the microtiterplate and cultured on fresh blood agar plates after serial dilution. The blood agar plates were incubated at 37 °C in a microaerophilic environment for 48 h and cfu were counted on appropriately diluted plates. Aliquots of the microtiterplate incubation samples were also taken for analysis of MGO and lactate. For MGO analysis, the liquid incubation samples were centrifuged and 100 µl of cell supernatant were derivatized according to the



MGO derivatization procedure (see section 1.4.5). For lactic acid analysis, the liquid incubation samples were centrifuged and 100  $\mu$ l of cell supernatant was analyzed with a D-/L-lactic acid kit (R-Biopharm, Darmstadt, Germany). The kit is based on the reaction of D-/L-lactic acid with D-/L-lactate dehydrogenase to form pyruvate and  $\text{NADH}+\text{H}^+$ , which can be detected photometrically at 340 nm.

#### 1.4.12. Studies on the structure of cyclodextrin inclusion complexes

Model complexes containing honey compounds and  $\alpha$ -cyclodextrin were prepared according to the protocol for the pilot scale production of “MGO 400+ Manuka Honey with Cyclopower™” (Manuka Health NZ Ltd., 2013) with slight modifications. Briefly, 10 ml ultrapure water was heated to 50 °C and 1 mmol of  $\alpha$ -CD was added. The turbid solution was stirred for 10 min and cooled down to 40 °C. The honey compounds (MGO or DHA) or the control compounds (1-propanol or hydroxyacetone) were added in the ratio presented in Table 9 and the solution was stirred for exactly ten minutes. The mixture was subsequently frozen and lyophilized. The lyophilized complexes were stored at -20 °C. As a negative control, starch and glucose instead of  $\alpha$ -cyclodextrin were used to prepare complexes with MGO and DHA. Approximately 80 mg of each complex was solubilised in 700  $\mu$ l  $\text{D}_2\text{O}$  and analysed with  $^1\text{H-NMR}$ . All  $^1\text{H-NMR}$  spectra were recorded at a Bruker Avance III 600 device with a central frequency of 600 MHz. The chemical shift is referenced to tetramethylsilane (TMS) resonance at 0 ppm. For visualization of spatial interactions between protons, ROESY-NMR was used. All spectra were acquired and processed using Topspin software (Bruker).

Table 9: Model complexes

Model complex	Consists of	Molar ratio
MGO-CD	MGO and $\alpha$ -cyclodextrin	1:1
DHA-CD	DHA and $\alpha$ -cyclodextrin	1:1
MGO-DHA-CD	MGO, DHA and $\alpha$ -cyclodextrin	1:2:1
MGO-DHA-Glc	MGO, DHA and glucose	1:2:1
MGO-Starch	MGO, DHA and starch	1:2:1
PrOH-CD	1-propanol and $\alpha$ -cyclodextrin	2:1
HA-CD	Hydroxyacetone and $\alpha$ -cyclodextrin	3:1

### 1.4.13. Enzyme inhibition with manuka honey

#### 1.4.13.1. Urease activity assay

The commercial jack bean urease was solubilized in ultrapure water (80 kU/l). To measure the enzyme activity, 25  $\mu$ l of urease solution were mixed with 10  $\mu$ l ninhydrin (2 % (w/w) in ethanol), 90  $\mu$ l phosphate buffer (200 mM, pH 6.8) and 100  $\mu$ l ultrapure water in a 96-well microtiter plate. The mixture was pre-incubated at 37 °C for 2 hours. The reaction was started by adding 50  $\mu$ l of urea solution (550 mM in ultrapure water). For the enzyme working at its maximum velocity, the final urea concentration for the assay was set to 100 mM, which is approximately 5 times the Michaelis-Menten constant (see below). The microtiter plate was further incubated at 37 °C for 80 min and the detection of ammonia released from urea cleavage was continuously monitored by measuring the absorption at 440 nm with a multimode reader Tecan Infinite M200 (Mainz, Germany). A blank with 50  $\mu$ l ultrapure water instead of the substrate urea was included in the assay to test whether ninhydrin reacts with any other compounds than ammonia to form a yellow complex which absorbs at 440 nm. Urease activity was defined as the linear slope of absorbance between 10-30 min of incubation.

#### 1.4.13.2. Urease inhibition assay

To measure the inhibition of the enzyme activity caused by honeys, methylglyoxal or dihydroxyacetone, respectively, 25  $\mu$ l of urease solution were mixed with 10  $\mu$ l ninhydrin (2 % (w/w) in ethanol), 90  $\mu$ l phosphate buffer (200 mM, pH 6.8) and 100  $\mu$ l of the solution of the inhibitory compound in a 96-well microtiter plate. The mixture was pre-incubated at 37 °C for 2 hours and the reaction was started by adding 50  $\mu$ l of the substrate urea solution (550 mM in ultrapure water). The microtiter plate was further incubated at 37 °C for 80 min and the detection of ammonia release from urea cleavage was continuously monitored by measuring the absorption at 440 nm with a multimode reader Tecan Infinite M200 (Mainz, Germany). A blank of each inhibitory compound without urease but 25  $\mu$ l ultrapure water instead was included in the assay to test for any interfering substances which absorb at 440 nm. Urease activity was defined as the linear slope of absorbance between 10-30 min of incubation. The results are expressed as a percentage of the residual activity measured in the presence of an inhibitor compared to the urease activity of a control (water) sample.

#### 1.4.13.3. Inhibitory test compounds

Lime, honeydew, canola and artificial honey, as well as four manuka honeys with MGO and DHA contents classified as low, medium, high and very high (see Table 4) were analysed for their inhibitory effect. Hydrogen peroxide, which is formed via enzymatic glucose oxidation in diluted honey, inhibits the ninhydrin-ammonia reaction, what leads to apparently decreased activities. Therefore, hydrogen peroxide was eliminated by the addition of 20  $\mu\text{l}$  catalase to each honey stock solution (75 % w/v). The honey stock solutions were diluted with ultrapure water to reach a final concentration of 0.04, 0.4, 1.8, 5.5, 10.9, 16.4, 21.8 and 27.3 % (w/v) in the assay. Eight concentrations ranging between 0.4 to 83.3 and 0.2 to 44.4 mM of methylglyoxal (MGO) and dihydroxyacetone (DHA), respectively, were tested for their inhibitory effect. Acetohydroxamic acid (AHA) was used as a positive control according to (Tanaka et al., 2004) and tested in eight concentrations ranging between 1.9 and 400.0  $\mu\text{M}$ . All tested substances were diluted in ultrapure water. Canola honey was artificially spiked with MGO and DHA by adding 114  $\mu\text{l}$  of a MGO stock solution (39.2 g/l) and 1 ml of a DHA stock solution (12.0 g/l) to 7.5 g honey in 10 ml ultrapure water. The aqueous solution with MGO and DHA was prepared as the spiked canola honey, but without honey addition. To eliminate the effect of MGO in manuka honey, glutathione (GSH) and glyoxalase were added in a final concentration of 0.5 mM and 141 mU/ml to the 75 % (w/v) stock solution of manuka honey sample MH 3, respectively. The honey sample MH 3 was a commercial manuka honey MGO 400+ with a MGO content of 595 mg/kg (determined with RP-HPLC-UV).

#### 1.4.13.4. Determination of Michaelis-Menten constant

To determine the affinity of urease to the substrate urea, the urease assay conditions mentioned above were used. The velocity of the reaction was measured using eight different concentrations of the substrate urea (15-100 mM) and a constant enzyme concentration in the absence of inhibitors.

#### 1.4.13.5. Chromatographic quantification of ammonia

In order to check values obtained from photometric quantitation of ammonia, data were compared with results obtained from quantitation via an amino acid analyser based on ion-exchange chromatography and post-column derivatization with ninhydrin. The ammonia content of the samples was further quantitated chromatographically. For this, incubation of urease with or without inhibitory substances was conducted without the addition of ninhydrin.

Volume correction was achieved by adding 10  $\mu$ l phosphate buffer (100  $\mu$ l phosphate buffer in total) instead of ninhydrin solution. Urease was pre-incubated with the inhibitors 2 h prior to start of the reaction with substrate addition (50  $\mu$ l urea, 550 mM). The samples were further incubated for 30 min and directly diluted 1:250 with lithium citrate buffer (0.12 N, pH 2.2) to stop the enzymatic reaction. The analyses were performed using a SYKAM S4300 amino acid analyser (Fuerstenfeldbruck, Germany) with conditions according to manufacturer's instructions. Ammonia eluted at 59.6 min and was detected after post-column derivatization with ninhydrin at 570 nm. External calibration with ammonia standards was performed.

#### 1.4.13.6. Further enzyme activity assays

To show that urease was specifically inhibited and other enzymes are less affected by methylglyoxal and dihydroxyacetone, two exemplary, physiologically relevant enzymes were tested for their inhibition with MGO and DHA.

Pepsin activity was measured in the presence and absence of MGO or DHA, respectively, according to (Minekus et al., 2014). All reagents were solubilised in ultrapure water unless otherwise stated. Trichloroacetic acid (TCA) was diluted to 5 % (w/w) and MGO stock solution was diluted to 4mM. DHA was solubilised and diluted to a final concentration of 7 mM. 0.5 g of the substrate haemoglobin was diluted in 20 mL of ultrapure water and further diluted with 5 ml HCl (300 mM) to reach a final concentration of 2 % (w/v) with a pH of 2. For the pepsin stock solution, 20 mg of pepsin was diluted in 20 mL NaCl solution (150 mM). To prevent autolysis, the pH was brought to 6.5 with 100 mM NaOH. The pepsin stock solution was diluted 1:10 in 100 mM HCl freshly for each test. Inhibitor solutions and diluted pepsin were pre-incubated at 37 °C for 2 h. The reaction was started with the addition of haemoglobin substrate and the reaction mixture was incubated for exactly 10 min at 37 °C. The reaction was stopped with the addition of TCA, followed by centrifugation at 10,000 rpm for 10 min. 200  $\mu$ l of the supernatant were transferred in a UV-star microtiter plate (from Greiner) and UV absorbance at 280 nm was measured with a multimode reader Tecan Infinite M200 (Mainz, Germany). A blank, containing no enzyme but inhibitor and substrate, was included in the assay and subtracted from the inhibitor sample and control sample. The results are expressed as a percentage of the residual activity measured in the presence of an inhibitor compared to the pepsin activity measured for a control sample.

ACE activity assay in the absence or presence of methylglyoxal (MGO) or dihydroxyacetone (DHA) was carried out according to Lunow et al. (2015). Briefly, the ACE-induced cleavage

of the fluorescence resonance energy transfer (FRET) substrate Abz-FRK(Dnp)P-OH was continuously monitored by measuring the fluorescence at  $\lambda_{\text{ex}}/\lambda_{\text{em}} = 320/420$  nm for 60 min at 37° C with a multimode reader Tecan Infinite M200 (Mainz, Germany). MGO stock solution was diluted to give a final concentration of 4 mM. DHA was dissolved and diluted in Tris-HCl buffer to a final concentration of 7 mM. Inhibitor solutions and ACE were pre-incubated at 37 °C for 2 h. The reaction was started with the addition of the FRET-substrate and substrate cleavage control samples, which correspond to 100 % activity, were prepared by adding Tris-HCl buffer instead of inhibitor solutions to the enzyme. A blank, containing no enzyme but inhibitor and substrate, was included in the assay and subtracted from the inhibitor sample and control sample. The results are expressed as a percentage of the residual activity measured in the presence of an inhibitor compared to the ACE activity measured for a control sample.

## 1.5. Results and discussion

### 1.5.1. Antibacterial compounds in honey

Honey is used as an antibacterial wound dressing since ancient time (Eteraf-Oskouei and Najafi, 2013). In the past, the antibacterial effect of honey was attributed to osmotic pressure, its acidic pH value or lysozyme and other minor compounds (Mandal and Mandal, 2011). This section will focus on two of the most potent antibacterial ingredients in honey: hydrogen peroxide and methylglyoxal.

The results of this section are partly originating from the experimental work of master student Constanze Polster and were primarily published in her master thesis (Polster, 2015).

#### 1.5.1.1. Hydrogen peroxide formation in honeys

To evaluate the antibacterial effect due to hydrogen peroxide, it was necessary to measure the hydrogen peroxide formation in honeys.  $H_2O_2$  is formed enzymatically in honey by the oxidation of glucose to glucono- $\delta$ -lactone with the bee-derived enzyme glucose oxidase. Due to the low water activity in undiluted honey and its acidic pH, the activity of glucose oxidase is rather low and thus, the formation of hydrogen peroxide in undiluted honey is negligible (White et al., 1963). Only after dilution of honey, the enzyme gets active and hydrogen peroxide is formed, which can act antibacterial. The measurement of hydrogen peroxide was carried out according to 1.4.6. Briefly, aqueous honey solutions were incubated to produce hydrogen peroxide, which was photometrically quantified at 540 nm after the reaction with o-dianisidine and peroxidase under acidic conditions. The limit of detection (LOD) was 0.9 mg/kg\*h and the limit of quantification was 2.7 mg/kg\*h (determined according to 1.4.6). The hydrogen peroxide formation of four commercial honeys is presented in Table 10.

Table 10: Hydrogen peroxide formation of commercial honey samples, results are expressed as mean values of triplicate measurement with standard deviation

Honey	Manuka MGO 400	Manuka MGO 550	Lime honey	Polyfloral honey
$H_2O_2$ mg/kg*h	7.1 ± 0.8	3.9 ± 0.3	66.7 ± 0.6	6.1 ± 1.3

The hydrogen peroxide formation of the two manuka honeys can be classified as low. Manuka honeys are known to produce relatively low amounts of hydrogen peroxide (Kwakman et al., 2011a; Müller, 2013), which might be due to reduced glucose oxidase activity in the presence of methylglyoxal (Majtan et al., 2013). In contrast, the tested non-manuka honeys gave a diverse picture: the lime honey formed around 10-fold higher amounts of hydrogen peroxide than the manuka honeys, whereas the polyfloral honey formed the same low hydrogen peroxide level as the manuka honeys. All honeys were tested after 1 h incubation as 5 % (v/v) solutions. The dilution plays an important role for the comparison of hydrogen peroxide levels in honey, since the activity of glucose oxidase depends on the water activity and thus increases with higher dilution. Moreover, highly diluted honey solution contain less substances, which counteract with hydrogen peroxide production through degradation reactions, leading to apparently higher H<sub>2</sub>O<sub>2</sub> values (White et al., 1963; Molan, 1992a). The incubation conditions were the same for all honey samples tested in this study, so the varying levels of H<sub>2</sub>O<sub>2</sub> are solely due to plant-derived characteristics. The hydrogen peroxide formation can be influenced by the botanical origin of the plant, climate conditions or environmental factors. Commercial processing and especially heat treatment can also significantly influence the hydrogen peroxide formation in honey (Chen et al., 2012). Since there was no information available about the treatment of the commercial honeys tested in this study, it was difficult to define factors responsible for the formation of hydrogen peroxide presented here. To exclude unpredictable influences on H<sub>2</sub>O<sub>2</sub> formation in honey, an artificial honey containing sugars only and the enzyme glucose oxidase (from *Aspergillus niger*) was prepared by spiking an artificial honey with 50 µg glucose oxidase per g honey, resulting in a specific activity of 2.4 U/g honey. The stock honey, named AH-GOX, was subsequently diluted with artificial honey (AH) to obtain seven model honeys with varying glucose oxidase concentrations (7-50 µg/g and 0.3-2.4 U/g). The model honeys were diluted to 5 % (v/v) with buffer and after 1 h incubation at 37 °C, the hydrogen peroxide formation was measured. Figure 4 shows the hydrogen peroxide formation of each AH-GOX dilution dependent on its GOX activity.

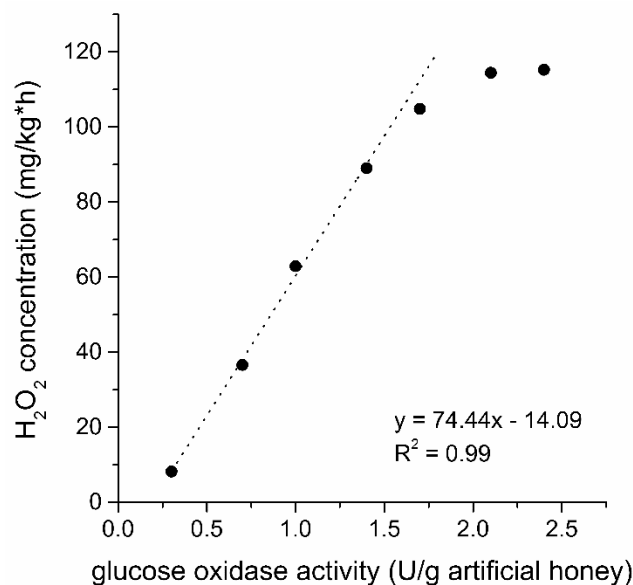


Figure 4: Hydrogen peroxide production in artificial honeys with varying activity of glucose oxidase, single determination in 5 % (v/v) solutions

The hydrogen peroxide formation in the artificial honeys increased with increasing GOX activity. The seven model honeys with varying GOX concentrations produced between 8 and 115 mg H<sub>2</sub>O<sub>2</sub>/kg honey after 1 h incubation. Until a GOX activity of 1.6 U/g honey, the hydrogen peroxide formation correlated linearly with the enzyme activity. At enzyme activities higher than 2.0 U/g honey, the H<sub>2</sub>O<sub>2</sub> formation reached saturation and no further increase of hydrogen peroxide was observable. Since glucose, the educt of the reaction is abundantly available, a continuous increase of H<sub>2</sub>O<sub>2</sub> concentration was expected. The flattening of the curve is a sign for an inhibition of the enzymatic reaction. This could be due to inhibition of glucose oxidase by one of the reaction products. Glucono- $\delta$ -lactone acts as a weak inhibitor of glucose oxidase by docking into the catalytic centre of the enzyme (Nakamura and Ogura, 1962; Gibson et al., 1964). Moreover, hydrogen peroxide was identified to inhibit glucose oxidase of *Aspergillus niger* (Kleppe, 1966; Buchholz and Goedermann, 1978). Hydrogen peroxide is a strong oxidative reagent, which can modify amino acid residues of proteins. Kleppe (1966) discusses the oxidation of methionine residues of glucose oxidase close to the catalytic centre of the enzyme and the subsequent loss of enzymatic activity. It was concluded that high amounts of hydrogen peroxide can decrease enzyme activity and thus lead to stagnation of the hydrogen peroxide formation in the AH-GOX model.



### 1.5.1.2. Influence of methylglyoxal on hydrogen peroxide formation in honey

The reactive compound methylglyoxal may react with enzymes and influences its enzymatic activity (Rabbani and Thornalley, 2008). The remarkably low levels of hydrogen peroxide formation in manuka honeys indicate that methylglyoxal may modify honey-derived glucose oxidase and thus decrease hydrogen peroxide accumulation in manuka honeys. This hypothesis was earlier expressed by Majtan et al. (2013), who described a dose-dependent effect of artificially added methylglyoxal to honeys on hydrogen peroxide accumulation. Moreover, the authors observed cross-linking of glucose oxidase after 48 h incubation with methylglyoxal, which might decrease enzymatic activity. To test, whether methylglyoxal is responsible for low levels of hydrogen peroxide formation, a non-manuka honey (lime honey) was mixed in a 1:1 ratio with either sugars only (AH), methylglyoxal and sugars (AH-MGO) or manuka honey MGO 400+. The blends were diluted to 5 % (w/v) and hydrogen peroxide production was analysed according to 1.4.6. The samples were incubated for 1 h at 37 °C prior to detection of hydrogen peroxide. The H<sub>2</sub>O<sub>2</sub> formation of the blends are shown in Table 11.

Table 11: Hydrogen peroxide formation of lime honey blends, results are expressed as mean values of triplicate measurement with standard deviation

<b>Honey 1</b>	Lime honey	Lime honey	Lime honey	Manuka honey
<b>Honey 2</b>	AH	AH-MGO	Manuka honey	AH
<b>H<sub>2</sub>O<sub>2</sub> mg/kg*h</b>	32.1 ± 0.6	33.7 ± 1.6	36.4 ± 3.3	5.4 ± 0.7

There was no significant decrease of hydrogen peroxide formation after the incubation of lime honey with methylglyoxal compared to the incubation of lime honey with sugars only (AH). The results suggest that after 1 h aqueous incubation, bee-derived glucose oxidase activity was not influenced by methylglyoxal. This is in accordance with Majtan et al. (2013), who neither detected a significant decrease of hydrogen peroxide production nor any cross-links of glucose oxidase after 2 h incubation at 37 °C. Only after 24-48 h aqueous incubation, a significant change of enzyme activity and molecular structure became detectable. The reason why both test systems failed to present any influence of MGO on glucose oxidase may be that the artificial adding of MGO to honey does not decently reproduce natural MGO formation in honey. Plant nectar contains up to 80 % water, which is evaporated during honey ripening in the comb down to a water content of 16-20 % in the final honey (Semkiw et al., 2008). This

process takes approximately 3-5 days at temperatures of 30-35 °C. These are optimal conditions for glycation reactions, which could lead to enzymatic inhibition of glucose oxidase in the commercial honey. For example, dihydroxyacetone, which is present in high concentrations in manuka nectar, is known for its ability to react with proteins (Molin et al., 2007). Moreover, Bilova et al. (2016) were able to show, that advanced glycation endproducts (AGE) are formed in plants and can be transported into plant tissue. The main glycating agents were identified to be phosphorylated sugars or triose phosphates. Because of the poor reaction conditions in honey (low water activity and slightly acidic) it is more likely that glycation reactions occur during earlier stages of honey formation, e.g. in the plant phloem or during nectar harvest by the bees. Nevertheless, it is also possible that hydrogen peroxide formation is rather low in manuka honey because the honey contains lower amounts of the enzyme glucose oxidase. According to Azeredo et al. (2003), the protein content of honey depends on the floral and geographical origin. Besides glucose oxidase, honey contains the enzyme catalase which catalyzes the reaction of hydrogen peroxide to water and oxygen. The ratio of both enzymes in honey ultimately determines its hydrogen peroxide level. Until now, no quantitative data of catalase and glucose oxidase activity in manuka honey is available.

#### 1.5.1.3. Methylglyoxal

Methylglyoxal (MGO) is only present in honey varieties from the plant family *Leptospermum*. It was described in New Zealand manuka honey (*Leptospermum scoparium*) for the first time (Mavric et al., 2008), but it was recently also found to be present in honeys from Australia (Windsor et al., 2012; Cokcetin et al., 2016). Honeys with increased levels of MGO belonged to the species *L. continentale*, *L. liversidgei* and especially to *L. polygalifolium*. Methylglyoxal in honey is stable towards light and heat (Molan and Russell, 1988). Moreover it was shown that the antibacterial effect of manuka honey was not affected by increasing the pH to 11 or storing the honey over 7 years at 4 °C (Bogdanov, 1997; Cokcetin et al., 2016). The varying levels of MGO in *Leptospermum* honey are caused by a wide concentration range of its precursor compound dihydroxyacetone in the plant nectar (Williams et al., 2014; Norton et al., 2015). The reason for the high variations of DHA is unknown. Effects of the environment or climate have been discussed (Williams et al., 2014). In commercial honeys, the MGO level is relatively stable during storage. Figure 5 shows the MGO and DHA concentration of a manuka honey with a starting concentration of 6 and 12 mmol/kg, respectively, during storage at room temperature over 90 days. There is a loss of 1

mmol/kg of DHA whereas the MGO level rises by 0.5 mmol/kg. The missing 0.5 mmol/kg could have reacted with other honey compounds, whereby it is not clear, whether DHA is initially dehydrated to MGO, which continues reacting or if DHA reacts with other honey compounds independently from MGO. Nevertheless, in comparison to hydrogen peroxide, MGO can be classified as a chemically stable compound in the honey matrix.

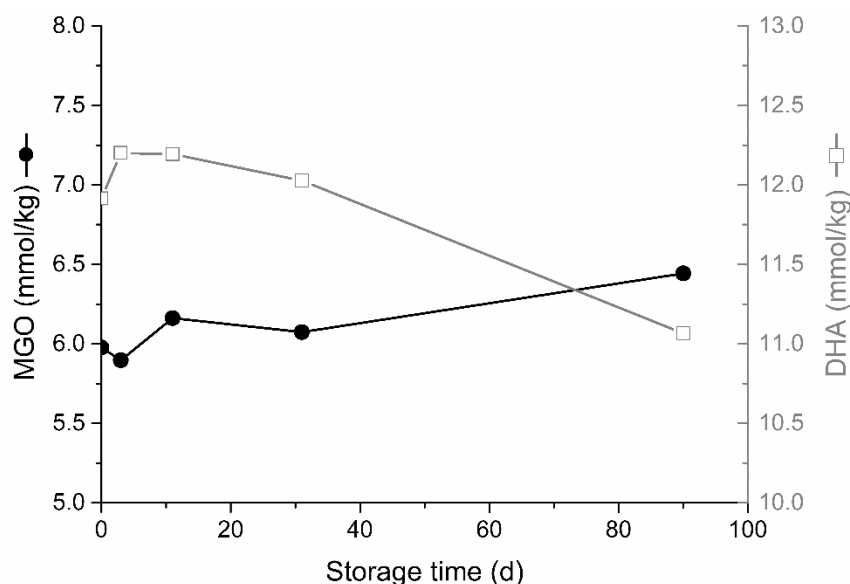


Figure 5: Concentration of methylglyoxal (MGO) and dihydroxyacetone (DHA) during 90 days storage at room temperature, results are expressed as mean values of duplicate measurement

### 1.5.2. The antibacterial effect of honey

The level of antibacterial activity in honey is highly variable and mostly depends on its floral source, processing and storage conditions. Antibacterial activity, which remains in honey after neutralization of hydrogen peroxide, is commonly referred to as “non-peroxide activity” (NPA) (Cokcetin et al., 2016). NPA was first identified in honey from New Zealand’s *Leptospermum* species (Molan and Russell, 1988; Allen et al., 1991). Until now, there exists no method to quantitatively compare PA and NPA in honey. The aim of this study was to evaluate the effect of manuka honey containing methylglyoxal and artificial honey, which produces hydrogen peroxide, on four different bacteria species. Eventually, a statement concerning the effectiveness of hydrogen peroxide in comparison to methylglyoxal in honey should be given.

### 1.5.2.1. Bacterial growth curves

To evaluate the effect of methylglyoxal and hydrogen peroxide in honey on bacterial growth, all tests were performed in solutions containing 5 % (w/v) sugars. In higher dilutions of honey, this amount was achieved by adding the additional amount of artificial honey (see Table 7 and Table 8). All dilutions were prepared in minimal medium and the assay was performed according to 1.4.7. The bacterial suspensions were incubated with different inhibitory solutions at 37 °C for 16 h. During that time, a photometric measurement of the optical density (OD) at 600 nm was performed every 30 min. The increase of OD indicates bacterial growth. Figure 6 shows the growth of *Escherichia coli* in media alone or in the presence of 5 % (v/v) artificial honey. Both controls were always included in every assay. The control of bacteria in media alone was carried out to test the overall conditions of the bacteria and the control in 5 % (v/v) artificial honey was used to calculate the growth delay of the inhibitor solutions.

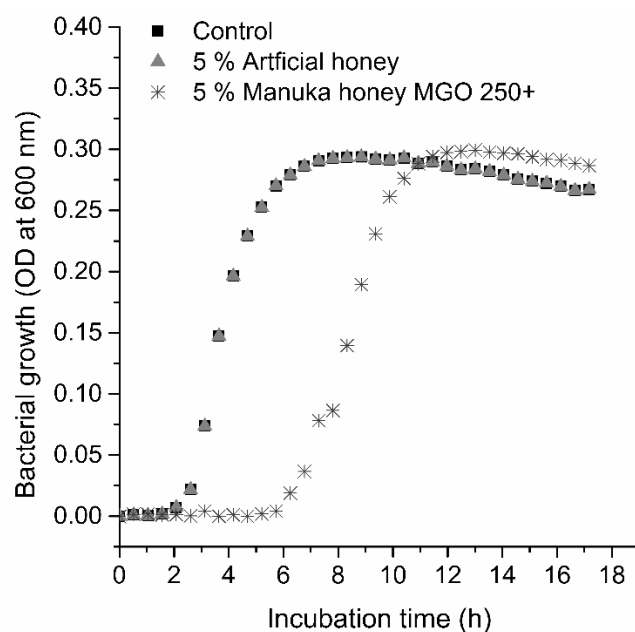


Figure 6: Growth curve of *Escherichia coli* in media alone, with artificial honey or manuka honey MGO 250+. Samples were incubated for 17 h at 37 °C.

Since the control with media alone contains no substances which could limit *E. coli* growth, this growth curve can be considered as optimal growth under the present conditions. After 2 h the bacteria leave the lag phase and enter exponential growth phase. After approximately seven hours, the maximum cell density is reached and no further growth occurs. At a concentration of 5 % (v/v) artificial honey and its osmotic effect does not influence the

growth of *E. coli*. In general, a bacteriostatic effect of artificial honey on all four tested bacteria was only detectable in concentrations above 20 % (v/v) (data not shown).

The presence of manuka honey delays the onset of bacterial growth. The cells incubated with 5 % (v/v) manuka honey MGO 250+ started growing after approximately 6 h, which is 4 h later than the control samples. Nevertheless, when the cells incubated with manuka honey entered the log phase of growth, they reached the same OD as the control sample, which indicates that the growth is delayed but not hindered completely. The incubation of bacteria cells in liquid media is an advantage compared to other established microbiological tests like the agar well or agar disc diffusion assay. In these tests, the inhibitory substance needs to diffuse through the media to interact with bacteria. Especially large molecules or viscous solutions can hamper these processes. Thus, incubation in liquid media reduces diffusion problems and the concentration of inhibitory substance is more homogenous. The continuous photometric measurement of the optical density is also a better way to study bacterial inhibition compared to detecting the growth after only one certain time point. With regard to the above mentioned growth curves of *E. coli*, when the OD would have been measured after 11 h incubation only, there would be no difference in the effect of artificial honey or manuka honey (see Figure 6). This could lead to an underestimation of the effect, which can be avoided by measuring the growth curve instead of measuring the OD at only one time point. Moreover, the presented assay allows studying various concentrations of inhibitory substances and enables the determination of dose-response curves. The effect of different antibacterial substances in honey will be discussed in the following sections in detail.

#### 1.5.2.2. The antibacterial effect of hydrogen peroxide

To study the antibacterial activity of hydrogen peroxide, dose-response curves for varying levels of H<sub>2</sub>O<sub>2</sub> were determined. Therefore, the artificial honey which contained glucose oxidase (AH-GOX) was diluted with artificial honey (AH) to yield different amounts of hydrogen peroxide in the assay. The final H<sub>2</sub>O<sub>2</sub> formation varied between 4 to 114 mg/kg\*h (see 1.4.7). In lime honey, which is described as a hydrogen peroxide-rich honey (Molan, 1992b; Müller, 2013), 67 mg H<sub>2</sub>O<sub>2</sub>/kg\*h was formed. Thus the model honey AH-GOX can be used to cover a wide range of hydrogen peroxide formation in honey. Figure 7 shows the dose-response curve of two gram-positive bacteria, namely *S. aureus* and *B. subtilis* and two gram-negative bacteria, namely *E. coli* and *P. aeruginosa*, against hydrogen peroxide. Hydrogen peroxide had a bacteriostatic effect on all bacteria, except *B. subtilis*. The growth delay (y-axis) was referenced to a 5 % (v/v) solution of sugars (AH). Therefore, a GD of 1

means the antibacterial compound has no stronger effect than a 5 % (v/v) solution of sugar. The dose-dependent effect of antibacterial compounds is reflected by an increase of the GD value. On the x-axis, the corresponding  $H_2O_2$  concentrations of the model honeys (AH-GOX  $\pm$  AH) are shown. The figure on the right side shows the linearization of GD by plotting the logarithm of the GD against the corresponding hydrogen peroxide formation. The red stars indicate the growth delay caused by lime honey. The inhibition values of the lime honey fitted well to the dose-response curves obtained with the model honey AH-GOX, which shows that the model honey is suitable to simulate hydrogen peroxide formation in honey.

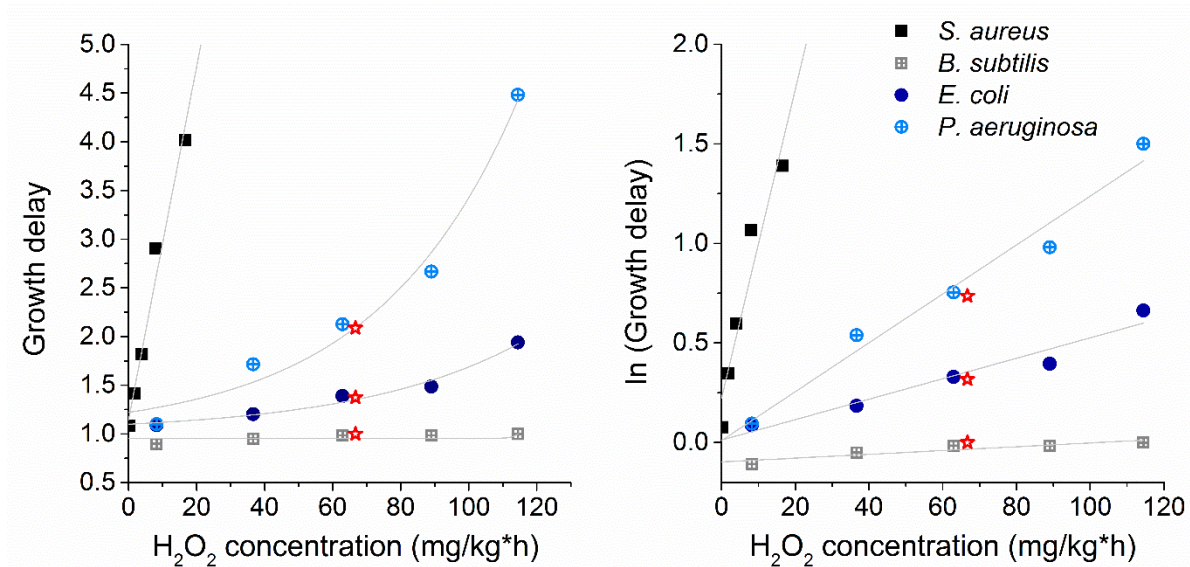


Figure 7: Dose-response curve of hydrogen peroxide towards *S. aureus*, *B. subtilis*, *E. coli* and *P. aeruginosa* before and after linearization. GD of hydrogen peroxide was referenced to 5 % (v/v) AH solution. Red stars indicate GD caused by 5 % (v/v) lime honey with 67 mg  $H_2O_2$ /kg\*h.

According to the dose-response curves, the influence of hydrogen peroxide on bacterial growth differed markedly between the four bacteria species. *B. subtilis* was the only microorganism tested, which was not inhibited by hydrogen peroxide over a honey relevant concentration range. The other bacteria showed a concentration-dependent growth delay. The sensitivity of the species towards  $H_2O_2$  can be described with the following ranking:

$$S. aureus \gg P. Aeruginosa > E. Coli$$

*S. aureus* was already inhibited in the presence of very low levels of hydrogen peroxide. A 5 % (v/v) solution of the model honey with a hydrogen peroxide formation of 16.6 mg/kg\*h

was able to delay *S. aureus* growth by 4 times compared to a 5 % (v/v) sugar solution. Hydrogen peroxide levels like this can easily be achieved in natural honeys (Bang et al., 2003; Majtan et al., 2013). In contrast, *B. subtilis*, which is also a gram-positive bacterium, was not inhibited by hydrogen peroxide in the tested concentration range. Previous studies showed, that some *B. subtilis* mutants can be resistant to hydrogen peroxide (Hartford and Dowds, 1994). The resistance is due to an over expression of enzymes, which decompose hydrogen peroxide, like catalase and alkyl hydroperoxide reductase, and thus inactivate it. The four test bacteria were studied for their ability to cleave hydrogen peroxide (see 1.4.8). Both *B. subtilis* and *E. coli* were able to cleave hydrogen peroxide, whereas *S. aureus* and *P. aeruginosa* lacked this ability. This explained the reduced sensitivity of *B. subtilis* and *E. coli* towards hydrogen peroxide in the bacterial assay. In the presence of a model honey with a hydrogen peroxide formation of 114 mg/kg\*h, *E. coli* growth was delayed by factor 2. To reach this H<sub>2</sub>O<sub>2</sub> level, a honey either needs to have a high formation capacity of hydrogen peroxide or the bacteria need to be incubated over a very long time with a honey with a moderate hydrogen peroxide formation. In consideration of the application of honey as a wound dressing, an incubation time of 24 h is possible. For other applications, like oral ingestion, this incubation time is rather unlikely. Bacteria without enzymes, which can cleave hydrogen peroxide are more sensitive to its antibacterial effect. Hydrogen peroxide is a strong oxidant, which can form hydroxyl radicals in the presence of metal ions (Brudzynski et al. 2011; Molan 1992a). The incubation of bacteria with hydrogen peroxide can lead to damage of the cell wall, proteins or even DNA. This results in cell lyses and thus reduced or completely inhibited bacterial growth (Davies, 1999; Finnegan et al., 2010). A protection mechanism can be the expression of enzymes, located in the cell wall, which can scavenge free radicals and thus prevent oxidative damage. Hence, the ability of bacteria to cope with hydrogen peroxide is an indication of its sensitivity towards oxidative stress in general (Brudzynski et al., 2011). To compare the sensitivity of the tested bacteria towards hydrogen peroxide, the slopes of the linearized dose-response curves were calculated and are shown in Table 12.

Table 12: Slopes of dose-response curves when growth delay is plotted logarithmically against hydrogen peroxide formation in mg/kg\*h

<b>Bacterium</b>	<i>S. aureus</i>	<i>B. subtilis</i>	<i>E. coli</i>	<i>P. aeruginosa</i>
<b>Slope</b>	0.078	0.001	0.005	0.012

The slope values confirmed the observation that *S. aureus* is the most sensitive bacterium towards hydrogen peroxide, followed by *P. aeruginosa* and to a lesser extent *E. coli*. To get a better idea of the effect of H<sub>2</sub>O<sub>2</sub> on different bacteria, the hydrogen peroxide formation, which would be necessary to delay bacterial growth 5-fold stronger than a 5 % (v/v) sugar solution was calculated. The results are shown in Table 13.

Table 13: Calculated hydrogen peroxide formation in honey, which would inhibit bacterial growth 5-fold stronger than a 5 % (v/v) sugar solution. n.d. stands for not determinable

Bacterium	<i>S. aureus</i>	<i>B. subtilis</i>	<i>E. coli</i>	<i>P. aeruginosa</i>
H <sub>2</sub> O <sub>2</sub> (mg/kg*h) to reach GD of 5	18	n.d.	311	130

According to previous results, which studied hydrogen peroxide formation in different honeys (Müller, 2013), the only honey relevant level would be the one necessary to inhibit *S. aureus*. All other hydrogen peroxide formation levels were higher than natural levels in honey. Hence, the bacteriostatic effect of hydrogen peroxide is varying towards different bacteria species. In honey-relevant concentrations, hydrogen peroxide was only effective against *S. aureus*.

#### 1.5.2.3. The antibacterial effect of methylglyoxal

To study the antibacterial activity of MGO in honey, a commercial manuka honey (MGO 550+) with a high MGO content of 690 mg/kg was diluted with artificial honey to obtain varying concentrations of MGO. 5 % (v/v) solutions of the diluted manuka honey were tested for their inhibitory effect on *S. aureus*, *B. subtilis*, *E. coli* and *P. aeruginosa*. The dose-response curves of the four bacteria are shown in Figure 8. MGO had a bacteriostatic effect on all studied bacteria. However, the extent of the antibacterial effect differed markedly between the bacterial species. Again, *S. aureus* was the most sensitive bacteria to the treatment. *P. aeruginosa* was not inhibited by MGO in manuka honey. The sensitivity of the species towards MGO can be described with the following ranking:

$$S. aureus \geq B. subtilis > E. coli$$



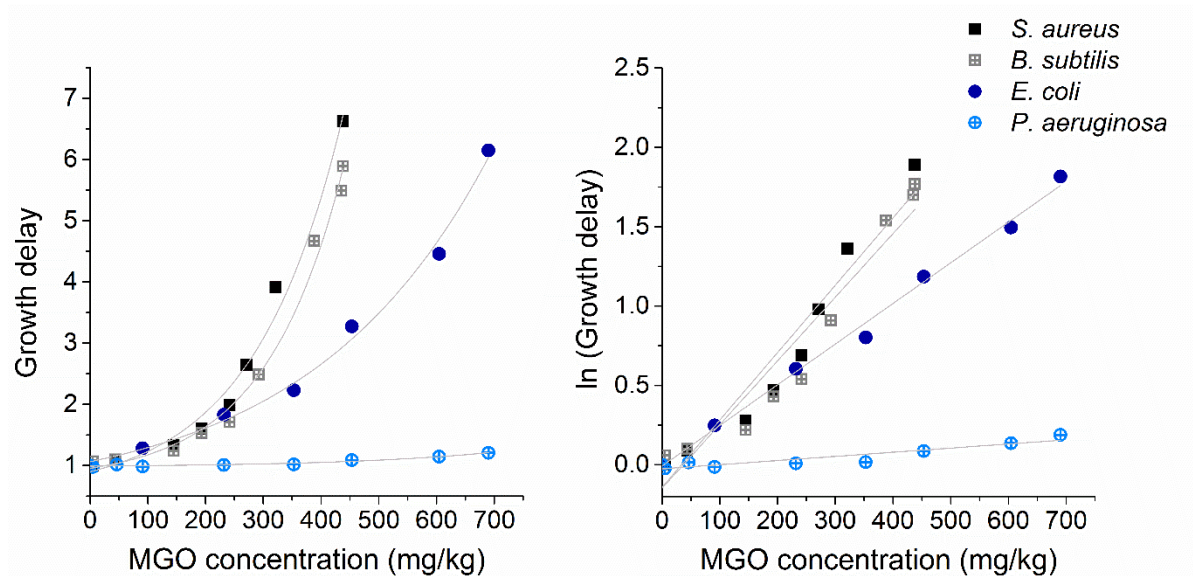


Figure 8: Dose-response curve of methylglyoxal towards *S. aureus*, *B. subtilis*, *E. coli* and *P. aeruginosa* before and after linearization. GD of MGO was referenced to 5 % (v/v) AH solution.

Similar results for the sensitivity towards MGO for these bacteria species were described by Lu et al. (2013). To compare the inhibition of the bacteria by MGO, the slopes of the linearized dose-response curves are presented in Table 14.

Table 14: Slopes of dose-response curves when growth delay is plotted logarithmically against methylglyoxal concentration in mg/kg

Bacterium	<i>S. aureus</i>	<i>B. subtilis</i>	<i>E. coli</i>	<i>P. aeruginosa</i>
Slope	0.004	0.004	0.003	0.0002

To compare the effect of MGO on the bacteria, the MGO concentrations which would be necessary to delay bacterial growth 5-fold stronger than a 5 % (v/v) sugar solution were calculated. The results are shown in Table 15.

Table 15: Calculated MGO levels in honey, which would inhibit bacterial growth 5-fold stronger than a 5 % (v/v) sugar solution. n.d. stands for not determinable

Bacterium	<i>S. aureus</i>	<i>B. subtilis</i>	<i>E. coli</i>	<i>P. aeruginosa</i>
MGO (mg/kg) to reach GD of 5	412	438	632	n.d.

The MGO concentrations which would be necessary to inhibit bacterial growth 5-fold stronger than a control sugar solution (412 to 632 mg/kg), are present in natural manuka honeys. There are several studies which show, that manuka honey can contain MGO in concentrations up to 1700 mg/kg (Windsor et al., 2012; Pappalardo et al., 2016). The sensitivity towards MGO depends on the bacteria species, but all bacteria, with the exception of *P. aeruginosa*, can be inhibited by MGO in manuka honey-relevant concentrations. A possible target for methylglyoxal in bacteria cells, are enzymes which are relevant for survival. Jenkins et al. (2011) showed that manuka honey influences the expression of murein hydrolase, an enzyme which regulates cell separation during cell division. The downregulation of enzyme activity resulted in decreased bacterial growth. However, since bacterial proliferation is a complex process, the precise mechanism by which MGO inhibits bacteria is unknown up to the present day.

In this study the gram-negative bacteria *E. coli* and *P. aeruginosa* were less sensitive to MGO compared to the gram-positive bacteria. Other studies found that also gram-negative bacteria can be inhibited by MGO in manuka honey (Alnaimat et al., 2012; Hayashi et al., 2014). Whether a bacterium is more or less sensitive towards MGO mostly depends on its ability to metabolize increasing concentrations thereof. There are several pathways known, which can lead to MGO detoxification like glyoxalase, reductase or dehydrogenase systems (Ferguson et al., 1998). Since MGO is a common by-product during glycolysis in bacteria, it is necessary to reduce its concentration so it will not negatively influence bacterial survival (Kalapos, 1999). Thus, bacteria which are naturally equipped with enzyme systems to reduce elevated MGO levels are more likely to survive treatment with manuka honey. In an earlier study, it was shown that *P. aeruginosa* has three glyoxalase encoding genes, instead of one (Sukdeo and Honek, 2007). This could be an explanation for the reduced sensitivity of *P. aeruginosa* towards MGO in this study. Another reason for bacterial growth after initial inhibition could be the loss of MGO in the medium. The medium consisted of glucose, sodium chloride and yeast extract. The yeast extract is the product of yeast autolysis and contains mainly protein degradation products. MGO is known for its reactivity towards proteins or peptides. It is possible, that MGO reacted with media components during incubation time and thus became unavailable for bacterial inhibition. According to our results, MGO in manuka honey decreased by 20 % after 6 h of incubation and by 55 % after 30 h of incubation. Moreover, the manuka honey matrix appeared to stabilize MGO to a certain extent, because in an artificial honey with added MGO and DHA in the same concentrations as present in manuka honey,

MGO is even less stable (see Figure 9). The MGO decrease needs to be taken into account when the antibacterial activity in the form of growth delay is plotted against the MGO concentration. Thus, the concentrations given in Figure 8 are only apparent MGO concentrations, calculated based on the MGO level of the corresponding honey.

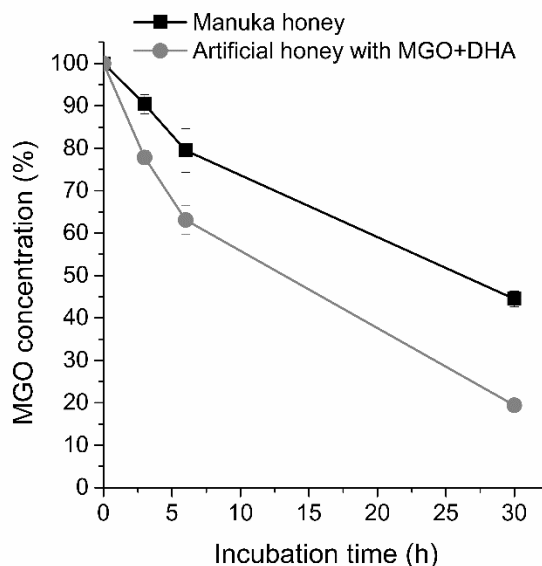


Figure 9: MGO stability in nutrient media. 5 % (v/v) solutions of manuka honey with 690 mg/kg MGO and of artificial honey with the same amount were incubated in nutrient media at 37 ° C for 30 h. Measurements were carried out in duplicate and error bars indicate standard deviation.

#### 1.5.2.4. Comparison of hydrogen peroxide and methylglyoxal as antibacterial compounds

The values of the slopes obtained for the inhibition with hydrogen peroxide (Table 12) can be directly compared to the slopes of inhibition with MGO (Table 14). For *S. aureus*, *E. coli* and *P. aeruginosa*, the values of the slopes of the linearized dose-response curves are higher than the slopes obtained for the inhibition with MGO. That means that these bacteria are more sensitive to hydrogen peroxide than to methylglyoxal. However, the concentrations in which hydrogen peroxide and methylglyoxal are present in honey differ. Whereas MGO amounts in manuka honey range between 40 to 760 mg/kg (Mavric et al., 2008), the formation of hydrogen peroxide depends on the honey dilution and reaches its maximum at approximately 200 mg/kg\*30 min in dilutions of 15 to 67 % (v/v) (Bang et al., 2003). During the current study, honeys were diluted to 5 % (v/v) and lime honey was the one with the highest level of hydrogen peroxide formation with 67 mg/kg\*h. The different levels of H<sub>2</sub>O<sub>2</sub> between our study and the one of (Bang et al., 2003) could be due to different methods to detect hydrogen peroxide. Bang et al. (2003) detected hydrogen peroxide by measuring the release of oxygen after the treatment of pre-incubated honey solutions with catalase. Kwakman et al. (2011b)

measured hydrogen peroxide with the same method presented in this work and found similar levels of approximately 50 to 100 mg/kg\*2 h. Moreover the effective amount of hydrogen peroxide in honey depends on the presence of compounds which can decompose it. Thus, the enzyme catalase or reducing compounds can decrease hydrogen peroxide levels in honey (Hartford and Dowds, 1994). The slopes of the linearized dose-response curves do not reflect this unequal distribution of the bioactive compounds MGO and hydrogen peroxide in honey. Thus, the calculation of the amount of hydrogen peroxide and methylglyoxal which exert the same antibacterial activity (e.g. GD of 5) can give a more accurate picture of the impact of MGO and H<sub>2</sub>O<sub>2</sub> to the antibacterial effect of honey. Except *P. aeruginosa*, which was not inhibited by manuka honey, all other bacteria can be inhibited by MGO in honey-relevant concentrations. Even though most bacteria are more sensitive to hydrogen peroxide, in manuka honey MGO is the predominantly antibacterial compound, because of its higher concentrations compared to hydrogen peroxide. Figure 10 shows the growth delay which is caused by peroxide activity (lime honey) and non-peroxide activity (manuka honey) on *S. aureus*, *B. subtilis*, *E. coli* and *P. aeruginosa*.

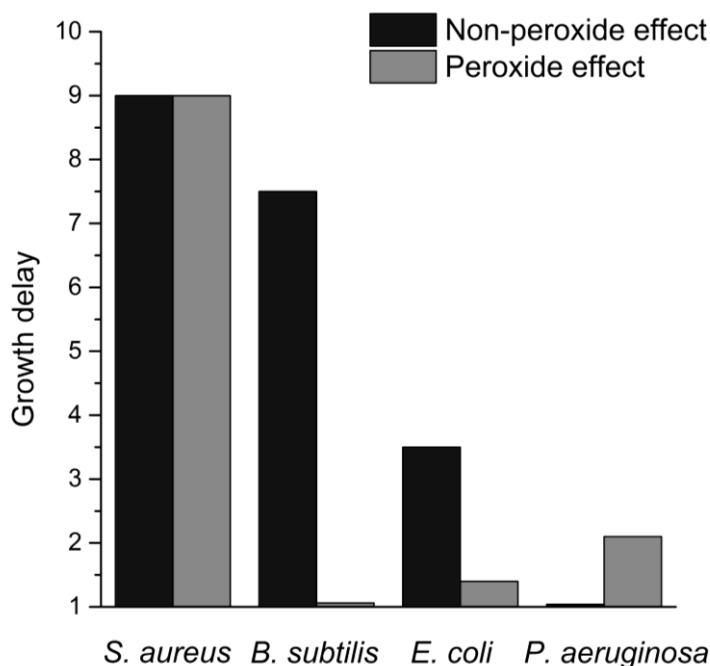


Figure 10: Antibacterial activity of manuka honey (non-peroxide effect) and lime honey (peroxide effect) on bacteria. Manuka honey contains MGO 488 mg/kg and lime honey contained H<sub>2</sub>O<sub>2</sub> 67 mg/kg\*h. Both honeys were diluted to 5 % (v/v) and incubated with bacteria for 18 h at 37 °C. Growth delay of 9 indicates no growth during the entire incubation time.

Taken together, both MGO and hydrogen peroxide can have a bacteriostatic effect on bacterial growth. The sensitivity of the bacteria towards the antibacterial compounds differ widely and it was found that most bacteria are more sensitive to hydrogen peroxide. However,

the amount of antibacterial compounds in manuka honey is higher than in non-manuka honey, what enhances the potential effect of manuka honey.

#### 1.5.2.5. Comparison of bacteriostatic versus bactericidal effect

The MIC (minimum inhibitory concentration) test, which is used to determine the antibacterial activity of bioactive compounds, cannot distinguish between bacteriostatic or bactericidal mode of action. Until now, there is no information about the potential bactericidal effect of honey compounds on bacteria. Thus, the assay developed in this project was used to study the bactericidal effect of hydrogen peroxide and methylglyoxal in honey. Therefore, bacterial solutions incubated with artificial honey containing GOX or with manuka honey, which did not show any bacterial growth after 16 h of incubation, were plated on fresh nutrient agar and further incubated for 24 h at 37 °C (see 1.4.10). Thereby, the concentration of the inhibitory compounds was diluted and cells which were resting but were not dead, can proliferate again. For *S. aureus* and *B. subtilis* incubated with MGO in manuka honey the concentrations without visible growth after 16 h incubation were  $\geq 510\text{mg/kg}$ , whereas with hydrogen peroxide only *S. aureus* growth was inhibited completely above concentrations of  $16.6\text{ mg/kg} \cdot \text{h}$ . The minimum bactericidal concentration (MBC) is the amount of test compound incubated with bacteria which prevented re-proliferation in fresh nutrient media completely. The maximum MGO concentration of manuka honey present in the assay was  $690\text{ mg/kg}$  whereas the maximum  $\text{H}_2\text{O}_2$  concentration was  $114\text{ mg/kg} \cdot \text{h}$  (artificial honey with added glucose oxidase). Table 16 shows the MBC values for *S. aureus* and *B. subtilis*. The growth of *E. coli* and *P. aeruginosa* was neither inhibited completely with MGO nor hydrogen peroxide over the entire incubation time. Thus, the effect of MGO and hydrogen peroxide on the two gram-negative bacteria can be described as bacteriostatic in honey-relevant concentrations.

Table 16: Bactericidal concentrations (MBC) of MGO in manuka honey and hydrogen peroxide in artificial honey with GOX on *S. aureus* and *B. subtilis* (one determination per sample)

Bacterium	<i>S. aureus</i>	<i>B. subtilis</i>
Hydrogen peroxide (mg/kg*h)	89	-
Methylglyoxal (mg/kg)	-	657

Although *S. aureus* growth was completely inhibited by MGO in manuka honey during 16 h of incubation, after plating the cells on fresh media they proliferated again. Thus, MGO in

manuka honey affects *S. aureus* bacteriostatically. In contrast, *B. subtilis* was not able to proliferate in fresh media after prior incubation in 5 % (v/v) manuka honey with MGO 657 mg/kg. Thus, the effect of MGO in manuka honey can be bactericidal for *B. subtilis* in certain concentrations. Figure 11 shows the nutrient agar plates incubated with *S. aureus* and *B. subtilis* which were previously incubated with MGO in manuka honey for 16 h.

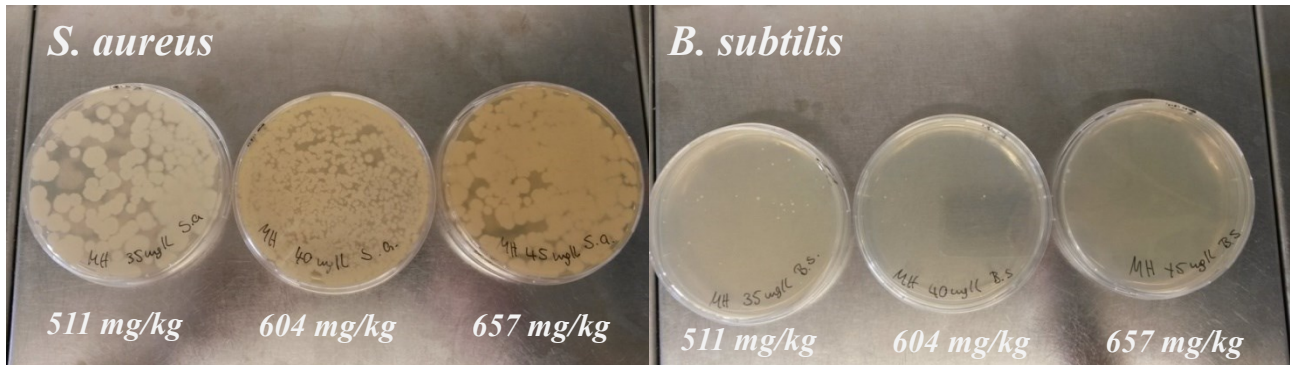


Figure 11: Proliferation of *S. aureus* and *B. subtilis* after plating on fresh media after 16 h incubation with MGO in manuka honey. Plates were incubated for 24 h at 37 °C.

The plates incubated with *B. subtilis* show remarkably less growth compared to the plates with *S. aureus*. Although *S. aureus* and *B. subtilis* showed almost the same growth delay by MGO in manuka honey (both linearized dose-response curves had a slope of 0.004), a bactericidal effect was only detectable for *B. subtilis*. This again showed the different sensitivity of the bacteria species towards the inhibitory compounds of honey, which suggests differences in the mode of action of MGO on bacteria. Hydrogen peroxide only had a bactericidal effect on *S. aureus* at a concentration of 89 mg/kg\*h. This concentration is higher than the one measured for lime honey as an example for a peroxide-rich honey (67 mg/kg\*h). Thus, it is unlikely that commercial honeys with peroxide activity are able to kill *S. aureus* cells completely.

Although bioactive compounds in honey were only able to kill bacteria to a very limited extent, this does not necessarily mean that their antibacterial activity is weak. The antibacterial treatment with bacteriostatic compounds is considered to be equally effective compared to bactericidal agents, when patients have uncomplicated infections and a healthy immune system (Pankey and Sabath, 2004). Most bacteriostatic agents win some time for the host defence system and enable the body to fight infections properly. Thus, manuka honey with MGO and honey with peroxide activity can present an alternative treatment for bacterial

infections, especially in times of increasing number of antibiotic-resistant bacteria (Alanis, 2005).

### 1.5.3. The antibacterial effect of manuka honey with cyclodextrin

The cyclic oligo saccharide  $\alpha$ -cyclodextrin can potentially form inclusion complexes with manuka honey compounds and thus increase its bioactive properties. Therefore, it was tested whether the commercial product “Manuka Honey with CycloPower™” (CP) has an increased antibacterial activity compared to manuka honey. The bacterial assay was performed according to section 1.4.7. To compare the antibacterial effect of MGO in CP to MGO in manuka honey, CP was mixed with artificial honey to obtain standardized 5 % (v/v) sugar solutions (referring to honey sugars). MGO in CP showed no increase of the antibacterial effect of manuka honey on *S. aureus*, *E. coli* and *P. aeruginosa* (data not shown). However, *B. subtilis* showed a significantly stronger growth delay when treated with CP compared to manuka honey (see Figure 12).

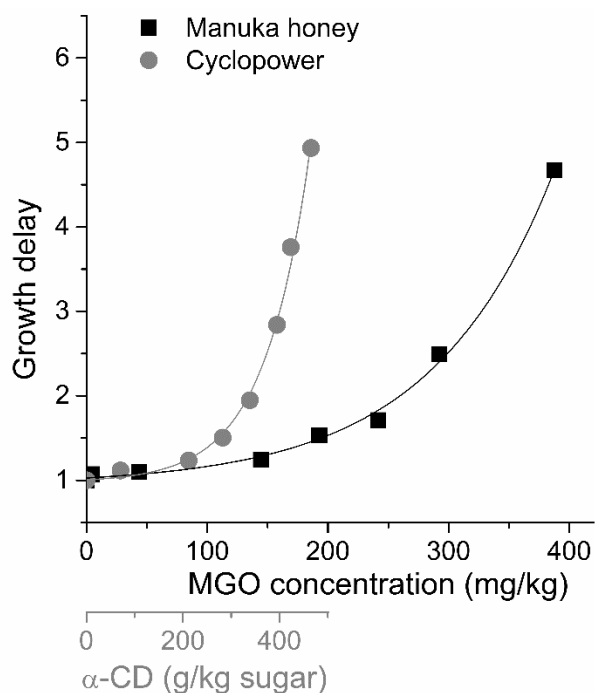


Figure 12: Dose-response curve of *B. subtilis* incubated with manuka honey and cyclopower. GD was referenced to 5 % (v/v) AH solution.

To check whether the increased activity of MGO in CP is based on an additive effect of the antibacterial effect of  $\alpha$ -cyclodextrin (CD) and manuka honey or on a synergistic effect of both compounds, a dose-response curve for CD (with 5 % (v/v) artificial honey) was

measured (see Figure 13).  $\alpha$ -Cyclodextrin alone does not have an antibacterial effect on most of the tested bacteria. This is in accordance with Zhang et al. (2008) and Swift et al. (2014), who also found no significant inhibition of *E. coli* and *S. aureus* by  $\alpha$ -cyclodextrin. Only *B. subtilis* was sensitive to  $\alpha$ -cyclodextrin in the concentration present in cyclopower. Since  $\alpha$ -cyclodextrin alone inhibits *B. subtilis* growth, it can be assumed that the inhibition of *B. subtilis* with cyclopower is not only due to methylglyoxal but also  $\alpha$ -cyclodextrin itself.

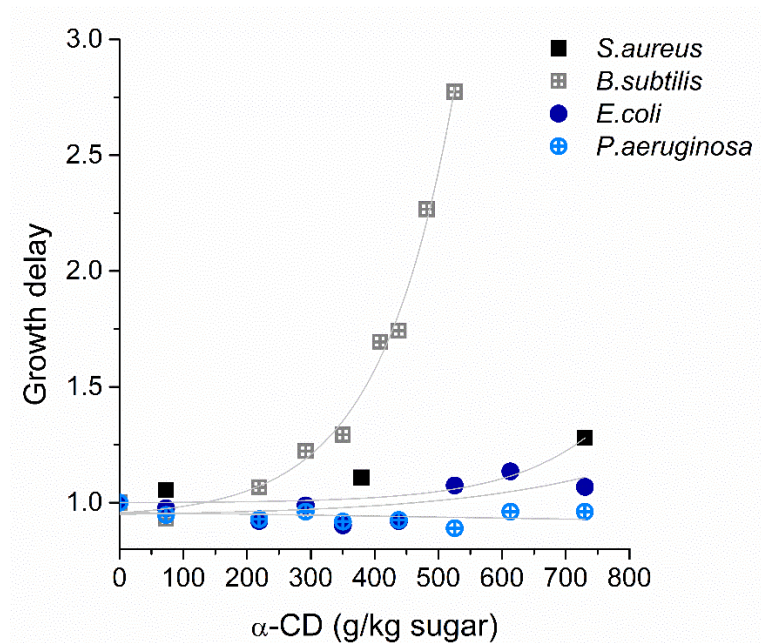


Figure 13: Dose-response curve of  $\alpha$ -cyclodextrin towards *S. aureus*, *B. subtilis*, *E. coli* and *P. aeruginosa* GD was referenced to 5 % (v/v) AH solution.

The growth delay caused by MGO in manuka honey and  $\alpha$ -cyclodextrin was determined individually and summed up (orange curve, Figure 14). The addition of the effect of MGO and  $\alpha$ -cyclodextrin did not fully explain the antibacterial effect caused by cyclopower on *B. subtilis*. This suggested that the antibacterial activity of manuka honey was synergistically enhanced by the complexation with  $\alpha$ -cyclodextrin. Zhang et al. (2008) were able to show, that  $\alpha$ -cyclodextrin can interact with certain protein-lipid complexes in the cell wall of *Bacillus* strains. The authors supposed that flotillin-like proteins form a complex with unknown lipid molecules present in the cell membranes of the strains and that the complex must be very important in the construction and stabilization of their structure. Similar complexes, which regulate biofilm formation are discussed by Vlamakis et al. (2013). Those complexes might be uniquely present in the membrane of *Bacillus* strains. The interaction of  $\alpha$ -cyclodextrin with these membrane microdomains might lead to a destabilization of the



bacteria membrane which eventually leads to lysis of the cells and a decrease of cell number. Thus, the synergistic effect of MGO and  $\alpha$ -cyclodextrin may be due to increased membrane permeability and therefore a facilitated effect of MGO on bacteria cells. As this effect is depending on the membrane structure of bacteria, the response of bacterial species to cyclopower can differ widely. To exert an antibacterial effect *in vivo*, the bioactive compound needs to interact with bacteria. If the bacteria are present in the gastrointestinal tract, the transit time of manuka honey is rather short. All honey compounds, especially sugars, are easily digestible and can be absorbed quickly. It was shown in earlier reports that  $\alpha$ -cyclodextrin itself is poorly digested and can slow down gastric emptying (Thompson, 1997; Gentilcore et al., 2011). Thus,  $\alpha$ -cyclodextrin may enhance the effect of MGO in manuka honey by increasing its interaction time with bacteria in the gastrointestinal tract. Nevertheless, further research is needed to elucidate the antibacterial effect of cyclopower on bacterial systems and to give more profound statements.

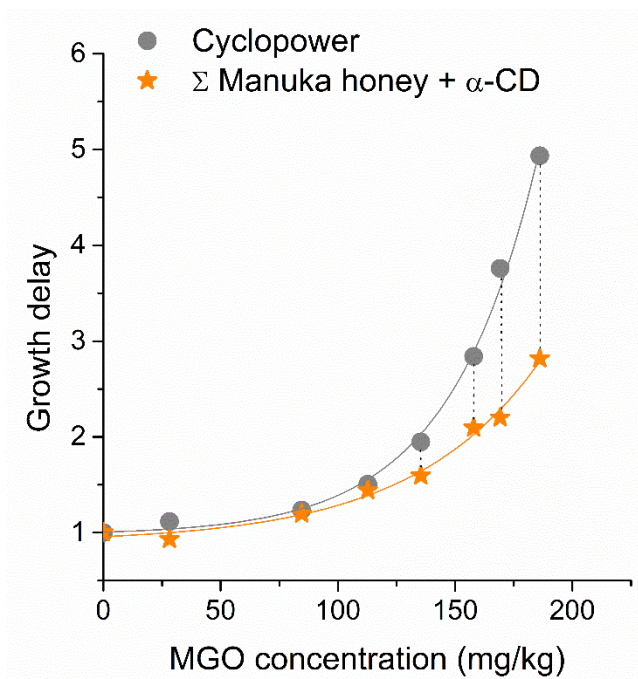


Figure 14: Dose-response curve for cyclopower and sum of growth delay caused by MGO in manuka honey and  $\alpha$ -cyclodextrin measured individually

#### 1.5.4. The structure of inclusion complexes of manuka honey and cyclodextrin

With the help of 2-D-NMR methods through-bond or through-space interactions of  $\alpha$ -CD and possible inclusion partners were analysed. The basis for this technique formed 1-D  $^1\text{H-NMR}$  spectroscopy. Thus, 1-D  $^1\text{H-NMR}$  spectra of  $\alpha$ -cyclodextrin, MGO and DHA were recorded and the signals were assigned to their corresponding protons (see Figure 15). In the  $^1\text{H-NMR}$  spectrum, all chemically different protons give a signal. For example,  $\alpha$ -cyclodextrin consists of six 1,4- $\alpha$ -glycosidically-linked D-glucose units, which form a symmetric cyclic molecule leading to the same chemical environment for the protons of each glucose unit. Therefore, the multiplet signals describe the  $-\text{CH}_2$  or  $-\text{CH}$  groups in each of the glucose units. The peak pattern (duplets and triplets) of  $\alpha$ -cyclodextrin is due to couplings between the adjacent protons. Generally the higher the magnetic shielding, which is caused by electron density, the lower the chemical shift. The shielding effect depends on the electronegativity of the adjacent atoms, whereby the following applies: the more electronegative neighboring groups, the less shielding, the higher the chemical shift.

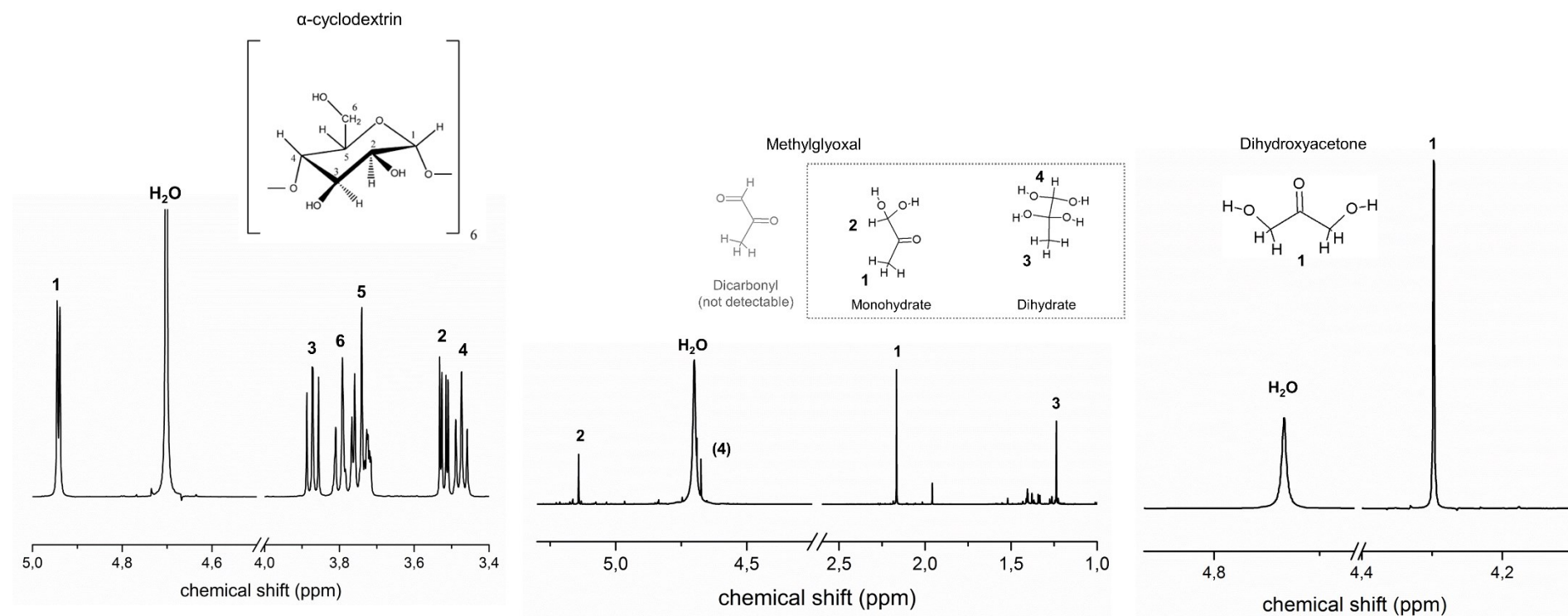


Figure 15: Molecular structures and  $^1\text{H-NMR}$  spectra of  $\alpha$ -cyclodextrin, methylglyoxal and dihydroxyacetone with proton assignment

For methylglyoxal, two structures were detected. In aqueous solutions, the dicarbonyl structure was not present, but the mono- or dihydrate forms dominated. The singlet resonances at 1.237 and 2.165 ppm corresponded to the methyl hydrogen atoms in methylglyoxal di- and monohydrate, respectively. The resonances at 4.674 and 5.141 ppm were assigned to the alkyl protons, although the alkyl proton signal of the methylglyoxal dihydrate was not observed well because of the overlapping water signal. The use of presaturation for water suppression did not significantly enhance signal separation. The resonance signal at 1.9 ppm could be acetic acid as a contamination in the methylglyoxal standard. For dihydroxyacetone, the four alkyl protons had all the same chemical environment, thus there was only one signal at 4.297 ppm present.

After the identification of MGO, DHA and  $\alpha$ -CD signals, the commercial product cyclopower was analyzed. Cyclopower contains manuka honey and  $\alpha$ -cyclodextrin in a ratio of 45 to 55 %, respectively. When cyclopower contains a manuka honey with MGO (500 mg/kg) and DHA (1000 mg/kg), this results in a molar ratio of MGO:CD of 1:190 and DHA:CD of 1:110. Figure 16 shows the corresponding  $^1\text{H}$ -NMR spectrum.

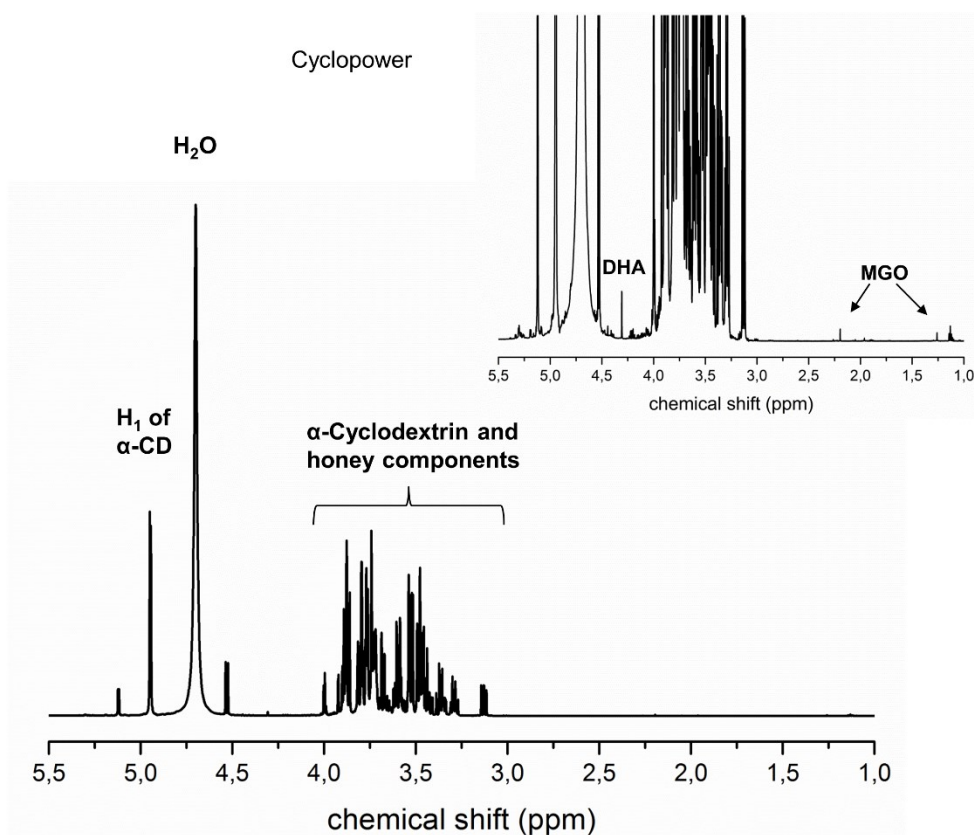


Figure 16:  $^1\text{H}$ -NMR spectra of cyclopower, upper right corner: zoom spectrum of cyclopower with MGO and DHA signal assignment

The large excess of  $\alpha$ -cyclodextrin compared to the MGO and DHA content of the honey led to a huge  $\alpha$ -CD signal, whereas MGO and DHA gave only very small signals. Both compounds were only visible in the zoom spectrum. These intensity differences made 2-D NMR studies, which were necessary to visualize interactions between  $\alpha$ -CD and MGO and DHA, impossible with this complex. Thus, model complexes were prepared, which contained MGO or DHA and  $\alpha$ -CD, but no monosaccharides in an equimolar ratio (see 1.4.12). The model complex which contained pure MGO and  $\alpha$ -CD was named MGO-CD and the complex formed of DHA and  $\alpha$ -CD was called DHA-CD. Figure 17 compares the spectra of MGO-CD and DHA-CD. In both spectra the intensity of the resonances of  $\alpha$ -CD as well as the signals of MGO and DHA were about the same size. The following 2-D NMR studies for investigating the interactions of  $\alpha$ -CD with MGO and DHA were recorded with these model complexes.

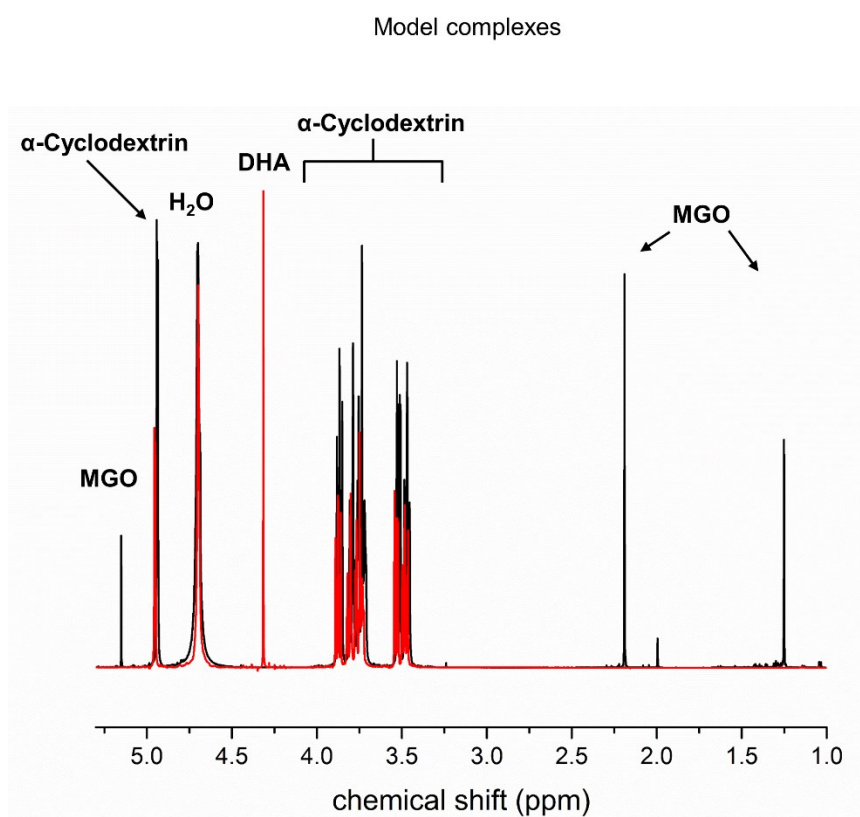


Figure 17: <sup>1</sup>H-NMR spectra of the complex MGO-CD (black) and DHA-CD (red) with proton assignment

The applied 2-D-NMR methods aimed to visualize through-bond or through-space interactions of  $\alpha$ -CD and possible inclusion partners. Through-bond correlations can be analyzed with homonuclear proton correlation spectroscopy (COSY, used for indicating correlation with

coupled protons), heteronuclear single-quantum correlation spectroscopy (HSQC, detects correlations between nuclei of two different types which are separated by one bond) and heteronuclear multiple-bond correlation spectroscopy (HMBC, visualizes interactions over longer ranges of about 2–4 bonds). The results for the MGO-CD and DHA-CD complexes showed that there is no covalent bond between MGO or DHA and  $\alpha$ -CD. With the help of rotating frame nuclear Overhauser effect spectroscopy (ROESY), non-covalent, through-space interactions of the complexes were examined.

Figure 18 shows the ROESY-NMR spectrum of the MGO-CD model complex. When protons interact through-space, it becomes visible in the ROESY plot with a cross peak. The cross-peaks of MGO protons with protons of  $\alpha$ -CD are marked with a circle. Concerning MGO, the methyl protons and the alkyl protons of the monohydrate form interacted with the protons number 3 and 5 of cyclodextrin (see Figure 15 for proton assignment). According to the literature, the protons number H-3 and H-5 are located inside of the  $\alpha$ -CD cone, whereas all other protons (H-1, H-2, H-4 and H-6) are located at the outside of the cage-like structure (Anselmi et al., 2008; Salústio et al., 2009). Therefore interactions with these protons were of special interest for revealing  $\alpha$ -CD inclusion complexes. The proposed structure of  $\alpha$ -CD is shown in Figure 19. According to the ROESY spectrum the alkyl protons of MGO monohydrate interacted slightly stronger with H-3 than H-5, whereas the methyl protons interacted with H-3 and H-5 in the same way. This might indicate that the methyl group of MGO was able to penetrate into the cone of  $\alpha$ -CD and interacted with the H-5 at the narrow end of the cone. The outside protons (H-1, H-2, H-4 and H-6) showed no interaction with the MGO protons. Moreover, no interaction of the MGO dihydrate protons and  $\alpha$ -CD was detectable.

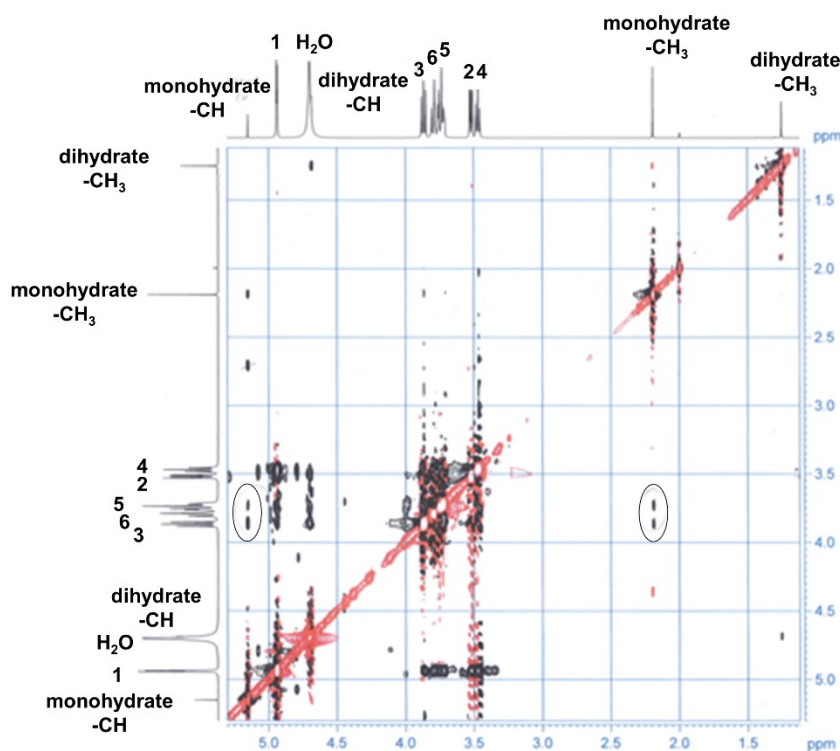


Figure 18: ROESY-NMR spectrum of model complex containing MGO and  $\alpha$ -CD in equimolar ratio, protons are assigned to MGO and  $\alpha$ -CD (protons 1-6), cross peaks of MGO and  $\alpha$ -CD are marked with black circle

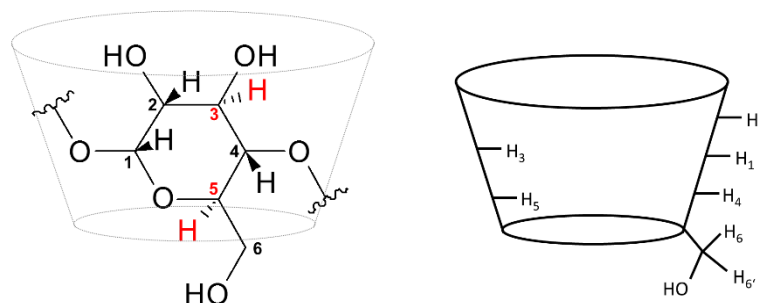


Figure 19: Structures of  $\alpha$ -cyclodextrin and spatial orientation of protons

Moreover, the model complex which contained DHA and  $\alpha$ -CD in a 1:1 ratio was studied with ROESY-NMR. Again, there were no through-bond but through-space correlations between DHA and  $\alpha$ -CD visible. Since DHA is even more hydrophilic than MGO, a strong interaction between the cone of  $\alpha$ -CD and DHA was not expected. The number of recorded spectra was the same for the measurement of the MGO-CD and the DHA-CD complex. According to the ROESY-NMR results, the alkyl protons of DHA interacted with the  $\alpha$ -CD proton H-3 (see Figure 20). Since proton H-3 is located at the wider end of the  $\alpha$ -CD cone and

there were no interactions with proton H-5 (narrow end) of  $\alpha$ -CD and DHA visible, it is quite unlikely that the hydroxyl or the keto group of DHA penetrated into  $\alpha$ -CD because of the cone's hydrophobic character. In comparison to the interactions between MGO and  $\alpha$ -CD, the interactions of DHA and the inner protons of  $\alpha$ -CD appeared weaker.

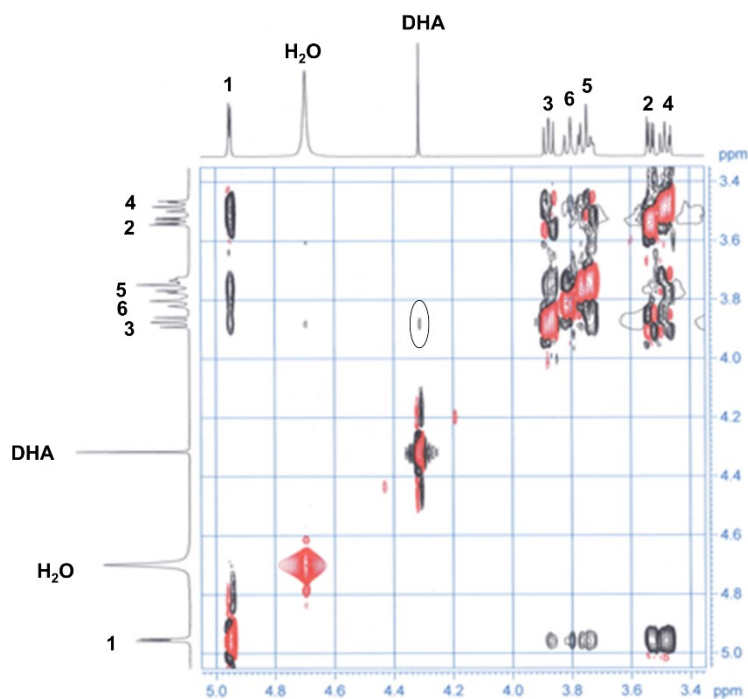


Figure 20: ROESY-NMR spectrum of model complex containing DHA and  $\alpha$ -CD in equimolar ratio, protons are assigned to DHA and  $\alpha$ -CD (protons 1-6), cross peak of DHA and  $\alpha$ -CD is marked with black circle

The experiments were performed with model complexes, which do not have the same composition as the commercial product cyclopower. To get closer to the conditions which are present in the commercial product, a model complex, which contained MGO, DHA and  $\alpha$ -CD in a 1:2:1 ratio was prepared (see 1.4.12). Figure 21 shows the ROESY spectrum of this model complex. Interestingly, when both compounds MGO and DHA were present in the model complex, only MGO interacted clearly with  $\alpha$ -cyclodextrin. Again, only the monohydrate form of MGO showed interaction with  $\alpha$ -CD. The methyl group interacted with both inner protons of  $\alpha$ -CD (H-3 and H-5), whereas the alkyl group only interacted with the proton H-3, which is located at the wider part of the  $\alpha$ -CD cone. For the alkyl protons of DHA, there appeared only a negligible cross peak with  $\alpha$ -CD proton H-3 (not marked with circle), which indicated very weak interactions between  $\alpha$ -CD and DHA in the presence of competitive MGO.



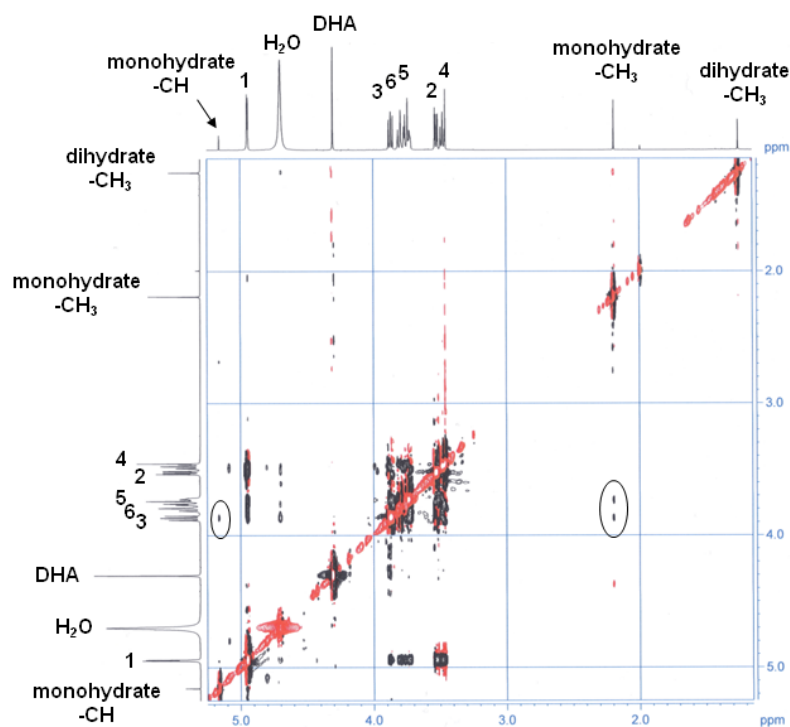


Figure 21: ROESY-NMR spectrum of model complex containing MGO, DHA and  $\alpha$ -CD in a 1:2:1 ratio, protons are assigned to DHA, MGO and  $\alpha$ -CD (protons 1-6), cross peaks of MGO and  $\alpha$ -CD are marked with black circle

A possible reason for the weaker interactions of MGO and DHA with  $\alpha$ -CD in the mixture compared to their complexes formed with  $\alpha$ -CD alone, could be the interactions between MGO and DHA itself. ROESY-NMR only allows visualizing proton interactions, but MGO and DHA probably interacted via hydrogen bridges, which were not visible in the presented spectra. The MGO-DHA interaction led to a more complex and hydrophilic nature of the compounds, which decreased the single interactions of each compound. Apparently, when MGO and DHA were present in the model complex, MGO interacted preferentially with  $\alpha$ -CD. Based on these results, Figure 22 shows proposed spatial structures of the model complexes. The proposed structure A (MGO inclusion complex) occurs more likely, whereas structure B (DHA inclusion complex) and C (MGO and DHA inclusion complex) are rather unlikely formed.

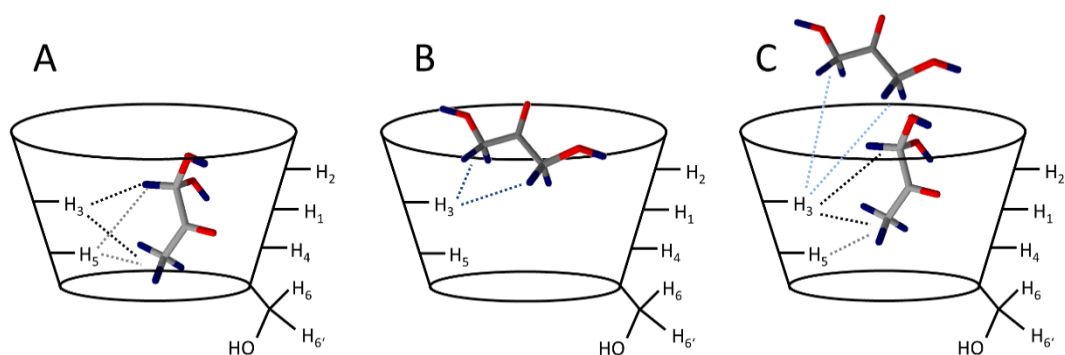


Figure 22: Proposed 2-D models structures of inclusion complexes formed by  $\alpha$ -CD and MGO (A),  $\alpha$ -CD and DHA (B) and  $\alpha$ -CD, MGO and DHA (C)

Cyclodextrins are cyclic products of enzymatic starch degradation. Alpha-cyclodextrin consists of six  $\alpha$ -D-glucose units. To assess if the interactions recorded by ROESY-NMR are specific for cyclodextrin, model complexes which contained MGO, DHA and glucose as well as MGO, DHA and starch were prepared (see 1.4.12). There was no interaction between the protons of starch or glucose and MGO and DHA detectable (see Annex-Figure 1 and Annex-Figure 2 for ROESY-NMR data). That means that neither glucose nor starch interacted with MGO or DHA in a manner seen with  $\alpha$ -cyclodextrin. Thus, the interactions of  $\alpha$ -CD with MGO and DHA were specific and proved the formation of inclusion complexes. Moreover, the strength of the MGO and DHA inclusion complex should be compared to other  $\alpha$ -CD complexes. In the literature, the complex of 1-propanol (PrOH) and  $\alpha$ -CD was described as very stable (Buvari et al., 1983; Funasaki et al., 2002). Thus, a complex of 1-propanol and  $\alpha$ -CD in a 2:1 ratio was prepared and the ROESY-NMR measurement performed according to 1.4.12. The number of recorded spectra was the same for the measurement of the PrOH-CD and the MGO-/DHA-CD complexes. Figure 23 shows the corresponding ROESY spectrum and a zoom part of the spectrum.

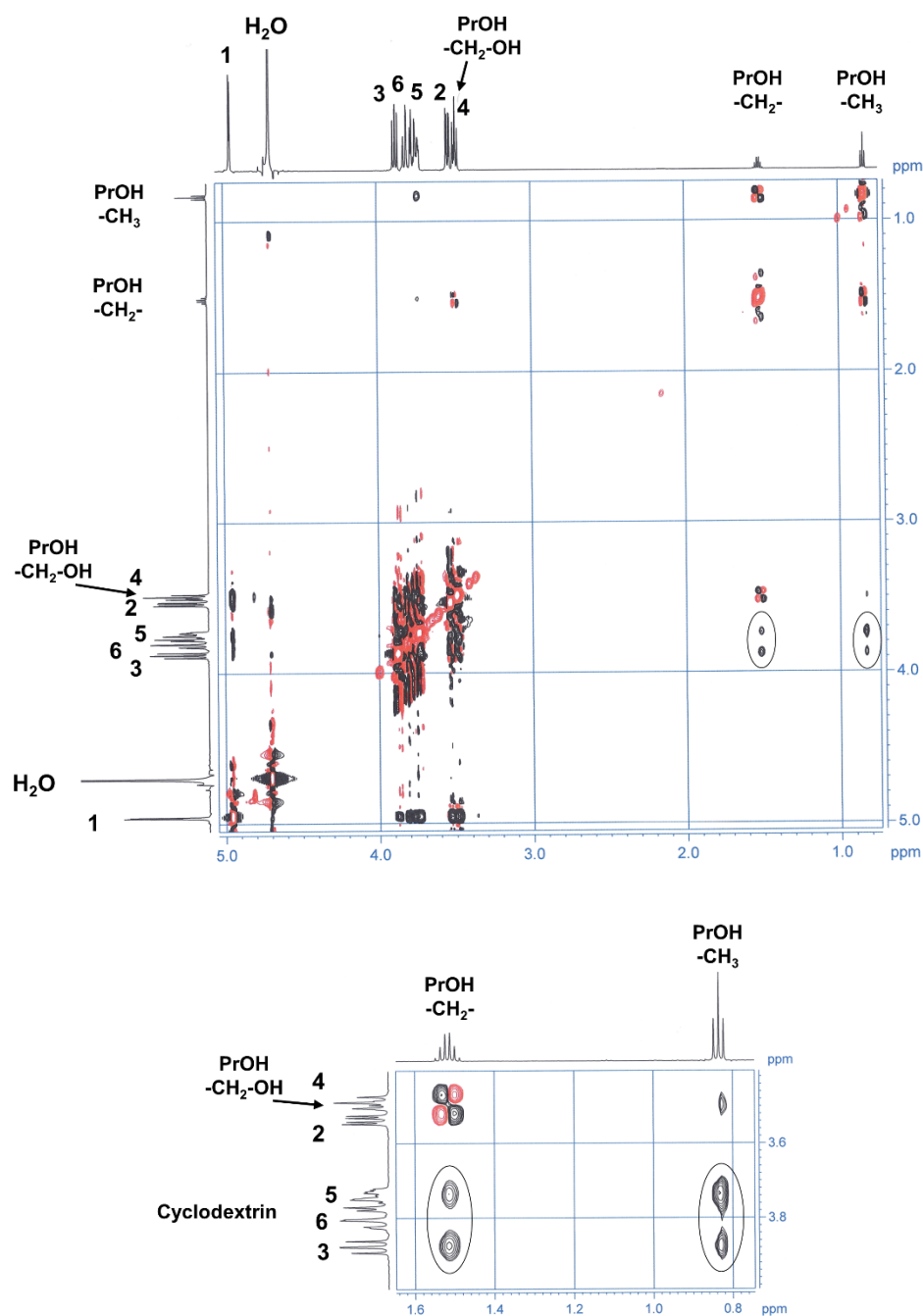


Figure 23: At top: ROESY-NMR spectrum of model complex containing 1-propanol (PrOH) and  $\alpha$ -CD in a 2:1 ratio, protons are assigned to 1-propanol and  $\alpha$ -CD (protons 1-6), cross peaks of 1-propanol and  $\alpha$ -CD are marked with black circle; at bottom: zoomed ROESY-NMR spectrum of PrOH/  $\alpha$ -CD complex

It becomes visible that the alkyl group of 1-propanol interacted stronger with the  $\alpha$ -CD proton H-3 than with H-5. For the methyl group the reversed effect was observed. Based on these results, the alkyl chain of 1-propanol entered the  $\alpha$ -CD cone deeply and formed a stable guest-host complex with  $\alpha$ -CD. Compared to MGO, the interactions with  $\alpha$ -CD appeared stronger.

Methylglyoxal has no molecule part which is as hydrophobic as the alkyl group of 1-propanol. Therefore the interactions with the inside of the hydrophobic cone were weaker. Weaker interactions are visualized by ROESY-NMR with the intensity and the size of the area of the cross peaks. The comparison of Figure 18 and Figure 23 shows, that the cross peaks of the MGO/ $\alpha$ -CD complex were smaller than the cross peaks of the 1-propanol/ $\alpha$ -CD complex. To compare MGO to a molecule with a more similar structure, a model complex containing hydroxyacetone (HA) and  $\alpha$ -CD was prepared (see 1.4.12). Hydroxyacetone differs only in one position from MGO, by carrying a hydroxyl instead of an aldehyd group. Therefore hydroxyacetone is slightly less hydrophobic than MGO. Figure 24 shows the ROESY-NMR spectrum of the HA/ $\alpha$ -CD complex. Only a very small cross peak between the  $\alpha$ -CD proton H-5 and the methyl group of hydroxyacetone was detectable.

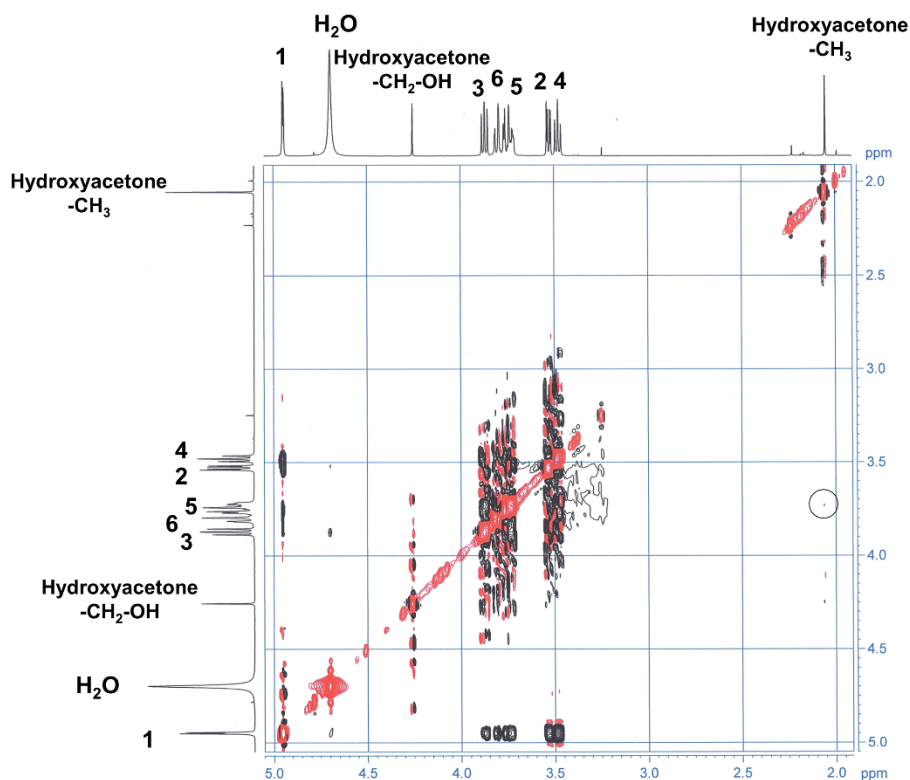
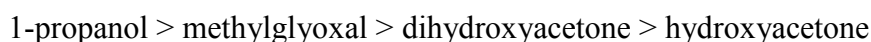


Figure 24: ROESY-NMR spectrum of model complex containing hydroxyacetone (HA) and  $\alpha$ -CD in a 2:1 ratio, protons are assigned to hydroxyacetone and  $\alpha$ -CD (protons 1-6), cross peak of hydroxyacetone and  $\alpha$ -CD are marked with black circle

In conclusion, the strength of interaction in  $\alpha$ -CD complexes can be ranked as follows:



Until now, it is not clear which influence these interactions have on the stability, bioavailability and the bioactive effect of MGO and DHA. Overall, the observed interactions were rather weak and are expected to have only a limited influence. Nevertheless, in the commercial cyclopower product,  $\alpha$ -cyclodextrin is present in an excess of factor 190 or 110 concerning MGO and DHA, respectively. The huge excess of host to guest molecules makes an inclusion of MGO or DHA more likely. However, honey contains also other compounds, like polyphenols or peptides, which could interact competitively with  $\alpha$ -cyclodextrin and limit its ability to complex MGO. During the antibacterial *in vitro* studies, no enhanced effect of cyclopower compared to manuka honey was found for most of the tested bacteria (see 1.5.3). However, the gram-positive bacterium *B. subtilis* showed an increased sensitivity towards manuka honey in the presence of  $\alpha$ -cyclodextrin. Swift et al. (2014) suggest that the improved antibacterial activity of cyclopower may be a result of a slow release of antimicrobial components to maintain a bacteriostatic concentration over an extended time period. The authors also suggest that  $\alpha$ -cyclodextrin may be able to deliver antimicrobial components to the bacterium allowing more efficient killing. Based on the results of the weak molecular interactions between MGO and  $\alpha$ -cyclodextrin, an enhanced effect of manuka honey encapsulated with  $\alpha$ -cyclodextrin may not be caused by inclusion reactions but could be due to synergistic effects. Further research is needed to clarify the influence of  $\alpha$ -cyclodextrin complexation of manuka honey on its effect and bioavailability.

#### 1.5.5. Influence of manuka honey on urease activity

Although manuka honey is known for its antibacterial activity for a long time, only limited knowledge about the mechanism of inhibition with MGO exists. Possible targets for the inhibition of bacteria are enzymes which are relevant for fundamental metabolic processes. The current study focused on the enzyme urease, which is present in the bacterium *Helicobacter pylori*. The gram-negative bacterium *H. pylori* colonizes the human stomach and causes chronic inflammation or gastric ulcers. The enzyme urease is an important virulence factor of *Helicobacter pylori*. It catalyzes the reaction of urea to carbon dioxide and ammonia, which neutralizes the acidic environment of the stomach. This reaction enables bacteria to adapt to an acidic environment, which normally prevents bacterial growth. It was shown that manuka honey inhibits *H. pylori* growth *in-vitro* (Al Somal et al., 1994; Keenan et al., 2010). The inhibition of *H. pylori* may be due to the inhibition of urease. An inhibition of the enzyme could be a possible cause for the decreased growth of *H. pylori* in the presence of

manuka honey. Therefore, the aim of this study was to characterize the effect of the compounds MGO and DHA and commercial honeys, including manuka and non-manuka varieties, on urease. Urease from jack bean (*Canavalia ensiformis*) was used for the studies. The study is supposed to contribute to the understanding of the mode of action of manuka honey on bacteria.

The results of this section are partly originating from the experimental work of master student Oliver Klemm and were published in his master thesis (Klemm, 2016) and in *Food Chemistry* (Rückriemen, Klemm, et al., 2017).

#### 1.5.5.1. Development of a photometric method to measure urease activity

There are several methods published in the literature to study urease activity in vitro. Tanaka et al. (2004) used an approach based on the pH increase caused by the continuous ammonia production to analyse the inhibitory effect of  $\alpha$ -hydroxyketones. Phenol red was used to indicate appropriate ammonia production through urease with a color change from yellow to pink. Sahin (2015) measured the urease inhibiting effect of dissolved honey samples and detected the ammonia production by using the indophenol method. During this reaction, known as Berthelot reaction, a phenol solution reacts with ammonia and sodium hypochlorite to form indophenol which can be detected photometrically at 625 nm. Both methods were tested in this study for their applicability. The Berthelot reaction in the presence of artificial honey was significantly suppressed (see Figure 25A). According to the results, the reducing sugars in honey, especially fructose, interfere with the oxidation of phenol to indophenol, thus leading to wrong positive inhibition values. Hence, the reducing nature of honey sugars makes this detection method unsuitable to study urease activity. Also the method used by Tanaka et al. (2004), based on the detection of ammonia via pH control with phenol red, was negatively influenced by reducing sugars (data not shown).

Therefore, the first aim of this study was to develop a new method for reliable quantitation of ammonia production by urease in vitro, which is not influenced by honey sugars. Ammonia reacts with ninhydrin to form a purple dye, called Ruhemann purple (Ruhemann, 1910). Based on this knowledge, urea and urease with or without inhibitors were incubated and the resulting ammonia was separated via ion exchange chromatography and detected via post-column derivatization with ninhydrin at 570 nm. The chromatographically quantitated amount of ammonia was depending on the presence or absence of an inhibitor (see Figure 26).

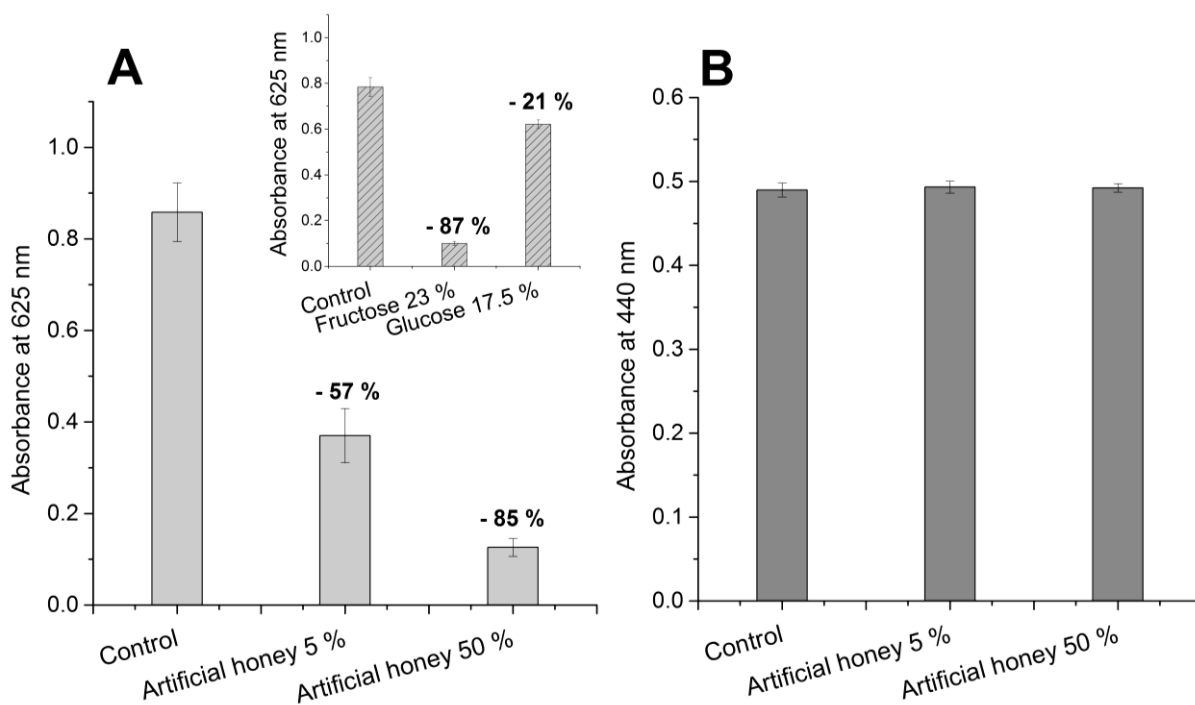


Figure 25: (A) Berthelot reaction in the presence of water (control) or artificial honey after 30 min incubation time with 280 mM ammonia, zoom figure: Berthelot reaction in the presence of water (control) or fructose and glucose after 30 min incubation time with 280 mM ammonia; (B) Reaction of ammonia with ninhydrin in the presence of water (control) or artificial honey after 30 min incubation time with 270 mM ammonia

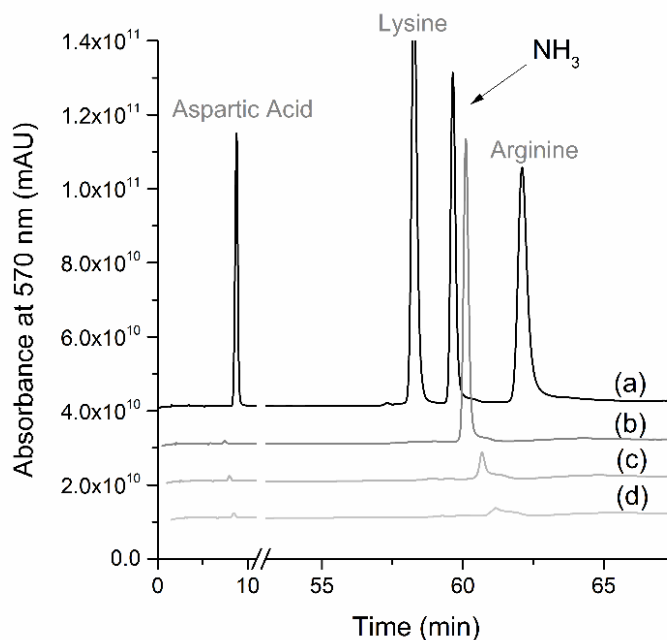


Figure 26: Amino acid analysis via ion-exchange chromatography and post-column ninhydrin detection (a) Amino acid standard solution with ammonia, (b) ammonia cleaved by urease from urea, (c) ammonia cleaved by urease from urea in the presence of 400  $\mu\text{M}$  acetohydroxamic acid, (d) blank solvent

It was concluded that ammonia quantitation via ninhydrin reaction was suitable to analyse urease activity. To quantitate urease activity with high sample throughput, the assay was optimized by using a photometric approach instead of chromatographic separation. Hence, urea and urease with or without inhibitor was incubated in a microtiter plate and ninhydrin was directly added to the reaction. The incubation resulted in the formation of a yellow coloured product, with an absorption maximum at 440 nm (see Figure 27A). The absorption maximum at this wavelength was unexpected, since Ruhemann purple detected via post-column derivatization of ammonia with ninhydrin absorbs at 570 nm. Nevertheless, the incubation of ammonia with ninhydrin in the microtiter plate resulted in the formation of a light-brown product with an absorption spectrum similar to the spectrum of the yellow product mentioned above. There was no increase at 440 nm when urease and urea were incubated without ninhydrin or ninhydrin was incubated with urease without urea. Moreover, the presence of artificial honey did not influence the reaction of ammonia with ninhydrin (see Figure 25B).

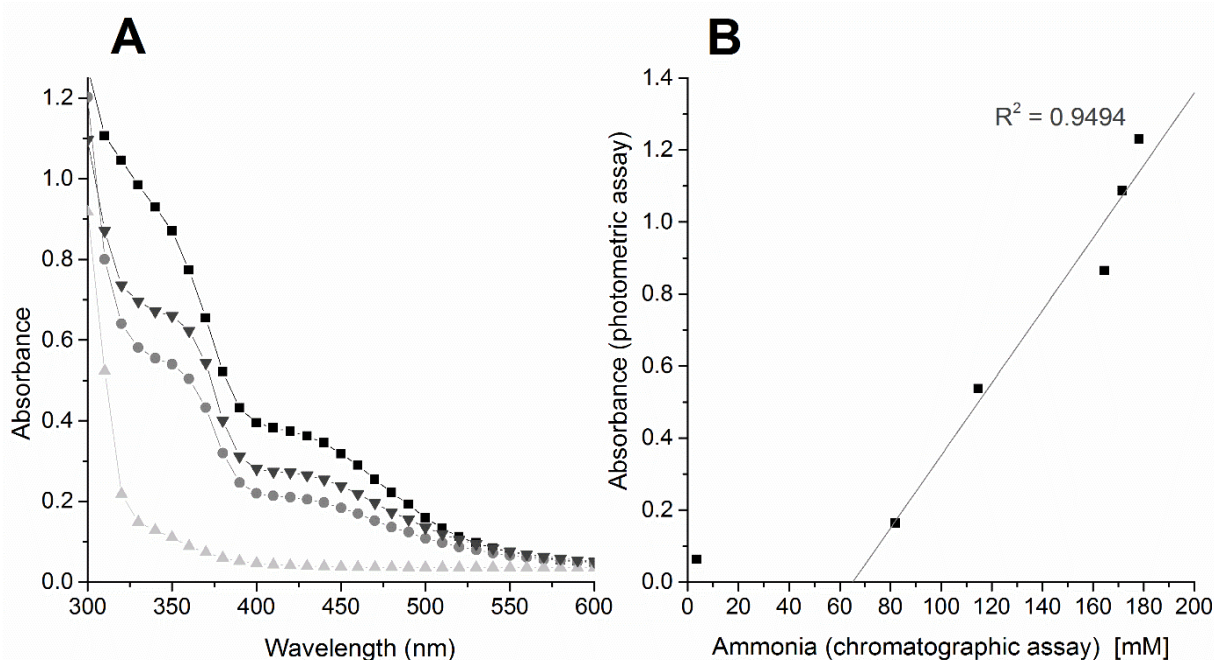


Figure 27: (A) UV spectra after incubation of urea with urease and ninhydrin (■), urea with ammonia and ninhydrin (●), ninhydrin and ammonia ("Ruhemann purple") (▼) and urea with ammonia (▲), (B) Correlation between ammonia, which was quantitated chromatographically and the UV absorbance of the photometric assay at 440 nm.

The absorbance measured using the photometric assay and the ammonia concentration as quantitated chromatographically correlated (see Figure 27B). That proves the hypothesis that the absorbance at 440 nm directly correlates with the ammonia concentration. The increase of



absorbance at 440 nm was therefore solely due to the formation of ammonia and subsequent reaction with ninhydrin. Moreover, Figure 27B illustrates the limit of detection of the microplate assay. At a concentration of 65 mM ammonia, no absorbance at 440 nm was detected. A minimum ammonia concentration of above 65 mM is necessary to detect ammonia photometrically. To ensure that a lack of absorption was not misinterpreted because of the limit of detection, the assay was incubated for 80 min. No increase of absorption after this time was observed, which was interpreted as complete inhibition of the enzyme. The inhibitor concentration, which inhibits 50 % of enzyme activity ( $IC_{50}$ ) was determined by plotting the percentage of urease inhibition against the logarithm of different concentrations of the inhibitor (see 1.4.13.2). The  $IC_{50}$  value of acetohydroxamic acid (AHA) was determined with the newly developed method to be 10.1  $\mu$ M (see Annex-Figure 3 for dose-response curves). In an earlier study an  $IC_{50}$  of 5  $\mu$ M after 3 h pre-incubation time (current assay: 2 h) was determined (Tanaka et al., 2004). This proves that the assay is suitable to determine inhibition constants similar to those previously published.

#### 1.5.5.2. Inhibition of urease activity

The aim of this study was to analyse urease inhibition by MGO and DHA and to evaluate the inhibitory potential of the carbonyl compounds in manuka honey. Therefore, aqueous solutions of MGO and DHA were studied for their urease inhibiting effect and the percentage of urease inhibition was plotted against the logarithm of the MGO and DHA concentrations. The fitting of the sigmoid dose-response curves resulted in  $IC_{50}$  values of  $2.8 \pm 0.2$  mM for MGO and  $5.0 \pm 0.1$  mM for DHA, what equals 202 mg/l and 450 mg/l, respectively (see Annex-Figure 3). Compared to other natural ingredients of food, which are known to inhibit urease like alkyl thiosulfates in garlic or onion juice ( $IC_{50}$  values between 1-27 mM)(Olech et al., 2014), MGO and DHA are moderate inhibitors. Jack bean urease contains 15 cysteine residues per subunit, whereby Cys-592 is crucial for its enzymatic activity. It was proposed, that the interaction of  $\alpha$ -hydroxyketones with the sulfhydryl group may be related to urease inhibition (Tanaka et al., 2004). Both MGO and DHA could interact with cysteine residues of urease and thereby decrease its enzymatic activity. Moreover, urease from jack bean contains 50 lysine and 37 arginine residues, which accounts for 6 % and 4 % of total amino acids, respectively (according to jack bean urease amino acid sequence, UniProt database entry P07374). Both amino acids are known to react quickly with MGO and form glycation products, which could lead to a decrease of urease activity. To check, whether enzyme activity is non-specifically affected by MGO or DHA, pepsin and angiotensin converting

enzyme (ACE) activity was measured in the presence of MGO and DHA (see 1.4.13.6). Both enzymes contain lysine (pepsin: 3 %, ACE: 4 %) and arginine (pepsin: 1 %, ACE: 6 %) residues (according to pepsin and ACE amino acid sequence, UniProt database entry P00791 and P12822, respectively). The hydrolytic activity of these physiologically relevant enzymes was not affected in the presence of MGO or DHA. The residual enzyme activity in the presence of 4 mM MGO or 7 mM DHA is presented in Figure 28.

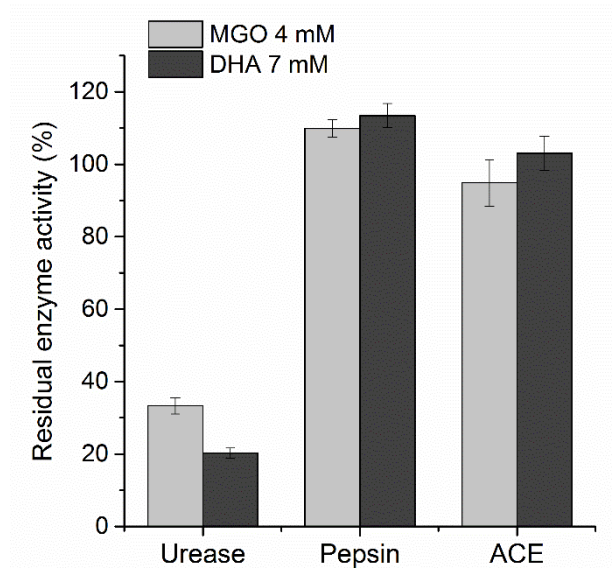


Figure 28: Residual enzyme activity of urease, pepsin and angiotensin-converting enzyme (ACE) in the presence of 4 mM MGO (grey) or 7 mM DHA (dark grey)

Similar results for pepsin and pancreatin were recently published (Daglia et al., 2013). The authors concluded that glycation of digestive enzymes may occur, but it does not influence the three-dimensional structure and thus enzyme activity. These “protecting effects” may be a consequence of protein evolution, since MGO is present in different food, which is commonly consumed and physiologically relevant enzymes got adapted to incubation with carbonyls. In contrast, the enzyme urease has no protective effect and is specifically inhibited by MGO and DHA. Besides naturally present MGO and DHA, manuka honey contains mainly fructose and glucose. The effect of a sugar matrix on the urease inhibition was studied by preparing an artificial honey. No influence on urease activity was observed until concentrations of 10.9 % (w/v) and above, with maximum inhibition of 32 % at 27.3 % (w/v) (see Figure 29A). This effect might be due to the osmotic activity of the sugars and the limited availability of water for the enzymatic reaction. Hence, in high concentrations, the effect of honey on urease is a combination of inhibition caused by sugars and other honey compounds, e.g. MGO and DHA,

whereas in small concentrations of honey, sugars do not influence the enzyme activity. To prove whether MGO and DHA also inhibit urease activity when present in manuka honey, four different manuka honeys with varying MGO and DHA contents were tested. Figure 29B shows the urease inhibition of manuka honeys in concentrations ranging between 0.04 and 27.3 % (w/v). The concentrations of MGO and DHA of the corresponding honeys are listed in Table 17. The results indicate that manuka honeys efficiently inhibit urease and that the effect is dose-dependent on the MGO and DHA content of the honeys. Figure 29A shows the inhibition of urease by non-manuka honeys, namely canola, lime and honeydew honey.

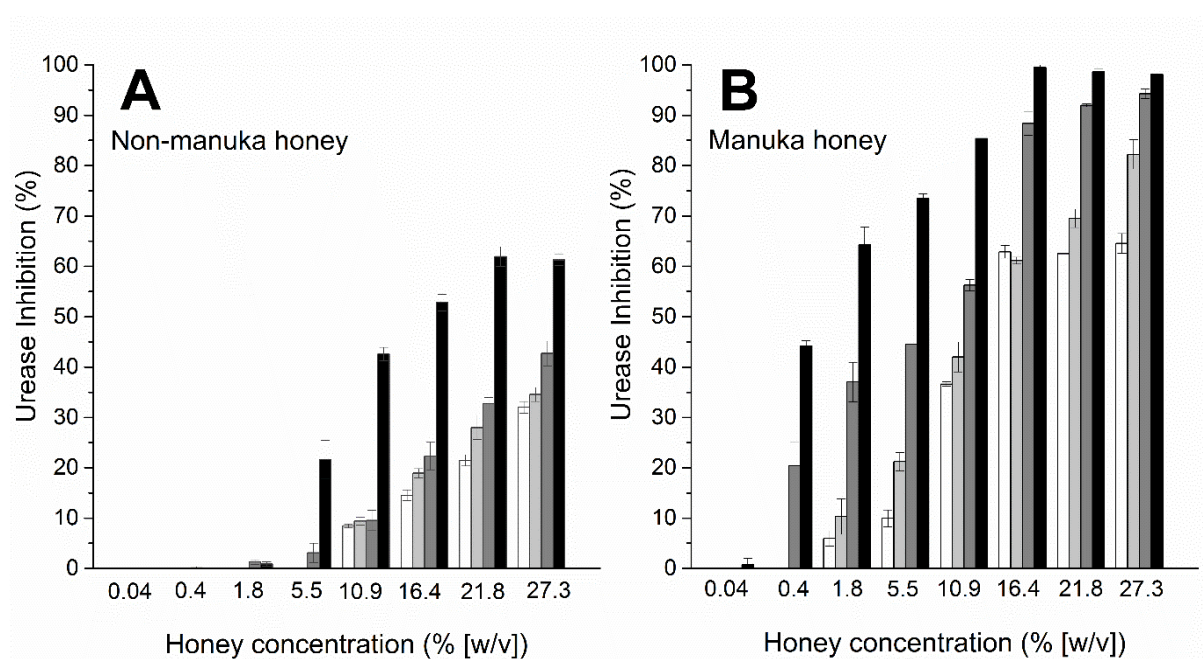


Figure 29: Urease inhibition caused by honeys. (A) Artificial honey (white) and non-manuka honeys, namely canola (light grey), lime (grey) and honeydew honey (black). (B) Manuka honeys, MH 1 (white), MH 2 (light grey), MH 3 (grey) and MH 4 (black). Results are expressed as mean values of three separate measurements and error bars indicate standard deviation.

Table 17: MGO and DHA concentrations of manuka honeys MH1 to MH 4. Results are expressed as mean values of three separate measurements.

Honey	MH 1	MH 2	MH 3	MH 4
<b>MGO (mg/kg)</b>	73	284	595	435
<b>DHA (mg/kg)</b>	350	722	1549	4342

Compared to manuka honeys, canola and lime honey showed significantly lower inhibitory activity on urease. This can be explained by the absence of MGO and DHA in these honeys (concentrations below 5 mg/kg). The inhibitory effect of the non-manuka honeys is mainly due to the effect of the sugars. A 27.3 % (w/v) solution of artificial honey resulted in 32 % inhibition of urease. For canola honey in the same concentration, 34 % and for lime honey 43 % urease inhibition was observed. The honeydew honey showed a stronger effect compared to the other honeys with 62 % inhibition at 27.3 % honey (w/v). Honeydew honeys are known to be rich in phenolic compounds originating from the plant phloem which is absorbed and excreted by the insects. These compounds may be responsible for the increased inhibitory effect of honeydew honey. Earlier reports already showed that honeydew honeys cause significantly stronger urease inhibition than other monofloral honeys (Sahin, 2015). This was confirmed by the results of the current study. In contrast, a 5.5 % (w/v) solution of manuka honey MH 3 inhibited around 50 % of the enzyme. This solution contained 33 mg/l MGO and 85 mg/l DHA. An aqueous solution of MGO and DHA in the same concentrations was prepared to study, if this effect found for honey MH 3 is solely due to these compounds. Figure 30 compares the inhibition of manuka honey MH 3 (S4) and the aqueous MGO and DHA sample (S3). Both solutions inhibited 50 % of the enzyme activity, thus demonstrating that the inhibition of manuka honey is exclusively caused by the effect of MGO and DHA. To test whether this inhibition is specific for manuka honey, MGO and DHA were artificially added to canola honey in concentrations similar to MH 3 (S2). After addition of MGO and DHA, the inhibitory effect of canola honey was higher than canola honey alone (S1), but not as strong as caused by manuka honey MH 3.

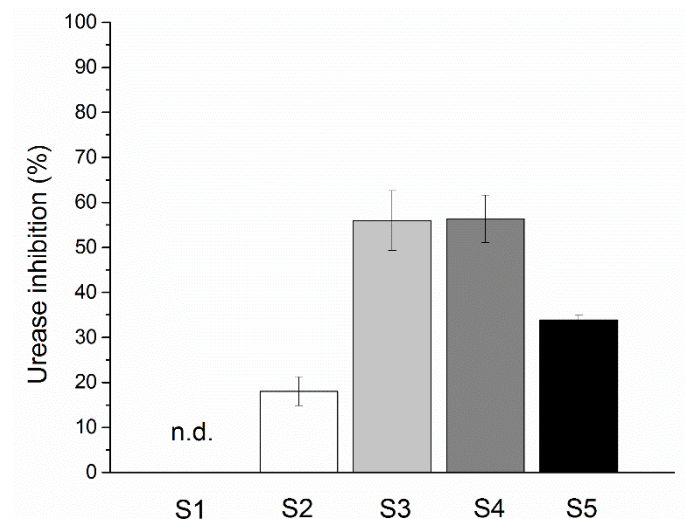


Figure 30: Urease inhibition caused by canola honey (sample S1), canola honey with added MGO and DHA (S2), a solution of MGO and DHA in water (S3), manuka honey MH 3 (S4) and manuka honey MH 3 after treatment with glyoxalase 1 and GSH (S5). All honeys were diluted to 5.5 % (w/v). MGO and DHA concentration was 33 mg/l and 87 mg/l, respectively, for the samples S2-S4. MGO and DHA concentration in S5 was not quantitated. Measurements were carried out in duplicate and error bars indicate standard deviation. Abbreviation: n.d., not detectable.

This indicates that the strong urease inhibition is exclusive for manuka honey and cannot be achieved by adding MGO or DHA to non-manuka varieties. The decreased effect of artificially added MGO and DHA in the canola honey matrix could be due to trapping reactions caused by honey polyphenols. Benzene structures with hydroxyl groups can form MGO adducts (Lo et al., 2011). That reaction may reduce the apparent MGO concentration and its urease inhibition capacity. In manuka honey, MGO is naturally formed during honey maturation, thus an equilibrium between trapped and free MGO should exist. To elucidate whether MGO depletion from manuka honey results in decreased urease inhibition, glyoxalase I and glutathione (GSH) were added to MH 3. GSH forms a hemithioacetal adduct with MGO which is isomerized to S-2-hydroxyacylglutathione by glyoxalase I (Racker, 1951). Thus, MGO should no longer be available for urease inhibition. After addition of glyoxalase I and GSH, the inhibitory effect of manuka honey MH 3 decreased by 23 %, but no complete decrease down to the level of a non-manuka honey was observed (see Figure 30, S5). The remaining inhibitory effect is due to DHA, which is not affected by glyoxalase or GSH. This unambiguously demonstrates that MGO and DHA are essentially responsible for urease inhibition with manuka honey.

A manuka honey concentration of 0.4 % (w/v) is sufficient to achieve 20 % urease inhibition. That corresponds to a dose of 4 g manuka honey containing 595 mg MGO per kg and 1549

mg DHA per kg, solubilized in 1 litre of stomach fluid. Thus, an amount of manuka honey which causes significant urease inhibition can easily be achieved with the diet. Further studies are needed to clarify if the inhibition of jack bean urease can be transferred to urease present in *Helicobacter pylori*. There are several studies published in the literature, which use jack bean urease as a model to study potential urease inhibition in *Helicobacter pylori* (Krajewska, 2011; Wu et al., 2013). Moreover, studies, which compared the inhibition of certain plant extracts on jack bean urease and urease from *Helicobacter pylori* did not find significant differences (Matsubara et al., 2003; Matongo and Nwodo, 2014). The results of this study are a contribution to explain the mechanism of the antibacterial activity of manuka honey against bacteria by inhibiting enzyme activity. According to our results, manuka honey might be a nutritional support for a treatment against *Helicobacter pylori* and might help to decrease the use of antibiotics.

## 1.6. Summary of Chapter A – The antibacterial effect of manuka honey

Manuka honey is merchandised as an antibacterial food which helps to prevent and fight bacterial infections. The antibacterial effect is often associated with the methylglyoxal (MGO) content of manuka honey. Other honeys show an antibacterial effect which is mostly due to hydrogen peroxide. Regarding this, the question arises, how much stronger the antibacterial activity of MGO is compared to hydrogen peroxide. The aim of this study was to characterize the effect of MGO and hydrogen peroxide on four bacteria and give a quantitative statement on the effectiveness of these compounds in honey. Moreover, the molecular structure of manuka honey inclusion complexes formed with  $\alpha$ -cyclodextrin were characterized and their antibacterial activity was studied. Furthermore, the mechanism of bacterial inhibition with manuka honey was studied by examining the inhibitory effect of MGO and dihydroxyacetone (DHA), present in manuka honey, on the enzyme urease. This enzyme ensures the survival of the bacterium *Helicobacter pylori* and, by decreasing its activity, bacterial growth may be inhibited. The results of chapter A can be summarized as follows:

- 1 Methylglyoxal (MGO) in honey-relevant concentrations had a bacteriostatic effect on *S. aureus*, *E. coli* and *B. subtilis*, whereas *P. aeruginosa* was not inhibited by MGO.
- 2 Hydrogen peroxide, which is formed in diluted honey, had a bacteriostatic effect on *S. aureus*, *E. coli* and *P. aeruginosa*, whereas *B. subtilis* was not inhibited by hydrogen peroxide.
- 3 By comparing the slopes of the linearized dose-response curves, it was found that *S. aureus*, *E. coli* and *P. aeruginosa* are more sensitive to hydrogen peroxide than to MGO.
- 4 Natural amounts of MGO in honey were higher than the formation of hydrogen peroxide. Although most bacteria were more sensitive to hydrogen peroxide, MGO was the predominant antibacterial compound in honey, because of its high concentrations compared to hydrogen peroxide formation. Certain bacterial species could be specifically inhibited by hydrogen peroxide and were insensitive to MGO (e.g. *P. aeruginosa*).
- 5 Studies on the molecular structure of  $\alpha$ -cyclodextrin inclusion complexes with MGO and DHA showed that protons inside the cone of  $\alpha$ -cyclodextrin interact preferentially with MGO. An inclusion of MGO with  $\alpha$ -cyclodextrin in the commercial product cyclopower is likely due to the excess of  $\alpha$ -cyclodextrin compared to MGO (190:1).

- 6 Presumably, the inclusion has only minor consequences on bioavailability and antibacterial activity. Cyclopower did not enhance the antibacterial activity of manuka honey on *S. aureus*, *E. coli* and *P. aeruginosa*.
- 7 The growth of *B. subtilis* was synergistically inhibited with cyclopower compared to manuka honey and  $\alpha$ -cyclodextrin alone.
- 8 Possible targets for bacterial inhibition with manuka honey are bacterial enzymes. It was shown that MGO and DHA inhibit jack bean urease, which was used as a model for *Helicobacter pylori* urease, with IC<sub>50</sub> values of 2.8 and 5.0 mM, respectively.
- 9 Urease inhibition of manuka honey correlated with its MGO and DHA content.
- 10 Non-manuka honeys, which lack MGO and DHA, showed significantly less urease inhibition. MGO depletion from manuka honey with glyoxalase reduced urease inhibition. Therefore, urease inhibition by manuka honey was mainly due to MGO and DHA.

The results of this chapter contribute to the understanding of the antibacterial activity of manuka honey and emphasize its unique effect compared to non-manuka honey.



---

## 2 Chapter B – Reactions of carbonyl compounds in honey

---

### 2.1. Introduction

Honey contains mostly mono- and disaccharides (80 g/100 g) and water (18 g/100 g). Minor compounds like polyphenols, melanoidins, free amino acids and proteins account for up to 2 g/100 g. Based on its composition, honey is highly susceptible to the Maillard reaction. Louis-Camille Maillard discovered that sugars react with amino acids to form brown compounds upon heating in 1912 (Maillard, 1912). Since then, the reaction has been studied intensively *in vivo* and *in vitro* (Hodge, 1953; Ledl and Schleicher, 1990; Tessier, 2010; Hellwig and Henle, 2014). The pattern of reaction products varies with the reaction conditions, whereby time, temperature and pH value have the strongest impact. The Maillard reaction is a complex of dehydration and fragmentation reactions and the irreversible binding of reaction products to amino compounds (glycation) can lead to advanced glycation end products (AGE). The reaction can have technological and biological consequences for proteins. It is widely accepted, that the Maillard reaction follows three main stages (early, advanced and final stage) and that dicarbonyl compounds are major reaction products (Ledl and Schleicher, 1990). Earlier studies reported the occurrence of 3-deoxyglucosone, glyoxal and methylglyoxal in honey (Weigel et al., 2004; Mavric et al., 2008). It was found that manuka honey has a unique composition of dicarbonyl compounds, whereby methylglyoxal (MGO) is present in concentrations up to 800 mg/kg (Mavric et al., 2008; Adams et al., 2009). Moreover, Kunze (2009) studied the protein and amino acid composition of honeys in her master thesis. Nevertheless, the extent of the Maillard reaction and its influence on proteins and amino acids in honey has not been studied yet. The focus of this chapter is based on the idea that the Maillard reaction also occurs in honey and that the pattern of reaction products differs between manuka and non-manuka honeys. The study focused on three reaction pathways, which are all part of the complex Maillard reaction system. Firstly, the occurrence of 2-acetyl-1-pyrroline, a product formed by the reaction of proline and MGO was studied. Secondly, proteins were isolated from honey and their fluorescence properties and molecular size were analysed. Thirdly, the isolated honey proteins were enzymatically hydrolysed and protein bound AGE were studied. The third part was a collaboration with Dr. Michael Hellwig (TU Dresden), who performed a study on the formation of AGE in honey. The

reactions were studied in model honeys with artificially added MGO and in commercial honey samples during storage.

## 2.2. Background

### 2.2.1 Carbonyl compounds in food

The term carbonyl compounds refer to all organic compounds which contain carbonyl groups in their molecular structure. Examples for carbonyl compounds are aldehydes, ketones, and carboxylic acids or amides. In food, these compounds are mainly present in the form of carbohydrates or peptides and proteins. Especially the group of carbohydrates generates various structures, which are referred to as carbonyl compounds. These could either be of the aldehyde type, e.g. glucose or of the ketone type, e.g. fructose. Moreover, compounds can contain more than one carbonyl group. Compounds with two adjacent carbonyl groups, called 1,2-dicarbonyls, are of particular interest for research. 1,2-Dicarbonyls are sugar degradation products, which occur in food after thermal treatment. They are preferentially formed at pH values below 3 or above 8. In fermented food 1,2-dicarbonyls can be formed by microorganisms and in plants they can occur during stress conditions (Yadav et al., 2005; Nemet et al., 2006). 1,2-Dicarbonyls are known to react with proteins and amino acids to form advanced glycation end products (AGE) (Brownlee et al., 1984). The effect of dietary AGE *in vivo* is discussed controversially (Henle, 2007). 3-Deoxyglucosone (3-DG), glyoxal (GO) and methylglyoxal (MGO) are quantitatively the most relevant dicarbonyl compounds in food (Gobert and Glomb, 2009). Figure 31 shows the molecular structures of 3-DG and MGO.

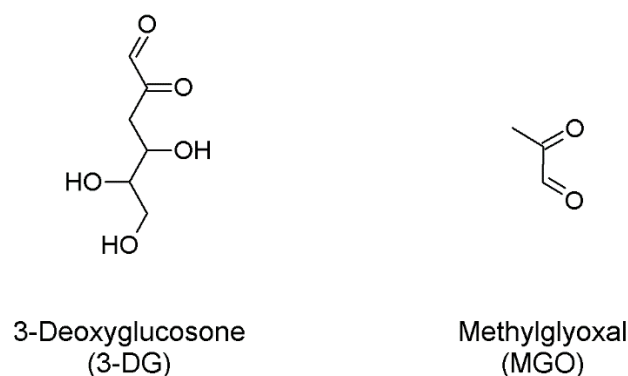


Figure 31: Molecular structures of 3-deoxyglucosone and methylglyoxal

Since 3-DG and MGO are also the most relevant 1,2-dicarbonyls in honey, these compounds will be discussed in detail. For 3-DG formation, an amino compound reacts with the aldehyde

group of glucose to form imines (Schiff base) in the early stage of the Maillard reaction. Via 1,2-enolization, the stable 1-amino-1-deoxyketose (Amadori product) is formed (Ledl and Schleicher, 1990) (see Figure 32).

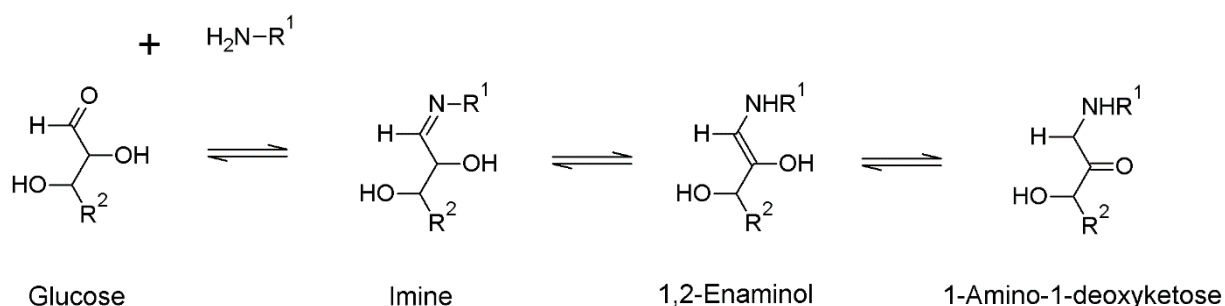


Figure 32: Formation of 1-amino-1-deoxyketose (Amadori product) from glucose,  $\text{R}^2 = \text{C}_3\text{O}_3\text{H}_7$

During the advanced stage, the Amadori product can rearrange via 1,2-enolization or 2,3-enolization and after water elimination and hydrolysis of the amino group, dicarbonyl compounds are formed. The formation of 3-DG is shown in Figure 33.

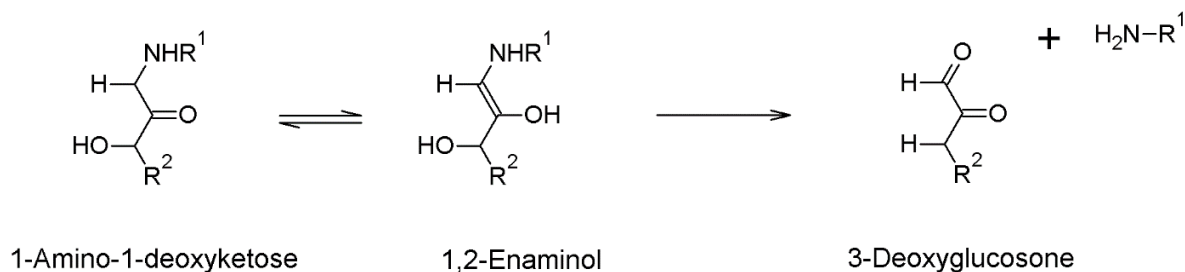


Figure 33: Formation of 3-deoxyglucosone from the Amadori product of glucose,  $\text{R}^2 = \text{C}_3\text{O}_3\text{H}_7$

In contrast, the short dicarbonyl methylglyoxal is formed from deoxyosones or from the Amadori product of glucose via retro-aldol fragmentation. The fragmentation is enhanced under alkaline conditions (Kroh, 1994; Thornalley et al., 1999).

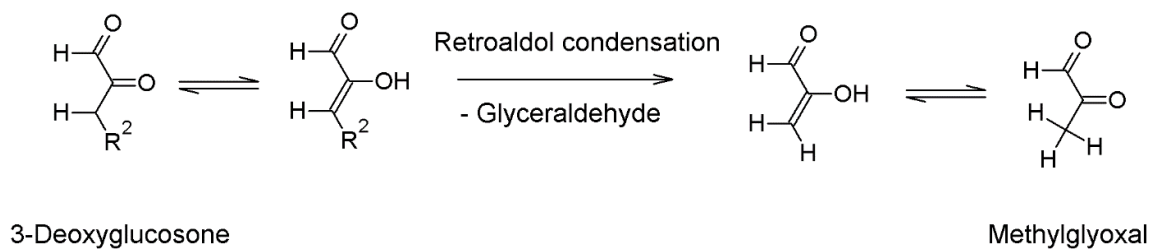


Figure 34: Formation of methylglyoxal from 3-DG,  $R^2 = C_3O_3H_7$

However, methylglyoxal and also 3-DG can be formed from other sources than glucose in food. For example caramelisation or lipid peroxidation can lead to an increase of 1,2-dicarbonyls (Belitz, Grosch, 2008). Moreover, methylglyoxal is formed in living organisms in small amounts from the dephosphorylation of triose phosphates (Richard, 1993; Kalapos, 1999). Triose phosphates like glyceraldehyde phosphate (GA3P) and dihydroxyacetone phosphate (DHAP) are metabolites of glycolysis. The enediol intermediate of the interconversion of DHAP and GA3P is a source of methylglyoxal. The reaction can occur in plants (Takagi et al., 2014; Bilova et al., 2016) and mammalian tissue (Allaman et al., 2015). Furthermore, MGO can arise directly from dihydroxyacetone (DHA). The occurrence of DHA is only insufficiently studied and it is not commonly found in food. Severin et al. (1984) reported that DHA occurs in pretzels, but they did not report quantitative data. The only exception where DHA is found in significant amounts is manuka honey. It was found that in honeys from the plant *Leptospermum scoparium* (manuka tree) the DHA level is significantly higher compared to other honeys and food. During storage, DHA is non-enzymatically dehydrated to MGO (Adams et al., 2009; Atrott et al., 2012). The quantitative data on the occurrence of 1,2-dicarbonyls in food is rather limited. Recent studies aimed to give a more accurate picture of the formation and distribution of 1,2-dicarbonyls in food. Table 18 summarizes the relevant findings concerning MGO and 3-DG.

Table 18: Concentrations of 1,2-dicarbonyls in food and their cause of formation

Food	Dicarbonyl mg/kg or mg/l		Cause of formation
	3-DG	MGO	
Vinegar	4.6-2622 <sup>[1]</sup>	1.7-53 <sup>[1]</sup>	Microorganisms
Soy sauce	32-832 <sup>[1]</sup>	n.d.-12 <sup>[1]</sup> 3.0-8.7 <sup>[2,3]</sup>	Microorganisms

Beer (Pilsener)	18-54 <sup>[1]</sup> 153-159 <sup>[4]</sup>	n.d.-1.0 <sup>[1]</sup> 0.1-5.1 <sup>[1,4,5]</sup>	Sugar, microorganisms
Malt beer	19-136 <sup>[1]</sup>	tr.-1.0 <sup>[1]</sup>	
Soft drink	n.d.-28 <sup>[1]</sup> 29-30 <sup>[6]</sup>	n.d. <sup>[1]</sup> 0.2-1.4 <sup>[2,3,6]</sup>	Sugar
Milk (UHT)	n.d-1.4 <sup>[7]</sup>	n.d. <sup>[7]</sup>	Sugar
Bread	13-619 <sup>[1]</sup>	n.d.-28 <sup>[1]</sup> 0.8-2.5 <sup>[3]</sup>	Sugar
Cookies	8-5-385 <sup>[1]</sup>	1.8-68 <sup>[1]</sup> 3.7-82 <sup>[8]</sup>	Sugar
Honey	271-1641 <sup>[1]</sup> 97-1266 <sup>[9]</sup>	0.4-5.4 <sup>[9]</sup>	Sugar
Manuka honey	563-1060 <sup>[10]</sup>	38.4-761 <sup>[10]</sup>	Sugar and DHA

<sup>[1]</sup>Degen et al. (2012), <sup>[2]</sup> Hayashi & Shibamoto (1985), <sup>[3]</sup> Nagao et al. (1986), <sup>[4]</sup> Bravo et al. (2008), <sup>[5]</sup> Yamaguchi et al. (1994), <sup>[6]</sup> Lo et al. (2008), <sup>[7]</sup> Hellwig et al. (2010), <sup>[8]</sup> Arribas-Lorenzo & Morales (2010), <sup>[9]</sup> Weigel et al. (2004), <sup>[10]</sup> Mavric et al. (2008)

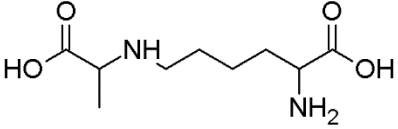
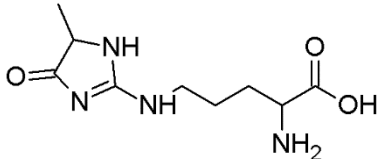
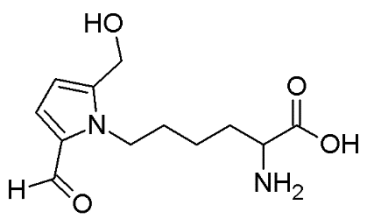
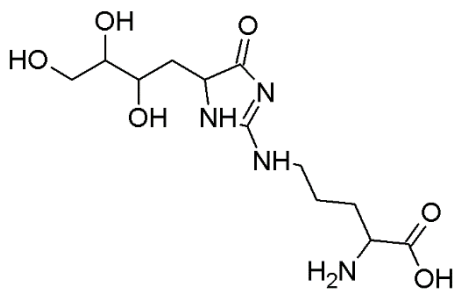
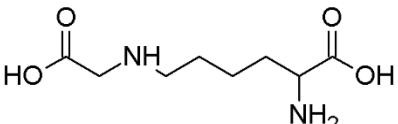
Since 1,2-dicarbonyls are reactive compounds, it is likely that they are only intermediately present in food and can react with other compounds to form a variety of reaction products. The next section gives an overview of the most important reaction pathways of 1,2-dicarbonyl compounds in food.

### 2.2.2 Reactions of carbonyl compounds in food

In comparison to glucose, 1,2-dicarbonyls can be up to 20,000-fold more reactive (Thornalley, 2005). The  $\alpha$ -oxoaldehydes can react with proteins to form protein-bound Maillard reaction products (MRP). The reactivity of individual proteins is dependent on the amino acid composition, the primary, secondary, and tertiary structure, and on the presence of cysteine (Ludwig, 1979; Hellwig and Henle, 2014). The amino acid derivatives resulting from the reaction with 1,2-dicarbonyls are called advanced glycation end-products (AGE). AGE can either be released from their protein linkage by enzymatic matters or can directly form at free, non-protein-bound amino acids. Table 19 summarizes some of the most important AGE formed in food. Besides modification of single amino acid residues, AGE formation can also lead to protein cross-linking when two dicarbonyl compounds react intramolecularly with two

amino acid residues. Popular representatives of this group are the lysine dimers MOLD and DOLD, which are formed by methylglyoxal and 3-DG respectively (Henle, 2005).

Table 19: Structures and starting material of advanced glycation end-products

AGE	Structure	Amino acid	Dicarbonyl
N-ε-Carboxyethyllysine (CEL)		Lysine	MGO
Methylglyoxal-derived hydroimidazolone (MG-H1)		Arginine	MGO
Pyrraline		Lysine	3-DG
3-Deoxyglucoson-derived hydroimidazolone (3-DGH)		Arginine	3-DG
N-ε-Carboxymethyllysine (CML)		Lysine	GO

AGE formation can lead to the biochemical blockage of amino acids, since the modified amino acids are not available for digestive enzymes during gastrointestinal digestion. Thus, glycated proteins cannot be used as a source of essential amino acids (Finot, 1982). However,

during food processing, the Maillard reaction and especially the reaction of 1,2-dicarbonyls with amino acids can also have positive impact on food components. During Strecker degradation of amino acids with dicarbonyls, various aroma compounds are generated (Wang and Ho, 2012). In the initial phase of Strecker reaction a Schiff base is formed. Later during the reaction, the intermediate is cleaved via decarboxylation of the carboxyl group of the amino acid and subsequent formation of Strecker aldehyde and the corresponding amino ketone. Strecker aldehydes can be aroma active themselves and the amino ketones are key precursors for the formation of flavour compounds such as pyrazines, oxazoles and thiazoles (Wang and Ho, 2012). Moreover, intramolecular reactions of 1,2-dicarbonyls can lead to aroma active compounds. For example, MGO can form furaneol via the Cannizzaro reaction (Wang and Ho, 2008) and 3-DG can form 5-hydroxymethylfurfuraldehyde (HMF) via dehydration (Belitz, Grosch, 2008). Finally, the multiple interactions of MRP generate a wide pattern of advanced stage low molecular weight (LMW) products. The final stage of the Maillard reaction can also lead to high molecular weight (HMW) products, like melanoidins. To date neither the mechanism of formation nor the detailed structure of these partly dark brown coloured compounds are clarified completely (Kroh et al., 2008). It is assumed that covalent binding of low molecular weight compounds to form high molecular weight structures is one possible mechanism of melanoidin formation and of acquiring their antioxidant properties (Hofmann, 1998; Delgado-Andrade and Morales, 2005). Moreover, the incorporation of polyphenols into melanoidins and their influence on melanoidin functions was discussed (Brudzynski and Miotto, 2011).

Concerning honey, reactions of carbonyls are rarely studied. Weigel et al. (2004) analysed the 1,2-dicarbonyls 3-DG, glyoxal and MGO in honey for the first time and discussed the results in context to the HMF contents of the honeys. It was shown that most honeys predominately contain 3-DG in amounts between 80 to 1300 mg/kg, followed by smaller amounts of 0.2 to 2.7 mg/kg of GO and 0.4 to 5.4 mg/kg of MGO. The HMF content of the honeys ranged between 0.6 and 44 mg/kg, which is predominantly in accordance with the European food regulation (Codex Alimentarius Commission, 2001). An exception of dicarbonyl content to honeys studied previously is manuka honey. It was found that manuka honey contains MGO in concentrations up to 100-fold higher than other commercial honeys (Adams et al., 2008; Mavric et al., 2008). MGO in manuka honey is non-enzymatically formed from dihydroxyacetone (DHA), which is present in the nectar of the manuka plant (Adams et al., 2009; Atrott et al., 2012). Since then, there are various reports on the occurrence of DHA and

MGO in manuka nectar and honey (Windsor et al., 2012; Williams et al., 2014; Cokcetin et al., 2016; Grainger et al., 2016a). Moreover, HMF was studied intensively as a quality parameter of honey and the influence of storage parameters and heat treatment was shown previously (Singh and Bath, 1998; Karabournioti and Zervalaki, 2001; Windsor et al., 2013). Thus, the current situation gives a good picture of the formation of reactive carbonyl compounds in honey, especially manuka honeys. Nevertheless, there is only minor knowledge available about the reactions which occur in honey when 1,2-dicarbonyls further react with other honey compounds. Previous research showed, that MGO in manuka honey is not stable during storage (Grainger et al., 2016a). The fate of MGO and other honey carbonyls during honey processing and storage shall be addressed in this chapter. The following section should give a brief overview of methods to study carbonyl reactions in food matrices.

### 2.2.3 Analysis of carbonyl reaction products

As presented previously, the Maillard reaction leads to a diverse field of reaction products. The chemical and physical nature of the compounds can vary widely. Thus, the quantification of reaction products resulting from the reaction of carbonyls with proteins and amino acids is mainly achieved by measuring specific structures as representative compounds, which are formed during the complex reaction. During the early stage of the Maillard reaction, Amadori products are formed as the first stable intermediate. A popular method to study the early Maillard reaction is to analyse the furosine content of food via HPLC (Pompei and Spagnolello, 1997; Villamiel et al., 2000). Furosine is formed during the acid hydrolysis of protein-bound Amadori product of lysine. Depending on the sugar residue bound to lysine, the rate of furosine formation during hydrolysis differs (Krause et al., 2003). Therefore, conversion factors for the formation of furosine from Amadori products were calculated, thus enabling the evaluation of the progress of the early Maillard reaction (Krause et al., 2003). The advanced stage of the Maillard reaction can be analysed by measuring specific AGE structures. There are several methods published, which deal with sample preparation and product detection. The analysis of AGE in food and body fluids is most often performed by enzyme-linked immunosorbent assay (ELISA) or LC-MS (Sajithlal et al., 1998; Schmitt et al., 2007; Poulsen et al., 2013; Thornalley and Rabbani, 2014). The ELISA method is often used by medical laboratories since no sophisticated instruments are required. However, the specificity of the antibodies for only one AGE structure is questionable (Poulsen et al., 2013). The ELISA method needs to be validated for different food matrices so that cross-reaction



with other AGE-modified structures can be prevented (Henle, 2008). In contrast the use of LC-MS/MS increases the sensitivity and in combination with isotopically labelled standards and the multiple reaction monitoring (MRM) mode the method is exact and suitable for quantification (Poulsen et al., 2013). Moreover, there are methods which do not measure specific glycation compounds but provide a more general view of the progress of the Maillard reaction. By measuring the colour of protein isolates from food matrices, statements concerning the extent of the Maillard reaction and the degree of cross-linking reactions can be given. As described in section 2.2.2, the final stage of the Maillard reaction provides complex reaction products, which are called melanoidins because of their colour properties (Hodge, 1953). The products are mostly yellow or brown and can absorb light at the wavelength 405-420 nm (De Marco et al., 2011). Moreover, the formation of fluorescent products during the Maillard reaction in milk is reported (Morales et al., 1996). For food stuff, the excitation wavelength studied were between 340 to 370 nm and the emission wavelength varied between 420 to 450 nm (Sajithlal et al., 1998; Morales and Jiménez-Pérez, 2001; Bosch et al., 2007). It is known that dicarbonyls and amino acids can form specific, fluorescent AGE. One example is the formation of argpyrimidine which results from the reaction of MGO and arginine (Shipanova et al., 1997). However, the maximum fluorescence excitation and emission wavelengths of argpyrimidine are situated at shorter wavelengths ( $\lambda_{\text{ex/em}} = 320/380$  for argpyrimidine). Besides specific structures, protein fluorescence can be caused by protein crosslinking, reactions at the peptide backbone or changes in the tertiary structure (Sajithlal et al., 1998). It was initially assumed that fluorescent structures are a precursor of brown melanoidin pigments (Berrens, 1966; Adhikari and Tappel, 1973). Later on it was shown that under certain reaction conditions (low pH, retardant salts) brown pigments can be formed before fluorescent structures are present (Matiacevich and Pilar Buera, 2006). After the incubation of casein with lactose or glucose it was found that fluorescent compounds can either be formed protein-bound or to a lesser extent also in free form (Morales and Boekel, 1997). The authors were able to show that fluorescence evolution was due to many different reactions products and that their formation was heat dependent. They concluded that the measurement of the sum of fluorescent AGE could be a valuable parameter to analyze the Maillard reaction in food matrices. Another rather unspecific method to pursue glycation reactions in food is size exclusion chromatography (SEC). SEC enables the user to differentiate molecules upon their molecular size. The detection of compounds is mostly based on UV or fluorescence. There exists a wide range of SEC columns which allow the

separation of proteins of various molecular sizes. It was recently shown, that the extent of browning reactions and the formation of fluorescent structures in bread crust and crumb can be followed by SEC (Helou et al., 2016). Moreover, SEC can also be used to distinguish between the precursors which are involved in the formation of HMW products. It was shown that the molecular size of melanoidins varies depending on the carbonyl compound which is involved in the formation (Fiedler et al., 2006). The authors were able to present that methylglyoxal is predominantly forming HMW products whereby 3-DG promotes the formation of lower molecular size domains. Besides, De Marco et al. (2011) showed that the increase of the molecular size of coffee melanoidins is an indicator for the progression of coffee bean roasting. The increase of the molecular size was explained by the incorporation of carbohydrates and phenolic compounds into a proteinaceous backbone. Taken together, both the analysis of concrete reaction products of the final stage of the Maillard reaction like AGE and the measurement of more general parameters like fluorescence or molecular size can be used to evaluate the extent of glycation reactions in food.

### 2.3. Aims

Despite the high ratio of reducing sugars to proteins and amino acids, there is only limited information available dealing with the extent of glycation reactions in honey. Although it was shown that MGO in manuka honey slowly decreases over storage time, it is unknown which reaction products are formed up to the present day. Based on the hypothesis that honey in general and especially manuka honey with its unique high level of MGO is prone to glycation reactions, different honey-derived reactions shall be analyzed. The study was divided into two parts. Firstly, the reaction of MGO with small honey compounds to form LMW products was investigated. Therefore, a reaction product of MGO and the amino acid proline, namely 2-acetyl-1-pyrroline (2-AP), was studied in honey and the concentrations were considered in relation to the MGO content of the honeys. Secondly, honey proteins were isolated and the formation of protein adducts was studied. Therefore, the molecular size and the fluorescence intensity of the HMW fraction of honey were analyzed. Moreover, a selection of protein-bound Maillard reaction products was studied. This project was part of a study performed in cooperation with Dr. Michael Hellwig (TU Dresden). The aim of this chapter is to elucidate the formation of mainly MGO-derived reaction products in manuka honey compared to non-manuka honey. The results of this study are supposed to contribute to the understanding of the unique reactions in manuka honey and could potentially be used to control honey authenticity and quality.

## 2.4. Methods

### 2.4.1 Chemicals

Table 20: Chemicals used for the studies presented in chapter B

Chemical	Specification	Supplier
1,3-Dihydroxyacetone dimer	97 %	Sigma-Aldrich, Steinheim, Germany
2,4,6-Trimethylpyridine	> 99 %	Sigma-Aldrich, Steinheim, Germany
2-Acetyl-1-pyrroline	10% w/w in DCM	Toronto Research Chemicals, Toronto, Canada
3-[(3-cholamidopropyl)-dimethylammonium]-1-propanesulfonate, CHAPS	99.3 %	Molekula, Dorset, UK
5-Hydroxymethylfurfuraldehyd	98+ %	Alfa Aesar, Karlsruhe, Germany
Acetic acid	100 %, p.a.	Carl Roth, Karlsruhe, Germany
Acetonitrile	HPLC grade	VWR, Darmstadt
Amino acid mix	2.5 mM each, in 0.1 M hydrochloric acid	Sigma-Aldrich, Steinheim, Germany
Ammonia	25 %	Merck, Darmstadt, Germany
Catalase	from bovine liver, suspension in water, 15 000 000 U/15 ml	Sigma-Aldrich, Steinheim, Germany
Copper(II) sulfate pentahydrate	≥99 %, Ph.Eur.	Carl Roth, Karlsruhe, Germany
D(-)Fructose	> 99.5 %, for biochemistry	Carl Roth, Karlsruhe, Germany
D(+)-Glucose	anhydrous, p.a.	Carl Roth, Karlsruhe, Germany
D(+)-Saccharose	≥ 99.5 %, p.a.	Carl Roth, Karlsruhe, Germany
Dichloromethane	HPLC grade	VWR, Darmstadt, Germany

Disodium hydrogenphosphate	99 %, p.a	Grüssing, Filsum, Germany
Dithiothreitol	>99 %	Molekula, Dorset, UK
Dodium dodecyl sulfate	min. 99.5 %	Serva, Heidelberg, Germany
Ferritin	Part of gel filtration calibration kit	GE Healthcare, Uppsala, Sweden
Folin Ciocalteu's phenol reagent		Fluka, Buchs, Switzerland
Formyline	Synthesis product, Michael Hellwig	TU Dresden, Germany
Glucose oxidase	from <i>Aspergillus niger</i> , 10 kU, 47200 U/g	Sigma-Aldrich, Steinheim, Germany
Helium	99.999 %, Alphagaz	Air Liquide
Hydrochloric acid	37 %	Sigma-Aldrich, Steinheim, Germany
Leucine aminopeptidase	Type IV-S, 18 U/mg protein	Sigma-Aldrich, Steinheim, Germany
Lithium chloride	p.a.	Merck, Darmstadt, Germany
Lithium citrate buffer	0.12 N, pH 2.2	Sykam, Fuerstenfeldbruck, Germany
Lithium citrate buffer	0.12 N, pH 2.9	Sykam, Fuerstenfeldbruck, Germany
Lithium citrate buffer	0.3 N, pH 4.2	Sykam, Fuerstenfeldbruck, Germany
Lithium citrate-/ borate buffer	0.3 N, pH 8.0	Sykam, Fuerstenfeldbruck, Germany
Lysozyme	from chicken egg white	Sigma-Aldrich, Steinheim, Germany
Maltosine	Synthesis product, Michael Hellwig	TU Dresden, Germany
Methanol	HPLC grade	VWR, Darmstadt, Germany
Methylglyoxal	~ 40 % (w/w), exact concentration was determined against 2-MQ	Sigma-Aldrich, Steinheim, Germany
Methylglyoxal-derived hydroimidazolone	Synthesis product, Michael Hellwig	TU Dresden, Germany
Ninhydrin	p.a., min. 99%	Serva Feinbiochemica,

		Heidelberg, Germany
Nonafluoropentanoic acid	97 %	Sigma-Aldrich, Steinheim, Germany
N- $\epsilon$ -Carboxyethyllysine	Synthesis product, Michael Hellwig	TU Dresden, Germany
N- $\epsilon$ -Carboxymethyllysine	Synthesis product, Michael Hellwig	TU Dresden, Germany
N- $\epsilon$ -fructosyllysine	Synthesis product, Michael Hellwig	TU Dresden, Germany
N- $\epsilon$ -maltulosyllysine	Synthesis product, Michael Hellwig	TU Dresden, Germany
ortho-Phenylenediamine (oPD)	$\geq 98$ %,	Sigma-Aldrich, Steinheim, Germany
Ovalbumin	from chicken egg white	Sigma-Aldrich, Steinheim, Germany
Pepsin	from porcine gastric mucosa, 3555 U/mg protein	Sigma-Aldrich, Steinheim, Germany
Potassium sodium tartrate tetrahydrate	$\geq 99$ %, p.a.	Carl Roth, Karlsruhe, Germany
Prolidase	from porcine kidney, 208 U/mg protein	Sigma-Aldrich, Steinheim, Germany
Pronase E	from <i>S. griseus</i> , 4000 PU/mg protein	Merck, Darmstadt, Germany
Pyrraline	Synthesis product, Michael Hellwig	TU Dresden, Germany
Sodium acetate	99 %	Grüssing, Filsum, Germany
Sodium carbonate	99.5 %, p.a.	Grüssing, Filsum, Germany
Sodium dihydrogenphosphate	99.5 %, p.a.	Grüssing, Filsum, Germany
Sodium hydroxide	98.56 %	Fisher Scientific, Loughborough, UK Sigma-Aldrich,
Sodium sulfate	Anhydrous, p.a.	Grüssing, Filsum, Germany
Trichloroacetic acid	$> 99$ %; p.a.	Carl Roth, Karlsruhe, Germany
Tris(hydroxymethyl)-	$\geq 99$ %, p.a.	Sigma-Aldrich, Steinheim,

aminomethan (TRIS)		Germany
Urea	> 99.5 %	Fluka AG, Basel, Switzerland
$\gamma$ -Globulin	from bovine blood	Sigma-Aldrich, Steinheim, Germany

## 2.4.2 Materials

Table 21: Materials used for the studies presented in chapter B

Name	Specification	Supplier
Amino acid analysator column	Cation exchange LCA K07/Li	Sykam, Fuerstenfeldbruck, Germany
Centrifuge tube, Kimax®	50 mL, O.D. $\times$ L 29 mm $\times$ 123 mm	Sigma-Aldrich, Steinheim, Germany
Dialysis tubings	Cellulose, 33 mm, MWCO 14 kDa	Sigma-Aldrich, Steinheim, Germany
GC column	TR-FFAP capillary column, 30.0 m $\times$ 0.25 mm inner diameter, with a 0.25 $\mu$ m film thickness	Thermo Scientific, Runcorn, U.K.
GC vials with crimp caps	1.5 ml, glass	VWR, Darmstadt, Germany
Glass vessel	10-50 ml	VWR, Darmstadt, Germany
HPLC column	Eurospher 100 RP18 material (250mm $\times$ 4.6 mm, 5 $\mu$ m particle size with integrated pre-column	Knauer, Berlin, Germany
HPLC column	Zorbax 100 SB-C18 column, 2.1 $\times$ 50 mm, 3.5 $\mu$ m	Agilent Technologies, Böblingen, Germany
HPLC vials with lit	1.5 ml, glass	VWR, Darmstadt, Germany
Ion-exchange resin Dowex 50WX8	100-200 mesh	Sigma-Aldrich, Steinheim, Germany
Membrane filter	Regenerated cellulose, 45 $\mu$ m, 26 mm	Phenomenex, Aschaffenburg, Germany
Membrane filter for solvents	GH Polypro 0,45 $\mu$ m, 47 mm hydrophilic polypropylene	Pall, Crailsheim, Germany
Microtiter plate	96 flat bottom, transparent, pureGrade, nonsterile	Brand, Wertheim, Germany
Microtiter plate	UV-star	Greiner Bio-One,

		Kremsmuenster, Austria
Microtiter plate	96 flat bottom, black, pureGrade, nonsterile	Brand, Wertheim, Germany
Multichannel pipette	10-100 $\mu$ l	Brand, Wertheim, Germany
Parafilm	4 in x 125 ft	Bemis, Neenah, USA
Pasteur pipettes	230 mm, glass	VWR International, Leuven, Netherlands
Pipette tips	1-1000 $\mu$ l	Brand, Wertheim, Germany
Septa for HPLC vials	8*0.4 mm, PTFE coated	VWR, Darmstadt, Germany
Superdex 200 column	10/30 GL	GE Healthcare Bio-Sciences AB, Uppsala, Sweden
Syringe	1 ml	B. Braun, Melsungen, Germany
Tubes	1.5 ml, 2 ml	Eppendorf, Hamburg, Germany

### 2.4.3 Devices

Table 22: Devices used for the studies presented in chapter B

Device	Specification	Supplier
Amino acid analyser	S 4300, Software: Chromstar 6.3 SCPA GmbH	Sykam, Fuerstenfeldbruck, Germany
Analytic balance	BP 121 S, accuracy: 0.0001 g, max. 120 g	Sartorius, Göttingen, Germany
Centrifuge	Eppendorf 5804-R	Eppendorf AG, Hamburg, Germany
CLN detector	8060	Antek, Houston, USA
Freeze dryer	Alpha 1 - 2	Martin Christ, Osterode, Germany
Freezer	Comfort	Liebherr, Bibrach an der Riss, Germany
Fridge	Econoic System, 5°C	Liebherr, Bibrach an der Riss, Germany
GC-MS	GC 7890A system, 7683 Series injector with sample tray, 5975C	Agilent Technologies, Böblingen, Germany



	MS detector in electron ionization (EI) mode	
HPLC system 1	Äkta basic system pump P-900 auto sampler A-900 UV detector UV-900 online degasser K-5004	Amersham Pharmacia Biotech, Uppsala, Sweden  Knauer, Berlin, Germany
HPLC system 2	Smartline 1000 pump Dynamic mixing chamber solvent organizer K-1500 online degasser K-5004 Basic Marathon auto sampler Azura DAD detector 2.1 L	Knauer , Berlin, Germany  Knauer , Berlin, Germany Knauer , Berlin, Germany Sparks , Netherlands Knauer, Berlin, Germany
HPLC system 3 (connected to CLN detector)	Quarternary pump G1311A, Autosampler G1313A, Variable Wavelength Detector G1314A, Column Thermostat G1316A, Degasser G1322A	Agilent Technologies, Böblingen, Germany
HPLC-MS/MS	binary pump (G1312A), online degasser (G1379B), autosampler (G1329A), column thermostat (G1316A), diode array detector (G1315D), triple-quadrupole mass spectrometer (G6410A)	Agilent Technologies, Böblingen, Germany
Incubator	BE 500	Memmert, Schwabach, Germany
Incubator	BE 400	Memmert, Schwabach, Germany
Incubator	ULM 500	Memmert, Schwabach, Germany
Laboratory pipette	1-1000 µl	Eppendorf AG, Hamburg, Germany
LabWater Purelab Plus water system	conductivity 0.055 µS/cm	ELGA, Celle, Germany filter from USFilter, Ransbach- Baumbach, Germany

Magnetic and heating stirrer	RH basic	IKA Labortechnik, Staufen, Germany
Multimode reader	Tecan infinite M200	Tecan, Mainz, Germany
pH meter	InoLab Level 1, electrode: InLab Semi-Micro	Mettler-Toledo, Weilheim, Germany
Photometer	Spekol 1500	Analytik Jena, Jena, Germany
Ultrasonic bath	Sonorex RK 510 Super	Bandelin, Berlin, Germany
Viscotester iQ	Peltier control	Haake/Thermo Fisher Scientific, Waltham, USA
Vortex	Uniprep Gyrotor	Uniequip, Freital, Germany
Vortex	Minishaker MS-1 IKA	IKA Labortechnik, Staufen, Germany

#### 2.4.4 Honey samples

Table 23: List of commercial honey samples, Chapter B

Honey	Quantity	Manufacturer, Best before
Buckwheat honey	1	Bienenhonig R. Feldt, 03/18
Chestnut honey	1	Imkerauslese L.W.C. Michelsen, 03/14
Cornflower honey	1	Hans Grundner Imkermeister, 01/17
Honeydew honey	1	Biophar, Fürsten-Reform, 11/17
Lime honey	1	Biophar, Fürsten-Reform, 12/17
Manuka honey active 10	1	Wellbeing, 07/2015
Manuka honey active 20	1	Wellbeing, 09/2016
Manuka honey active 5	1	Wellbeing, 03/2016
Manuka honey Bio	1	Hoyer GmbH, 08/2011
Manuka honey MGO 250	2	Manuka Health NZ Ltd
Manuka honey MGO 30	3	Manuka Health NZ Ltd
Manuka honey MGO 400	2	Manuka Health NZ Ltd
Manuka honey MGO 550	2	Manuka Health NZ Ltd

Manuka honey Miel de Manuka IAA 15 +	1	Compoirs & Compagnies, 05/18
Manuka honey Miel de Manuka IAA 18 +	1	Compoirs & Compagnies, 05/18
Manuka honey Miel de Manuka IAA 5 +	1	Compoirs & Compagnies, 05/18
Manuka honey Pure Gold 18	1	Pure Gold, 08/16
Manuka honey Pure Gold 8	1	Pure Gold, 09/16
Manuka honey UMF 15	1	Comvita, 10/2016
Manuka honey UMF 20	1	Comvita, 05/2016
Manuka honey UMF 5	1	Comvita, 09/2016
Manuka honey, Queen Bee active 15	1	Queen Bee, 04/16
Manuka honey, Steen Raw 25	1	Steens limited, 11/15
Polyfloral honey	1	Dr. Krieger, 08/17
Polyfloral honey	1	Nektarquell, Ulis Hongimarkt 04/14
Canola honey	1	Bienen Wirtschaft Meißen, 06/16
Scottish heather honey	1	John Mellies' Apiaries, 10/14
Thyme honey	1	Imkerauslese L.W.C. Michelsen, 03/14
Ulmo honey	1	Bienenhonig R. Feldt, 08/15

Table 24: List of spiked honey samples, Chapter B

Honey	Specification	Manufacturer
Manuka honey MGO 30 + MGO/DHA for MRP studies	A: spiked with MGO 500 mg/kg and DHA 1000 mg/kg, stored at 30°C	Manuka Health NZ Ltd
Polyfloral honey +/- MGO/DHA for 2-AP studies	A: spiked with MGO 100 mg/kg, stored at room temp. B: spiked with MGO 100 mg/kg stored at 37 °C C: spiked with MGO 500 mg/kg, stored at room temp. D: spiked with MGO 500 mg/kg stored at 37	Nektarquell

	°C E: spiked with MGO 100 mg/kg and DHA 200 mg/kg, stored at room temp. F: spiked with MGO 100 mg/kg and DHA 200 mg/kg, stored at 37°C G: spiked with MGO 500 mg/kg and DHA 1000 mg/kg, stored at room temp. H: spiked with MGO 500 mg/kg and DHA 1000 mg/kg, stored at 37°C	
Polyfloral honey +/- MGO/DHA for fluorescence and SEC studies	A: spiked with MGO 100 mg/kg and DHA 200 mg/kg, stored at room temp. B: spiked with MGO 100 mg/kg and DHA 200 mg/kg, stored at 37°C C: spiked with MGO 500 mg/kg and DHA 1000 mg/kg, stored at room temp. D: spiked with MGO 500 mg/kg and DHA 1000 mg/kg, stored at 37°C	Dr. Krieger

#### 2.4.5 Quantification of methylglyoxal and dihydroxyacetone via RP-HPLC-UV

The quantification of methylglyoxal and dihydroxyacetone is described in section 1.4.5. All honey samples were analysed following the same procedure as mentioned above.

#### 2.4.6 Quantification of hydroxymethylfurfural

The determination of HMF was performed according to the literature (Jeuring and Kupperts, 1980) with some modifications. Briefly, 1 mL aliquots of 10% honey solutions in ultrapure water were membrane-filtered (0.45 µm) and subsequently analyzed via HPLC-UV. Separation was achieved by using HPLC system 1 (see Table 22) connected to a stainless steel column filled with Eurospher 100 RP18 material (250mm x 4.6 mm, 5 µm particle size with integrated pre-column; Knauer, Berlin, Germany). The mobile phase consisted of 0.05 M phosphate buffer at pH 5.5 (solvent A) and HPLC-grade methanol (solvent B). The elution was carried out isocratically with 15% solvent B over 30 min. The flow rate was 1.0 mL/min at ambient temperature; 50 µL sample solution was injected; and peaks were detected by measurement of UV absorbance at 283 nm. Quantitation was achieved by external calibration with freshly prepared HMF standard solution.

#### 2.4.7 Isolation and quantification of 2-acetyl-1-pyrroline

A total of 10 g of honey was dissolved in 10 mL of ultrapure water. A total of 50  $\mu$ L of the internal standard 2,4,6-trimethylpyridine (TMP) solution (195 mg/L) was added, and the pH was adjusted to 8 with 1 M sodium hydroxide solution. The alkaline honey solution was mixed with 5 mL of dichloromethane, agitated vigorously for 60 s, and centrifuged afterwards. The organic layer was collected, and extraction with dichloromethane was repeated once. The collected organic layer was washed with 5 mL of water and dried with anhydrous sodium sulfate. An aliquot of 1 mL was transferred to a GC vial and subjected to GC-MS analysis. Matrix calibration was achieved by adding known amounts of 2-AP to an artificial honey, which was then extracted as described above. The artificial honey was prepared following Wahdan (1997). Briefly, 46.5 g of fructose, 35 g of glucose, 1.5 g of saccharose, and 17 g of water were mixed and stirred until a fine crystalline suspension was formed. The artificial honey/2-AP mixture was diluted with pure artificial honey, and 10 g of each mixture was analyzed according to the extraction procedure above. The actual 2-AP concentration of the commercial standard was determined by RP-HPLC with a chemiluminescent nitrogen detector (CLND) according to Penndorf et al. (2007). GC-MS analysis of 2-AP was performed using the GC-MS system described in Table 22. The GC system was equipped with a TR-FFAP capillary column (30.0 m  $\times$  0.25 mm inner diameter, with a 0.25  $\mu$ m film thickness) from Thermo Scientific (Runcorn, U.K.). Helium was used as the carrier gas with a constant flow of 1 mL/min. The injector temperature was set to 250  $^{\circ}$ C, and a 1  $\mu$ L sample was injected using the pulsed splitless mode. The auxiliary temperature was set to 235  $^{\circ}$ C, and the ion source and quadrupole temperatures were set to 230 and 150  $^{\circ}$ C, respectively. The initial oven temperature was set to 40  $^{\circ}$ C and held for 2 min, then raised at 2.25  $^{\circ}$ C/min to 80  $^{\circ}$ C, finally raised at 30  $^{\circ}$ C/min to 235  $^{\circ}$ C, and held for 5 min. The mass spectrometer was working in EI mode at 70 eV in the scan (mass range of  $m/z$  40.0–300.0) and selected ion monitoring (SIM) mode. For quantitation, the SIM mode was used with the monitoring of the following ions:  $m/z$  111 and 83 (2-AP) and  $m/z$  121 and 79 (TMP). The ions underlined were used for quantitation. The retention time of the analytes was 15.0 min for 2-AP and 17.9 min for TMP, respectively. Data acquisition and evaluation were performed with MSD ChemStation software (Agilent, Germany). Results are expressed as mean values of two separate measurements, except otherwise indicated. Hypothesis testing was performed via a two sample t test with a significance level of 0.01. Intraday variation of 2-AP analysis was investigated using five replicate injections of a 2-AP standard solution.

Interday precision was determined using four calibration standards, which were analyzed during 8 months.

#### 2.4.8 Protein isolation from honey

High molecular-weight (HMW) fractions were isolated from honey either by dialysis or by precipitation with trichloroacetic acid (TCA). For the former approach, ca. 10 g of honey was dissolved in 10 mL of water and transferred to a dialysis tube (MWCO, 14 kDa, Sigma). The samples were dialyzed against distilled water for 2 days with the water changed twice per day. The retentates were then lyophilized and stored at -18 °C. For TCA precipitation, 10 mL of TCA (20%, w/v) was added to 10 g of honey, and the suspension was stored at -20 °C for 30 min after mixing. Following centrifugation (4 °C, 5000 rpm, 10 min), the supernatant was decanted and discarded, and the precipitate was suspended in water (10 mL). After centrifugation (4 °C, 5000 rpm, 10 min), the supernatant was discarded, and the precipitate was washed once more in the same way. Finally, the precipitate was suspended in 5 ml of water lyophilized and stored at -18 °C.

#### 2.4.9 Protein determination

##### Acid precipitates

Proteins extracted via TCA precipitation are denatured and therefore only soluble in detergent buffers. To analyze the protein content of TCA precipitates, a modification (Harrington, 1990) of the Lowry assay (Lowry et al., 1951) was used. Briefly, precipitates were solubilized in sodium dodecyl sulfate solution (1 %) in ultrapure water with a final concentration of 0.3 mg/mL. In a microtiter plate, 50  $\mu$ L of the diluted samples were incubated with 150  $\mu$ L dye solution for 10 min at room temperature. The dye solution consisted of 1 mL  $\text{CuSO}_4 \times 5 \text{H}_2\text{O}$  (0.16 M) and 10 mL of an aqueous solution containing  $\text{Na}_2\text{CO}_3$  (0.2 M), NaOH (0.1 M), potassium sodium tartrate (5.6 mM) and SDS (1 %). After 10 min, 15  $\mu$ L of Folin Ciocalteu's phenol reagent (1:1 with ultrapure water) was added and the mixture was incubated for 45 min at room temperature. Absorbance at 700 nm was measured using a multimode reader Tecan Infinite M200 (Mainz, Germany). Calibration was achieved using  $\gamma$ -globulin, which was precipitated with TCA and thus denatured prior to analysis (according to protein extraction mentioned in section 2.4.8). The denatured  $\gamma$ -globulin was solubilized in SDS (1 %) and the calibration range was 0.08 to 0.8 mg/L. 50  $\mu$ L of calibration solutions were treated like samples described above.

### Dialysis retentates

The protein content of the retentates was calculated as the sum of amino acids measured by amino acid analysis after acid hydrolysis. The amino acid analysis and acid hydrolysis is described in section 2.4.10.

#### 2.4.10 Amino acid determination

##### Free proline

A total of 1 g of honey was dissolved in 10 mL of phosphate buffer (0.1 M, pH 2) and subjected to a column (25×110 mm) filled with ion-exchange resin Dowex 50WX8, 100-200 mesh. The ion-exchange resin was previously activated with 50 mL of HCl (2 mol/L). The amino acids were eluted with 100 mL of a solution of ammoniac (7 mol/L). The eluate was evaporated to dryness, and the dry residue was dissolved in ultrapure water. After lyophilization, the sample was dissolved in 1 mL of lithium citrate buffer (0.12 M, pH 2.2), diluted (1:10), and subjected to amino acid analysis. The analyses were performed using a SYKAM S4300 amino acid analyzer (Fuerstenfeldbruck, Germany) with conditions according to the instructions of the manufacturer. The ninhydrin derivate of proline was detected at 440 nm.

##### Protein-bound amino acids

Acid hydrolysis of protein isolates was performed by adding 2 mL of 6 M HCl to 2-3 mg of the fractions and heating of the mixture at 110 °C for 23 h in a pre-heated oven. Then, 500 µL of the hydrolyzate was evaporated to dryness in a vacuum concentrator (SPD Speed Vac; Thermo Fisher Scientific, Karlsruhe, Germany). The residue was reconstituted in 1 mL of sample buffer for amino acid analysis (0.12 N lithium citrate, pH 2.2). Proteinogenic amino acids were quantitated with a SYKAM S4300 amino acid analyser (Fuerstenfeldbruck, Germany). The effluent was derivatized with ninhydrin, and detection of products was performed with an integrated two-channel photometer ( $\lambda = 440 \text{ nm}, 570 \text{ nm}$ ). External calibration was performed with an amino acid mixture (Sigma-Aldrich, Steinheim, Germany). The injection volume was between 50 and 100 µL. Leucine was taken as an internal reference for the evaluation of amino acid concentrations due to its abundance in the honey protein. Amino acid analysis was also used to calculate the protein content of HMW isolates obtained by dialysis and the efficiency of enzymatic hydrolysis. The release of amino acids during enzymatic hydrolysis was calculated by regarding the release during acid hydrolysis as 100%.

#### 2.4.11 Fluorescence measurement of honey proteins

To analyze fluorescence characteristics, 1 mg of protein precipitate was solubilized in 1 mL of 0.1 M sodium phosphate buffer, pH 6.8, containing 6 M urea, 0.1 M sodium chloride, and 0.1% 3-[(3-cholamidopropyl)-dimethylammonium]-1-propanesulfonate. Ultra-sonication for 15 min was used to completely solubilize the precipitates. The solutions were diluted 1:10 with buffer and 200  $\mu$ L were transferred to a black microtiter plate (Brand, Germany). The hydrolyzed precipitates were directly diluted 1:10 with ultrapure water and subsequently analyzed. Fluorescence intensities were measured at  $\lambda_{\text{ex}} = 350$  and  $\lambda_{\text{em}} = 450$  nm using a multimode reader Tecan Infinite M200 (Mainz, Germany).

#### 2.4.12 Size exclusion chromatography of honey proteins

Size exclusion chromatography was performed using the HPLC system 1 (see Table 22). Separation of the samples was achieved using a Superdex 200 10/300 GL column (GE Healthcare Bio-Sciences AB, Uppsala, Sweden). Analysis was carried out at room temperature and flow rate was set to 0.5 mL/min. The elution was performed isocratically for 60 min with the 0.1 M phosphate buffer system which was also used for fluorescence measurement. 50  $\mu$ L of the samples were injected with a protein concentration of 5 mg/mL. Prior to analysis, samples were either solubilized in elution buffer only or incubated at 6 °C in phosphate buffer with 1% dithiothreitol (DTT) over night. Detection was achieved by monitoring UV absorbance at 220 nm. The relative peak areas were calculated by relating the respective peak area to the total area under the curve. Calibration of molecular size was achieved by comparing the elution volume of protein standards with the elution volume of the samples. Protein standards used for calibration were ferritin (440 kDa), catalase (240 kDa), glucose oxidase (160 kDa), ovalbumin (43 kDa) and lysozyme (15 kDa).

#### 2.4.13 Enzymatic hydrolysis of proteins

This was performed according to Hellwig et al. (2015). Briefly, 2-3 mg of the precipitates were suspended in 1 mL HCl (0.02 M) and 50  $\mu$ L pepsin (1 U/sample) in 0.02 M HCl were added. After 24 h, 250  $\mu$ L of TRIS buffer (2 M, pH 8.2) and 50  $\mu$ L of pronase E (400 U/sample) were added. After 24 h, 5  $\mu$ L aminopeptidase (0.4 U/sample) and 10  $\mu$ L prolidase (1 U/sample) were added. The samples were further incubated for 24 h. All incubations were performed at 37 °C. A blank, containing only digestive enzymes but no honey proteins, was included.



#### 2.4.14 Analysis of Maillard reaction products via HPLC-MS/MS

Protein-bound MRPs were quantitated on an HPLC-MS/MS system consisting of a binary pump (G1312A), an online degasser (G1379B), an autosampler (G1329A), a column thermostat (G1316A), a diode array detector (G1315D), and a triple-quadrupol mass spectrometer (G6410A; all from Agilent Technologies, Böblingen, Germany). At the ESI source, nitrogen was utilized as the nebulizing gas (gas flow, 11 L/min; gas temperature, 350 °C; nebulizer pressure, 35 psi), and the capillary voltage was at 4000 V.

For chromatographic separation, the column Zorbax 100 SB-C18 (2.1 × 50 mm, 3.5 µm; Agilent) was used at a column temperature of 35 °C. HPLC solvent A was a solution of 10 mM nonafluoropentanoic acid (NFPA) in water, and solvent B was a solution of 10 mM NFPA in acetonitrile. The solvents were pumped at a flow rate of 0.25 mL/min in the gradient mode (0 min, 5% B; 15 min, 32% B; 16 min, 85% B; 20 min, 85% B; 21 min, 5% B; 27 min, 5% B). The injection volume was 5 µL. Data were acquired and evaluated with the software Mass Hunter B.02.00 (Agilent).

The standard addition method was used for quantitation of MRPs. All samples were analyzed at least in duplicate. In the sample without addition, 100 µL of enzymatic hydrolyzate was mixed with 20 µL of water. In the second run, 100 µL of hydrolyzate was mixed with 10 µL of water and 10 µL of a standard solution. In the last run, 100 µL of hydrolyzate was mixed with 20 µL of standard solution. All samples were centrifuged before injection (10,000 rpm, 10 min). In the standard solution added to Manuka honeys, *N*-ε-fructosyllysine (87.5 µg/mL), *N*-ε-maltosyllysine (35.2 µg/mL), CML (13.4 µg/mL), CEL (19.9 µg/mL), formyllysine (0.4 µg/mL), MG-H1 (5.0 µg/mL), maltosine (0.11 µg/mL), and pyrrolidine (2.0 µg/mL) were dissolved in water. In the standard solution added to non-Manuka honeys, the same concentrations were used, except for CEL (1.0 µg/mL), and MG-H1 (0.25 µg/mL).

#### 2.4.15 Model studies on 2-acetyl-1-pyrroline formation in honey

A commercial non-manuka multifloral honey from Germany was mixed with MGO alone (100 mg/kg, labeled as “low”, or 500 mg/kg, labeled as “high”, respectively) or MGO and DHA in a 1:2 ratio (100 and 200 mg/kg, labeled as “low”, or 500 and 1000 mg/kg, labeled as “high”, respectively). The samples were stirred vigorously and stored in the dark at room temperature and 37 °C. The storage temperature of 37 °C was chosen to simulate accelerated ripening and to study chemical reactions that occur during longer storage. Samples were taken after 0, 2, 4, 8, and 12 weeks of storage. A control (multifloral honey without added MGO)

was stored under the same conditions, and samples were taken after 0, 4, and 12 weeks of storage. The samples were analyzed according to the extraction procedure mentioned in section 2.4.7.

#### 2.4.16 Model studies on protein reactions in honey

Commercial non-manuka honey (multifloral honey from Germany) was spiked with MGO and DHA in a 1:2 ratio (100 and 200 mg/kg labeled as “low” and 500 and 1000 mg/kg labeled as “high”). The samples were stirred vigorously and stored at room temperature and 37 °C. The elevated temperature was chosen to simulate accelerated ripening and to study chemical reactions occurring during longer storage. Samples were taken after 1, 14, 35, 56 and 84 days. Protein extraction and fluorescence measurement of the samples were performed according to the procedure mentioned above.

#### 2.4.17 Model studies on Maillard reactions in honey

Commercial manuka honey (Manuka Health MGO 30) was spiked with MGO and DHA in a 1:2 ratio (500 and 1000 mg/kg). The sample was stirred vigorously and stored at 30 °C. The elevated temperature was chosen to simulate accelerated ripening and to study chemical reactions occurring during longer storage. Samples were taken after 0, 14, 42, 70 and 112 days. A control (manuka honey MGO 30 without added MGO and DHA) was stored under the same conditions, and samples were taken after 0, 4, 14, 42, 70 and 112 days of storage. The proteins were extracted according to 2.4.8, enzymatically hydrolyzed according to 2.4.13 and MRP were analyzed according to 2.4.14.

#### 2.4.18 Rheological studies

##### Thixotropy loop

Prior to analysis the honey samples were kept at room temperature over night to warm up. The rheological properties were studied by Haake Viscotester iQ (Thermo Scientific) rheometer using a parallel plate system (35mm diameter) at a gap of 1 mm. The rheological measurement data were analysed with rheometer software RheoWin. The honey samples were placed in the rheometer measuring system, then relaxed and equilibrated for 2 min to obtain required temperature. The temperature was set at 20 °C and kept constant during the measurement. The curves were obtained in CR mode with shear rate increasing from 1 to 100

$s^{-1}$  in 180 s, followed by a plateau at  $100 s^{-1}$  for 180 s and finally decreasing the shear rate from 100 to  $1 s^{-1}$  in 180 s.

#### Creep recovery

The same rheometer instrument was used as described in the section above. The honey samples were placed in the rheometer measuring system, then relaxed and equilibrated for 2 min to obtain required temperature. The temperature was set at  $20\text{ }^{\circ}\text{C}$  and kept constant during the measurement. The curves were obtained in CR mode with shear rate kept at  $0.5 s^{-1}$  for 60 s, followed by an increase to a plateau at  $50 s^{-1}$  for 30 s and finally decreasing the shear rate back to  $0.5$  to  $1 s^{-1}$  and keeping it for 300 s.

## 2.5. Results and discussion

Manuka honey contains the carbonyl compounds methylglyoxal (MGO) and dihydroxyacetone (DHA) in amounts up to 700 and 1600 mg/kg, respectively, whereas conventional honeys contain only 5 to 10 mg/kg of MGO and DHA (Atrott et al., 2012). MGO and DHA are highly reactive substances, leading to a variety of unique chemical reactions during honey maturation and storage. This chapter deals with MGO-derived reactions in manuka honey and the possibility to use this reaction to distinguish manuka honey from other honey varieties.

### 2.5.1 Identification and quantification of 2-acetyl-1-pyrroline in manuka honey

Besides MGO and DHA, manuka honey also contains amino compounds like amino acids. Proline is the most abundant amino acid in honey, accounting for 260–890 mg/kg, which represents 70% of the total free amino acids (Bernal et al., 2005). Despite the unusual ratio of highly reactive carbonyls and amino acids, there are no studies available concerning Strecker reactions in manuka honey. Therefore, the aim of this study was to investigate the possible occurrence of 2-acetyl-1-pyrroline (2-AP), a direct reaction product of proline and MGO, in manuka honey and its dependency upon the MGO content. The studies presented here were published in the *Journal of Agricultural and Food Chemistry* (Rückriemen et al., 2015). The volatile molecule 2-acetyl-1-pyrroline (2-AP) originates from the reaction of MGO with the amino acids ornithine or proline (Hofmann and Schieberle, 1998) and is the main aroma compound in aromatic rice varieties and bread crust (Buttery et al., 1986; Schieberle and Grosch, 1987; Grimm et al., 2011). Its smell is described as “popcorn-like” or “roasted”, with an odor threshold of 0.1 µg/kg (Belitz H.-D., Grosch W., 2008). Reactive carbonyl species, such as MGO, play an important role in flavor chemistry (Wang and Ho, 2012). This process is affected by water activity, temperature, and pH value (Hellwig and Henle, 2014). The aim of this study was to investigate whether 2-AP, a specific flavor compound formed from MGO and proline, is present in manuka honeys from New Zealand. Identification and quantitation of 2-AP in manuka honey was achieved using GC-MS based on a method recently described in the literature for 2-AP analysis (Wu et al., 2009). For sample preparation, a crucial step for reliable quantitation of 2-AP, solid-phase microextraction (SPME), or solvent extraction methods are reported (Schieberle and Grosch, 1987; Wu et al., 2009; Grimm et al., 2011). Because 2-AP formation in manuka honey is probably enhanced by a high temperature, an

extraction procedure using dichloromethane without heating was chosen (see 2.4.7). Furthermore, concentration steps like drying with nitrogen were avoided to prevent a loss of 2-AP during sample preparation. 2,4,6-Trimethylpyridine (TMP) was used as an internal standard to check the recovery during the extraction procedure. Comparing peak areas for 2-AP standard samples extracted from aqueous solutions or from an artificial honey matrix, the mean recovery of 2-AP resulted in an estimated 60%. Therefore, quantitation was carried out via external matrix calibration, using a synthetic 2-AP standard in artificial honey. The actual 2-AP concentration of the commercial standard was checked with RP-HPLC and chemiluminescent nitrogen detection (CLND) to be 83.3% of the specification given by the supplier. The actual concentration of the standard was used for calculation. A regression coefficient  $R^2$  of 0.998 was calculated for the linear calibration range from 0.1 to 2.0 mg/kg. The limit of detection (LOD) was 0.04 mg/kg, and the limit of quantitation (LOQ) was 0.09 mg/kg. LOD and LOQ were calculated on the basis of the signal-to-noise-ratio. Inter- and intraday precisions were 3.1 and 6.1%, respectively (see 2.4.7 for validation parameters). 2-AP was unequivocally identified in commercial samples of manuka honey by comparing retention time and corresponding mass spectra of honey samples and standard solutions (panels A and C of Figure 35). The comparison of the fragmentation pattern and the characteristic ratio of the quantifier ion to the qualifier ion ( $m/z$  83 and 111, respectively) of the 2-AP standard and the 2-AP peak in honey yields identical relative intensity ratios.

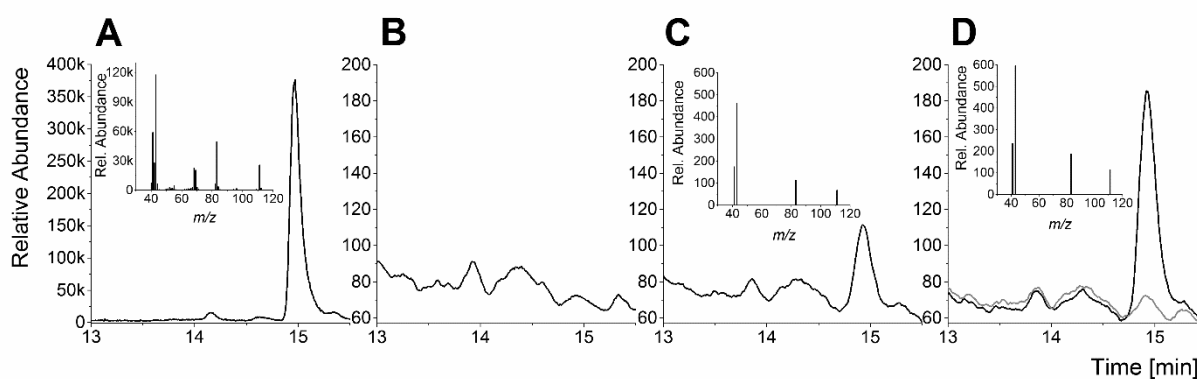


Figure 35: GC-MS data for identification and quantitation of 2-AP. (A) synthetic standard solution, (B) manuka honey, (C) lime honey, (D) artificial honey spiked with proline and MGO (black line) and DHA (grey line) incubated for 20 weeks at 37 °C (D)

The hypothesis, that 2-AP in manuka honey results from the reaction of MGO and proline was confirmed by significantly smaller signals of 2-AP in non-manuka honeys without MGO (Figure 35B) and the detection of 2-AP in an artificial honey containing MGO and proline

after 20 weeks of incubation (Figure 35D). For 11 commercially available manuka honeys, amounts of 2-AP ranging from 0.08 to 0.45 mg/kg were measured (Figure 36A). In contrast to this, the majority of non-manuka honeys analyzed in this study contained 2-AP only in very small amounts between 0.08 and 0.11 mg/kg. However, some aromatic non-manuka honeys, namely, buckwheat, lime, and thyme honey, contained 2-AP in concentrations ranging between 0.20 and 0.31 mg/kg. According to the literature, 2-AP has been found in different sorts of food as an aroma active compound. The concentrations vary between 78  $\mu\text{g}/\text{kg}$  for white-bread crust and 0.8 mg/kg for cooked rice (Buttery et al., 1986; Schieberle and Grosch, 1987). Concerning honey, 2-AP has already been detected in lime honey from the linden tree (Blank et al., 1989). The authors pointed out that 2-AP is an important odorant of linden honey but did not report on quantitative amounts of 2-AP. Interestingly, no 2-AP was detected in the blossoms of the linden tree, what supports the hypothesis that 2-AP originates from reactions in the honey matrix. The 2-AP concentration of manuka honey with a MGO concentration below 250 mg/kg is comparable to the non-manuka honeys (see Figure 36A, manuka group 1). However, the concentration of 2-AP in manuka honeys with a MGO concentration above 250 mg/kg was significantly increased in comparison to the non-manuka group (Figure 36A, manuka group 2). The average amount of 2-AP in manuka honeys with MGO contents above 250 mg/kg was 0.36 mg/kg, and the average amount of 2-AP in non-manuka honeys was 0.16 mg/kg.

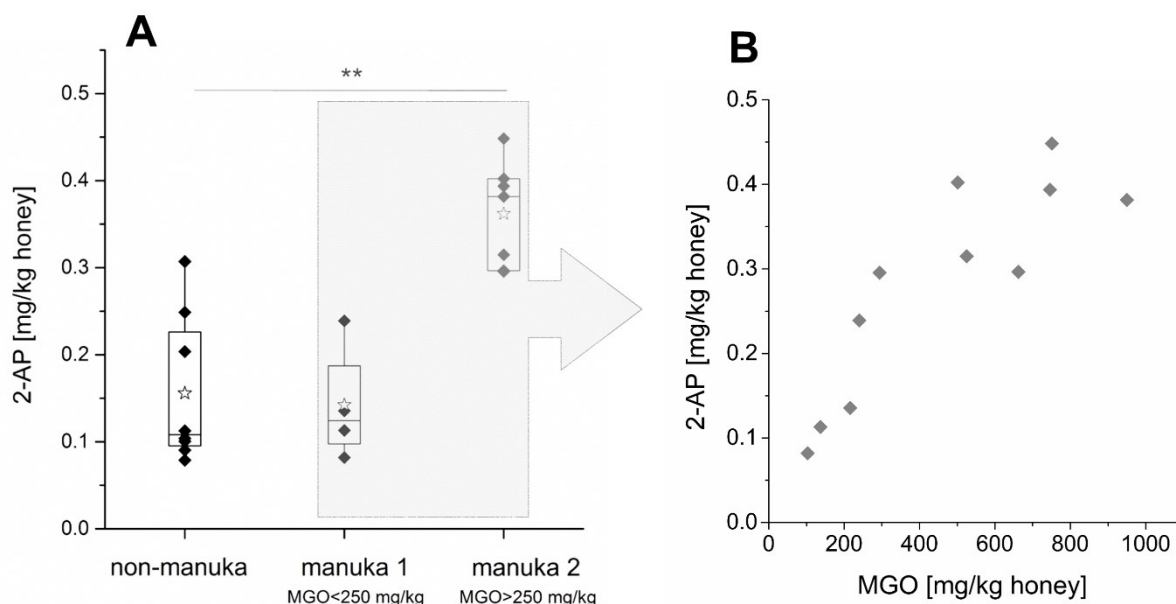


Figure 36: (A) 2-AP concentration of commercial samples of non-manuka honey (n=8), manuka honey with MGO below 250 mg/kg (manuka 1) (n=4) and above 250 mg/kg (manuka 2) (n=7), stars indicate average value for each group, (B) correlation of 2-AP concentration and MGO content of manuka honeys (group 1 and 2)

For the manuka honey samples, the 2-AP content increased with increasing MGO concentrations up to a MGO value of approximately 500 mg/kg honey (see Figure 36B). For concentrations of 600–1000 mg of MGO/kg of honey, no further increase of 2-AP was found. Proline is the most abundant amino acid in honey, accounting for 260–890 mg/kg, which represents 70% of the total free amino acids. The analysis of the proline concentration of the studied honeys showed no significant difference between the non-manuka and manuka honeys with varying MGO contents. The proline concentration ranged between 200 and 540 mg/kg and did not correlate with the MGO content. In fact, MGO appears to be the crucial factor for 2-AP formation. The observation that MGO contents between 600 and 1000 mg/kg do not lead to a further increase of 2-AP in manuka honeys could be explained by competitive reactions. MGO can react with other honey compounds or with another MGO molecule to form adducts or aroma-active compounds, such as furaneol, respectively. To assess whether storage of non-manuka honey containing artificially added MGO or DHA results in the formation of 2-AP, a commercial multifloral honey was spiked with MGO alone or a 1:2 mixture of MGO and DHA, respectively, and stored at room temperature and 37 °C for 12 weeks.

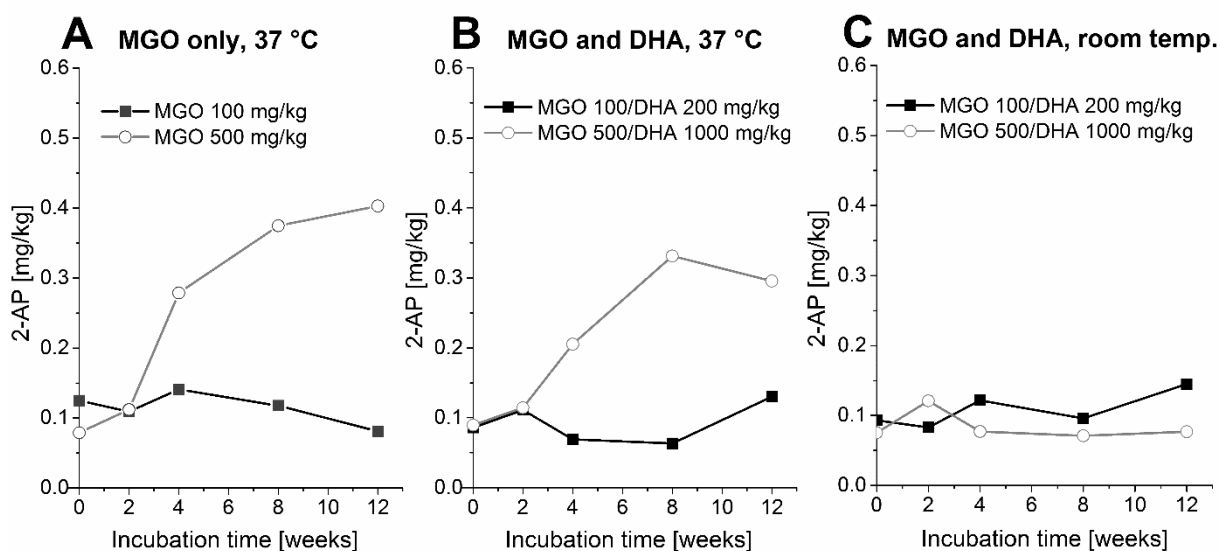


Figure 37: 2-AP formation in a non-manuka multifloral honey with (A) added MGO stored at 37 °C, (B) added MGO and DHA stored at 37°C and (C) added MGO and DHA stored at room temperature (n=2 for each time point and sample).

Panel A and B of Figure 37 show the 2-AP concentration depending upon the incubation time. When high amounts of MGO (500 mg/kg) were added to the honey, 2-AP significantly

increased after 4 weeks of storage at 37 °C. After 12 weeks, the 2-AP concentration reached the amount that was quantitated in the commercial manuka honey samples with high MGO contents, followed by no further increase. No increase of 2-AP was found during storage of non-manuka honey with artificially added MGO and DHA at ambient temperature (Figure 37C) and non-manuka honey without MGO (ambient temperature and 37 °C; data not shown). There was also no increase in 2-AP when low MGO concentrations (100 mg/kg) were added to non-manuka honey and stored at an elevated temperature for 12 weeks (see Figure 37 A and B). This is in accordance with the 2-AP amounts of commercial manuka honeys containing MGO below 250 mg/kg. The average 2-AP content of these samples was 0.14 mg/kg. The non-manuka honey with artificially added low amounts of MGO had approximately the same amount of 2-AP, which did not increase after storage. This indicates that a “threshold level” of MGO of approximately 250 mg/kg is necessary to initiate a reaction of proline and MGO and significantly increase the 2-AP content in manuka honey. Competitive reactions as a possible reason for the disproportionate conversion of MGO and proline to 2-AP were discussed above. The 2-AP concentration in non-manuka honey was not influenced by the addition of DHA and subsequent storage (Figure 37A and B). This indicates that DHA is not a promoter of 2-AP formation. For the spiked honey samples, which were stored for 8 weeks or longer at 37 °C, a significant increase in the concentration of HMF in addition to the formation of 2-AP was observed. At the first day of storage, the honeys had a mean HMF value of 10 mg/kg. Storage at 37 °C for 12 weeks resulted in a HMF increase up to 80 mg/kg, whereas samples stored at room temperature contained a maximum HMF level of 13 mg/kg after 12 weeks. HMF is used as a quality parameter of honey and should not exceed 40 mg/kg (Codex Alimentarius Commission, 2001). All commercial manuka honeys in this study were below this threshold level. This result points to the fact, that following “artificial” spiking of a non-manuka honey with MGO, 2-AP concentrations do only increase during storage at elevated temperatures, which also leads to increasing amounts of HMF. Therefore, 2-AP might be an interesting indicator to control the storage conditions and the quality of manuka honey. High amounts of 2-AP, as a result of high MGO levels, together with an increased concentration of HMF may point to a fraudulent addition of MGO and storage at increased temperatures for “artificially” producing high-price manuka honey products. A manuka honey with a high MGO content together with a high 2-AP concentration and a low HMF level has likely been stored at low temperatures over a longer time period. This “natural” ripening process cannot be simulated by MGO addition followed by high



temperature storage. Thus, in addition to MGO and DHA, 2-AP as a direct reaction product of MGO and proline could be a suitable parameter to characterize the quality of manuka honey.

According to the literature, the storage of manuka honey initially leads to MGO increase as a result of continuous formation from DHA, followed by a MGO decrease, probably as a result of reactions of MGO with other honey components (Atrott et al., 2012; Grainger et al., 2016a).

This study demonstrates that 2-AP is one of the reaction products which can be formed from MGO during storage. Nevertheless, the conversion rate from MGO to 2-AP is very low and the reaction of MGO with the amino acid proline can only explain a small percentage of MGO loss. Hence, other reactions leading to unique MGO-derived reactions products could be mainly responsible for MGO decrease during storage. In proteins, many amino groups are available for the reaction with the electrophile carbonyl compounds. The next section will focus on reactions of MGO with honey proteins.

### 2.5.2 Reactions of carbonyl compounds with honey proteins

Proteins are minor compounds in honey and can be plant-derived like catalase (Weston, 2000) or bee-derived like major royal jelly protein 1 (MRJP1) (Won et al., 2008). Proteins can quickly react with reducing sugars or dicarbonyl compounds to form Maillard reaction products. Previous reports have shown that MGO in manuka honey can modify honey proteins and influence its bioactive effect (Majtan et al., 2012). From a chemical point of view, these reactions are interesting, because they might explain the fate of MGO during honey storage. The unique chemical reactions of MGO may be useful to differentiate manuka honey from non-manuka honey. This section will deal with MGO mediated reactions with proteins and will focus on unspecific cross-linking reactions on the one hand (2.5.2.1 and 2.5.2.2) and specific protein-bound amino acid side chain modifications on the other hand (2.5.2.3).

#### 2.5.2.1 Cross linking of honey proteins

The results of the following sections 2.5.2.1 and 2.5.2.2 are partly originating from the experimental work of master student Christoph Hohmann and were primarily published in his master thesis (Hohmann, 2015) and in *Food Research International* (Rückriemen, Hohmann, et al., 2017). Proteins from food matrices can be extracted with various techniques such as ultracentrifugation or dialysis. The aim of this study was to analyze the molecular size of

honey proteins. Therefore it was important that the isolates were rich in protein and do not contain high amounts of other honey-derived compounds such as polyphenols or sugars. As methods for protein isolation from honey, dialysis and acid precipitation were tested in this study. Due to the simplicity and the time saving when acid precipitation was performed, the studies dealing with the molecular size and the fluorescence properties of honey proteins were conducted using TCA precipitates of honey. The obtained isolates were analyzed for their protein content, which was  $\geq 92\%$  (data not shown). To assess the molecular size of honey proteins, honey precipitates were analyzed with size exclusion chromatography with subsequent UV detection at 220 nm. A typical chromatogram of manuka proteins and non-manuka proteins is shown in Figure 38A. Manuka honey proteins were shifted towards higher molecular weights ( $> 510$  kDa) compared to the non-manuka honey proteins, which were distributed mainly between 510 to 100 kDa. For this study, the high molecular weight fraction (HMW) with a molecular size  $> 510$  kDa was of special interest since it is probably formed by cross-linking reactions. To rule out that the absorption increase of manuka honey protein was caused by hyperchromic effects, UV absorption of the protein precipitates was measured without chromatographic separation and no correlation of total UV absorption and MGO content of the honeys was found (data not shown). The shift of manuka honey proteins to higher molecular weights was described earlier. Majtan et al. (2012) reported that the antibacterial peptide bee defensin 1 experiences a molecular shift from 55 kDa to around 60 kDa in manuka honey. Nevertheless, the authors studied single protein structures. The high molecular weight fraction presented in the current work is more likely caused by cross-linking reactions of more than one protein. The principle of separation for size exclusion chromatography is based on the hydrodynamic diameter of molecules. For polymers of the same type (e.g. fibrous or globular proteins), the hydrodynamic diameter is proportional to their molecular mass. For calibration, only globular proteins were used, since the molecular structure of honey protein complexes was expected to be globular as well. Nevertheless, calibration with natural proteins provides an appropriate estimation for the molecular size of the analyzed proteins, but cannot be considered as accurate. Besides, proteins were extracted from honey by acid precipitation. During acid treatment of proteins, amino acid chains are protonated, which triggers protein unfolding by disrupting the electrostatic interactions that stabilize the native conformation of proteins. Thereby, protein oligomers can form which may not recover their natural conformation after solubilisation (Rajalingam et al., 2009). To enhance solubilisation of polymerised proteins to prevent overestimation of protein size, a

buffer containing 6 M urea was used (see 2.4.11). More precise statements concerning the size of honey protein complexes could be made with electron microscopy. The distribution of the relative amount of high molecular weight protein compared to total protein is shown in Figure 38B. Manuka honey proteins have an average amount of HMW fraction to total protein of 34 %. Most of the honeys without MGO (non-manuka) did not exhibit a large signal at high molecular weights. Nevertheless, some non-manuka honeys have an amount of high molecular weight fractions similar to the manuka honeys. The average amount of HMW fraction of all non-manuka proteins was 28 %. Besides of MGO-induced reactions, proteins can aggregate due to disulfide bonds. Thiol groups in honey proteins can be oxidized, e.g. with oxidizing reagents such as hydrogen peroxide present in honey, and form disulfide bonds. Therefore, honey proteins were incubated with dithiothreitol (DTT) prior to SEC. Dithiothreitol reduces disulfide bonds to thiol groups, thus reversing disulfide-derived crosslinking in proteins. With DTT, non-manuka honey proteins had an average amount of HMW fraction of 21 %, whereas manuka honey proteins contained 36 % of HMW fraction. The HMW fraction of non-manuka honey proteins decreased by 7% after incubation with DTT since disulfide crosslinks were reduced. The remaining HMW fraction could be originated from the reaction of honey proteins and carbonyl compounds, e.g. 3-deoxyglucosone, which are present in different types of honeys (Weigel et al., 2004).

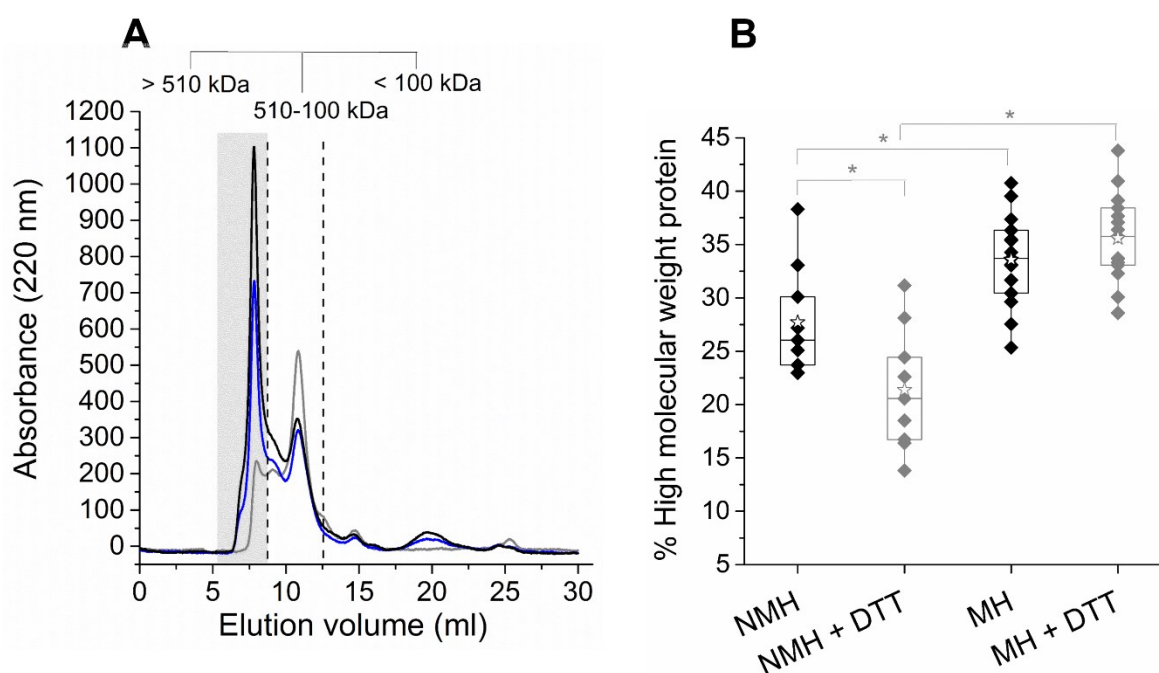


Figure 38: (A) Size exclusion chromatography with UV detection at 220 nm of proteins isolated from manuka honey with high MGO content (MGO 900 mg/kg; black line), low MGO content (MGO 118 mg/kg; blue line) and canola honey (MGO 10 mg/kg; grey line). Calibration was achieved by analyzing natural proteins with defined molecular weights. Grey box indicates high molecular weight

protein. (B) Relative amount of high molecular weight protein fraction in non-manuka honey (NMH) and manuka honey (MH) without addition of DTT (black) and after addition of DTT (grey). Stars indicate the average value of each group.

In contrast, HMW fraction of manuka honey protein apparently increased after incubation with DTT. This could be due to the loss of low molecular weight fragments with disulfide bonds, which contributed to the total amount of protein. A decrease of the total area under the curve, but a stable signal of the HMW fraction would result in an apparent increase of HMW fraction. Moreover, it is possible that thiol groups in the manuka honey protein are directly involved in formation of high-molecular weight fragments. Thus, the incubation with DTT does not influence manuka honey protein, since thiols did not form disulfide bonds, but might have reacted with MGO. The results lead to the conclusion that HMW fraction in manuka honey is mainly caused by MGO-derived reactions, whereas HMW fraction in non-manuka honey is a result of disulfide bonds. The formation of HMW proteins can lead to characteristic changes in their absorption properties. Therefore, the next section will focus on the influence of protein cross-linking on the fluorescence properties of honey proteins.

#### 2.5.2.2 Fluorescence properties of honey proteins

During the advanced stage of Maillard reaction, proteins are modified into colored and fluorescent compounds. Typical fluorescence excitation and emission wavelength to study these changes in food are  $\lambda_{\text{ex}} = 340\text{-}370$  and  $\lambda_{\text{em}} = 420\text{-}450$  (Morales and Jiménez-Pérez, 2001; Schmitt et al., 2005; Matiacevich and Pilar Buera, 2006). To detect the wavelength with the highest intensity for the honey protein matrix, the purified honey proteins (acid precipitates) were dissolved in phosphate buffer containing 6 M urea and the fluorescence excitation spectra were recorded at emission wavelength 440 nm with excitation wavelengths between 230 to 420 nm (2 nm step size). A maximum excitation wavelength of 350 nm was observed. With the excitation wavelength set at 350 nm, emission spectra were recorded between 380 to 600 nm (2 nm step size) and an emission maximum was found to be at 450 nm (see Figure 39). According to these results, the wavelength pair  $\lambda_{\text{ex}} = 350$  and  $\lambda_{\text{em}} = 450$  nm was used for further studies.

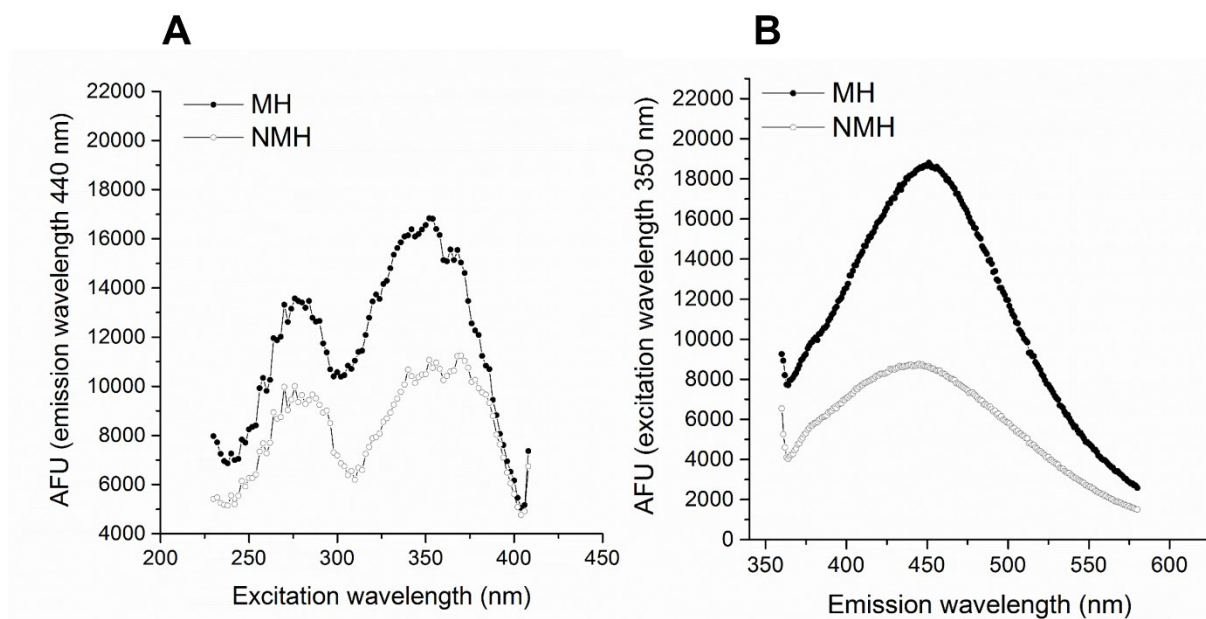


Figure 39: (A) Fluorescence excitation spectrum of manuka honey protein (MH) and non-manuka honey protein (NMH), recorded at emission wavelength 440 nm with excitation wavelengths between 230 to 420 nm, (B) Fluorescence emission spectrum of manuka honey protein (MH) and non-manuka honey protein (NMH), recorded at excitation wavelength 350 nm with emission wavelength between 380 to 600 nm

Non-manuka and manuka honey proteins were extracted and screened for their fluorescence intensities at  $\lambda_{\text{ex}} = 350$  and  $\lambda_{\text{em}} = 450$  nm. Non-manuka honey protein displayed fluorescence intensities between 23 000 to 71 000 AFU per mg precipitate. The highest AFU values were obtained for heather or chestnut honey protein. Isolated manuka honey protein gave fluorescence intensities from 24 000 to 145 000 AFU per mg precipitate. For proteins isolated from manuka honey, AFU correlated with the corresponding MGO contents of the honeys (see Figure 40A). The dicarbonyl compound MGO can react with proteins or amino acids to form fluorescent products (Riley and Harding, 1995), such as argpyrimidine, which results from the reaction of MGO and the amino acid arginine (Shipanova et al., 1997). However, the maximum fluorescence excitation and emission wavelengths of argpyrimidine are situated at shorter wavelengths as compared to the fluorescence maxima in our study ( $\lambda_{\text{ex/em}} = 320/380$  for argpyrimidine). Nevertheless, specific AGE could potentially be formed in manuka honey and will be discussed in section 2.5.2.3. Besides specific structures, protein fluorescence can be caused by protein crosslinking, reactions at the peptide backbone or changes in the tertiary structure (Sajithlal et al., 1998). To assess how much of the honey protein fluorescence was caused by protein-protein interactions compared to single fluorophore structures, honey proteins were enzymatically hydrolyzed. Fluorescence measurement of the hydrolyzed honey

protein precipitates resulted in a decrease of the slope of the regression equation by 50% (see Figure 40B).

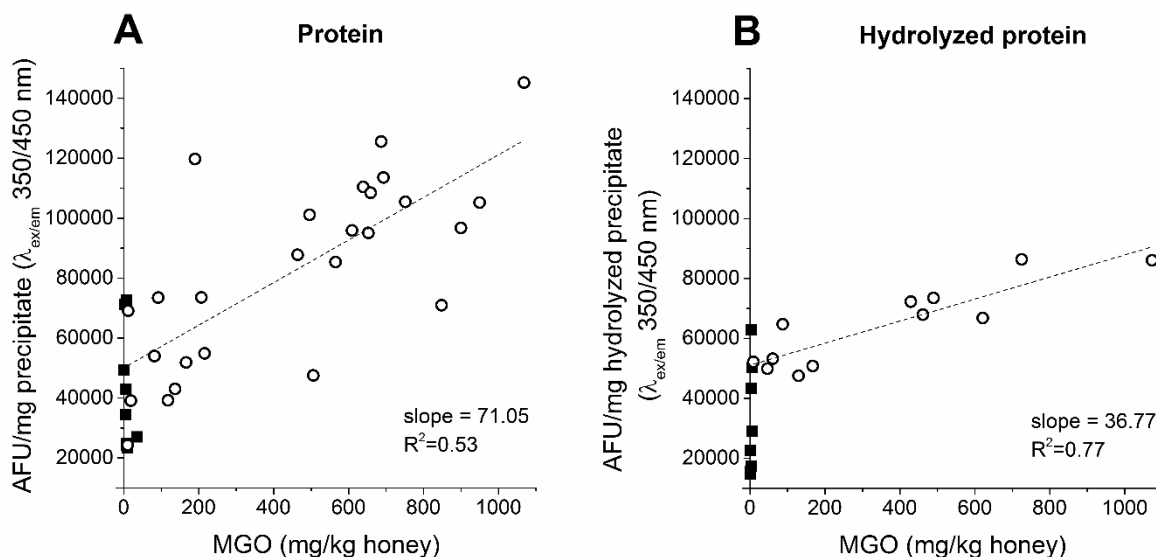


Figure 40: Fluorescence intensities before (A) and after (B) enzymatic hydrolysis of non-manuka honey protein precipitate (■) and manuka honey protein precipitate (○) against honey MGO concentration. Fluorescence of the precipitates was recorded at an excitation wavelength of 350 nm and an emission wavelength of 450 nm. MGO content was analyzed via RP-HPLC-UV.

This points to the fact that fluorescence of intact honey proteins is equally caused by specific fluorophores, such as glycated amino acids on the one hand, and interactions in the protein network on the other hand. When manuka honey proteins were treated with DTT, which reduces disulfide bonds, no decrease of HMW fraction was detectable (see Figure 38 in section 2.5.2.1). This might be due to the formation of thiol-MGO adducts, which may be fluorescent or form transient fluorophores due to the interaction with peptide bonds. Enzymatic cleavage of the protein and breakup of the network, could lead to the decrease which was observed for the hydrolyzed protein. The higher fluorescence intensities of manuka honey protein compared to non-manuka honey protein is not only dependent on MGO content, but also on storage conditions. The extent of Maillard reaction depends on incubation time and water content and it occurs preferentially at elevated temperatures. The honeys used in this study were commercial samples and stored at 6 °C in our lab. There is no information available about storage conditions prior to purchase. Variations in storage conditions could lead to higher variances in the fluorescence to MGO plot. To elucidate whether protein fluorescence in the range observed for manuka honeys can be induced by adding synthetic MGO and DHA to honey, a non-manuka honey was spiked with low or high amounts of

MGO and DHA (MGO/DHA 100/200 and 500/1000 mg/kg respectively) and stored at room temperature and 37 °C for 84 days. At certain time points, samples were taken and proteins were extracted. Fluorescence measurements were performed and the results are shown in Figure 41.

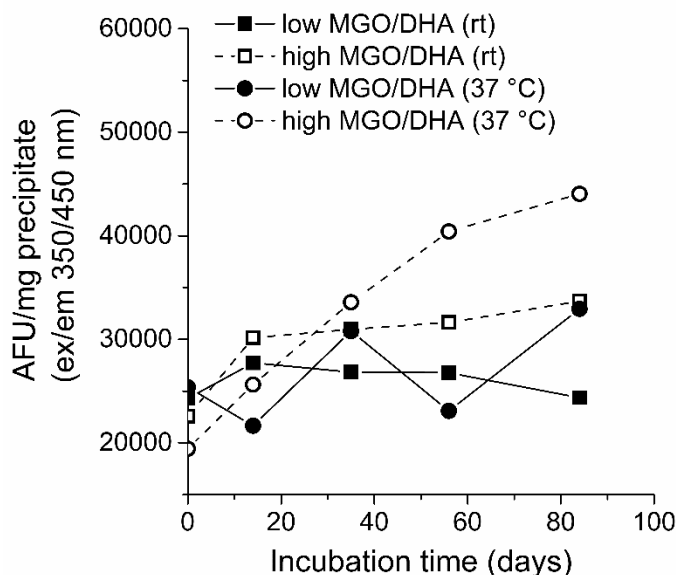


Figure 41: Fluorescence intensities of protein isolated from honey samples with added MGO and DHA stored at room temperature and 37 °C for 84 days. The label “low” corresponds to 100 and 200 mg/kg of MGO and DHA and “high” to 500 and 1000 mg/kg of MGO and DHA, respectively.

The storage experiment showed that fluorescence intensity increases from 20 000 to 40 000 AFU per mg precipitate only when high amounts of MGO and DHA are added to the honey and the honey is stored at 37 °C. In contrast, manuka honey protein with similar MGO concentrations as measured for the original honey yielded approximately 80 000 AFU/mg precipitate. Chemical reactions in the honey matrix are rather slow, because of its low water activity. Hence, the formation of fluorescent proteins takes either long time or requires elevated temperatures. This leads to the conclusion that protein fluorescence of manuka honey is uniquely formed during honey maturation from the nectar and cannot be achieved by artificially spiking a matured honey with MGO and DHA and subsequent storage.

A recent study which analyzed fluorescence properties of manuka honey, reported manuka-specific fluorescence at  $\lambda_{\text{ex}} = 330$  and  $\lambda_{\text{em}} = 470$  nm (Bong et al., 2016). The same research group claimed that 3,6,7-trimethylmazine, also called lepteridine, is responsible for this honey-derived fluorescence (Lin et al., 2017). According to our results, since fluorescence reading is performed with the original, non-extracted honey, the fluorescence measured by the

authors is also at least partially caused by MGO-derived reactions in honey proteins. A more accurate picture of the progress of Maillard reaction at honey proteins can be achieved when proteins are extracted from honey and are subsequently analyzed with fluorescence reading. Moreover, the Maillard reaction can be studied by analyzing representative compounds which are formed during glycation of proteins, which will be discussed in section 2.5.2.3.

### 2.5.2.3 Maillard reaction products in honey proteins

After fluorescence measurement and detection of an HMW fraction in manuka honey proteins, it is likely that the abundance of MGO in manuka honey also results in the formation of specific protein-bound Maillard reaction products (MRP). Therefore, proteins from twelve manuka and eight non-manuka honeys were isolated by dialysis (see 2.4.8). The proteins were enzymatically hydrolysed and subsequently analysed with LC-MS/MS for eight Maillard reaction products. The study was initiated by Dr. Michael Hellwig and his master student Daniel Sandner and was expanded in cooperation with me later on. The results of the study were published in *Journal of Agricultural and Food Chemistry* (Hellwig et al., 2017).

The Maillard reaction products which were analysed during the investigation were the Amadori products *N*- $\epsilon$ -fructosyllysine and *N*- $\epsilon$ -maltulosyllysine, which arise from the reaction of the  $\epsilon$ -amino group of lysine with glucose and maltose, respectively. Moreover, the advanced stage Maillard reaction products carboxymethyllysine (CML), carboxyethyllysine (CEL), pyrroline, formyllysine, maltosine, and methylglyoxal-derived hydroimidazolone 1 (MG-H1) were quantified, which arise from the reaction of amino or guanidine groups of proteins and 1,2-dicarbonyl compounds. The summary of the study presented here will focus on protein-bound MRP, which are remarkably increased in manuka honeys compared to non-manuka honeys, namely MG-H1 and CEL. Concentrations of all other quantified MRP can be found in the published paper (Hellwig et al., 2017). Also, for method validation parameters and synthesis of reference compounds please refer to the published manuscript.

The mean 5-hydroxymethylfurfural (HMF) concentration of the non-manuka honeys was 6 mg/kg, whereas the average HMF value of manuka honey was 16 mg/kg. The higher HMF value of manuka honey is in accordance with earlier studies, which showed that DHA, which is only present in manuka honey, has an influence on HMF levels (Atrott, 2013). The chemical pathway for the increased HMF formation is not studied yet. The MGO concentration of all non-manuka honeys was below 7 mg/kg, whereas the manuka honeys had a mean MGO level of 358 mg/kg. To assess the level of protein-bound MRP in food protein,



enzymatic hydrolysis is required. The efficiency of the enzymatic hydrolysis procedure was assessed by comparing the concentrations of amino acids in enzymatic hydrolyzates with those in acid hydrolyzates. The mean concentration of serine, alanine, valine, isoleucine, leucine, and phenylalanine in the enzymatic hydrolyzated was slightly lower for manuka (77-93%) than for non-manuka honeys (88-97%), with the release of individual amino acids being reduced by 3-12%. It was shown in previous reports that the release of certain amino acids can be decreased depending on the progress of glycation reactions in proteins (Hellwig et al., 2016). To overcome the limitations of enzymatic release of amino acids and to prevent an underestimation of MRP in manuka honey because of a decreased hydrolysis rate, the concentrations of MRP are calculated on the basis of the leucine content of the protein. Leucine is not modified during the Maillard reaction and thus can be used as an internal reference. Moreover, leucine concentration is not significantly different in manuka and non-manuka honey proteins. The quantification of protein-bound MRP in honey was achieved by HPLC-MS/MS with the standard addition method. The pattern of protein-bound MRP in honey revealed that CEL and MG-H1 are present in particularly high levels in manuka honey protein hydrolyzates (see Figure 42). Non-manuka honey proteins contain CEL and MG-H1 only in levels below the limit of quantification. Manuka honey proteins contain CEL and MG-H1 in concentrations up to 102.8 and 24.2  $\mu\text{mol}/\text{mmol}$  leucine, respectively.

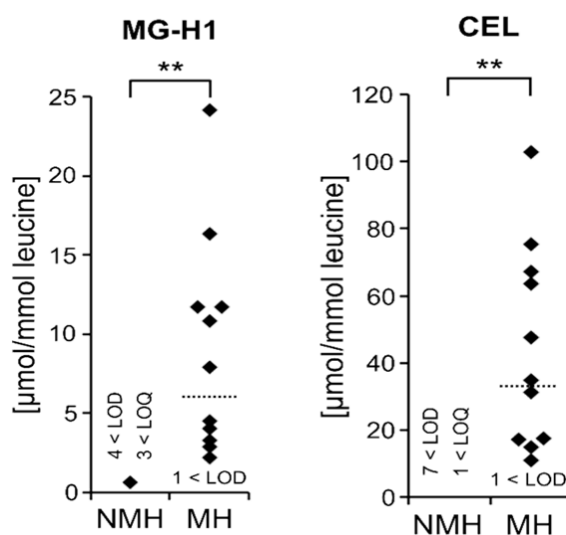


Figure 42: Concentrations of protein-bound MRP MG-H1 and CEL in enzymatically hydrolyzed HMW fractions (dialysis retentates) of 8 non-Manuka honeys (NMH) and 12 Manuka honeys (MH). Dotted lines indicate the medians. Significance of differences between MH and NMH medians was assessed by the Mann-Whitney U test. Figure taken from Hellwig et al. (2017).

CEL and MG-H1, which are formed during modification of the amino side chain of lysine or the guanidine group of arginine with MGO, are almost exclusively formed in manuka honeys. Compared to the reaction product of the free amino acid proline and MGO, namely 2-acetyl-1-pyrroline, the differences of non-manuka and manuka honey are more pronounced (see section 1). The CEL and MG-H1 concentrations correlated with the MGO content of the honeys (see Figure 43) and the CEL to MG-H1 ratio was approximately 5:1 (determined for the manuka honeys where both compounds were detected (n=11)). Moreover protein-bound CEL is the most abundant MRP in manuka honey with even higher concentrations than CML or *N*- $\epsilon$ -fructosyllysine, which are normally described as the MRP with the highest concentrations in food stuff (He et al., 2014; Scheijen et al., 2016). Based on the CEL and MG-H1 concentrations in the protein fractions of manuka honey, it can be assumed that approximately 1 % of total MGO has reacted with honey proteins.

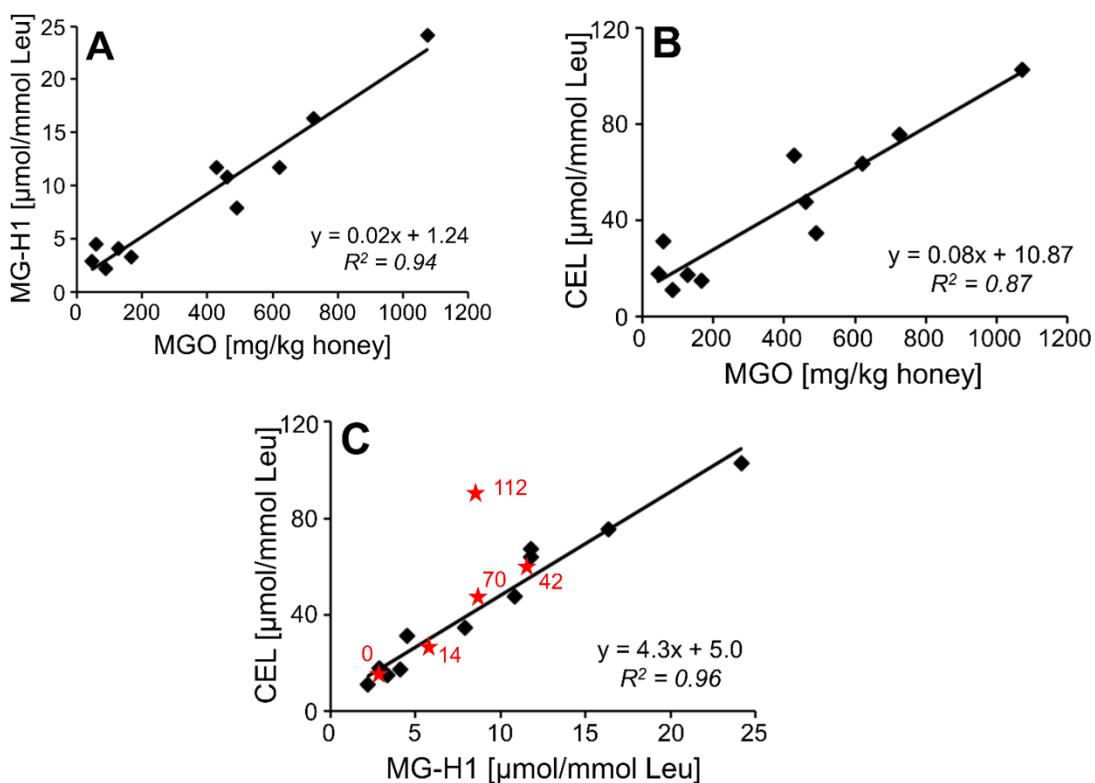


Figure 43: (A) Correlation of MGO with protein-bound MG-H1 concentrations and (B) CEL concentrations in manuka honey (n=11). (C) Correlation of protein-bound MG-H1 and CEL in manuka honey (black squares) and in artificially spiked honey with MGO (500 mg/kg) and DHA (1000 mg/kg) (red stars) after storage at 30 °C. Number of storage days is given in red. Figures taken from Hellwig et al. (2017) and partly modified.

Taken together, protein-bound MRP in Manuka honey show a unique pattern compared to other food stuff and especially in contrast to non-manuka honey proteins. The pathways and the kinetic of the formation of CEL and MG-H1 in Manuka honey are not studied yet. Besides MGO, also DHA could play an interesting role in the formation of protein-bound MRP during honey maturation. DHA is present in very high concentrations not only in the honey, but also in nectar, where MGO only plays a minor role (Adams et al., 2009; Williams et al., 2014). Nectar is derived from the plant phloem, which has a pH value of 7.4-8.7 (Vreugdenhil and Koot-Gronsveld, 1989; Schopfer and Brennicke, 2005). Moreover, the water content of honey nectar can vary between 50 to 90 % since it is mostly depending on floral microclimate and is affected by evaporation in the exposed flowers (Nicolson et al., 2007; Heil, 2011). Bees incorporate specific enzymes into the nectar matrix and during honey maturation in the beehive the pH value decreases through the enzymatic formation of organic acids to a pH value of approximately 4 (Molan, 1992a; Bogdanov, 1997). The water content slowly decreases and the  $a_w$ -value of the final honey reaches 0.5-0.65 (Gleiter et al., 2006). Under these circumstances, it is more likely that the conditions in the nectar or even the plant phloem favour the Maillard reaction. Nevertheless, the increase of protein by the addition of bee-derived enzymes to the honey could also lead to an increase of MRP, although the reaction conditions in the honey matrix (low pH and water activity) are less favourable. More profound knowledge about formation pathways of glycation compounds is necessary to determine if CEL and MG-H1 are convenient compounds to study the fraudulent addition of MGO and DHA to a less valuable honey. To study whether the formation of CEL and MG-H1 can be simulated by the addition of MGO and DHA to a honey matrix, a manuka honey was spiked with MGO and DHA and stored for 17 weeks at 30 °C. The manuka honey chosen for this experiment contained 96 mg MGO/kg and 464 mg DHA/kg. Thus, based on the recently quantified amounts of protein-bound CEL and MG-H1 in commercial manuka honeys, only low amounts of CEL and MG-H1 were expected to be present in this honey (3  $\mu\text{mol}$  MG-H1/mmol leucine and 19  $\mu\text{mol}$  CEL/mmol leucine as calculated from the regression curve presented in Figure 43. The aim of the storage experiment was to elucidate whether a fraudulent addition of MGO and DHA to a ripened honey leads to an increase of CEL and MG-H1. The concentrations of MGO, DHA and HMF in the storage samples are presented in Figure 44. During 17 weeks of storage at 30 °C, the MGO content in the natural honey increased by 2.4 % and the sample spiked with MGO increased by 36.2 % during storage. In contrast, DHA decreased slightly in the natural honey and the spiked sample. The smaller

DHA content at day 0 compared to day 4 is probably due to limited solubility of solid DHA in the honey matrix. Thus, DHA might not be dispersed thoroughly in the honey matrix at day 0. The HMF concentration of the commercial honey and the spiked honey increases over 17 weeks of storage at 30 °C. Again, HMF increases more quickly when DHA is present in high amounts. This was described previously in the PhD thesis of Atrott (2013) and leads to the conclusion that honeys with high levels of DHA need to be stored at especially mild conditions to prevent violation of the regulatory limit of HMF of 40 mg/kg (Codex Alimentarius Commission, 2001). The commercial sample exceeds the HMF limit at approx. 75 d and the spiked honey at 30 d of storage.

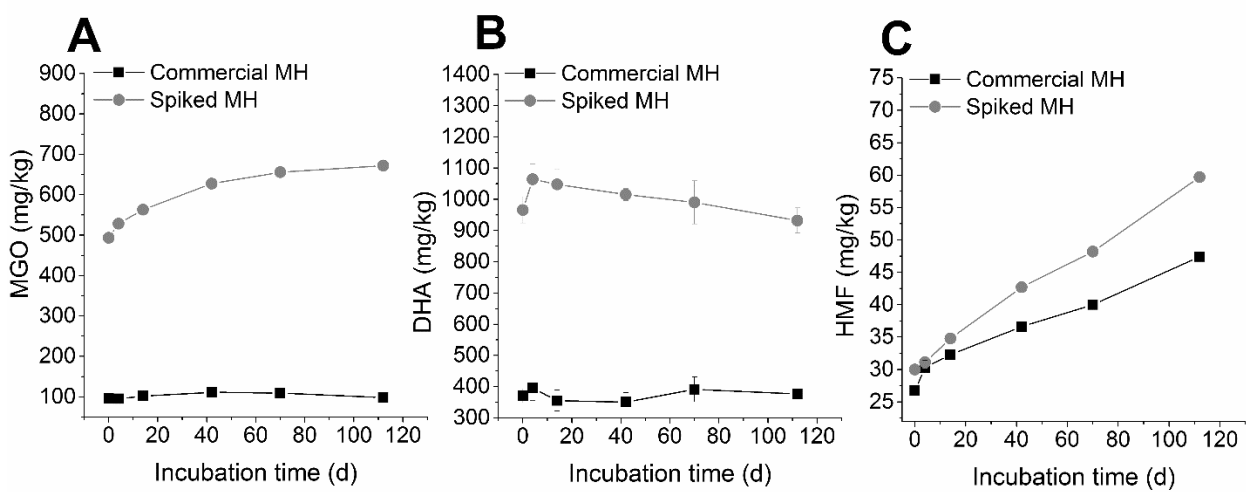


Figure 44: Concentration of MGO (A), DHA (B) and HMF (C) in commercial manuka honey MGO30+ (■) and in manuka honey MGO30+ with added MGO and DHA (●) over 17 weeks of storage at 30 °C. Dotted line marks regulatory limit of HMF in commercial honey (40 mg/kg).

The results for the protein-bound Maillard reaction products CEL and MG-H1 are shown in Figure 45.

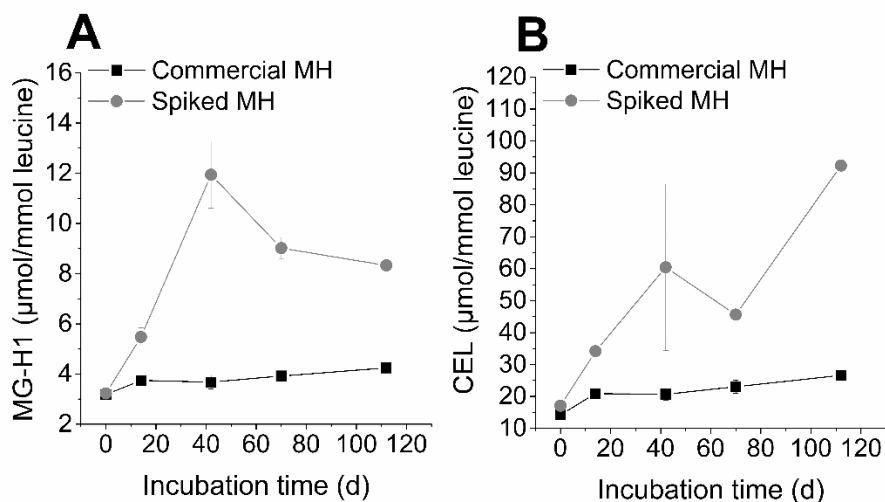


Figure 45: Concentration of protein-bound MG-H1 (A) and CEL (B) in commercial manuka honey MGO30+ (■) and in manuka honey MGO30+ with added MGO and DHA (●) over 17 weeks of storage at 30 °C.

The concentration of MG-H1 in the commercial manuka honey sample without added MGO and DHA increased from 3.2 to 4.2  $\mu\text{mol}/\text{mmol}$  leucine over 17 weeks. The concentration of the sample, which was spiked with MGO and DHA quadruples after 42 d up to 11.9  $\mu\text{mol}/\text{mmol}$  leucine. The quick increase is followed by a decrease of MG-H1, which resulted in a concentration of 8.3  $\mu\text{mol}/\text{mmol}$  leucine after 17 weeks. For CEL, the concentration of the commercial sample increased from 14.2 to 26.6  $\mu\text{mol}/\text{mmol}$  leucine. In contrast, the CEL concentration of the spiked sample increased up to 60.4  $\mu\text{mol}/\text{mmol}$  leucine on day 42, followed by slight decrease and reaches a concentration of 92.3  $\mu\text{mol}/\text{mmol}$  leucine after 17 weeks of storage. Both protein-bound Maillard reaction products, MG-H1 and CEL, significantly increased in honey, when artificial MGO and DHA were spiked to the commercial sample. On the one hand that demonstrates the unambiguous role of MGO and DHA in the formation of protein-bound Maillard reaction products. On the other hand this questions the application of CEL and MG-H1 as parameters to study the fraudulent addition of MGO and DHA to natural honey. For commercial, natural manuka honeys a constant CEL to MG-H1 ratio of 5:1 was found (see Figure 43). The increase of CEL and MG-H1 in the spiked manuka honey also led to a median CEL to MG-H1 ratio of 5:1. However, since MG-H1 started declining after day 42 whereas CEL increased further, the final CEL to MG-H1 ratio after 17 weeks of storage is 11:1 (see red stars in Figure 43). The decrease of MG-H1 might be due to consecutive reactions, such as protein cross linking. For example, protein-bound MG-H1 could react with amino groups of lysine residues and form methylglyoxal-derived imidazolium cross-links (MODIC). Moreover, the decrease of MG-H1 and a further

increase of CEL at the same time confirmed that the reactivity of MGO in manuka honey towards lysine residues appeared to be higher compared to arginine residues. When MGO is added to a honey without natural MGO, it will primarily react with lysine residues and arginine residues, which are easily accessible. When all available arginine residues reacted with MGO, the formation of MG-H1 will stagnate, whereas the formation of lysine-derived CEL further increased. This could be either due to the reactivity of MGO towards the amino acid residues or depend on the steric accessibility of the amino or guanidine groups. However, the role of DHA in the formation of glycation compounds in manuka honey should be further elucidated for a better understanding of the unique pattern of MRP in manuka honey.

In manuka honey, a discrepancy of the CEL to MG-H1 ratio of 5:1 together with an increased concentration of HMF might be an indicator for fraudulent addition of MGO and storage at increased temperatures for “artificially” producing high-price manuka honey products. Kinetic studies of the Maillard reaction in manuka honey at different temperatures should be continued to gain a more detailed insight in the spectrum of reaction products, which might prove useful for manuka honey authentication.

## 2.6. Summary of Chapter B - Reactions of carbonyl compounds in honey

Chapter B deals with unique chemical reactions which occur in manuka honey during storage. The aim is to identify exceptional reactions arising in manuka honey and evaluate their suitability to control quality and authenticity of manuka honey. Honey mainly consists of sugars and water accounting for 98 % of honey constituents. The key compounds for honey identification may be found in the missing 2 %. Therefore, the low molecular weight fraction of manuka honey is studied to identify the reaction product of MGO and the amino acid proline, namely 2-acetyl-1-pyrroline. Moreover, the extent of glycation reactions in manuka honey proteins is studied by the means of fluorescence measurement and size exclusion chromatography. Additionally, specific protein-bound Maillard reaction products derived from MGO and lysine and arginine, namely CEL and MG-H1, respectively, are studied. The results of chapter B can be summarized as follows:

- 1 In honey, methylglyoxal (MGO) reacted with proline to form 2-acetyl-1-pyrroline (2-AP). In manuka honey containing  $\geq 250$  mg/kg MGO, the 2-AP concentration was 0.3 to 0.5 mg/kg and was significantly increased compared to non-manuka honey, which contained  $\leq 0.1$  mg 2-AP/kg.
- 2 The addition of high amounts of MGO and DHA (500 and 1000 mg/kg, respectively) to a non-manuka honey and subsequent storage at room temperature did not lead to an increase of 2-AP. Storing the spiked honey at 37 °C led to a 2-AP increase to the same level present in commercial manuka honeys. However, 5-hydroxymethylfurfural (HMF) level also rose and exceeded the regulatory limit of 40 mg/kg, making this honey nonsalable.
- 3 The molecular size of manuka honey proteins was significantly shifted to high molecular weights (HMW) with a size above 510 kDa. The amount of HMW protein in manuka honey compared to non-manuka honey was significantly increased and cannot be decreased by cleavage of disulphide bonds. It was hypothesized that MGO cross-linking of proteins is mainly responsible for the formation of HMW adducts in manuka honey.
- 4 HMW proteins of manuka honey showed higher fluorescence intensities at  $\lambda_{\text{ex}}=350$  nm and  $\lambda_{\text{em}}=450$  nm compared to non-manuka honeys. The fluorescence intensity of manuka honey proteins depended on the MGO content of the honey.
- 5 The artificial addition of MGO and DHA to a non-manuka honey did not lead to an increase of fluorescence to the level of commercial manuka honeys. Thus protein

fluorescence could be used as an indicator for the Maillard reaction in honey and to control natural origin of MGO and DHA.

- 6 The protein-bound Maillard reaction products N- $\epsilon$ -carboxyethyllysine (CEL) and methylglyoxal-derived hydroimidazolone 1 (MG-H1) were quantified in manuka honey. Their amount was significantly higher in manuka compared to non-manuka honey, where the concentrations were mostly below LOQ. CEL and MG-H1 concentrations correlated with the MGO content of the honey.
- 7 The addition of MGO and DHA to a manuka honey with naturally low amounts of MGO, DHA and the Maillard reaction marker CEL and MG-H1, led to an increase of CEL and MG-H1 up to the level of commercial manuka honeys after 17 weeks of storage at 30 °C. In this sample, HMF exceeded the regulatory limit after 30 days of storage, leaving it nonsalable.

Taken together, unique MGO-derived reactions in manuka honey could be useful for analyzing the genuineness of manuka honey. To evaluate fraudulent addition of MGO or DHA to manuka honey, a combination of parameters like MGO, DHA, HMF, 2-AP, MRP and physicochemical parameters like pH and water content should be taken into account, since the consideration of only a single compound may lead to wrong conclusions. The reactions between MGO and honey proteins cannot be fully induced by artificial spiking of a ripened non-manuka honey with MGO and DHA, which is probably due to the low water activity of honey. The results contribute to the understanding of the unique chemistry of MGO in manuka honey and its role in manuka honey characterization.



---

## 3 Chapter C – Metabolic transit of carbonyl compounds

---

### 3.1. Introduction

Carbonyl compounds, especially 1,2-dicarbonyls compounds are discussed to pose a risk to human health when ingested with food. This discussion is based on *in vitro* studies, which indicated cytotoxic effects of 1,2-dicarbonyl compounds (Lee et al., 2009; Amoroso et al., 2013; Daglia, Amoroso, et al., 2013). This discussion poses two difficulties: The concentrations used for testing cytotoxicity are usually much higher than concentrations found in the human body and thus results are not directly transferable to the human system. Moreover, a distinction between endogenously formed 1,2-dicarbonyl compounds, which can be elevated under certain metabolic conditions (e.g. diabetes) and 1,2-dicarbonyl compounds which are taken up with the diet is necessary. Until now, there is only minor knowledge about the dietary influence of the endogenous “1,2-dicarbonyl load”. The background of this chapter focuses on studies revealing sources and concentrations of 1,2-dicarbonyl compounds in the human body and explaining important reaction pathways and the formation of by-products with potential adverse side effects.

### 3.2. Background

#### 3.2.1 Carbonyl compounds in living organisms

Since 1,2-dicarbonyl compounds are important intermediates of sugar degradation, their formation pathways and concentrations in body fluids were studied increasingly during recent years (see Table 25 for concentrations and corresponding literature). Since glucose is frequently regarded as the precursor compound for the formation of 1,2-dicarbonyls (in food and endogenously), its concentrations in body fluids and the impact of the diet is well documented. Despite the fact, that fructose can be converted into glucose *in vivo*, the interest in this precursor compound for dicarbonyl formation was rather low so far. The concentrations of 1,2-dicarbonyls *in vivo*, with 3-DG and MGO as the most important representatives, are presented in Table 25. For 3-DG and MGO a dietary influence after the consumption of food was shown (Degen et al., 2013; Degen et al., 2014; Maessen et al., 2015). Nevertheless, there appears to exist a certain base level of dicarbonyl compounds *in vivo*, which can either be explained by endogenous formation or by incomplete metabolism

after dietary intake. The next section will focus on endogenous formation pathways of 3-DG and MGO.

Table 25: Concentrations of glucose, fructose, 3-deoxyglucosone and methylglyoxal in body fluids of healthy subjects before (F: fasting) and after (P: postprandial) ingestion of compounds.

Compound	Body fluid	Concentration
<b>Glucose</b>	Blood plasma <sup>[1]</sup>	<b>F:</b> 5 mmol/l <b>P:</b> 6-8 mmol/l (consumption of 75 g glucose)
	Urine <sup>[2]</sup>	0.1-0.8 mmol/l (24 h urine)
	Saliva <sup>[3]</sup>	<b>F:</b> 80 $\mu$ mol/l <b>P:</b> 160-200 $\mu$ mol/l
<b>Fructose</b>	Blood serum <sup>[4]</sup>	<b>F:</b> 100 $\mu$ mol/l <b>P:</b> 200-300 $\mu$ mol/l (consumption of 10 g fructose)
	Blood serum <sup>[5]</sup>	8 $\mu$ mol/l
	Cardiac blood (murine) <sup>[6]</sup>	<b>F:</b> 20 $\mu$ mol/l <b>P:</b> 150-250 $\mu$ mol/l (consumption of sucrose 2g/kg)
	Urine <sup>[7],[8]</sup>	11-110 $\mu$ mol/d (24 h urine)
	Saliva <sup>[9]</sup>	<b>F:</b> < 1.8 $\mu$ mol/l
<b>3-Deoxyglucosone</b>	Blood plasma <sup>[1]</sup>	<b>F:</b> 1000 nmol/l <b>P:</b> 1500 nmol/l (consumption of 75 g glucose)
	Blood serum <sup>[10]</sup>	<b>F:</b> 500 nmol/l <b>P:</b> 700-1100 nmol/l (consumption of 125 g honey)
	Urine <sup>[10],[11]</sup>	1.8-7.6 $\mu$ mol/d (24 h urine)
<b>Methylglyoxal</b>	Blood plasma <sup>[1]</sup>	<b>F:</b> 350 nmol /l <b>P:</b> 420 nmol/l (consumption of 75 g glucose)
	Urine <sup>[10],[12]</sup>	0.1-0.7 $\mu$ mol/d (24 h urine)

<sup>[1]</sup>Maessen et al. (2015), <sup>[2]</sup>Burtis et al. (2013), <sup>[3]</sup>Jurysta et al. (2009) <sup>[4]</sup>Anderstam et al. (2013), <sup>[5]</sup>Kawasaki et al. (2002), <sup>[6]</sup>Sugimoto et al. (2010), <sup>[7]</sup>Johner et al. (2010), <sup>[8]</sup>Tasevska et al. (2005), <sup>[9]</sup>Luke et al. (1999) <sup>[10]</sup>master thesis Stephanie Schultes (2016), <sup>[11]</sup>Degen et al. (2014), <sup>[12]</sup>Degen et al. (2013)

### Formation of 3-deoxyglucosone

The reaction of reducing sugars with proteins leads to glycated amino groups of protein side chains. During the early stage of the Maillard reaction, Amadori products, also called ketoamine compounds, are formed. Depending on the chemical nature of the reacting sugar, fructosamines and ribulosamines from glucose and ribose, respectively, can be formed (Van Schaftingen et al., 2012). Amadori products can be enzymatically repaired by the enzymes fructoseamine-3-kinase (FN3K) and fructoseamine-3-kinase-related protein (FN3KRP). Both enzymes lead to phosphorylation of the Amadori compound, which results due to instability of the intermediate in the release of the native protein, anorganic phosphate and a 1,2-dicarbonyl compound (see Figure 46) (Delpierre et al., 2000, 2002). The enzymes FN3K and FN3KRP are ubiquitously present in all human tissues and are regenerating native proteins and forming new glycating agents at the same time (Collard et al., 2004). 3-DG, which is released after the reaction of FN3K and fructosamine, is considered to be the main metabolite of protein repair *in vivo* (Kato et al., 1987).

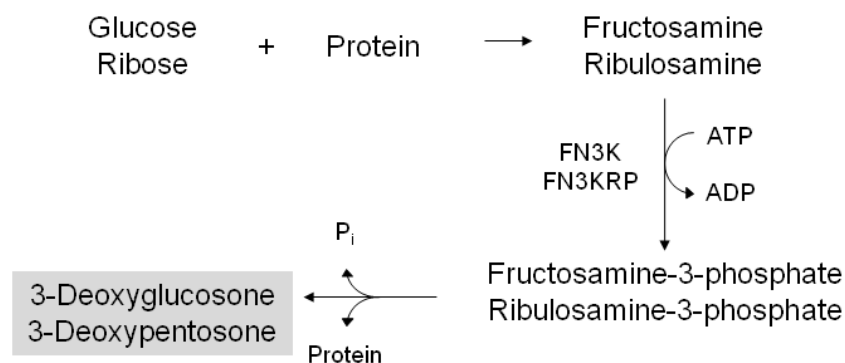


Figure 46: Formation of 1,2-dicarbonyl compounds from enzymatic repair of glycated proteins

Besides enzymatic protein repair, 1,2-dicarbonyl compounds can be formed via the polyol pathway. Under hyperglycaemic conditions, an excess of glucose can be converted to sorbitol by aldose reductase. Sorbitol can be further converted into fructose, which either leads to 3-DG via enolization and oxidation or via enzymatic phosphorylation and subsequent hydrolysis (see Figure 47) (Niwa, 1999). The phosphorylating enzyme for this conversion was identified to be fructose-3-kinase or 3-phosphokinase in rat and mammalian lenses (Lal et al., 1993, 1995). However, when Delpierre et al. (2000) studied human erythrocytes, they found a 300-fold lower affinity of the enzyme to fructose compared to fructosamines. These results indicated that the physiological function of the enzyme that is able to convert fructose into fructose 3-phosphate in erythrocytes is probably to phosphorylate fructosamines. Therefore, it

is assumed that the earlier discovered 3-phosphokinase and FN3K, which was studied later, are the same enzymes.

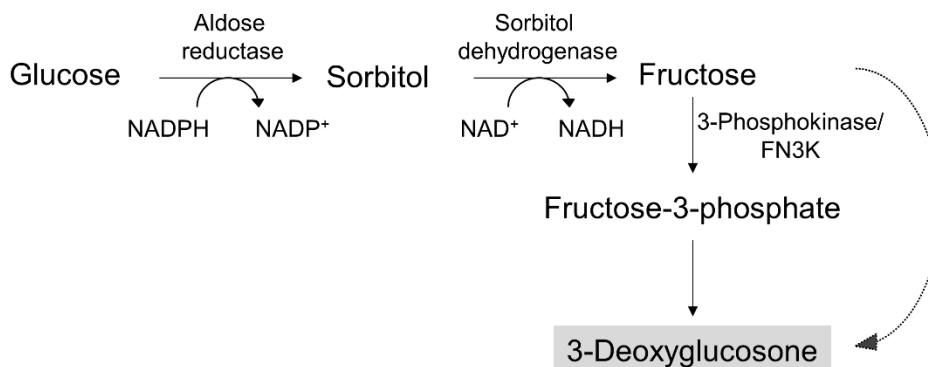


Figure 47: Formation of 3-DG from the polyol pathway

Under normoglycaemic conditions, the intracellular concentration of sorbitol is very low due to a low affinity of aldose reductase for glucose (Schalkwijk et al., 2004). The polyol pathway is indirectly linked to oxidative stress by decreasing the concentration of NADPH. NADPH serves as a cofactor for glutathione reductase, which restores glutathione levels in tissues. A decrease of NADPH via the polyol pathway may also lead to decreased levels of GSH, which results in enhanced oxidative stress (Schalkwijk et al., 2004). Moreover, 3-DG can be formed non-enzymatically via the advanced stage of the Maillard reaction, which is discussed in chapter 1. However, the formation of the 1,2-enaminol is enhanced under acidic conditions. The slightly basic conditions *in vivo* make the enzymatic formation more likely. Under healthy conditions, endogenously formed 3-DG can be metabolized enzymatically and eliminated by renal clearance. These reactions will be further discussed in section 3.2.2.

#### Formation of methylglyoxal

There are several pathways known, which can lead to endogenous formation of methylglyoxal making it a normal by-product of metabolic processes *in vivo*. It can be formed during glycolysis from the triose phosphates dihydroxyacetone phosphate and glyceraldehyde phosphate (Phillips and Thornalley, 1993). This can occur enzymatically via methylglyoxal synthase or non-enzymatically via fragmentation and dephosphorylation (Ray and Ray, 1981; Thornalley, 1996). Moreover, acetone, which is released during metabolism of ketone bodies, can be converted by cytochrom P450 monooxygenase into methylglyoxal via hydroxyacetone (Thornalley, 1996). During catabolism of threonine the compound aminoacetone is formed,

which can also lead to MGO via an enzymatic oxidation. The potential pathways of MGO formation *in vivo* are summed up in Figure 48.

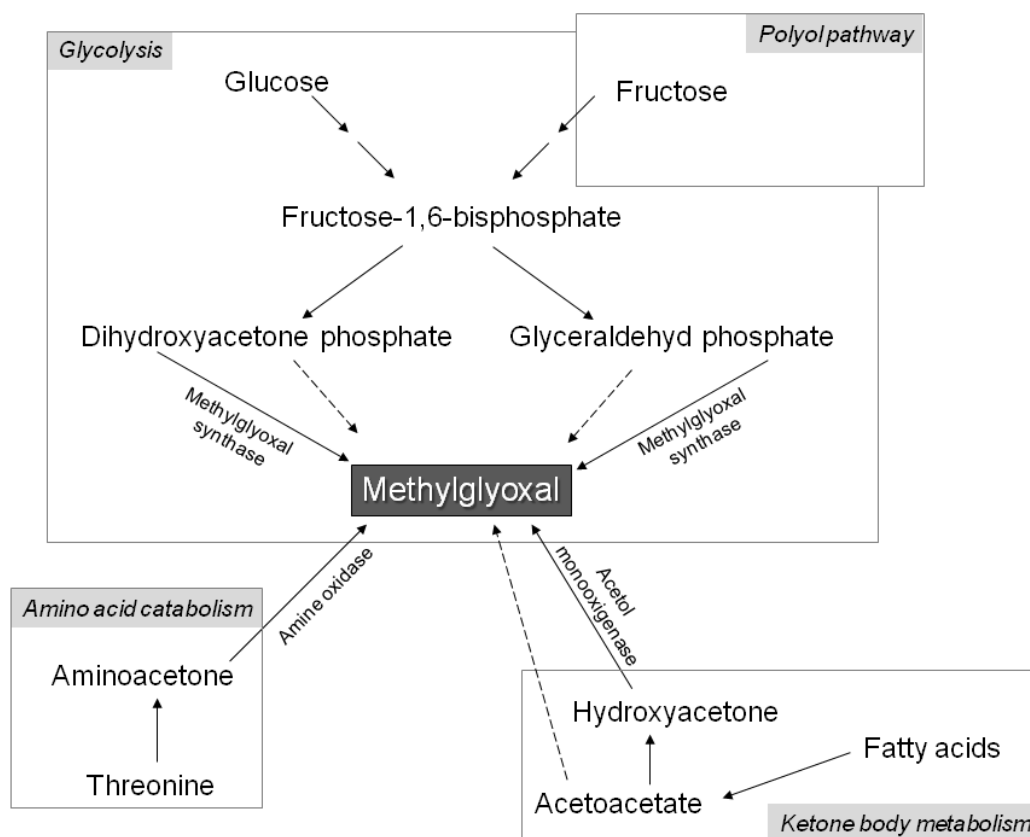


Figure 48: Formation of methylglyoxal *in vivo* (dashed arrows: non-enzymatic pathway)

Besides endogenous formation of 3-DG and MGO, carbonyl compounds can be taken up with the diet. The next section explains how the human body handles carbonyl compounds during digestion.

#### Dietary uptake of carbonyl compounds

Based on the concentration of 3-DG and MGO in commonly consumed foods, Degen et al. (2012) estimated the daily dietary intake of 3-DG to 0.1 to 1 mmol, whereas MGO is taken up in significantly lower amounts ranging from 0.1 to 0.3 mmol/day. There is only a limited number of food known, which contains very high amounts of 1,2-dicarbonyl compounds. One popular example is New Zealand manuka honey. Its MGO concentration can reach up to 800 mg/kg (Mavric et al., 2008). Moreover, honey is known to contain 3-DG in amounts up to 1300 mg/kg (Weigel et al., 2004). Thus, the alimentary levels of 3-DG and MGO are

exceeding the levels found *in vivo* by factor 100 to 1000 (see Table 25). This indicates that dietary dicarbonyl compounds are either not absorbed in the gastrointestinal tract or can be rapidly metabolized by the human body. The presence of dicarbonyl compounds *in vivo* is of special interest, since their reactivity towards proteins is increased by factor 10000 (for MGO) compared to glucose (Thornalley, 2005). Until now, there exists only minor knowledge about the resorption mechanisms of dicarbonyl compounds. It is not clear whether 3-DG and MGO are actively transported into the blood stream or can pass intestinal cells by diffusion. It was assumed that MGO and glyoxal (GO) can cross cell membranes, possibly by passive diffusion (Abordo et al., 1999). Hoffmann (2012) studied in her master thesis the 3-DG absorption and metabolism by Caco-2-cells. She found that a small proportion of 3-DG can cross the cell membrane (presumably passively) and can be recovered intracellularly. A further indication for potential transportation systems of dicarbonyl compounds into cells and the blood stream might be the increase of dicarbonyl compounds in body fluids after food consumption (see Table 25, fasting (F) versus postprandial (P) concentrations). Nevertheless, it is also possible that glucose and fructose, which are ingested with carbohydrate rich food, are precursor compounds leading to the endogenous formation of dicarbonyl compounds. According to the HELENA study (Healthy Lifestyle in Europe by Nutrition in Adolescence) European adolescents are consuming approximately 138 g sugars per day (defined as mono- and disaccharides), whereby 110 g of sugars are consumed as “free” sugars, which were added during processing or preparation of food (Mesana et al., 2016). This free sugar is also called extrinsic sugar, whereas intrinsic sugar describes sugars which are naturally incorporated into the cellular structure of foods, such as sugars in intact fruits and vegetables. The average consumption of fructose in the United States of America was 49 g per day, whereby 41 g were extrinsic fructose and only 8 g per day occurred naturally in food (Marriott et al., 2009). Tasevska et al. (2009) estimated that extrinsic sugars account for 60 % of the total sugar consumption. The authors also reported on the analysis of sucrose and fructose in urine as a good biomarker for the consumption of extrinsic sugar. According to the World Health Organization (WHO), the daily sugar intake should not be above 50 g, whereby extrinsic sugars should only contribute with 25 g (World Health Organization 2015). After dietary intake, the monosaccharide glucose is actively transported into mucosa cells by the sodium-dependent SGLT1 transporter and passed to the blood stream via the GLUT2 transporter. The uptake by tissue cells and the metabolism of glucose is strictly regulated since higher levels of free, circulating glucose can lead to protein damage (Cerami, 1986). In contrast to glucose,

the monosaccharide fructose is transported via the GLUT5 and facilitated diffusion into the mucosa cell and passed through the GLUT2 transporter to the blood stream (Löffler et al., 2007). Fructose is quickly resorbed by the liver and subsequently metabolized. Thus, the resorption and metabolism of glucose and fructose in healthy individuals leads to human plasma levels below 5 mmol/l and 1 mmol/l, respectively (Schalkwijk et al., 2004; Teichert et al., 2015).

### 3.2.2 Reactions of carbonyl compounds *in vivo*

When tissue levels of carbonyl compounds are rising due to dietary uptake or bad health conditions, enzymatic control mechanisms will lead to the turning-on of metabolic reactions. The following section will deal with the enzymatic metabolism of 3-DG and MGO as representatives of dicarbonyl compounds and glucose and fructose as the main monosaccharides commonly consumed with the diet.

#### Metabolism of 3-DG

The reactive intermediate 3-DG is rapidly metabolized to its reduced form 3-deoxyfructose (3-DF) via the enzymes aldose reductase (EC 1.1.1.21) and aldehyde reductase (EC 1.1.1.2), which belong to the enzyme family of aldo-keto-reductases (Kato et al., 1990; Hayase et al., 1991; Knecht et al., 1992). 3-DF is less reactive than 3-DG and can be excreted via the urine. The reductive enzymes are present in all tissues with high expression in the kidneys, the small intestine and the human colon (Cao et al., 1998; Zhong et al., 2009). 3-DG can also be oxidized to 3-deoxy-2-ketogluconic acid (3-DGA) via aldehyde dehydrogenase ALDH1A1 and 2-oxoaldehyde dehydrogenase (Fujii et al., 1995; Collard et al., 2007) (see Figure 49). The enzymes are mainly present in erythrocytes, but also in liver and lung tissue (Vander Jagt and Hunsaker, 2003; Collard et al., 2007).

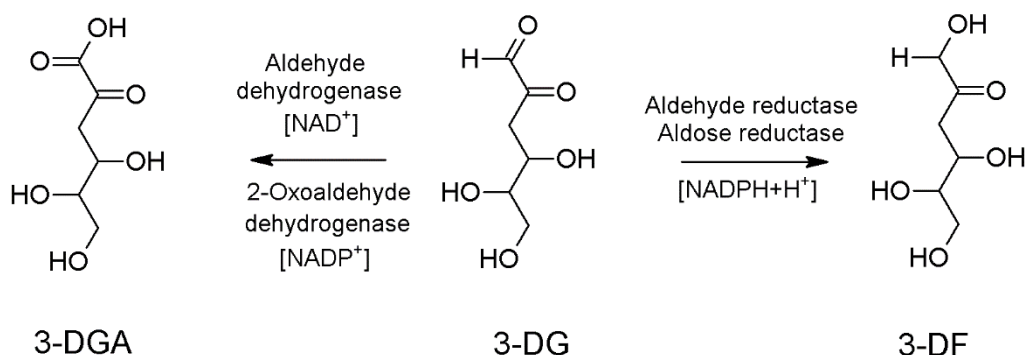


Figure 49: Metabolic degradation of 3-DG to 3-DF (reductive pathway) and 3-DGA (oxidative pathway), grey arrows represent approximate ratio of degradation

3-DF was found in the urine of healthy individuals in a concentration of 32  $\mu\text{mol/g}$  creatinine (Knecht et al., 1992), whereas 3-DGA was only found in amounts of 17  $\mu\text{mol/g}$  creatinine (Collard et al., 2007). This indicates that the metabolism of 3-DG to 3-DF is the main route of degradation, whereas the detoxification of 3-DG via the formation of 3-DGA may be an important pathway for tissues which miss the reductive enzymes (e.g. erythrocytes) (Fujii et al., 1995).

Degen et al. (2014) studied the dietary influence on the urinary excretion of 3-DF and 3-DG. It was shown that a diet, which avoids 3-DG and other Maillard products followed by a dose of honey containing 505  $\mu\text{mol}$  of 3-DG, significantly increases the urinary level of 3-DG and 3-DF by factor 10 and 20, respectively. In total, 6-25 % of the dietary 3-DG could be recovered as urinary 3-DG and 3-DF. These data demonstrated for the first time, that dietary 3-DG might be bioavailable and is rapidly metabolized to 3-DF. Until now, there are no data available for the dietary influence on the oxidative metabolite 3-DGA.

#### Metabolism of MGO

The 1,2-dicarbonyl compound MGO is even more reactive towards amino and thiol groups and thus might be a risk factor in altering protein structures *in vivo*. Thus, the human system detoxifies MGO via an enzymatic cascade, which is called the glyoxalase system (Thornalley, 1993). The enzymes of the glyoxalase pathway are found in the cytosol of all eukaryotic and prokaryotic cells. The glyoxalase system consists of glyoxalase I, which catalyzes the glutathione-dependent formation of the intermediate S- D-lactoylglutathione, and glyoxalase II, which hydrolyzes the glutathione-MGO adduct to D-lactate and glutathion. D-Lactate is subsequently excreted with the urine, but might also be converted into pyruvate via D-lactate dehydrogenase (Ewaschuk et al., 2005). The glyoxalase system is shown in Figure 50.

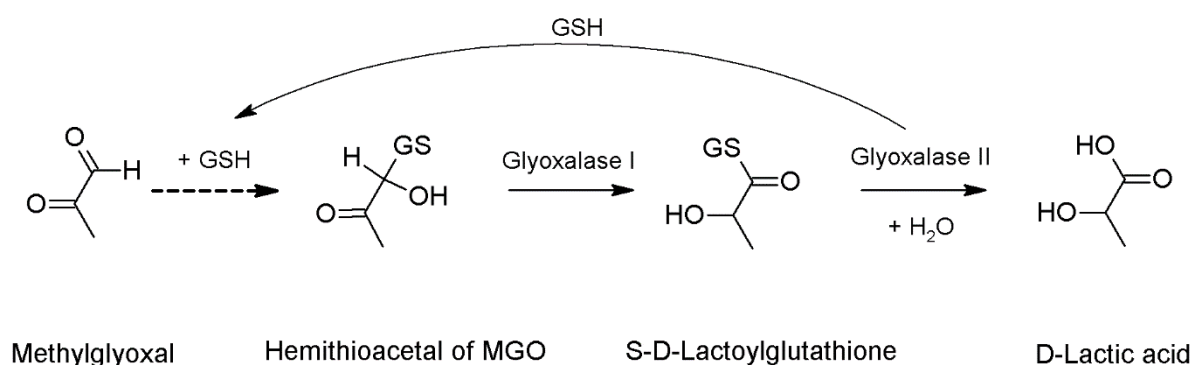


Figure 50: Metabolic degradation of MGO to D-lactate via the glyoxalase system, dashed arrow indicates non-enzymatic reaction



Besides the conversion to D-lactate, MGO can be enzymatically reduced to acetol with aldose reductase or oxidized to pyruvate with methylglyoxal dehydrogenase. Moreover, aldehyde dehydrogenase can convert MGO into lactaldehyde, which is further metabolized to pyruvate (Ko et al., 2005; Chakraborty et al., 2014).

The disposal of MGO by the glyoxalase system or other metabolic enzymes depends on the cellular pool of reduced glutathione. Finally, MGO is either converted to lactate or pyruvate, which are intermediates in several metabolic processes. Recently, it was concluded, that tissues with high energy requirements and high glycolytic fluxes (e.g. the brain) also produce higher amounts of the by-product MGO (Allaman et al., 2015). The authors hypothesized that the glyoxalase defence mechanism of the cells in these tissues evolutionary adapted to the energetic differences by up-regulating glyoxalase activity and thus protecting against high levels of MGO. However, most studies dealing with MGO elimination pathways are analysing endogenously formed MGO. The available data for dietary MGO and its metabolism is rather limited by now.

#### Metabolism of glucose and fructose

Glucose is metabolized in nearly all living organisms via the glycolysis pathway indicating that this is one of the most ancient known metabolic pathways (Romano and Conway, 1996). The uptake of glucose into cells is regulated by insulin. Via enzymatic cascades, the C<sub>6</sub>-sugar glucose is degraded into two molecules of pyruvate (C<sub>3</sub>-sugar). The aim of the glycolytic pathway is the production of the high-energy molecule adenosine triphosphate (ATP) and reduced nicotinamide adenine dinucleotide (NADH+H<sup>+</sup>). Under normal conditions the cellular uptake of glucose and its metabolic degradation is strictly enzymatically regulated, so that glucose plasma concentration remains in a narrow range between 4 to 7 mmol/l (Löffler et al., 2007). However, under diabetic conditions, which are caused by insulin deficiency or resistance, higher levels of glucose are present in the blood stream. The subsequent dysregulation of glycolysis is due to inappropriate amount and/or activities of metabolic and regulatory enzymes of glycolysis (Guo et al., 2012). Additionally, glucose can enter the polyol pathway and is reduced to sorbitol via aldose reductase. Sorbitol can either be converted to fructose with sorbitol dehydrogenase or it can accumulate and can cause cellular osmotic stress and damage cellular proteins.

Fructose is metabolized via entering the glycolytic pathway and also delivers ATP. In enterocytes but mainly in the liver, fructose can be phosphorylated with fructokinase to fructose-1-phosphate which is cleaved by aldolase B to glyceraldehyde and dihydroxyacetone

phosphate (DHAP). Glyceraldehyd is phosphorylated to glyceraldehyde phosphate (GAP) and both, GAP and DHAP pass glycolysis. Fructose metabolism is independent from the enzyme phosphofructokinase, which is regulated by insulin. Thus, fructose is metabolized even under diabetic conditions (Löffler et al., 2007). Moreover, fructose can also be converted into glucose via the vice-versa polyol pathway and is then metabolized insulin-dependent via glycolysis. In contrast to the elimination of glucose, the cellular uptake and metabolism of fructose is less regulated. Thus, under diabetic conditions, the production of fructose via the polyol pathway combined with the kinetically less controlled metabolism, can pose a risk for side reactions of fructose.

#### Beyond metabolism: Reactions of carbonyl compounds *in vivo*

Among the reactions of carbonyl compounds, the Maillard reaction is one of the most important pathways. Some details concerning the Maillard reaction in food were discussed in chapter 2.2.2. Therefore, this section will focus on reaction products which are present in body fluids. Under physiological conditions (pH 7.4, 37 °C), 1,2-dicarbonyl compounds preferentially react with the nucleophilic  $\epsilon$ -amino group of lysine, the guanidine group of arginine and the thiol group of cysteine. Under physiological conditions the initial reversible reactions form hemithioacetals from cysteine and glycosylamine derivatives from arginine and lysine (Thornalley, 1996). Further irreversible reactions may form more stable products like methylglyoxal-derived hydroimidazolones or N- $\epsilon$ -carboxyethyllysine. The analogue reaction products from 3-DG are 3-deoxyglucosone-derived hydroimidazolone and pyrraline (Thornalley et al., 2003). The hydroimidazolones derived from arginine and 3-DG or MGO together with the lysine modification with glyoxal, N- $\epsilon$ -carboxymethyllysine, respectively, are the most important glycation products *in vivo* (Ahmed et al., 2005). Further reactions of lysine and arginine with 1,2-dicarbonyl compounds include the formation of protein cross-linking, whereby two lysine or arginine side chains react with two molecules of the respective 1,2-dicarbonyl compound. Since these cross-linked structures can cause fluorescence, their analysis is used in clinical biochemistry as a marker for the Maillard reaction *in vivo* (Münch et al., 1997). In general, the formation and accumulation of AGEs in tissues is discussed as a risk to overall health. It was found to be related to the development of retinopathy, neuropathy and nephropathy as complication of diabetes (McCance et al., 1993). Moreover, also individuals with unimpaired glucose metabolism can be affected by the impact of AGEs through the development of age-related diseases like Alzheimer's and cataract (Lyons et al.,

1991; Vitek et al., 1994; Sell et al., 1996). More recently, a novel Maillard reaction compound formed from the reaction of creatine and MGO, namely N-(4-Methyl-5-oxo-1-imidazolyl)sarcosine (MG-HCr), was discovered (Löbner et al., 2015). The incubation of creatine and MGO under physiological conditions resulted in a rapid decrease of MGO to only 13 % of the initial concentration after 1 h at 37 °C. This indicates a “scavenging” role of creatine in trapping MGO, which may delay the formation of AGEs *in vivo* (Löbner et al., 2015). Moreover, with the analysis of the urinary MG-HCr concentration of non-vegetarians (0.4-3.8 µmol/24 h urine) and vegetarian volunteers (0.1-0.3 µmol/24 h urine), it was shown that MG-HCr excretion is influenced by the dietary uptake of creatine. The unique role of scavenging compounds in the human body and their mechanism to protect physiological proteins from glycation reactions is only rarely studied until now. Whether creatine reacts also with other 1,2-dicarbonyl compounds is currently studied in our group. The formation of AGEs and MG-HCr are important reactions of 1,2-dicarbonyl compounds which are formed endogenously under physiological conditions. However, the question whether dietary carbonyl compounds are absorbed during gastrointestinal digestion and increases “carbonyl stress” is discussed controversially. In our group, the stability of 3-DG and MGO during a simulated *in vitro* digestion was studied. Degen (2013) studied in her PhD thesis the stability of 3-DG during gastrointestinal digestion (incubation for 2 h at pH 2 with pepsin) and ileal digestion (incubation for 6 h at pH 7.5 with trypsin and pancreatin). She found that 3-DG was stable during gastrointestinal digestion and that 70 % of the initial 3-DG concentration can be recovered after 6 h of simulated ileal digestion. The missing 30 % were assumed to have reacted with digestive enzymes. The results demonstrate that 3-DG is rather stable under physiological conditions. However, when MGO was incubated under the same conditions it was stable under gastric conditions but showed a rapid decrease to 15 % of the initial concentration in the presence of ileal conditions (Degen et al., 2013). If these results can be transferred to human digestion, it is assumed that 3-DG might be bioavailable, whereby the resorption of MGO is unlikely because its concentration *in vivo* is quickly decreased by the reaction with physiological proteins or other food components. However, this assumption needs further research to elucidate the distinct role of dietary carbonyl compounds and their contribution to the “1,2-dicarbonyl load” of the human body. Since 1,2-dicarbonyl compounds are generally regarded as harmful and were related to severe diseases like multi-organ failure (van Bussel et al., 2017) or cardiovascular diseases (Maessen et al., 2017) very recently, the fate of dietary carbonyl compounds deserves reinforced research.

### 3.3. Aims

The modern western diet leads to an uptake of millimolar amounts of carbonyl compounds every day. Although the metabolism of the energy delivering monosaccharide glucose is well studied, the metabolism of fructose and of sugar fragmentation products like 1,2-dicarbonyl compounds is understood poorly. A previous study of our group showed that healthy individuals are capable of metabolising 3-deoxyglucosone (3-DG) to the less reactive 3-deoxyfructose (3-DF) and that dietary methylglyoxal (MGO) is probably not absorbed during digestion. However, especially the simultaneous uptake of a combination of carbonyl compounds and its impact on individual metabolic pathways needs further research. Since 1,2-dicarbonyl compounds are discussed as a risk to human health because of their increased reactivity towards endogenous proteins, the current work will focus on the recovery of dietary carbonyl compounds and the quantification of their metabolites. Manuka honey served as a model food to study the metabolic transit of carbonyl compounds. The main carbonyl compounds of honey are fructose, glucose and 3-DG. Moreover, manuka honey is characterised by additional high amounts of MGO and its precursor dihydroxyacetone (DHA). During the first part of the study, the gastrointestinal stability of carbonyl compounds was studied under simulated, physiological conditions. The loss of MGO and its reaction partners during simulated digestion, which were described in previous reports, should be considered in detail. The stability of MGO in manuka honey, which was complexed with  $\alpha$ -cyclodextrin (cyclopower) shall be studied for the first time. Moreover, a dietary intervention study was performed to evaluate the fate of carbonyl compounds during digestion. Therefore, two different approaches were used: By analysing the 24 h urine, the excretion of the initial carbonyl compounds and also their metabolites was studied (transit to the urine). Furthermore, the release of carbonyl compounds into the blood stream was studied by monitoring carbonyl compounds in plasma from fasting state until two hours after dietary intervention (transit to blood). The aim of this study was to achieve a better understanding of the influence of dietary carbonyl compounds on the endogenous level of sugar fragments and the clearance mechanism of the human body. Finally, a possible “risk” posed by the uptake of manuka honey and therefore high amounts of carbonyl compounds should be assessed.

### 3.4. Methods

#### 3.4.1. Chemicals

Table 26: Chemicals used for the studies presented in chapter C

Chemical	Specification	Supplier
[ <sup>13</sup> C]-MGO	Synthesis product 2016 (T. Hofmann)	TU Dresden, Germany
[ <sup>13</sup> C <sub>6</sub> ]3-DG	Synthesis product 2014 (master thesis F. Hahne)	TU Dresden, Germany
[ <sup>13</sup> C <sub>6</sub> ]3-DGA	Synthesis product 2014 (master thesis F. Hahne)	TU Dresden, Germany
1,3-Dihydroxyacetone dimer	97 %	Sigma-Aldrich, Steinheim, Germany
3-DF	Synthesis product 2010 (master thesis H. Beyer)	TU Dresden, Germany
3-DG	Synthesis product 2011 (PhD thesis M. Hellwig) and 2014 (master thesis F. Hahne)	TU Dresden, Germany
3-DGA	Synthesis product 2014 (master thesis F. Hahne)	TU Dresden, Germany
Acetic acid	100 %, p.a.	Carl Roth, Karlsruhe, Germany
Acetonitrile	HPLC grade	VWR, Darmstadt
Amino acid mix	2.5 mM each, in 0.1 M hydrochloric acid	Sigma-Aldrich, Steinheim, Germany
Bile extract	from porcine	Sigma-Aldrich, Steinheim, Germany
Calcium chloride dihydrate	99.5 %	Grüssing, Filsum, Germany
D(-)Fructose	> 99.5 %, for biochemistry	Carl Roth, Karlsruhe, Germany
D(+)-Glucose	anhydrous, p.a.	Carl Roth, Karlsruhe, Germany
D(+)-Saccharose	≥ 99.5 %, p.a.	Carl Roth, Karlsruhe, Germany

Dihydroxyacetone phosphate	Lithium salt, $\geq 95.0$ % (TLC)	Sigma-Aldrich, Steinheim, Germany
Disodium hydrogenphosphate	99 %, p.a.	Grüssing, Filsum, Germany
Ethanol	96%, denatured with light petroleum	Berkel, Berlin, Germany
Helium	99.999 %, Alphagaz	Air Liquide
Hydrochloric acid	37 %	Sigma-Aldrich, Steinheim, Germany
Hydroxylamine hydrochloride	99 %, p.a.	Grüssing, Filsum, Germany
Leucine aminopeptidase	19 U/mg protein, 3.7 mg protein/mg	Sigma-Aldrich, Steinheim, Germany
Lithium chloride	p.a.	Merck, Darmstadt, Germany
Lithium citrate buffer	0.12 N, pH 2.2	Sykam, Fuerstenfeldbruck, Germany
Lithium citrate buffer	0.12 N, pH 2.9	Sykam, Fuerstenfeldbruck, Germany
Lithium citrate buffer	0.3 N, pH 4.2	Sykam, Fuerstenfeldbruck, Germany
Lithium citrate-/ borate buffer	0.3 N, pH 8.0	Sykam, Fuerstenfeldbruck, Germany
Magnesium chloride hexahydrate	p.a.	Merck, Darmstadt, Germany
Methanol	HPLC grade	VWR, Darmstadt, Germany
Methylglyoxal	$\sim 40$ % (w/w), exact concentration was determined against 2-MQ	Sigma-Aldrich, Steinheim, Germany
Mucin	from porcine stomach; Type III	Sigma-Aldrich, Steinheim, Germany
N,O-bis(trimethylsilyl)trifluoroacetamide (BSTFA + TCMS)	99:1	Sigma-Aldrich, Steinheim, Germany
n-Hexane	HPLC grade	VWR, Darmstadt, Germany
Ninhydrin	p.a., min. 99 %	Serva Feinbiochemica, Heidelberg, Germany
O-(2,3,4,5,6-Pentafluorobenzyl)hydroxylamine)	$\geq 99.0$ %	Sigma-Aldrich, Steinheim, Germany

hydrochloride (PFBOA)		
o-Chlorobenzaldehyde	N/A	N/A
ortho-Phenylenediamine (oPD)	≥98 %,	Sigma-Aldrich, Steinheim, Germany
Pancreatin	from porcine pancreas	Sigma-Aldrich, Steinheim, Germany
Pepsin	from porcine gastric mucosa, 3555 U/mg protein	Sigma-Aldrich, Steinheim, Germany
Potassium chloride	99.5 %, p.a.	Grüssing, Filsum, Germany
Potassium dihydrogenphosphate	p.a.	VEB Laborchemie, Apolda, Germany
Potassium hydroxide	85 %	Grüssing, Filsum, Germany
Prolidase	from porcine kidney, 208 U/mg protein	Sigma-Aldrich, Steinheim, Germany
Pronase E	from <i>S. griseus</i> , 4000 PU/mg protein	Merck, Darmstadt, Germany
Pyridine	anhydrous	VWR, Darmstadt, Germany
Sodium acetate	99 %	Grüssing, Filsum, Germany
Sodium chloride	p.a.	VWR, Darmstadt, Germany
Sodium dihydrogenphosphate	99.5 %, p.a.	Grüssing, Filsum, Germany
Sodium hydrogencarbonate	99.5 %, p.a.	Grüssing, Filsum, Germany
Trypsin	from porcine pancreas; Type IX- S, 1500 U/mg protein	Sigma-Aldrich, Steinheim, Germany
Urea	> 99.5 %	Fluka AG, Basel, Switzerland
Urease from <i>Canavalia ensiformis</i> (Jack bean)	Type III; 34310 U/g solid	Sigma-Aldrich, Steinheim, Germany
α-Cyclodextrin	≥98 %, CAVAMAX® W6 FOOD	Wacker Chemicals AG, Supplied by Manuka Health NZ Ltd.

## 3.4.2. Materials

Table 27: Materials used for the studies presented in chapter C

Name	Specification	Supplier
Amino acid analyser column	Cation exchange LCA K07/Li	Sykam, Fuerstenfeldbruck, Germany
Blood collection system	BD Vacutainer SST II Advance containing clot activator	Becton Dickinson, Franklin Lakes, USA
Dialysis tubings	Cellulose, 33 mm, MWCO 14 kDa	Sigma-Aldrich, Steinheim, Germany
GC column	ZB-5 capillary column, 30 m x 0.25 mm i.d., 1.0 µm film thickness and a Zebron Z-guard guard column, deactivated, 5 m x 0.25 mm i.d.	Phenomenex, Aschaffenburg, Germany
GC vials with crimp caps	1.5 ml, glass	VWR, Darmstadt, Germany
Glass vessel	10-50 ml	VWR, Darmstadt, Germany
HPLC column	Eurospher 100 RP18 material (250mm x 4.6 mm, 5 µm particle size with integrated pre-column)	Knauer, Berlin, Germany
HPLC vials with lit	1.5 ml, glass	VWR, Darmstadt, Germany
Hydrolysis tubes	12 mm x 100 mm, glass	Schott AG, Mainz, Germany
Membrane filter	Regenerated cellulose, 45 µm, 26 mm	Phenomenex, Aschaffenburg, Germany
Membrane filter for solvents	GH Polypro 0,45 µm, 47 mm hydrophilic polypropylene	Pall, Crailsheim, Germany
Parafilm	4 in x 125 ft	Bemis, Neenah, USA
Pasteur pipettes	230 mm, glass	VWR International, Leuven, Netherlands
Pipette tips	1-1000 µl	Brand, Wertheim, Germany
Plastic containers	5 l	N/A
Septa for HPLC vials	8*0.4 mm, PTFE coated	VWR, Darmstadt, Germany
Syringe	1 ml	B. Braun, Melsungen, Germany



Tooth brush	soft	Various suppliers
Tubes	1.5 ml, 2 ml	Eppendorf, Hamburg, Germany

### 3.4.3. Devices

Table 28: Devices used for the studies presented in chapter C

Device	Specification	Supplier
Amino acid analysator	S 4300, Software: Chromstar 6.3 SCPA GmbH	Sykam, Fuerstenfeldbruck, Germany
Analytic balance	BP 121 S, accuracy: 0.0001 g, max. 120 g	Sartorius, Göttingen, Germany
Blood glucose meter	ACCU CHEK aviva	Roche, Mannheim Zymark,
Centrifuge	Eppendorf 5804-R	Eppendorf AG, Hamburg, Germany
Freeze dryer	Alpha 1 - 2	Martin Christ, Osterode, Germany
Freezer	Comfort	Liebherr, Bibrach an der Riss, Germany
Fridge	Econoic System, 5°C	Liebherr, Bibrach an der Riss, Germany
GC-MS	GC 7890A system, 7683 Series injector with sample tray, 5975C MS detector in electron ionization (EI) mode	Agilent Technologies, Böblingen, Germany
HPLC system 1	Äkta basic system pump P-900 auto sampler A-900 UV detector UV-900 online degasser K-5004	Amersham Pharmacia Biotech, Uppsala, Sweden  Knauer, Berlin, Germany
HPLC system 2	Smartline 1000 pump Dynamic mixing chamber solvent organizer K-1500 online degasser K-5004	Knauer , Berlin, Germany  Knauer , Berlin, Germany Knauer , Berlin, Germany

	Basic Marathon auto sampler Azura DAD detector 2.1 L	Sparks , Netherlands Knauer, Berlin, Germany
Incubator	BE 500	Memmert, Schwabach, Germany
Incubator	BE 400	Memmert, Schwabach, Germany
Incubator	ULM 500	Memmert, Schwabach, Germany
Laboratory pipette	1-1000 $\mu$ l	Eppendorf AG, Hamburg, Germany
LabWater Purelab Plus water system	conductivity 0.055 $\mu$ S/cm	ELGA, Celle, Germany filter from USFilter, Ransbach- Baumbach, Germany
Magnetic and heating stirrer	RH basic	IKA Labortechnik, Staufen, Germany
pH meter	InoLab Level 1, electrode: InLab Semi-Micro	Mettler-Toledo, Weilheim, Germany
Ultrasonic bath	Sonorex RK 510 Super	Bandelin, Berlin, Germany
Vacuum concentrator	Thermo Savant SPD SpeedVac, Kühlfalle RVT 4104, Vakuumpumpe OFP 400	ThermoSavant, Holbrook, USA
Vortex	Uniprep Gyrator	Uniequip, Freital, Germany
Vortex	Minishaker MS-1 IKA	IKA Labortechnik, Staufen, Germany

#### 3.4.4. Honey samples

Table 29: List of commercial honey samples, Chapter C

Honey	Quantity	Manufacturer, Best before
Artificial honey (AH)	100g AH contain 46.5g fructose + 34g glucose + 1.5g sucrose + 18g ultrapure	-

	water	
Cyclopower capsules, Manuka honey 400+ with $\alpha$ -cyclodextrin	0.05 mg/capsule Batch: G4189	Manuka Health, 07/2017
Manuka honey MGO 550 +	2	Manuka Health NZ Ltd
Polyfloral honey	Batch: C080331	Dr. Krieger`s, 08/2017
RewaRewa honey	1	Manuka Health NZ Ltd, 03/2019

Table 30: List of food used for intervention studies (except honey), Chapter C

Honey	Specification	Manufacturer, Best before
Fructose	99.8 %	Lorenz & Lihn GmbH & Co. KG, Zarrentin, Germany, 07/2019
Glucose	91 %	Dextro Energy GmbH & Co. KG, Krefeld, Germany, 02/2020
$\alpha$ -Cyclodextrin	$\geq 98$ %, CAVAMAX® W6 FOOD	Wacker Chemicals AG, Supplied by Manuka Health NZ Ltd.

### 3.4.5. Simulated gastrointestinal digestion

The *in vitro* digestion model was performed according to Hellwig et al. (2014). In brief, the synthetic gastric juice contains NaCl (2.9 g/l), KCl (0.7 g/l) and KH<sub>2</sub>PO<sub>4</sub> (0.27 g/l) and the synthetic pancreatic juice contains KCl (0.3 g/l), CaCl<sub>2</sub> \* 2 H<sub>2</sub>O (0.5 g/l), urea (0.3 g/l), MgCl<sub>2</sub> \* 6 H<sub>2</sub>O (0.2 g/l), NaHCO<sub>3</sub> (1 g/l) and lyophilized porcine bile (9 g/l). Directly before the incubation, the digestive enzymes pepsin (2.5 mg) and mucin (7.5 mg) were solubilized in 4 ml of the gastric juice and trypsin (1 mg) and pancreatin (24 mg) were homogenized in 3 ml pancreatic juice. The gastric phase was started by mixing 2 ml sample solution with 4 ml of gastric juice. The samples solutions were prepared by solubilizing the samples in 5 ml ultrapure water (see Table 31). The pH value was adjusted to pH 2  $\pm$  0.1 with HCl (3 N) and the samples were incubated in a water bath at 37 °C for two hours. After the stomach phase, 3 ml of pancreatic juice were added to the samples and the pH value was adjusted with solid NaHCO<sub>3</sub> to 7.5  $\pm$  0.1. The samples were further incubated for six hours at 37 °C. The pH

value was controlled every hour and adjusted to  $\text{pH } 7.5 \pm 0.1$  with HCl (3 N) if necessary. For the analysis of DHA in the samples, a higher sample volume was required. Therefore, the simulated digestion was performed with 3-times higher volume of sample solution, gastric juice and pancreatic juice. During incubation, samples were taken at 0, 1 and 2 hour of simulated gastric digestion and 0, 2, 4 and 6 hours of simulated ileal digestion. For HPLC-UV analysis the sample volume was 0.5 ml for MGO and 1.5 ml for DHA analysis, respectively. For amino acid analysis, 2 ml samples were taken. A blank, containing the MGO standard solution, but no digestive juices was included in the sample set.

Table 31: Preparation of sample solutions for the simulated gastrointestinal digestion

Sample	MGO in sample (mg/kg)	Sample weight (g)	MGO in sample solution (mg/l)	MGO in simulated gastric digestion (mg/l)
MGO standard solution (436.7 g/l)	-	-	174.7	58.2
Manuka honey	488.5	1.8	175.9	58.6
Cyclopower	221.3	1.8	79.7	26.6
CD-complex 1	437.5	1.4	122.5	53.3*
CD-complex 2	74377.9	0.012	178.5	59.5
CD-complex 3	221.0	1.8	79.6	26.5

\* 3 ml of sample solution was mixed with 4 ml gastric juice

The CD-complexes containing MGO and  $\alpha$ -cyclodextrin were prepared according to the protocol for the pilot scale production of “MGO 400+ Manuka Honey with Cyclopower<sup>TM</sup>” (Manuka Health NZ Ltd., 2013) with slight modifications. Briefly, ultrapure water was heated to 50 °C and  $\alpha$ -CD was added. The turbid solution was stirred for 10 min and cooled down to 40 °C. MGO and artificial honey were added and the solution was stirred for exactly ten minutes. The sample volumes and concentrations are presented in Table 32. The mixture was subsequently frozen and lyophilized. The lyophilized complexes were stored at -20 °C.

Table 32: Preparation of model CD-complexes for the simulated gastrointestinal digestion

Sample	Molar ratio CD:MGO	Ultrapure water (ml)	$\alpha$ -CD (g)	MGO (ml), concentration given in parentheses	Artificial honey (g)
CD-complex 1	190:1	100	15	0.015 (436.7 g/l)	-
CD-complex 2	1:1	50	5	0.85 (436.7 g/l)	-
CD-complex 3	190:1	50	14.4	1 (5.76 g/l)	11.6*

\* preparation of artificial honey see 3.4.4.

#### Influence of the pH value on the simulated gastrointestinal digestion

To check the influence of the pH value on the stability of the MGO standard solution, the pH value was adjusted according to Table 33. The gastric pH was adjusted to 7.5 directly after the sample after 1 h incubation was taken and the sample was further incubated for one hour. The ileal pH was initially kept at 2.0 and a sample was taken after 0 min of incubation. Then, the pH was adjusted to 7.5 and a sample was taken directly. The sample was further incubated at pH 7.5 for 2 hours and the final sample was taken and analysed for its MGO concentration.

Table 33: Modifications of pH value during simulated gastrointestinal digestion

Digestion	Time point (h)	pH of sample in standard digestion	pH of sample variation
Gastric	0	2.0	2.0
	1	2.0	2.0
	2	2.0	7.5
Ileal	0	7.5	2.0
	0	7.5	7.5
	2	7.5	7.5

#### Influence of human saliva on MGO stability

The samples were solubilized in human saliva instead of ultrapure water and incubated for 5 min at 37 °C. The human saliva was obtained according to (Hu et al., 2013). Briefly, a healthy volunteer rinsed the mouth with water for 30 s. After starting spitting, saliva which was obtained in the first 30 s was discarded. The saliva obtained after following 2 min of spitting was stored and the procedure was repeated until enough saliva was available. The collected saliva was centrifuged at 5000 rpm for 10 min and the supernatant was used as the salivary digestive fluid. The MGO standard solution, manuka honey and CD-complex 1 were studied

for their MGO stability towards human saliva. The samples were solubilised in human saliva instead of water in concentrations according to Table 31 (column 3). For simulated digestion, 3 ml of saliva with solubilized sample were incubated at 37 °C for 5 min and after taking samples at  $t = 0$  min and  $t = 5$  min (0.5 ml each), the residual 2 ml were used for gastrointestinal digestion.

#### 3.4.6. Quantification of methylglyoxal and dihydroxyacetone via RP-HPLC-UV

The quantification of methylglyoxal and dihydroxyacetone is described in section 1.4.5. All honey samples were treated as described in the mentioned section. The samples of the simulated gastrointestinal digestion taken at each time point were directly mixed with 1 ml of methanol and kept at -18 °C for 1 h to precipitate proteins. After centrifugation at 10,000 rpm for 10 min at 4 °C, 500  $\mu$ l of the supernatant was used for MGO and DHA analysis. The volume of the derivatization reagent and the phosphate buffer were adjusted to the reduced sample volume (150  $\mu$ l of each solution instead of 300  $\mu$ l).

#### 3.4.7. Sample preparation of simulated digestion samples for amino acid analysis

Based on the results from the master thesis of Zeitz (2013), the recovery of amino acids from the digestive proteins after enzymatic hydrolysis of the simulated digestion samples is rather limited. Therefore, proteins were supposed to be extracted from the residual sample matrix before subjecting them to enzymatic hydrolysis. The results of the enzymatic hydrolysis with previous protein extraction were compared to the amino acid yield after acid hydrolysis of the digestion samples.

#### Protein isolation

The proteins of the simulated digestion samples were either isolated by protein precipitation with methanol or by dialysis. For protein precipitation, 2 ml of the digestion samples were mixed with 4 ml methanol and kept at -18 °C for 1 h. After centrifugation (10,000 rpm, 10 min) the supernatant was discarded and the protein pellet was washed with 2 ml acetone and centrifuged again (10,000 rpm, 10 min). The supernatant was discarded and the protein pellet was dried under a nitrogen stream. For dialysis, the digestion samples were transferred to dialysis tubings (MWCO 14 kDa) and were dialyzed against distilled water for 3 days at 6 °C with the water changed twice per day. The retentates were then lyophilized and stored at -18 °C.

### Enzymatic hydrolysis

For enzymatic hydrolysis, 2-3 mg of the protein retentate or precipitate was solubilized in 1 mL of 0.02 M hydrochloric acid and 50  $\mu$ l pepsin solution (14 kU in 2 ml 0.02 N HCl) was added. After incubation (37 °C, 24 h), 250  $\mu$ l of potassium phosphate buffer (0.05 M, pH 7.4), 50  $\mu$ l KOH (260 mM) and 50  $\mu$ l of pronase E solution (16 kU Pronase E in 2 ml 0.05 M potassium phosphate buffer, pH 7.4) were added. After further incubation (37 °C, 24 h), 4  $\mu$ l of aminopeptidase solution (ready to use, Sigma) and 20  $\mu$ l prolidase (98.5 U in 1 ml ultrapure water) were added. After incubation (37 °C, 24 h), the samples were lyophilized and reconstituted in 1 ml lithium citrate buffer (0.12 M, pH 2.2) and membrane filtered (0.45  $\mu$ m) prior to analysis.

### Acid hydrolysis

The acid hydrolysis was performed according to Förster (2006) with the protein retentates and precipitates and with the digestion samples without previous protein extraction. For acid hydrolysis of protein isolates and digestion samples, 3 mg of the solid samples were dissolved in 3 ml 6 N HCl and 2 ml of the liquid digestion samples were mixed with 2 ml 12 N HCL.

The mixture was heated at 110 °C for 23 h in a preheated oven. Then, 1 ml of the hydrolysate was evaporated to dryness in a vacuum concentrator (SPD Speed Vac; Thermo Fisher Scientific, Karlsruhe, Germany). The residue was reconstituted in 1 mL of sample buffer for amino acid analysis (0.12 N lithium citrate, pH 2.2) and membrane filtered (0.45  $\mu$ m) prior to analysis.

#### 3.4.8. Amino acid determination

Proteinogenic amino acids were quantitated with a SYKAM S4300 amino acid analyser (Fuerstenfeldbruck, Germany). The effluent was derivatized with ninhydrin at 130 °C and detection of products was performed with an integrated two-channel photometer ( $\lambda$  = 440 nm, 570 nm). External calibration was performed with an amino acid mixture (Sigma-Aldrich, Steinheim, Germany). The injection volume was between 10 and 90  $\mu$ L. The parameters of the amino acid analysis are summarized in Table 34.

Table 34: Parameters of amino acid analysis

		Eluent	A: Lithium citrate buffer, 0.12 M, pH 2.9 B: Lithium citrate buffer, 0.3 M, pH 4.2 C: Lithium citrate/borate buffer, 0.3 M, pH 8.0 D: Lithium hydroxide, 0.5 N		
		Flow rate	0.45 ml/min		
		column	Cation exchange LCA K07/Li		
<b>Gradient Elution</b>	Time (min)	A %	B %	C %	D %
	0	85	15	0	0
	3.0	85	15	0	0
	4.0	79	21	0	0
	21.0	43	57	0	0
	25.0	43	57	0	0
	33.0	0	100	0	0
	39.0	0	0	100	0
	43.0	0	0	77	23
	61.0	0	0	77	23
	61.1	0	0	0	100
	64.1	0	0	0	100
	64.2	85	15	0	0
	77.2	85	15	0	0
<b>Post Column Derivatization</b>	Tim (min)	Valve		Temperature (°C)	
	0	30 % Isopropanol in water		42	
	0.1	SYKAM Ninhydrin		42	
	25.0	SYKAM Ninhydrin		42	
	40.4	SYKAM Ninhydrin		60	
	46.0	SYKAM Ninhydrin		74	
	61.0	SYKAM Ninhydrin		74	
	69.0	30 % Isopropanol in water		74	
	71.0	30 % Isopropanol in water		42	
	81.0	30 % Isopropanol in water		42	



### 3.4.9. Determination of carbonyl compounds via GC-MS

The sample preparation and analysis parameters of the GC-MS method depend on the sample matrix and will be described in detail for the physiological samples urine, blood and saliva.

#### 3.4.9.1. In urine

##### MGO

The analysis of MGO was performed according to Degen et al. (2013). After the urine had been thawed and centrifuged at 10,000 rpm for 10 min, an aliquot of 400  $\mu$ l was mixed with 400  $\mu$ l of acetic acid-acetate buffer (0.5 M, pH 5.0) and spiked with 50  $\mu$ l of the internal standard *o*-chlorobenzaldehyde (17.8  $\mu$ M in ethanol/water (1:1, v/v)). For derivatization, 100  $\mu$ l of a freshly prepared *O*-(2,3,4,5,6-pentafluorobenzyl)hydroxylamine) hydrochloride (PFBOA) solution (15 mg/l in water) was added to the sample solution and vigorously mixed by vortex. After 6 h of derivatization at room temperature, the samples were extracted with 250  $\mu$ l of *n*-hexane for 5 min. An aliquot of 100  $\mu$ L of the organic layer was transferred to a GC vial and then analyzed. GC-MS analysis was performed using an HP7890A gas chromatograph, coupled with an HP7683 automatic liquid sampler and an HP5975C mass spectrometer equipped with an ZB-5 capillary column (30 m, 0.25 mm i.d., 1.0  $\mu$ m film thickness; Phenomenex, USA) and a Zebron Z-guard guard column (deactivated, 5 m, 0.25 mm i.d.; Phenomenex, Germany). The carrier gas was helium with a constant flow at 1.0 ml/min, the injector temperature was 250  $^{\circ}$ C, and 1  $\mu$ l of sample was injected using the pulsed splitless injection mode. MS quadrupole temperature was set at 150  $^{\circ}$ C and MS source temperature at 230  $^{\circ}$ C. The oven temperature program started at 120  $^{\circ}$ C (hold time of 1 min) elevated to 230  $^{\circ}$ C at a rate of 25  $^{\circ}$ C/min (hold time of 2 min), and finally heated to 300  $^{\circ}$ C at 30  $^{\circ}$ C/min with a subsequent post run at 300  $^{\circ}$ C for 3 min, resulting in a complete run time of 13 min. The mass spectrometer was used with electron impact ionization (70 eV) in SCAN and SIM modes. In SIM mode, the dwell time of the analytes was 80 ms and the quantifier and qualifier ions for *o*-chlorobenzaldehyde were 335 and 300, respectively, and for methylglyoxal 265 and 462, respectively. Data acquisition and evaluation were performed with MSD ChemStation software (Agilent, Germany). For external calibration, stock solutions of MGO in water (0.1-1.9  $\mu$ M) were prepared, and 100  $\mu$ l of each stock solution was mixed with 400  $\mu$ l of acetic acid-acetate buffer (0.5 M, pH 5.0) and spiked with 50  $\mu$ l of the internal standard *o*-chlorobenzaldehyde (17.8  $\mu$ M in ethanol/water (1:1, v/v)). For derivatization, 100  $\mu$ l of a freshly prepared *O*-(2,3,4,5,6-pentafluorobenzyl)hydroxylamine hydrochloride (PFBOA) solution (15 mg/l in water) was added to each standard solution and

vigorously mixed by vortex. After 6 h of derivatization at room temperature, the samples were extracted with 250  $\mu\text{l}$  of n-hexane for 5 min. An aliquot of 100  $\mu\text{l}$  of the organic layer was transferred to a GC vial and then analyzed. The procedure resulted in a calibration range of 0.010–0.19 nmol MGO per derivatization assay. Due to the formation of stereoisomers with PFBOA, MGO and o-chlorobenzaldehyde were quantified on the basis of the sum of their signals. Quantitative evaluation was then carried out by the use of the ratio of the area of summarized analyte peaks and the summarized internal standard peaks. The limits of detection (LOD) and quantification (LOQ) in urine were calculated as the concentrations of the analyte necessary to show a peak at a signal-to-noise ratio of 3 and 10, respectively.

### 3-Deoxyglucosone, 3-deoxyfructose and 3-deoxy-2-ketogluconic acid

The analysis of 3-DG, 3-DF and 3-DGA was performed according to Degen et al. (2014). An aliquot of 100  $\mu\text{l}$  of the thawed urine was spiked with 10  $\mu\text{l}$  of internal standard solution (containing 45  $\mu\text{M}$  [ $^{13}\text{C}_6$ ]3-DG and 170  $\mu\text{M}$  [ $^{13}\text{C}_6$ ]3-DGA in water) and was then treated with 30  $\mu\text{l}$  of urease (1 mg/mL in 0.2M sodium phosphate buffer, pH 7.0) for 10 min at 37 °C in a water bath. Termination of the enzymatic reaction was realized by addition of 900  $\mu\text{l}$  of ice-cold ethanol. After centrifugation (10,000g rpm for 15 min), the resulting supernatant was transferred to a new tube and evaporated to dryness under a nitrogen stream. The dry residue was incubated with 50  $\mu\text{l}$  of hydroxylamine hydrochloride solution (10 mg/mL in anhydrous pyridine) for 30 min at 80 °C followed by evaporation to dryness. Then 50  $\mu\text{l}$  of N,O-bis(trimethylsilyl)trifluoroacetamide (BSTFA + TCMS) was added to the residue and vigorously mixed by vortex and incubated at room temperature for another 2 h. Subsequently, 50  $\mu\text{l}$  of n-hexane was added and an aliquot of 80  $\mu\text{l}$  was transferred to a vial. The GC-MS system used for analysis was the same mentioned above for MGO analysis. The carrier gas was helium with a constant flow at 1.0 mL/ min, the injector temperature was 250 °C, and injection mode was 1  $\mu\text{L}$  pulsed splitless. The oven temperature program started at 80 °C (hold time of 2 min) elevated to 260 °C at 7 °C/min and finally heated to 300 °C at 20 °C/min, resulting in a complete run time of 31 min. Mass spectrometer was used with electron ionization (70 eV) in scan and SIM modes. In SIM mode, the dwell time of the analytes was 100 ms and the quantifier and qualifier ions of the analytes are presented in Table 35.

Table 35: SIM mode parameters for the GC-MS analysis of 3-DG, 3-DF and 3-DGA in urine and blood

Analyte	Quantifier ion (m/z)	Qualifier ion (m/z)
3-DF	214	524
3-DG	347	537
[ <sup>13</sup> C <sub>6</sub> ]3-DG	351	543
3-DGA	348	538
[ <sup>13</sup> C <sub>6</sub> ]3-DGA	352	544

For quantification, stock solutions of the analytes in water (0.1  $\mu$ M to 1.1 mM) were pipetted (10-150  $\mu$ l) to yield concentrations between 0.003 to 1.5 nmol per derivatization assay for 3-DG, 0.6 to 69.5 for 3-DF and 0.01 to 6.9 for 3-DGA. Each calibration sample was mixed with 10  $\mu$ l internal standard and subjected to the derivatization procedure after evaporation to dryness (see above). The analytes formed syn- and *anti*-stereoisomers, but for quantification only the ratio of the area of the most prominent analyte peak and the internal standard peak of the corresponding quantifier ions were used. For quantification of 3-DF, the internal standard [<sup>13</sup>C<sub>6</sub>]3-DG was used. The limits of detection (LOD) and quantitation (LOQ) in standard solution and urine were calculated as the concentrations of the analyte necessary to show a peak at signal-to-noise ratios of 3 and 10, respectively.

#### 3.4.9.2. In blood

##### MGO

The blood samples were centrifuged (6,000 rpm, 12 min) in the hospital and 60  $\mu$ l aliquots of the supernatant blood serum were stored at -80 °C. Prior to analysis, the serum samples were thawed and homogenized by gentle vortexing. After the addition of 240  $\mu$ l ultrapure water and 600  $\mu$ l ice-cold acetonitrile/methanol solution (v/v 70:30), the samples were stored at -18 °C for 1 h. Then, the samples were centrifuged (6,500 rpm, 10 min) and 600  $\mu$ l of the supernatant was transferred in a fresh 1.5 ml tube and subsequently evaporated to dryness under a nitrogen stream. Then, 50  $\mu$ l of the internal standard ([<sup>13</sup>C]-MGO, 5.6  $\mu$ M in 0.5 M acetic acid-acetate buffer, pH 5.0) and 50  $\mu$ l of acetic acid-acetate buffer (0.5 M, pH 5.0) were added. For derivatization, 300  $\mu$ l of a freshly prepared O-(2,3,4,5,6-pentafluorobenzyl)hydroxylamine hydrochloride (PFBOA) solution (15 mg/l in water) was added and vigorously mixed by vortex. After 6 h of derivatization at room temperature, the samples were extracted with 150  $\mu$ l of n-hexane for 5 min. An aliquot of 100  $\mu$ l of the organic

layer was transferred to a GC vial for GC-MS analysis. The GC-MS parameters were the same mentioned in section 3.4.9.1 and in SIM mode, the quantifier and qualifier ions for [ $^{13}\text{C}$ ]-MGO were 266 and 463, respectively, and for ([ $^{12}\text{C}$ ]-MGO) 265 and 462, respectively. For quantification of MGO, a matrix calibration was used. Therefore, different volumina of a stock solution in water (91  $\mu\text{M}$ ) were diluted in 10 ml acetic acid-acetate buffer (0.5 M, pH 5.0) to yield concentrations between 0.9 to 27.3  $\mu\text{M}$ . Then, eight blood serum samples (from a healthy volunteer in fastened state) was prepared as mentioned above. To the dried serum samples, 50  $\mu\text{l}$  of the internal standard solution ([ $^{13}\text{C}$ ]-MGO, 5.6  $\mu\text{M}$  in 0.5 M acetic acid-acetate buffer, pH 5.0) and 50  $\mu\text{l}$  of the corresponding standard solutions were added. The derivatization procedure was performed according to the serum samples.

### 3-Deoxyglucosone, 3-deoxyfructose and 3-deoxy-2-ketogluconic acid

The blood samples were centrifuged (6,000 rpm, 12 min) and 60  $\mu\text{l}$  aliquots of the supernatant blood serum were stored at  $-80\text{ }^{\circ}\text{C}$ . Prior to analysis, the serum samples were thawed and homogenized by gentle vortexing. After the addition of 10  $\mu\text{l}$  internal standard (containing 45  $\mu\text{M}$  [ $^{13}\text{C}_6$ ]3-DG and 170  $\mu\text{M}$  [ $^{13}\text{C}_6$ ]3-DGA in water), 240  $\mu\text{l}$  ultrapure water and 600  $\mu\text{l}$  ice-cold acetonitrile/methanol solution (v/v 70:30), the samples were stored at  $-18\text{ }^{\circ}\text{C}$  for 1 h. Then, the samples were centrifuged (6,500 rpm, 10 min) and 600  $\mu\text{l}$  of the supernatant was transferred in a fresh 1.5 ml tube and subsequently evaporated to dryness under a nitrogen stream. The derivatization procedure was performed according to 3.4.9.1. The GC-MS SIM parameters were also described in the previous mentioned section. Moreover, dihydroxyacetone phosphate (DHAP) was included in the SIM mode with the quantifier ion 315 and the qualifier ions 299 and 458. The internal standard [ $^{13}\text{C}_6$ ]3-DG was used for the evaluation of peak areas of DHAP. Since DHAP and 3-DG are physically and chemically different, there were no absolute amounts of DHAP quantified. However, the ratio of the peak area of DHAP to the peak area of [ $^{13}\text{C}_6$ ]3-DG was calculated and the ratio of the fastened state was defined as 100 %. For quantification of 3-DG, 3-DF and 3-DGA, a matrix calibration was used. Therefore, stock solutions of the analytes in water (9.8 nM to 4.5  $\mu\text{M}$ ) were pipetted (10-300  $\mu\text{l}$ ) to yield concentrations between 0.0005 to 0.12 nmol per derivatization assay for 3-DG, 0.001 to 1.0 for 3-DF and 0.002 to 0.55 for 3-DGA. The calibration standards were mixed with 10  $\mu\text{l}$  internal standard solution and were evaporated to dryness. Then, 60  $\mu\text{l}$  of blood serum (from a healthy volunteer in fastened state) were added and the samples were treated according to the blood serum samples.

## 3.4.9.3. In saliva

The freshly collected saliva (see 0 for collection protocol) was stored on ice and subsequently membrane filtered (0.45  $\mu\text{m}$ ). After the addition of 100  $\mu\text{l}$  saliva filtrate to 40  $\mu\text{l}$  of MGP solution (6.3 mg/l) and 30  $\mu\text{l}$  of [ $^{13}\text{C}$ ]MGO solution (4.2 mg/l), the samples were frozen and lyophilized. The dry residue was incubated with 50  $\mu\text{l}$  of hydroxylamine hydrochloride solution (10 mg/mL in anhydrous pyridine) for 30 min at 80  $^{\circ}\text{C}$  followed by evaporation to dryness. Then 50  $\mu\text{l}$  of N,O-bis(trimethylsilyl)trifluoroacetamide (BSTFA + TCMS) was added to the residue and vigorously mixed by vortex and incubated at room temperature for another 2 h. Subsequently, 70  $\mu\text{l}$  of n-hexane was added and after centrifugation (10,000 rpm, 10 min) an aliquot of 50  $\mu\text{l}$  was transferred to a vial. The GC-MS system used for analysis was the same mentioned above (see Table 28). The carrier gas was helium with a constant flow at 1.0 mL/ min, the injector temperature was 250  $^{\circ}\text{C}$ , and injection mode was 1  $\mu\text{L}$  pulsed splitless. The oven temperature program started at 70  $^{\circ}\text{C}$  (hold time of 1 min) elevated to 130  $^{\circ}\text{C}$  at 4  $^{\circ}\text{C}/\text{min}$ , followed by an increase of 10  $^{\circ}\text{C}/\text{min}$  to 162  $^{\circ}\text{C}$ , elevated to 184  $^{\circ}\text{C}$  at 2  $^{\circ}\text{C}/\text{min}$  and finally heated to 254  $^{\circ}\text{C}$  at 7  $^{\circ}\text{C}/\text{min}$ , resulting in a complete run time of 40.2 min. A post run at 320  $^{\circ}\text{C}$  for 7 min was subsequently performed. Mass spectrometer was used with electron ionization (70 eV) in scan and SIM modes. In SIM mode, the dwell time of the analytes was 50 ms and the quantifier and qualifier ions of the analytes are presented in Table 36.

Table 36: SIM mode parameters for the GC-MS analysis of MGO, DHA, DHAP, 3-DG, 3-DF, 3-DGA, fructose and glucose in saliva, \*internal standard

Analyte	Quantifier ion (m/z)	Qualifier ion (m/z)
[ $^{13}\text{C}$ ]MGO*	232	247
MGP*	204	217
MGO	231	246
DHA	221	158
DHAP	315	299
Fructose	217	307
Glucose	319	205
3-DG	347	537
3-DF	214	524
3-DGA	348	538

For quantification, an external matrix calibration with 100  $\mu\text{l}$  freshly collected and filtered saliva was used. Stock solutions of the analytes in water were pipetted to yield concentrations between 0.0005 to 0.03 nmol per 100  $\mu\text{l}$  saliva for MGO, 0.03 to 0.3 for DHA, 0.3 to 11.8 for DHAP, 0.0009 to 0.4 for 3-DG, 0.006 to 0.12 for 3-DF, 0.0002 to 0.2 for 3-DGA, 0.005 to 50 for fructose and 0.05 to 40 nmol/100  $\mu\text{l}$  saliva for glucose. Each calibration sample was mixed with the same internal standards like the samples (MGP and [ $^{13}\text{C}$ ]MGO) and was subjected to the derivatization procedure after evaporation to dryness (see above). The analytes formed syn- and *anti*-stereoisomers, but for quantification only the ratio of the area of the most prominent analyte peak and the internal standard peak of the corresponding quantifier ions were used. For quantification of MGO and DHA, the internal standard [ $^{13}\text{C}$ ]MGO was used. For all other analytes, MGP was used as internal standard.

#### 3.4.10. Conception of nutrition studies

Within the scope of the master thesis of Stephanie Schultes (Schultes, 2016) and Lisa-Marie Blasse (Blasse, 2017), the metabolic transit of carbonyl compounds was studied. On this occasion, two approaches to study human carbohydrate metabolism were used. By collecting the 24 h urine of healthy individuals, which followed a dietary protocol, the daily urinary excretion rate of carbonyl compounds and their metabolites was studied over 5 days (long-term metabolic transit) (Schultes, 2016). Moreover, by taking blood (Schultes, 2016) or saliva samples (Blasse, 2017) from healthy volunteers in fastened state and at certain time points after a dietary intervention, the current metabolic state of the individuals was studied (short-term metabolic transit).

##### 3.4.10.1. Metabolic transit in urine

The group of subjects comprised 18 volunteers (see Table 38 for characterisation of study subjects), which were divided into five groups. The intervention study lasted for five days, whereby on day 1 and 5 the individuals had no dietary restrictions, on day 2-4 they followed a diet consisting solely of raw fruits and vegetables, avoiding heated and fermented food such as dairy and bakery products, coffee, juices, and beer to ensure a diet virtually free of dicarbonyl compounds (“raw-food” diet). In the morning of day 3 the subjects were administered their intervention food. The diet on intervention day for the five groups is described in Table 37. Prior to the intervention study, a control group followed the dietary protocol without intervention, whereby day 1 had no dietary restrictions, day 2-6 consisted of

a raw-food diet and on day 7 the subjects went back to no dietary restrictions again. The results of the control group showed that one day for the wash-out of residual dicarbonyl compounds in the urine is sufficient, so the intervention study was shortened to 5 days in total. The subjects were asked to collect their 24 h urine in plastic containers, which were stored at 6 °C during the collection time. On the following morning of each day, the total volume of the 24 h urine was measured and a aliquot of the 24 h urine was subsequently stored at -80 °C until analysis of MGO, 3-DG, 3-DF and 3-DGA was performed (see section 3.4.9.1). The subjects were further asked to keep records of the kind and amount of the daily ingested food, their physical activity and the amount of cigarettes smoked during each study day.

Table 37: Dietary restrictions during the intervention study

Day	Diet		Number of subjects
1	Raw-food		15
2	Raw-food		15
3	Group 2:	Raw-food + 125 g manuka honey	4
	Group 3:	Raw-food + 12 cyclopower capsules	4
	Group 4:	Raw-food + 2.7 g cyclodextrin powder	4
	Group 5:	Raw-food + 125 g non-manuka honey	3
4	Raw-food		15
5	Raw-food		15

The subjects of group 3 and 4 were administered the dose of 6 capsules or 1.35 g  $\alpha$ -cyclodextrin powder in the morning of day 3 and further 6 capsules or 1.35 g  $\alpha$ -cyclodextrin powder during mid-day. This was done to prevent digestion complications like flatulence. Based on a voluntarily questionnaire, the subjects were classified as healthy individuals with an average body mass index (BMI) of 23 kg/m<sup>2</sup> and fastened-state glucose level of 4.8 mmol/l. Table 38 gives an overview of the study subjects. In total, 18 subjects took part in the study, whereby two subjects participated two times.

Table 38: Characterisation of study subjects for metabolic transit in urine

Parameter	Subjects
n	18
Sex	14 female, 4 male
Age (years)	25.6 ± 4.8 (range: 21-41)
BMI (kg/m <sup>2</sup> )	23.0 ± 3.7 (range: 20.8-36.3)
Fastened-state glucose (mmol/l)	4.8 ± 0.4 (range: 4.1-5.8)
Vegetarians	4
Smokers	2

#### 3.4.10.2. Metabolic transit in blood

Two subjects participated in a short-term intervention study, which was designed in the style of an oral glucose tolerance test (OGTT). Venous blood was withdrawn from the subjects via a vascular access and after the subjects gave a fastened-state blood sample, they orally administered either 125 g manuka honey (subject 1) or 125 g artificial honey (subject 2). The subjects were asked to consume the samples within 10 min and blood was withdrawn after 30, 60 and 120 min of administration. Parallel to the blood withdrawal, the blood glucose level was detected with a blood glucose meter. The venous blood was stored in the BD Vacutainer SST II Advance containing clot activator for 30-60 min and was centrifuged after complete coagulation at 6,000 rpm for 12 min. Aliquots of the blood serum were stored at -80 °C until analysis of MGO, 3-DG, 3-DF, 3-DGA and DHAP (see section 3.4.9.2). The subjects are characterised in Table 39.

Table 39: Characterisation of study subjects for metabolic transit in blood

Parameter	Subject 1 (manuka honey)	Subject 2 (artificial honey)
Sex	female	male
Age (years)	24	31
BMI (kg/m <sup>2</sup> )	20.5	26.8
Fastened-state glucose (mmol/l)	4.9	4.3



Vegetarian	yes	yes
Smoker	no	no

#### 3.4.10.3. Metabolic transit in saliva

The study subjects were divided into five groups, which were administered five different food products. Group 1 was administered 75 g of glucose, group 2 had 40 g of fructose, group 3 had a fructose/glucose mix (34.7/30.3), which resembled the honey sugar matrix, group 4 had 65 g of manuka honey (MGO 550+) and group 5 had 65 g of rewarewa honey. The study was performed in the morning of the according day and the participants were asked to be in fastened state. The food stuff was weighed in a plastic beaker and dissolved in 150 ml water. The administration was performed in a time period of 1 min and the subjects were allowed to drink water afterwards. Saliva samples were collected prior to the food administration (0 min) and 15, 30, 60 and 120 min after. Prior to each saliva sample collection, the subjects rinsed their mouth with 30 ml water for 10 s, brushed their teeth for 60 s without toothpaste and rinsed again with 30 ml water for 10 s. After the cleaning procedure, the subjects waited 5 min and then swallowed the residual saliva in their oral cavity. For the following 3 min, the subjects collected the saliva, which pooled in their mouth, into a 10 ml glass vessel. The freshly collected saliva was stored on ice until analysis (see 3.4.9.3). The sample collection at 0 min was referred to as fastened state, whereas the following time points (15, 30, 60 and 120 min) were referenced to the time at which the subjects administered the corresponding food product. The subjects are characterised in Table 40.

Table 40: Characterisation of study subjects for metabolic transit in saliva

Parameter	Subjects
Sex	13 female, 21 male
Age (years)	28 (21-60)
BMI (kg/m <sup>2</sup> )	22.6 (18.8-27.2)
Omnivore	20
Vegan	2
Vegetarian	12
Smoker	7

### 3.5. Results and discussion

#### 3.5.1. Stability of carbonyl compounds during simulated digestion

When manuka honey is taken up with the diet, mainly the monosaccharides glucose and fructose, but also significant amounts of methylglyoxal and dihydroxyacetone can reach the gut. Whereas there is profound knowledge of the metabolic transit of sugars and their gastrointestinal metabolism (Löffler et al., 2007), there are only limited information available dealing with the metabolic fate of MGO and DHA. The results of this section are partly originating from the experimental work of master student Constanze Polster and are originally published in her master thesis (Polster, 2015).

#### Stability of MGO and DHA in manuka honey

The simulated gastrointestinal digestion is a model experiment to evaluate the stability of certain compounds during digestion. Concerning MGO and DHA, metabolic reactions like degradation or enzymatic modification were unlikely since the simulated gastrointestinal fluids contained only peptidases, which are not able to metabolise MGO and DHA. Nevertheless, the measurement of MGO and DHA during the simulated digestion process, enabled the estimation of the stability of these compounds under physiological conditions. The conditions (e.g. salt and enzyme concentration, pH value and temperature) during the gastric and ileal phase were chosen to simulate human physiological circumstances (Hellwig, 2011). Besides the gastric and ileal fluids also saliva contains potential reaction partners for MGO. Although saliva contains mainly water (99.5 %), it comprises also proteins like mucine and enzymes like lysozyme and amylase (Löffler et al., 2007). To assess whether these compounds react with MGO thus leading to an apparent decrease of MGO in food, human saliva was incubated with manuka honey and a MGO standard solution (see section 3.4.5 for experimental). The incubation did not lead to a decrease of MGO, which is shown in Table 41. This might be due to the short incubation time of 5 min, the limited amount of proteins ( $\leq 0.5$  %) or the slightly acidic pH value of 5.5-6.5 (Benedé et al., 2014; Minekus et al., 2014). The results of the simulated saliva phase showed that high amounts of MGO in food may reach the gut without prior degradation.

Table 41: Concentration of MGO after 5 min incubation in human saliva, based on initial MGO concentration

Sample	Manuka honey solubilized in human saliva (MGO:176 mg/l)	MGO standard solution solubilized in human saliva (MGO: 175 mg/l)
MGO (%) of initial concentration after 5 min incubation	98.4 ± 2.6	100.8 ± 1.5

Following the hypothesis that MGO in manuka honey reaches the gastrointestinal system, a simulated digestion of manuka honey with continuous monitoring of the bioactive compounds MGO and DHA was performed.

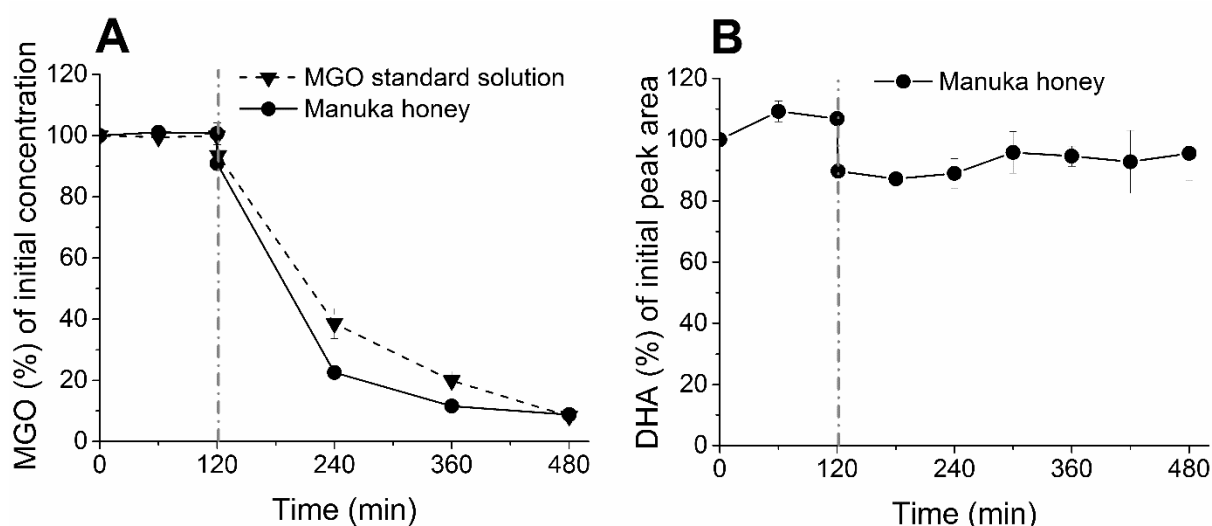


Figure 51: Stability of (A) MGO during simulated gastrointestinal digestion of MGO standard solution or manuka honey and (B) stability of DHA during simulated gastrointestinal digestion of manuka honey

Figure 51 shows the gastrointestinal stability of MGO and DHA. For analysing free MGO and DHA at each time point, methanol was added to the samples directly after sample collection to precipitate proteins and thus terminate reactions with proteins. The supernatant was separated from proteins and analysed according to 3.4.6. For MGO, absolute concentrations were calculated, whereas for DHA only peak areas were compared. The determination of MGO can be achieved with an external calibration of an aqueous standard since the MGO derivatization to the quinoxaline derivative is complete. In contrast DHA did neither

completely react to a quinoxaline derivative nor formed only one reaction product with o-PD. These limitations were overcome in honey by quantifying DHA via the standard addition method and by modifying the derivatization procedure (Atrott, 2013). However, because of the size of the sample set and the limited amount of sample volume for each time point, this was not performed during the simulated digestion experiment. Therefore, only the peak areas of the main DHA quinoxaline derivative (elutes at 12.5 min when performed according to 1.4.5) was compared for each time point.

The behaviour of MGO during simulated digestion (see Figure 51A) showed that MGO is stable in the presence of gastric fluids at pH 2. In contrast during ileal phase, the MGO concentration rapidly decreased down to 10 % of the initial concentration. The comparison of manuka honey with the MGO standard solution showed that the MGO concentration in manuka honey appeared to decrease a bit faster. However, in the end of the incubation after 6 h of ileal digestion, there were only minor differences between the MGO concentrations of the samples, indicating that the matrix did not exert a significant influence on MGO stability. The results for MGO confirmed the findings of Degen et al. (2013), who also described a rapid decrease of MGO during ileal digestion down to a level of 20 % of the initial MGO concentration. The stability of MGO during the gastric phase was surprising since the available reaction sites at protein residues were as many as in the ileal phase. However, the acidic pH of 2 ensured that the amino groups were protonated and thus less available for reactions with MGO. To prove this hypothesis, an additional simulated digestion experiment was performed in which the pH 2 of the gastric phase was either kept also after the addition of the pancreatic enzymes or the pH value was set at 7.5 already at the beginning of the gastric phase (see section 3.4.5 for experimental). The results are presented in Figure 52.

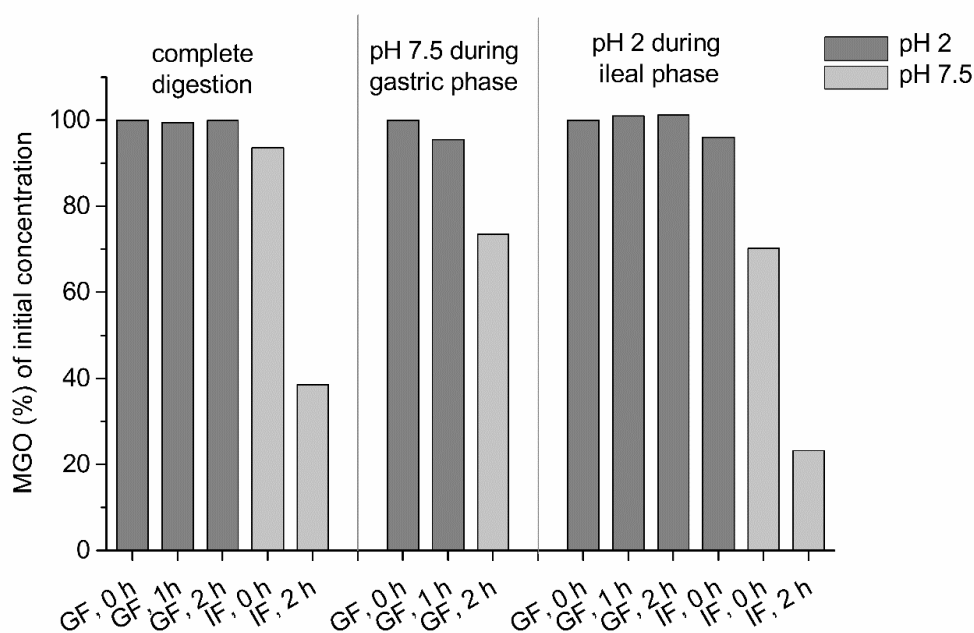


Figure 52: Stability of MGO standard solution in gastric fluids (GF) and ileal fluids (IF) at pH 2 or pH 7.5

When the pH value was set to 7.5 in the presence of the gastric fluids, MGO decreased to 74 % of the initial MGO concentration. However, when the gastric pH of 2 was kept also when pancreatic fluids were added, MGO did not decrease. Only when the pH was set to 7.5, MGO started decreasing. This unambiguously showed that not the type of enzymes but the pH value was the critical factor for the loss of MGO during the simulated digestion. Glycation reactions due to MGO are well described at physiological pH values (Lo et al., 1994; Rabbani and Thornalley, 2008).

In contrast to MGO, the precursor compound DHA seemed to be stable over the whole simulated digestion period. In comparison to MGO, the hydroxyketone DHA has only one reactive keto groups, which can react with amino groups of proteins to form Schiff base adducts (Li et al., 2008; Seneviratne et al., 2012). In the literature, this is mainly described for dihydroxyacetone phosphate, which is endogenously present as a metabolic intermediate of glycolysis. In the presence of human serum albumin (HSA), DHA appears to be even more reactive than DHAP, especially at pH levels greater 7 (Seneviratne et al., 2012). However, the authors report a significant decrease of DHA and DHAP only after 10 days of incubation. This might explain why no decrease of DHA was found in this work, since the maximum incubation time during simulated digestion is 8 h (6 h at basic pH). Similar results for DHA stability during simulated digestion compared to the present work were reported recently (Parkar et al., 2017). The stability of DHA could also be due to competitive reactions of MGO

and DHA. Since MGO is more reactive, its presence might suppress reactions of DHA with amino groups. However, technically there is an excess of reaction sites for DHA and MGO present during simulated digestion, which is shown in Table 42. The amount of amino acids was calculated based on the results of the acidic hydrolysis of the digestion enzymes performed by Zeitz (2013) and corrected for the dilution factors used in the present work.

Table 42: Concentration of lysine, arginine and cystin based on the analysis of acidic hydrolysates by Zeitz (2013) in simulated ileal phase. MGO and DHA concentrations are calculated from the initial concentrations under consideration of the dilution factor

Compound	Lysine	Arginine	Cystin	MGO	DHA
Concentration in simulated ileal phase ( $\mu\text{mol/l}$ )	771	607	301	325	566
In total ( $\mu\text{mol/l}$ )	1679			891	

To check whether the stability of DHA was due to the simultaneous presence of MGO, a simulated digestion of a DHA standard solution could be performed. However, for the application in food this is only of minor relevance, since there is no food described with high concentrations of DHA alone. Regardless of the application in food, it would be interesting to study the reactivity of DHA since its phosphorylated form also appears to be an important physiological intermediate.

#### Stability of MGO and DHA in cyclodextrin complexes

The commercial product cyclopower contains  $\alpha$ -cyclodextrin and manuka honey in the ratio 175:1. To elucidate whether CD influences the MGO and DHA stability during simulated digestion, cyclopower and two model complexes, which contained  $\alpha$ -CD and MGO, were digested according to 3.4.5. The model CD-complex 1 contained  $\alpha$ -CD and MGO in the ratio 175: 1, whereas the model CD-complex 2 contained both compounds in an equimolar ratio.

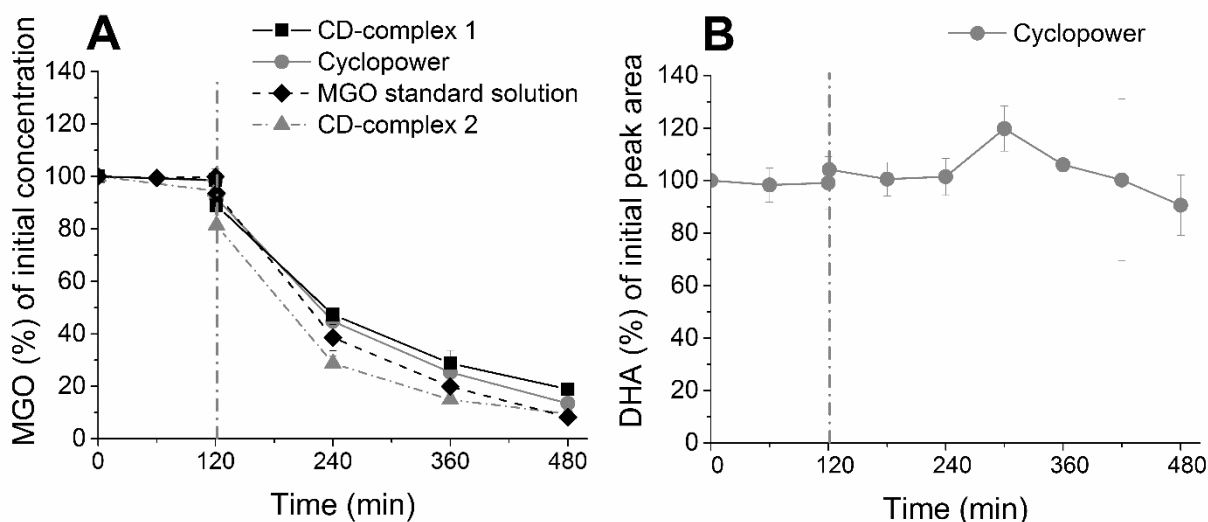


Figure 53: Stability of (A) MGO during simulated gastrointestinal digestion of a MGO standard solution and CD complexes of manuka honey (cyclopower) or CD complexes of MGO in the ratio 175:1 (complex 1) and in the ratio 1:1 (complex 2) and (B) stability of DHA during simulated gastrointestinal digestion of the CD complex of manuka honey (cyclopower)

Figure 53 shows the results of the MGO and DHA analysis of the digestion samples. For MGO, the simulated digestion of cyclopower and the model CD-complex 1 resulted in a decrease of MGO down to 13 and 19 % of the initial concentration, respectively. Compared to the decrease to 8 % when a MGO standard solution is incubated, this indicated a slightly stabilizing effect of  $\alpha$ -CD. However, this effect is only found when  $\alpha$ -CD is present in a great excess compared to MGO. The model CD-complex 2 contained MGO and  $\alpha$ -CD in an equimolar ratio and did not stabilize MGO towards reactions during the simulated digestion (decrease of MGO to 9 %). Figure 53B shows the stability of DHA during the simulated gastrointestinal digestion of cyclopower. The complexation of manuka honey with  $\alpha$ -CD did not influence DHA stability, since DHA showed the same stability in the presence or absence of  $\alpha$ -CD.

The slightly stabilizing effect of  $\alpha$ -CD on MGO, when an excess of  $\alpha$ -CD was present, might be due to either an encapsulation of MGO (compare chapter 1.5.4) or interactions of amino acid side chains with the inner side of  $\alpha$ -CD. The interaction of MGO and DHA with  $\alpha$ -CD was shown to be rather weak, therefore a strong effect on the stability of MGO and DHA was not expected. However, amino acid residues of the gastrointestinal proteins might interact with  $\alpha$ -CD and thus are less available for reactions with MGO and DHA. The slight enhancement in the stability of MGO is probably without physiological relevance and confirmed the rather weak interactions between MGO and CD. The stability of DHA in the

presence and absence of  $\alpha$ -CD is an interesting result, which needs further research. We speculate that DHA reaches the colon and may have an effect on the intestinal microbiota. Moreover, DHA could also reach the blood system via gastrointestinal resorption. The metabolic transit of DHA will be discussed in section 3.5.3.2 in detail.

### 3.5.2. Amino acid modification during simulated digestion

In her master thesis, Zeitz (2013) identified bile extracts and enzymes as the main reaction partners of MGO. The MGO derivative of arginine, MG-H1, was identified as the major reaction product and accounted for 5 % of the MGO loss. The lysine modification CEL was not detected. It was concluded that the incomplete recovery of MGO is due to the low release of 12 % of proteinogenic amino acids during the enzymatic hydrolysis (Zeitz, 2013). The low release might be due to reactions of MGO and the enzymes used for enzymatic hydrolysis leading to a reduced enzymatic cleavage. To increase the recovery of protein-bound amino acids after enzymatic cleavage, the sample preparation was adjusted. Instead of directly incubating the digestion samples with the solutions for enzymatic hydrolysis, the digestion samples were treated with methanol to separate MGO and proteins. The precipitated proteins were washed and subjected to enzymatic hydrolysis. After enzymatic hydrolysis of the precipitated protein, only 2 % of lysine residues and 5 % of arginine residues were recovered in comparison to the acid hydrolysis of the same protein. Apparently the hydrolytic enzymes were not able to cleave the precipitated protein, which might be due to denaturation followed by aggregation and blockage of the enzymatic cleaving sites. The same experiment was performed with lysozyme to check whether the low lysine and arginine recovery is due to the protein structure or the methanol treatment. With lysozyme as a model protein, 78 % of lysine residues were recovered when solubilized lysozyme was enzymatically cleaved, whereas only 16 % of lysine residues were recovered when lysozyme was treated with methanol prior to enzymatic hydrolysis. Thus, the methanol treatment of digestion samples to separate MGO and proteins followed by enzymatic cleavage is unsuitable for sample preparation. To prevent protein denaturation, the digestion samples were dialyzed against water instead treatment with methanol. After lyophilisation, the retentates were enzymatically hydrolysed. The enzymatic hydrolysis of the model protein lysozyme after dialysis resulted in a 86 % and 96 % recovery of lysine and arginine residues, respectively. A blank, which contained the enzymes of the simulated gastric phase but no MGO gave 79 % recovery of lysine and 84 % recovery of arginine residues after enzymatic hydrolysis. This result showed that digestive gastric



enzymes can be enzymatically cleaved when they have not been denatured. However, when the digestion samples, which additionally contained the ileal enzymes after 6 h incubation, were enzymatically hydrolysed, only 34 % of lysine and 54 % of arginine residues were recovered. These results point to the fact that indeed dialysis is a more appropriate sample preparation for the digestion samples, compared to protein precipitation, but that the release of amino acids after incubation is mainly dependent on the enzyme species. Apparently, the gastric enzymes pepsin and mucin might be cleaved more effectively by the enzymatic hydrolysis, whereas the ileal enzymes trypsin and pancreatin might be more resistant to this treatment. Moreover, the “enzymatic load” is much higher when the ileal samples are subjected to enzymatic hydrolysis compared to the gastric phase. Ultimately, the enzymes used for simulated digestion are able to cleave the enzymes added for enzymatic hydrolysis, thus making them ineffective.

When manuka honey was digested for 2 h with gastric fluids and 6 h with pancreatic fluids and the final sample was enzymatically hydrolysed, 29 % of lysine and 45 % of arginine residues were recovered. In comparison to the blank, which contained no honey, this was a 5 % decrease of lysine and a 9 % decrease of arginine residues. Taken together, the modification of lysine and arginine explained 7 % of the MGO loss, which was detected during the 8 h incubation. Up to now, there is no complete recovery of the MGO loss possible. On the one hand this was probably due to the reduced release of protein-bound amino acids after enzymatic hydrolysis and on the other hand lysine and arginine are only some of the residues which were modified by MGO. The results of the enzymatic hydrolysis of the digestion samples are summarized in Table 43.

Table 43: Summary of the lysine and arginine recovery after enzymatic hydrolysis of the digestion samples with sample preparation via methanol precipitation or dialysis

<b>Recovery after enzymatic hydrolysis</b>	<b>Precipitated lysozyme</b>	<b>Precipitated Ileal enzymes</b>	<b>Dialysed lysozyme</b>	<b>Dialyzed gastric enzymes</b>	<b>Dilayzed ileal enzymes</b>
Lysine (%)	16	2	86	79	34
Arginine (%)	-	5	96	84	54

To overcome the effects, which were caused by self-hydrolysis of the digestive enzymes and to fully recover the MGO loss, the simulated digestion should be performed in the presence of a non-enzymatic protein (e.g. casein) instead of pepsin, mucin, trypsin and pancreatin. It

should be tested whether the loss of MGO is the same in the presence of casein and if so whether the incubated protein can be enzymatically hydrolysed more effectively. Moreover, the MGO modification of casein residues should be studied by analysing MGO-derived MRPs via LC-MS/MS.

### 3.5.3. Metabolic transit of carbonyl compounds

The intake of carbohydrate rich food, which was heated or fermented, mostly comes along with the uptake of dicarbonyl compounds. The aim of this study was to obtain more profound knowledge about the metabolic transit of those compounds. Therefore, the excretion of carbonyl compounds and their metabolites was studied in urine (section 3.5.3.1) and in blood (3.5.3.2). The samples were obtained in small intervention studies with healthy subjects (see section 3.4.10).

#### 3.5.3.1. Metabolic transit in urine

Urine is an ultrafiltrate of blood, which is produced in the kidneys. Urine production regulates the water and electrolyte balance system of the human body and ensures clearance of metabolic by-products. Thus, the urinary excretion of dietary compounds is a reflection of their metabolic transit. In this study, the influence of dietary 3-DG and MGO on their concentration and their metabolites in human urine was studied. During the first trial, four healthy subjects chose their food with no dietary restrictions on day 1 and 7 and followed a raw-food diet on day 2 to 6. The raw-food diet was chosen to ensure a diet virtually free of dicarbonyl compounds. The subjects were asked to collect their 24 h urine, which was subsequently analysed for MGO and 3-DG and the metabolites 3-DF and 3-DGA.

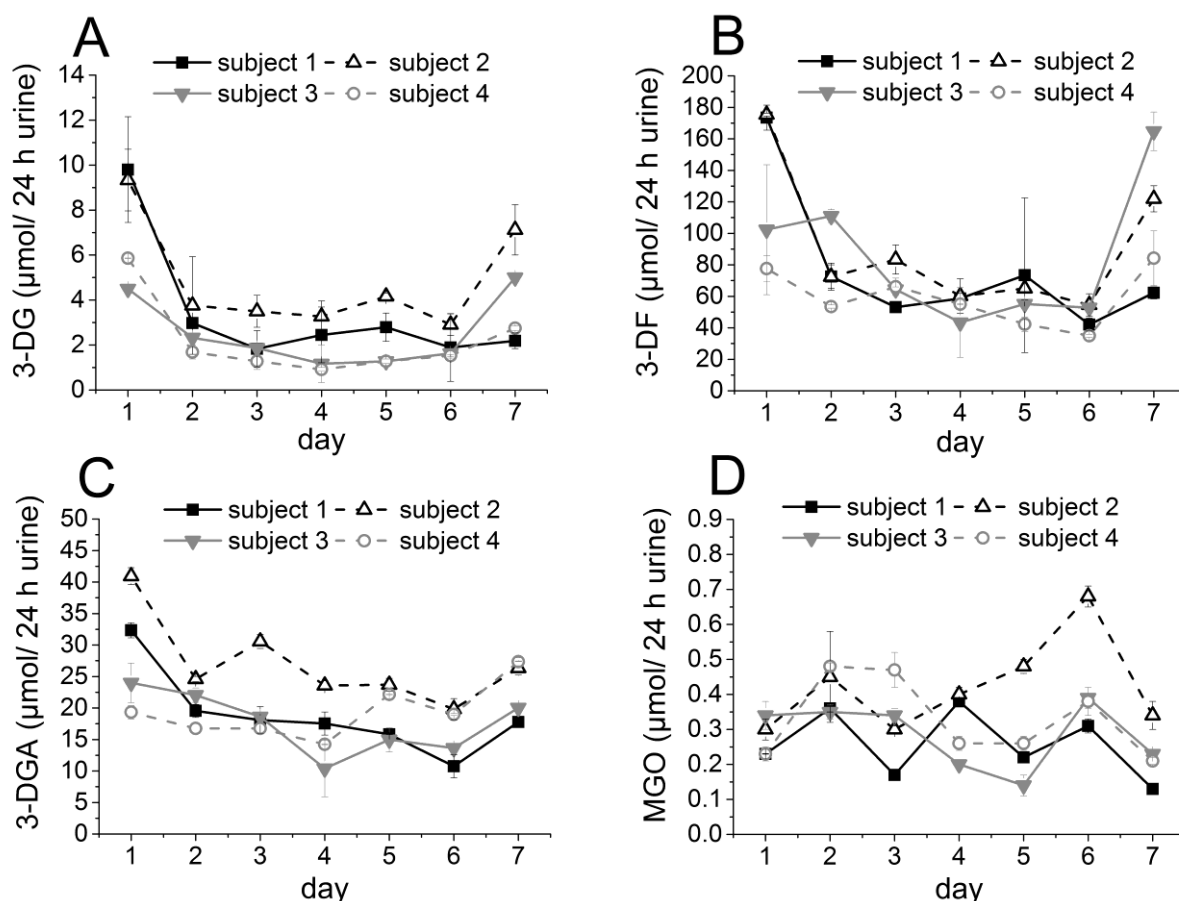


Figure 54: Urinary excretion in 24 h urine of 3-DG (A), 3-DF (B), 3-DGA (C) and MGO (D) during a mixed diet (day 1 and 7) and a raw-food diet (day 2-6)

Figure 54A shows the dietary influence of 3-DG on its urinary concentration. The urinary 3-DG excretion of all subjects was higher at day 1 and 7, when the participants consumed a mixed diet, whereas the 3-DG excretion was lowered from day 2 to 6. It was concluded that the reduction of dietary dicarbonyl compounds by eating a raw-food diet, subsequently reduced the 3-DG level *in vivo* and therefore led to a decrease of urinary 3-DG. The median urinary concentration of 3-DG during a mixed diet was  $7.6\ \mu\text{mol}/24\text{ h urine}$  on day 1 and was reduced to  $2.3\ \mu\text{mol}/24\text{ h urine}$  on day 2. The same pattern can be seen for the 3-DG metabolites 3-DF and 3-DGA. The median urinary excretion of 3-DF (panel B) was  $137.9\ \mu\text{mol}/24\text{ h urine}$  on day 1 and decreased to  $72.5\ \mu\text{mol}/24\text{ h urine}$  on day 2. The metabolite 3-DF is formed via the enzymes aldose reductase and aldehyde reductase and the loss of the dicarbonyl function of 3-DG leads to a decreased reactivity towards amino groups. In contrast, the oxidative metabolite 3-DGA, which was found in urine of subjects with a mixed diet at a median concentration of  $28.2\ \mu\text{mol}/24\text{ h urine}$ , 3-DF appeared to be the main

metabolite of 3-DG. However, the 3-DGA excretion was also decreased when the mixed diet was replaced with a raw-food diet to a median level of 20.8  $\mu\text{mol}/24\text{ h}$  urine (panel C). The remaining level of 3-DG, 3-DF and 3-DGA during the raw-food diet (day 2-6) can be explained by endogenously formed 3-DG, which was also metabolized to 3-DF and 3-DGA. Endogenous 3-DG can either be formed from glucose via the Maillard reaction (Maessen et al., 2015) or can arise from the enzymatic degradation of fructosamines (Van Schaftingen et al., 2012). Although dietary 3-DG exerted an influence on the endogenous level of 3-DG and its metabolites, apparently it was not the only source of 3-DG *in vivo*.

In contrast, the endogenous level of the dicarbonyl compound MGO (see Figure 54D) was not influenced by the diet. The urinary MGO concentration ranges from 0.1 to 0.7  $\mu\text{mol}/24\text{ h}$  urine during mixed diet and raw-food diet, with no apparent increase on the days with mixed diet. Endogenous MGO can also be formed from glucose (Maessen et al., 2015) or as a by-product of glycolysis from dihydroxyacetone phosphate (Phillips and Thornalley, 1993). MGO can be enzymatically metabolized via the glyoxalase pathway to ultimately form D-lactate, which is excreted by the urine. However, Degen et al. (2013) did not find a dietary influence of MGO on urinary D-lactate levels. Based on the findings of the simulated digestion experiments (see section 3.5.1), it is more likely that dietary MGO which reaches the ileum, reacts with proteins to form MGO-derived Maillard reaction products and thus becomes unavailable for absorption from the gut. The modified proteins might then reach the colon and may be fermented by bacteria. The ability of intestinal bacteria to degrade MRP was recently shown by Hellwig et al. (2015). Although in the mentioned study only free and not protein-bound MRPs were incubated in human faecal suspensions, it clearly demonstrated that colonic bacteria are able to degrade modified amino acids and may use them as a source of carbon or nitrogen. The metabolic transit of glycated proteins and their stability towards colonic bacteria will be an interesting upcoming research topic.

The following section will deal with the results of the dietary intervention with manuka honey, multifloral honey, cyclopower capsules or  $\alpha$ -cyclodextrin on the urine metabolome during a raw-food diet.

#### Manuka honey

During this 5-day intervention, four healthy subjects followed a mixed diet (day 1 and 5), which was changed to a raw-food diet on day 2 lasting for 3 days. On day 3 of the study, the

subjects consumed 125 g of manuka honey, which contained 275  $\mu\text{mol}$  3-DG and 769  $\mu\text{mol}$  MGO. All subjects were asked to collect their 24 h urine, which was subsequently analysed. Figure 55 shows the urinary excretion of 3-DG and its metabolites and MGO during the intervention week with manuka honey.

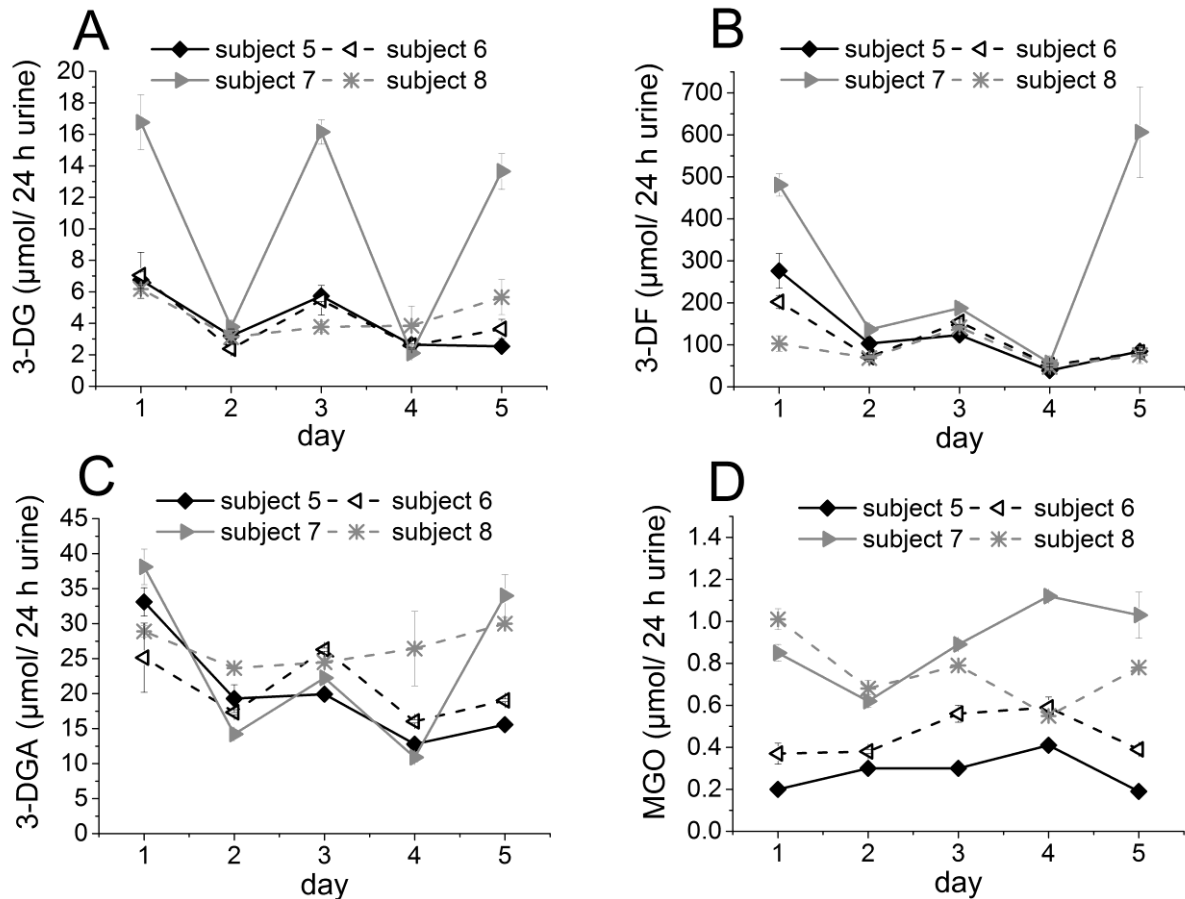


Figure 55: Urinary excretion in 24 h urine of 3-DG (A), 3-DF (B), 3-DGA (C) and MGO (D) during a mixed diet (day 1 and 5) followed by a raw-food diet (day 2-4) and a dietary intervention on day 3 with 125 g manuka honey

The median level of urinary 3-DG at day 1 (mixed diet) was 6.9  $\mu\text{mol}/24 \text{ h urine}$ , which decreased to 3.2  $\mu\text{mol}/24 \text{ h urine}$  at day 2 (raw-food diet). On day 3, the uptake of 125 g manuka honey, containing 275  $\mu\text{mol}$  3-DG, increased the median urinary 3-DG level to 5.6  $\mu\text{mol}/24 \text{ h urine}$ . At day 4, the subjects consumed only raw-food and the median 3-DG level decreased again to 2.6  $\mu\text{mol}/24 \text{ h urine}$ . On day 5, all subjects had a mixed diet which led to an increase of 3-DG uptake and therefore also an increase of urinary 3-DG. Although the pattern was the same for all study participants, it became clear that there were strong inter-individual differences between the uptake and metabolism rate of 3-DG. For example,

participant number 7 had exceptional high levels of 3-DG excretion (approx. 14-16  $\mu\text{mol}/24\text{ h}$  urine) during the mixed diet and also showed a high increase of 3-DG after the uptake of manuka honey. However, the endogenous 3-DG level during the raw-food diet (day 2 and 4) was almost the same for all participants. This may be due to various factors including the gastrointestinal resorption rate of 3-DG, the enzyme activity of metabolizing enzymes and the stability of 3-DG in the presence of other food stuff. For example participant 8 had no increased level of 3-DG excretion after the uptake of manuka honey. In contrast to all other subjects who consumed a vegetarian diet, participant 8 ate raw minced meat on day 2 and 3 of the intervention study. Löbner et al. (2015) showed that the dicarbonyl compound MGO can react with creatine to form N-(4-methyl-5-oxo-1-imidazolin-2-yl)sarcosine (MG-HCr). In consideration of the structural similarities of MGO and 3-DG, it is likely that creatine can also scavenge 3-DG. Recent studies in our laboratory have shown that indeed 3-DG reacts with creatine, although to a lesser extent than MGO (personal message by S. Treibmann, unpublished data). This might explain the missing increase of urinary 3-DG concentration after manuka honey intervention in subject 8.

Another reason for inter-individual differences of the 3-DG level in urine might be the activity of the metabolizing enzymes. The median excretion of the metabolite 3-DF on day 1 (mixed diet) was 239.2  $\mu\text{mol}/24\text{ h}$  urine, which decreased to 87.1  $\mu\text{mol}/24\text{ h}$  urine on day 2 (raw-food diet). The uptake of 275  $\mu\text{mol}$  3-DG with manuka honey led to an increase of the median 3-DF level to 148.1  $\mu\text{mol}/24\text{ h}$  urine. On day 3, all subjects consumed a raw-food diet and additionally 125 g manuka honey. The increase of the metabolite 3-DF compared to day 2 (raw-food only) was in the same range for all participants. That showed that, at least for these four participants, inter-individual differences in the activity of the 3-DG reducing enzymes were rather small. The big variance in the 3-DF excretion on day 1 and 5 (mixed diet) was probably rather due to differences in the food matrix and composition which was taken up by the subjects. The influence of a food matrix on the 3-DG resorption and metabolism to 3-DF could be studied by administering the same raw-food diet to all participants and additionally serve manuka honey in the presence or absence of a protein or creatinine rich matrix.

The second metabolite of 3-DG, namely 3-DGA, showed the same excretion pattern as 3-DF: The median urinary excretion rate was 31.0  $\mu\text{mol}/24\text{ h}$  urine on day 1, which decreased to 18.3  $\mu\text{mol}/24\text{ h}$  urine on day 2 and showed a slight increase to 23.4  $\mu\text{mol}/24\text{ h}$  urine after the uptake of 125 g manuka honey. In comparison to 3-DF, the concentration of 3-DGA in the urine is 2-10 times smaller. This, again, emphasized the role of 3-DF as the main metabolite

of 3-DG. This might be due to a rather wide distribution of the aldose reductase enzymes in the human body, which was found to be present in high concentrations in the liver but also in all other relevant tissues (Nishimura et al., 1990). In contrast, the oxoaldehyde dehydrogenase, which catalyses the oxidation of 3-DG to 3-DGA, was found in high concentrations in erythrocytes (Fujii et al., 1995). The authors concluded that erythrocytes can actively take up 3-DG, enzymatically degrade it to 3-DGA and therefore could function as a scavenger for 3-DG *in vivo*. This pathway could serve as an additional protective mechanism in the blood vessels when high concentrations of 3-DG are present. Hahne (2014) observed in her master thesis that in erythrocytes the oxidation of 3-DG to 3-DGA was indeed the main metabolic route.

For MGO, no correlation between dietary intake and the urinary MGO level was found. The urinary MGO excretion ranged between 0.2-1.1  $\mu\text{mol}/24\text{ h}$  urine during the 5 day intervention week. There was no decrease when the diet was changed from mixed to raw-food and also no significant increase when the subjects consumed 125 g of manuka honey on day 3. Based on the results of the simulated gastrointestinal digestion (see section 3.5.1), approximately 90 % of MGO which was taken up with the diet, reacted with proteolytic enzymes and thus became unavailable for resorption. Regarding the administered dose of 769  $\mu\text{mol}$  MGO in this intervention study, that means only 77  $\mu\text{mol}$  MGO would be available for gastrointestinal resorption. Richard (1991) estimated the daily endogenous MGO formation to be approximately 400  $\mu\text{mol}$ . Compared to the dietary MGO uptake of 100 to 300  $\mu\text{mol}$  per day, which is achieved with a common western diet (Degen et al., 2012), the endogenous MGO concentration exceeds the dietary amount. Therefore, the variations of the daily urinary MGO excretion seen in Figure 55D are more likely due to variations of endogenously formed MGO.

### Multifloral honey

During this 5-day intervention, four healthy subjects followed a mixed diet (day 1 and 5), which was changed to a raw-food diet on day 2 lasting for 3 days. On day 3 of the study, the subjects consumed 125 g of a multifloral honey from Germany, which contained 202  $\mu\text{mol}$  3-DG and only minor amounts of MGO ( $< 5\text{ mg/kg}$ ,  $< 7\text{ }\mu\text{mol}/125\text{ g}$ ). All subjects were asked to collect their 24 h urine, which was subsequently analysed. Figure 56 shows the urinary excretion of 3-DG and its metabolites and MGO during the intervention week with multifloral honey. It became clear that the pattern and the concentrations of 3-DG and 3-DG metabolites excretion were very similar to the intervention week with manuka honey. Interestingly, participant 8, who already showed a very low 3-DG increase during the manuka honey trial, was the only

subject whose 3-DG excretion did not increase after the consumption of multiflora honey containing 202  $\mu\text{mol}$  3-DG. Since the study was performed in two different weeks with a two weeks break in between, this indicated that either the metabolism of 3-DG in participant 8 was very efficient and/or the resorption of 3-DG was hindered. Moreover, the participant consumed 100 g minced meat at day 2 and 3 of the multiflora honey intervention. The influence of the food matrix on the 3-DG absorption was discussed previously. However, the fact that subject 8 participated in both studies, allowed us to compare the intra-individual differences. There was no significant difference in the 3-DG excretion during the mixed diet (manuka honey trial: 5.7-6.2  $\mu\text{mol}/24$  h urine and multiflora honey trial: 5.3-6.7  $\mu\text{mol}/24$  h urine) or the raw-food diet (manuka honey trial: 3.1-3.8  $\mu\text{mol}/24$  h urine and multiflora honey trial: 3.5-4.6  $\mu\text{mol}/24$  h urine). This indicated a rather well controlled metabolic system of 3-DG elimination.

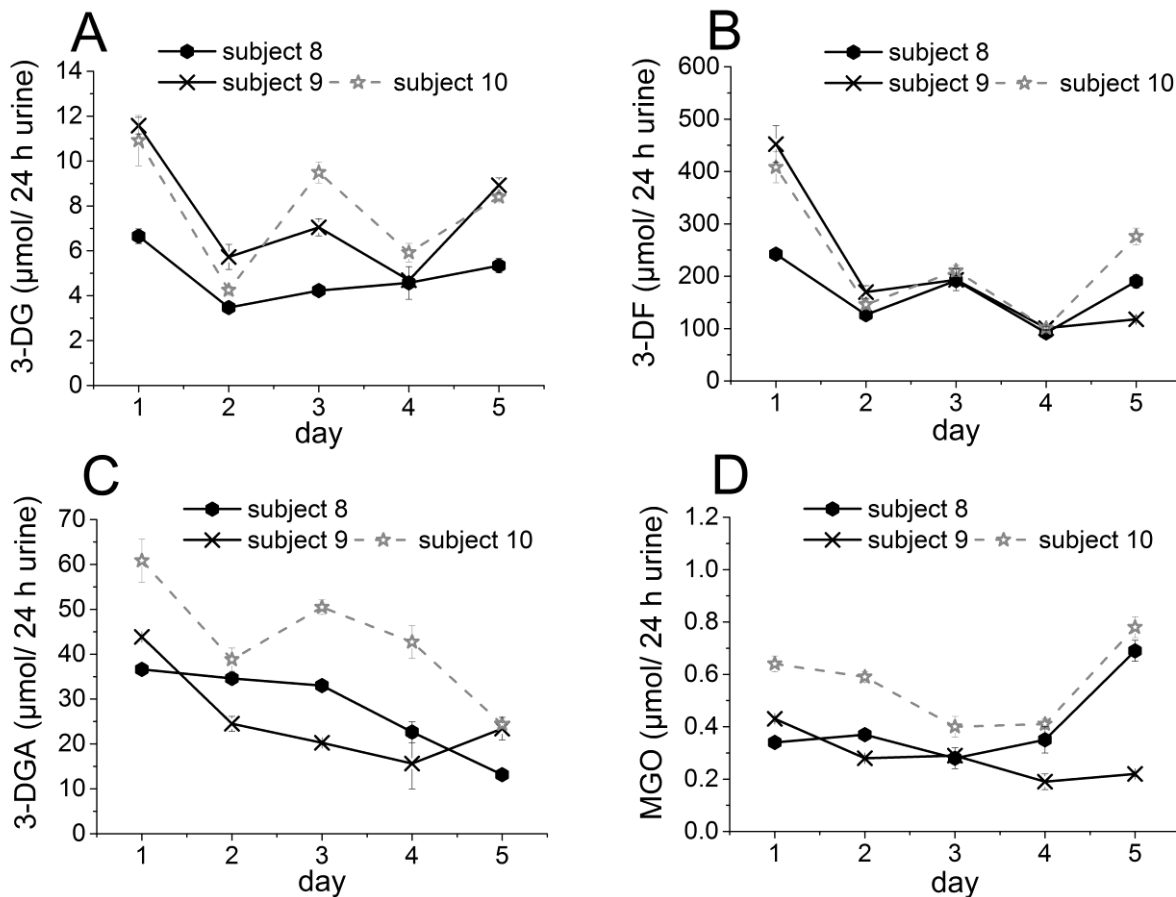


Figure 56: Urinary excretion in 24 h urine of 3-DG (A), 3-DF (B), 3-DGA (C) and MGO (D) during a mixed diet (day 1 and 5) followed by a raw-food diet (day 2-4) and a dietary intervention on day 3 with 125 g multiflora honey

Compared to the increase of the median 3-DG excretion after the consumption of manuka honey, the increase after the uptake of multiflora honey was something smaller. This might



be due to the lower concentration of 3-DG in the serving of multifloral honey (202  $\mu\text{mol}$  instead of 275  $\mu\text{mol}$  in manuka honey), but could also be due to inter-individual differences in the 3-DG metabolism. Except participant 8, the group of volunteers during the multifloral honey intervention was different compared to the manuka honey trial. These differences also became obvious in the urinary 3-DF excretion. Although the pattern of 3-DF excretion was similar to the 3-DG excretion, what gave evidence to 3-DF being the main metabolite of 3-DG, the daily median excretion rates were lower compared to the manuka honey week. For participant 8, the 3-DF excretion on day 2 and 4 (only raw-food diet) was higher during the multifloral honey week compared to the manuka honey week (multifloral honey week: 91.9 - 126.6  $\mu\text{mol}/24$  h urine; manuka honey week: 47.4 – 68.6  $\mu\text{mol}/24$  h urine). Although the participants followed a raw-food diet, they were still consuming glucose by eating fruits or vegetables. The dietary glucose can lead to a post-prandial increase of dicarbonyl compounds, e.g. 3-DG, *in vivo* (Maessen et al., 2015). The fact that participant 8 excreted the same amount of 3-DG during the raw-food diet of both intervention weeks, but an increased amount of 3-DF, indicated that the body ensured a 3-DG homeostasis by varying the level of 3-DF excretion.

In contrast to 3-DF, the 3-DGA excretion was not significantly influenced by dietary 3-DG from multifloral honey. Again, that showed the importance of 3-DF as the main metabolite of 3-DG. Moreover, it may be that 3-DGA is only an intermediate in the 3-DG metabolism and therefore no significant increase during a 3-DG uptake was detected. For gluconic acids, an oxidative pathway ultimately leading to  $\text{CO}_2$  is discussed (Stetten and Stetten, 1950). Whether this pathway is also applicable for deoxygluconic acids was not studied yet.

For MGO, there was no dietary influence found during the intervention with multifloral honey. The MGO concentration in urine ranged from 0.2-0.8  $\mu\text{mol}/24$  h urine during the trial week. This was in the same range as the urinary MGO excretion during the manuka honey week. There was also no increase of urinary MGO when a dose of 125 g of multifloral honey was administered to the participants on day 3, which is in accordance with the low level of MGO in the multifloral honey.

#### Cyclopower and $\alpha$ -cyclodextrin

The commercial product cyclopower contained 45% manuka honey and 55%  $\alpha$ -cyclodextrin. The complexation of manuka honey and its bioactive compound MGO was supposed to increase the bioavailability during gastrointestinal digestion. To study whether the consumption of cyclopower enhances dicarbonyl availability, four subjects consumed 12

cyclopower capsules and four participants consumed the equivalent amount of  $\alpha$ -cyclodextrin contained in 12 capsules (control group).

The results of the urinary 3-DG, 3-DF, 3-DGA and MGO excretion during both interventions are shown in Figure 57 ( $\alpha$ -cyclodextrin) and Figure 58 (cyclopower). The excretion of the dicarbonyl compounds and the metabolites of 3-DG showed the same pattern which was observed during the first trial when the subjects followed a mixed diet on day 1 and 7 and had a raw-food diet from day 2-6. During the mixed, diet the 3-DG and therefore also the 3-DF and 3-DGA excretion increased, which was probably due to the uptake of dietary 3-DG. During the raw-food diet, the subjects had a diet virtually free of dicarbonyl compounds which is reflected in the decrease of 3-DG, 3-DF and 3-DGA on day 2. The uptake of 2.7 g  $\alpha$ -cyclodextrin did not increase the excreted concentration of either 3-DG or its metabolites. This was expected since  $\alpha$ -cyclodextrin is a fibre and does neither contain digestible monosaccharides nor dicarbonyl compounds. Therefore, an excretion pattern similar to the raw-food diet was expected.

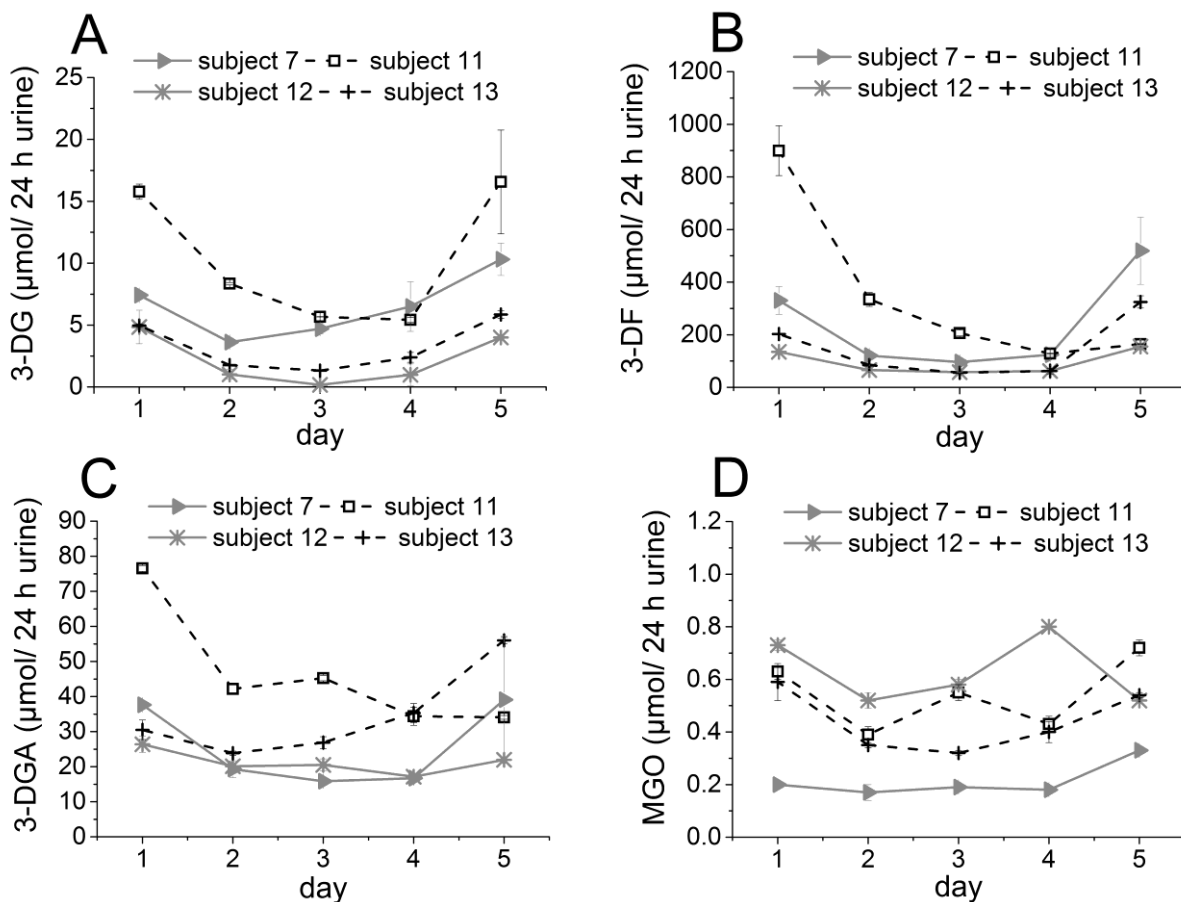


Figure 57: Urinary excretion in 24 h urine of 3-DG (A), 3-DF (B), 3-DGA (C) and MGO (D) during a mixed diet (day 1 and 5) followed by a raw-food diet (day 2-4) and a dietary intervention on day 3 with 2.7 g  $\alpha$ -cyclodextrin powder

For MGO, the same concentration in the urine was found compared to the other interventions. The urinary MGO excretion ranged between 0.2 and 0.8  $\mu\text{mol}/24\text{ h}$  urine and no dietary influence was observed.

The dose of 12 cyclopower capsules accounted for 6.9  $\mu\text{mol}$  3-DG and 9.0  $\mu\text{mol}$  MGO, which was 30-40 times lower in comparison to the amount taken up with multifloral and manuka honey. The curve characteristics of the 3-DG, 3-DF and 3-DGA excretion resemble the excretion rates which were observed during the  $\alpha$ -cyclodextrin week. The uptake of 12 cyclopower capsules on day 3 did not increase the excretion of 3-DG or its metabolites. That was probably due to the low dose of dietary 3-DG compared to endogenously formed 3-DG. Although the cyclopower product aimed to complex bioactive compounds of manuka honey and thereby increase their bioavailability, there was no increase of MGO found when 12 cyclopower capsules are consumed (see Figure 58D). This is in accordance with the studies of the molecular interaction between MGO and  $\alpha$ -cyclodextrin (see section 1.5.4).

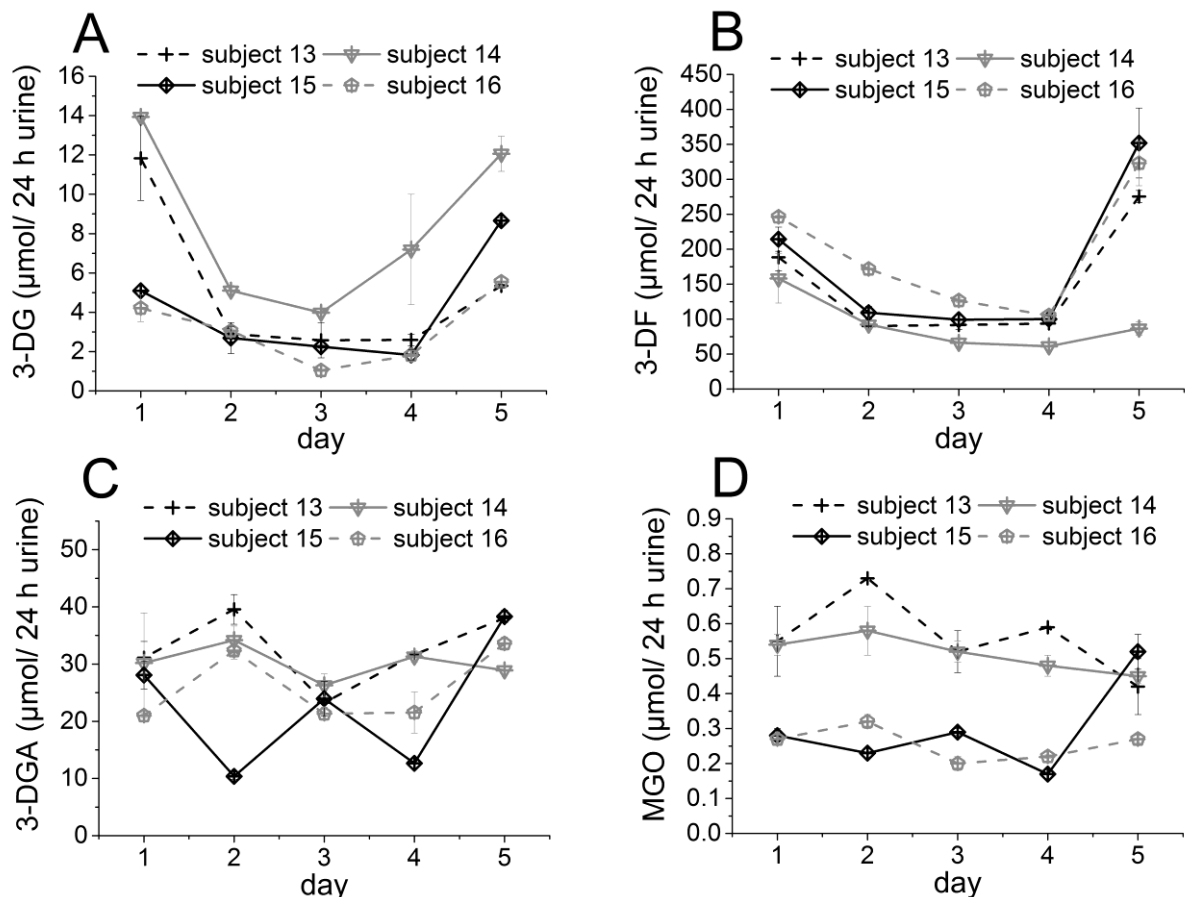


Figure 58: Urinary excretion in 24 h urine of 3-DG (A), 3-DF (B), 3-DGA (C) and MGO (D) during a mixed diet (day 1 and 5) followed by a raw-food diet (day 2-4) and a dietary intervention on day 3 with 12 cyclopower capsules

The weak interaction between MGO and  $\alpha$ -cyclodextrin which was shown via 2-D NMR, are confirmed by the intervention study. Moreover, the results of the simulated gastrointestinal digestion of cyclopower were reflected in the missing MGO increase during the intervention. When cyclopower was digested under simulated conditions *in vitro* (see 3.5.1), the MGO content decreased to 14% of the initial concentration. That means, that only 1.3  $\mu\text{mol}$  of the initial MGO dose of 9  $\mu\text{mol}$  in 12 capsules would be available for gastrointestinal resorption. Compared to the endogenously formed MGO, which accounts for approximately 400  $\mu\text{mol}/\text{day}$ , this concentration is too low to have an impact on the urinary MGO content. The complexation of manuka honey apparently did not lead to an increased bioavailability of MGO. Based on these results, MGO in manuka honey and cyclopower capsules did not influence the “dicarbonyl load” of the human body. Dicarbonyl compounds, and especially MGO, are discussed as risk factors for ageing, cell vitality and diabetes (Brownlee et al., 1984; Kalapos, 1999; Allaman et al., 2015). Concerning dietary MGO, the present results indicated that MGO from manuka honey or cyclopower did not influence the MGO level *in vivo* and therefore did not pose a risk to human health. Although MGO in manuka honey and cyclopower might not reach the blood circulation it might have an effect on gastrointestinal health. There are several reports on the positive effect of manuka honey towards the gastritis causing bacterium *H. pylori* (Al Somal et al., 1994; Keenan et al., 2010, 2012). Moreover, Parkar et al. (2017) found that faecal bacteria in the presence of the digesta of manuka honey and cyclopower, generated metabolites which favour gut health. Mannina et al. (2016) were able to show that the gastroduodenal digesta of manuka honey had an antibacterial effect against the pathogenic bacterium *Staphylococcus aureus*. These studies demonstrated that MGO might have a positive effect on the body although, based on our results, it did not reach the blood circulation.

#### Discussion of carbonyl transit to the urine

The results of the intervention study are summarized in Table 44. The concentrations during day 2 and 4 (raw-food diet) were considered to represent the endogenous level of the analytes, whereas the concentrations during day 1 and 5 (mixed diet) depended on the choice of food by the subjects. The results of the raw-food diet and the mixed diet demonstrated inter-individual differences of the analyte levels *in vivo*. During the raw-food diet, the subjects consumed a diet virtually free of dicarbonyl compounds like 3-DG and MGO. Thus the inter-individual differences might be due to varying activities of the enzymes, which are

responsible for dicarbonyl degradation or formation. For instance, the deglycation enzyme FN3K (see section 3.2.1), which catalyzes the release of 3-DG from Amadori products, was found to vary in its activity by the factor 4 in erythrocytes of humans (Delpierre et al., 2006). During the raw-food diet of this study, the concentration of 3-DG in the urine of 23 subjects was found to vary by factor 8, what corresponds with earlier findings. Moreover, during the mixed food diet, variations between the subjects by factor 4-8 occur. Although, the dietary intake of 3-DG ranges approximately from 0.1 to 1.0 mmol/day (Degen et al., 2012), only minor changes between the excretion variances of the raw-food diet and the mixed diet were found. This indicated that although the dietary 3-DG influence could lead to a wide range of 3-DG *in vivo*, the inter-individual variations were independent from the amount of 3-DG which is taken up with the diet.

Table 44: Concentrations of 3-DG, 3-DF, 3-DGA and MGO in 24 h urine of all subjects (n=23) during raw-food diet and mixed diet

	Level during raw-food diet ( $\mu\text{mol}/24\text{ h urine}$ )		Level during mixed diet ( $\mu\text{mol}/24\text{ h urine}$ )	
	Median of urinary excretion of all subjects at		Median of urinary excretion of all subjects at	
	Day 2	Day 4	Day 1	Day 5
<b>3-DG</b>	3.2 (range: 1.0-8.4)	2.6 (range: 1.0-7.2)	7.1 (range: 4.2-16.8)	5.9 (range: 2.2-16.6)
<b>3-DF</b>	109.2 (range: 53.3-334.2)	62.0 (range: 35.0-128.6)	214.3 (range: 77.6-899.6)	190.1 (range: 62.2-606.3)
<b>3-DGA</b>	23.8 (range: 10.4-42.2)	19.8 (range: 10.8-42.7)	32.4 (range: 19.3-76.5)	28.5 (range: 13.2-56.0)
<b>MGO</b>	0.38 (range: 0.17-0.73)	0.41 (range: 0.18-1.12)	0.37 (range: 0.20-1.01)	0.42 (range: 0.13-1.03)

The results of the 3-DF excretion were in accordance with the results of Degen et al. (2014), who detected 3-DF concentrations in urine of subjects following a mixed diet between 91-306  $\mu\text{mol}/24\text{ h urine}$  and following a raw-food diet between 62-130  $\mu\text{mol}/24\text{ h urine}$  (n=9). The formation of 3-DF from 3-DG is catalysed by the enzyme aldehyde reductase, which is ubiquitarily present in human tissues, whereby the expression mainly occurs in the liver (Barski et al., 2005, 2008). During the raw-food diet, the 3-DF concentration in the urine of all study subjects varied by factor 4-6, whereas the variation increased during the mixed diet to a factor

of 10-12. This increase in inter-individual differences during the mixed diet indicated that 3-DF is the metabolite which “buffered” dietary 3-DG variations. When high amounts of 3-DG were taken up with the diet, the metabolic systems kept the level of 3-DG relatively constant, whereas the level of 3-DF increased rapidly. This hypothesis is backed up by the observation that 3-DGA, another metabolite of 3-DG, was varying by factor 4 between the different subjects independently from the diet which was consumed. Together with the fact that 3-DF occurred in 30-fold higher concentrations in the urine compared to 3-DG and 5-fold higher concentrations than 3-DGA, this emphasized the role of 3-DF as the main metabolite of endogenous, but also dietary 3-DG.

The urinary 3-DGA excretion was in accordance with the results of Collard et al. (2007), who detected a mean 3-DGA excretion of 16.7  $\mu\text{mol/g}$  creatinine ( $n=4$ ), which equals 21.7  $\mu\text{mol/day}$  when the daily creatinine excretion is approximately 1.3 g. No information about the dietary state of these subjects was available. The present work demonstrated for the first time, that the urinary 3-DGA level was influenced by the diet. The inter-individual differences of the 3-DGA concentration might be due to the varying enzyme activities of the metabolising enzymes. Johnson et al. (1992) found varying activities of the enzyme ALDH by the factor 5 ( $n=145$ ). Moreover, the activity of 3-DGA was correlating with alcohol consumption. However, Hansell et al. (2005) found no significant effect of alcohol consumption on ALDH activity. The inter-individual differences of the urinary 3-DGA excretion in our study varied by factor 4, which is in accordance with the results of Johnson et al. (1992).

During the intervention study, the subjects consumed either a dose of 275 (manuka honey) or 202  $\mu\text{mol}$  (conventional honey) of 3-DG at day 3. The recovery of 3-DG, 3-DF and 3-DGA in the urine of the subjects, who took part in the manuka honey intervention and the 3 subjects, who participated in the multifloral honey intervention are graphically shown in Figure 59. The results showed that 8.2-40.0 % of the dietary 3-DG can be recovered in the urine as the sum of 3-DG, 3-DF and 3-DGA. Kato et al. (1990) detected 6 % of isotopic labelled 3-DG in the urine of rats two hours after oral administration, whereas 60 % were detected in the small intestine. When the labelled 3-DG was administered intravenously, the main percentage of radioactivity was found to be present in the urine (72 %) after 3 h. The significantly lower recovery of 3-DG after oral administration compared to our study might be due to the one-time sampling after 2 h of administration. The metabolic transit of 3-DG and its metabolites apparently takes a certain amount of time and therefore the analysis of 24 h urine is more reliable in this context. However, when 3-DG was administered intravenously 72 % of 3-DG

and its metabolites were already recovered in the urine after 3 h. This indicated that 3-DG is not biologically utilized by the rats, but rapidly excreted in the urine. The longer transit time after oral administration showed that the resorption of 3-DG and its transport to the urine is a rather slow process.

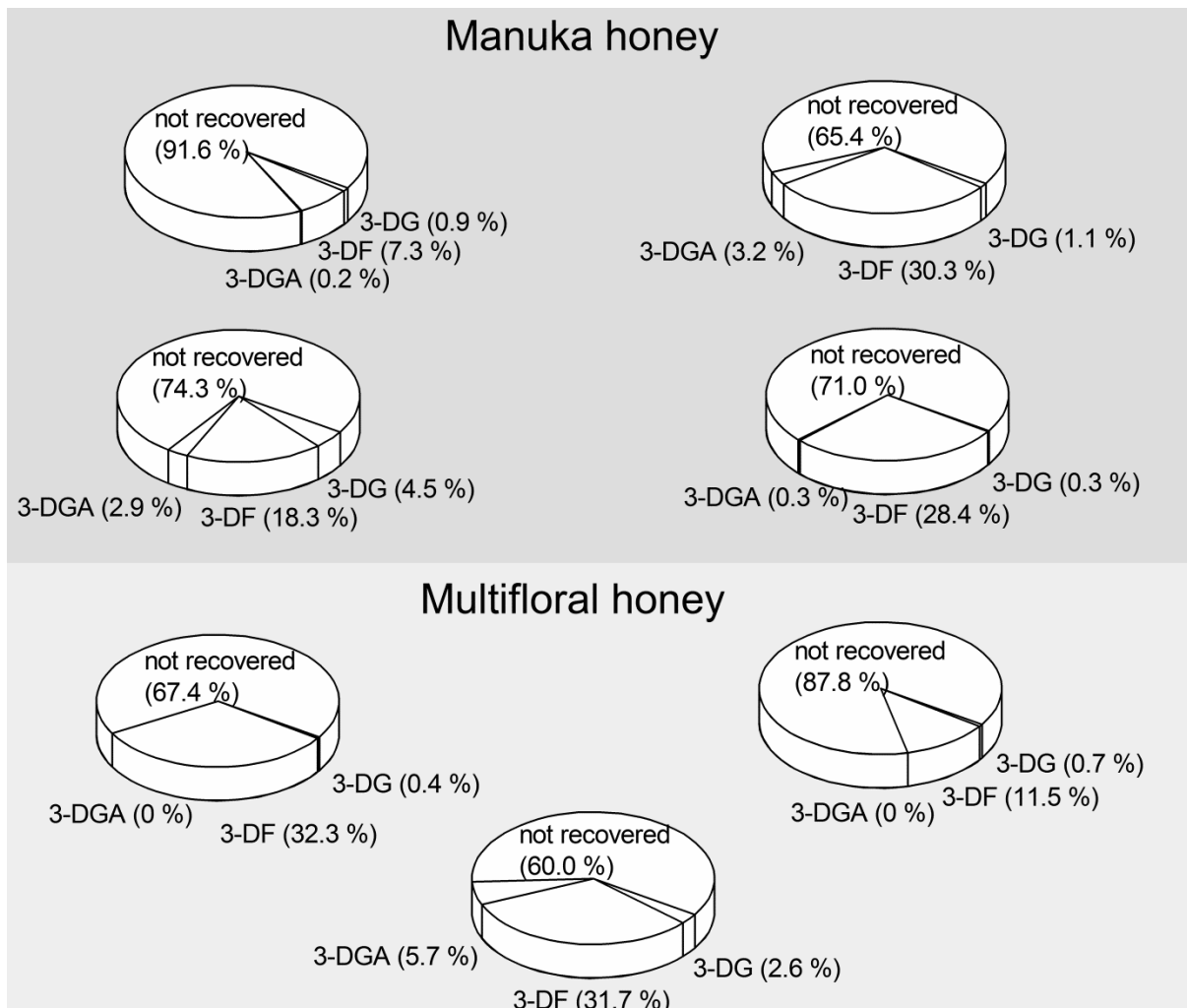


Figure 59: Urinary recovery of 3-DG, 3-DF and 3-DGA from the dietary 3-DG during manuka honey intervention (3-DG dose was 275  $\mu\text{mol}$ ) and multifloral honey intervention (3-DG dose was 202  $\mu\text{mol}$ ). Each pie chart stands for one participant.

Degen et al. (2014) were able to recover 10-15 % of 3-DG, which was administered with a dose of honeydew honey, as 3-DF in the urine of healthy participants. This confirmed the results of the present study, where 7-32 % of 3-DG were recovered as 3-DF. Moreover, Richter (2012) performed in her master thesis a simulated gastrointestinal digestion of 3-DG in the presence of gastrointestinal enzymes. The results showed a 20-40 % loss of 3-DG after 8 h of incubation in the digestive fluids. This led to the conclusion that a full recovery of

dietary 3-DG in urine was not possible, since a loss of 3-DG already occurred during gastrointestinal digestion.

In contrast to 3-DF, the metabolite 3-DGA appeared to play only a minor role in dietary 3-DG metabolism. Only 0-5.7 % of dietary 3-DG was recovered as 3-DGA in the urine of the subjects. The endogenous 3-DGA concentration was approx. 6 times higher than the 3-DG concentration, which indicated that 3-DGA was an important metabolite of endogenous 3-DG. Fujii et al. (1995) found significantly higher concentrations of 3-DGA in erythrocytes compared to plasma levels. The authors assumed that 3-DG is rapidly taken into erythrocytes and is converted to 3-DGA to prevent glycation of haemoglobin and blood vessels. Originated 3-DGA is not excreted from erythrocytes back into blood plasma (Fujii et al., 1995). In our study, the urinary 3-DGA level was analyzed. The scavenging of 3-DGA into erythrocytes might explain the reduced recovery of 3-DGA in the urine. Further studies should focus on the quantification of 3-DGA in erythrocytes after dietary intervention with 3-DG rich food.

Figure 60 shows the correlation of the urinary 3-DF excretion with 3-DGA. The regression coefficient of 0.5 indicated that the metabolites 3-DF and 3-DGA were excreted in a constant ratio and that the metabolising enzyme systems interacted.

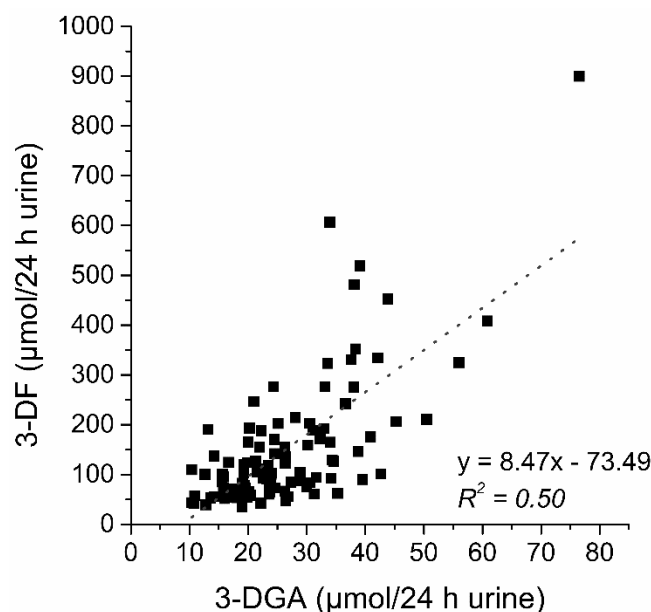


Figure 60: Correlation of urinary 3-DF with 3-DGA

Moreover, the urinary excretion of 3-DF and 3-DGA correlated with the 3-DG level in urine, which confirmed 3-DF and 3-DGA were metabolites of 3-DG (see Figure 61). Closer



examination of the 3-DF to 3-DG plot revealed a two-branched graph with a steeper and a lower curve progression. This might indicate that there are individuals who are able to rapidly metabolize 3-DG and therefore excrete high amounts of 3-DF and 3-DGA, whereas others are only able to metabolize 3-DG to a lesser extent and thus excreting rather low levels of 3-DGA and 3-DF. Closer examination of the raw data revealed that the graph separation was caused by the 3-DG and metabolite data during the mixed diet but not during the raw food diet. Apparently, only when the body was challenged with higher amounts of dietary 3-DG, variations in the metabolic processes between the subjects became visible. An explanation for those “strong” and “weak metabolisers” might be differences in the enzyme activity of aldehyde reductase and aldehyde dehydrogenase. Variations of the level of 3-DG and its metabolites in urine of different subjects might indicate different metabolism characteristics for dicarbonyl compounds in food and the tendency of certain individuals to accumulate higher levels of dicarbonyl compounds from the diet. In contrast, endogenously formed 3-DG was equally well metabolised by all subjects, which can be seen in the lower, more uniform part of the curves in Figure 61. However, since dietary 3-DG was not fully recovered it might also be possible that other metabolic pathways, yet unknown, contributed to the metabolism of 3-DG, which might vary between different individuals.

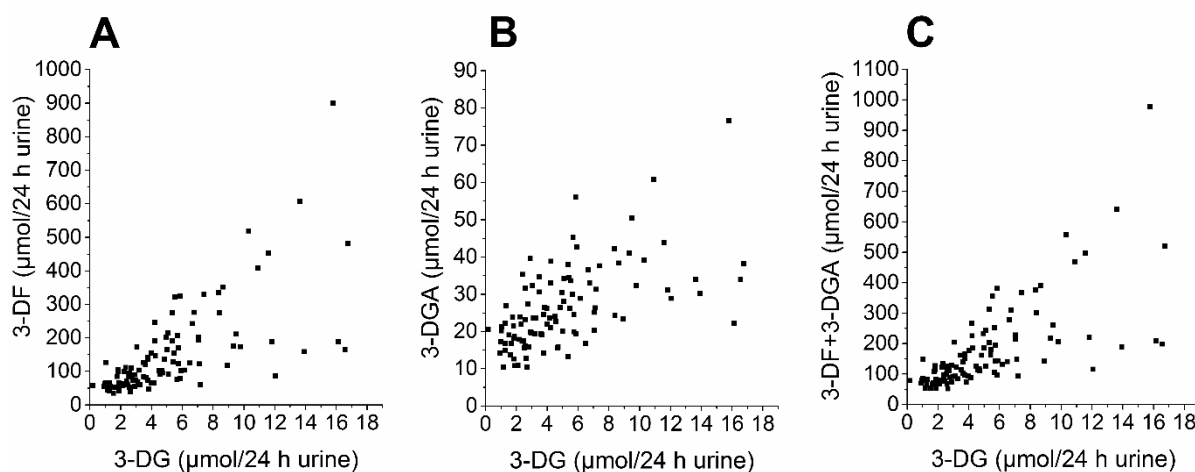


Figure 61: Correlation of urinary 3-DG level with urinary 3-DF (A), 3-DGA (B) and the sum of 3-DF and 3-DGA (C) of all participants

### 3.5.3.2. Metabolic transit in blood

The analysis of 24 h urine indirectly showed that dietary dicarbonyl compounds reach the blood circulation and are excreted via the urine. However, the study gave no information about the direct transit into the blood circulation. The analysis of plasma samples aimed to

gain information about the temporal course of the resorption and elimination process of dietary compounds. In contrast to the study of 24 h urine, the analysis of blood plasma gave a snapshot of the current metabolic state of an individual, which might elucidate the timing of dicarbonyl metabolism after dietary uptake.

To study the contribution of dietary dicarbonyl compounds to the “dicarbonyl load” of the human body, two subjects consumed either 125 g of manuka honey, which contained 3-DG, MGO and DHA or 125 g of an artificial honey, which was a mixture of glucose, fructose and sucrose and contained virtually no dicarbonyl compounds. The blood withdrawal was performed in a hospital prior to the intervention, the subjects were asked to consume the honeys in 10 min and further blood was withdrawn after 30, 60 and 120 min. The subsequent analysis of the samples was performed according to 3.4.9.2. The glucose concentration of the samples was analyzed with a blood glucose meter directly in the hospital.

### Glucose

Both subjects had a fasting glucose level below 5.6 mmol/l and therefore were classified as normoglycemic individuals (World Health Organization, 2016). Figure 62 shows the increase of plasma glucose level after the consumption of 125 g of manuka or artificial honey.

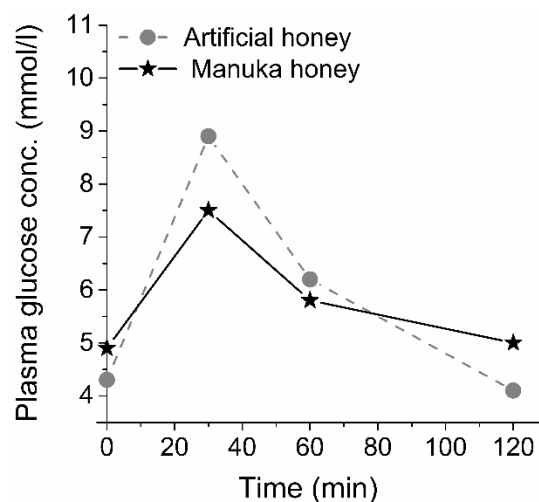


Figure 62: Progression of plasma glucose level after the consumption of 125 g of manuka honey or artificial honey

Dietary glucose is absorbed in the small intestine and transported via the blood circulation to the portal vein. The liver is considered to be the central organ of carbohydrate metabolism and is responsible for a constant blood glucose concentration. During the dietary intervention with manuka or artificial honey, an amount of approx. 43 g glucose was ingested. The liver was

temporary not able to keep a constant blood glucose concentration, what explained the increased blood glucose level 30 min after start of the intervention. The metabolism of glucose ensured the clearance of glucose from the blood stream and its transfer into tissues by phosphorylation. After 2 h, the blood glucose concentration was at the same level as prior to the intervention in both subjects. This indicated that both subjects had a normal glucose metabolism and did not suffer from diabetes or impaired glucose metabolism. The inter-individual differences in the increase of glucose concentration might be due to different enzyme activities or varying affinities of the glucose transport protein SGLT1 in the tissues of the subjects. However, the slightly lower glucose increase during the manuka honey intervention could indicate a lower glycemic index of honeys in comparison to pure glucose. Atayoğlu et al. (2016) reported similar results for some Turkish honeys in comparison to glucose. In contrast, Raatz et al. (2015) found no difference in the glycemic response to honey, sucrose or high fructose corn syrup. In our study, the glucose concentration of the commercial manuka honey was not quantified, thus it might ultimately be that the subject, who consumed the artificial honey, ingested a slightly higher dose of glucose compared to the manuka honey. To check whether the different glucose increase was due to the honeys or the inter-individual differences, the study should be performed with a cross-over design.

### 3-Deoxyglucosone

The fasting subjects had a 3-DG level of 480 and 530 nmol/l, which was in accordance with previously published 3-DG concentration in plasma and serum (Niwa, 1999; Maessen et al., 2015). Figure 63A shows the increase of 3-DG plasma concentration after the consumption of manuka or artificial honey. The uptake of artificial honey and manuka honey both led to an increase of 3-DG in plasma. This confirmed the results of Maessen et al. (2015), who showed that dietary glucose was degraded to 3-DG, which led to a postprandial increase of plasma 3-DG concentration. With the consumption of manuka honey, besides glucose also dietary 3-DG was taken up. However, the 3-DG concentration in plasma showed no higher increase when manuka honey was consumed instead of artificial honey. This raised the question whether dietary 3-DG was bioavailable or whether 3-DG *in vivo* is only a product of glucose.

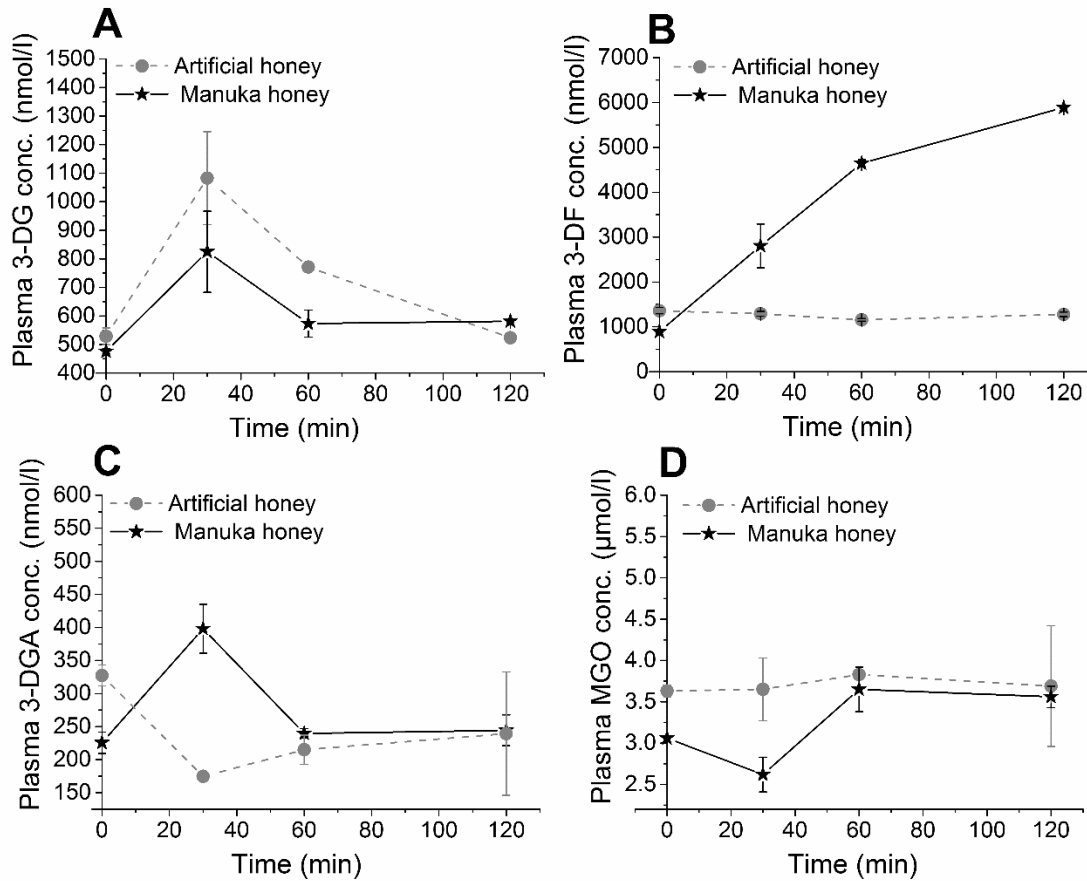


Figure 63: Progression of plasma 3-DG (A), 3-DF (B), 3-DGA (C) and MGO (D) level after the consumption of 125 g of manuka honey or artificial honey

### 3-Deoxyfructose

The fasting levels of plasma 3-DF concentrations were 890 and 1360 nmol/l. Knecht et al. (1992) and Teichert et al. (2015) reported 3-DF levels of 494 and 2700 nmol/l in human plasma, respectively. The intervention with artificial honey did not lead to an increase of 3-DF during the 2 h study time. However, when manuka honey was consumed, which contained dietary 3-DG, the plasma concentration of the metabolite 3-DF increased (see Figure 63B). In contrast to glucose and 3-DG, which showed the highest increase after 30 min followed by a decrease to the initial level, the 3-DF concentration increased continuously over the 2 h in which blood samples were taken. Since there was no further blood withdrawal, it was not possible to predict the highest 3-DF concentration after the intervention and also the time point at which the 3-DF level reached its initial concentration. The artificial honey did not contain significant levels of dietary 3-DG and its consumptions did not rise the 3-DF plasma level. This emphasized the role of 3-DF as a metabolite of dietary 3-DG. However, it was shown that the uptake of glucose led to a postprandial increase of 3-DG. This

endogenously formed 3-DG from glucose apparently was not metabolized to 3-DF. This indicated that the metabolism of dietary 3-DG underlied a different mechanism or occurred in different cells than the metabolism of endogenously formed 3-DG.

#### 3-Deoxy-2-ketogluconic acid

The subjects had a fasting plasma 3-DGA concentration of 226 and 327 nmol/l, which was in accordance with the findings of Fujii et al. (1995), who detected 450 nmol/l of 3-DGA in human plasma. The consumption of artificial honey led to a slight decrease of 3-DGA during the first 30 min of the intervention. In contrast, the subject who consumed manuka honey showed an increase to 176 % of plasma 3-DGA after 30 min, followed by a decrease to the initial 3-DGA concentration after 2 h (see Figure 63C). We assumed that the increase of plasma 3-DGA level was due to the dietary uptake of 3-DG with manuka honey and its metabolism to 3-DGA. Again, the missing increase of 3-DGA after the consumption of artificial honey, although glucose uptake produced postprandial 3-DG, indicated the unique role of dietary 3-DG and its metabolism. Additionally, in this study only plasma 3-DGA levels were analyzed. It was reported that erythrocytes scavenge 3-DG and metabolize it to 3-DGA (Fujii et al., 1995). Further studies could show, whether the uptake of 3-DG rich food does also lead to an increase of 3-DGA in erythrocytes, which might be even more significant than the increase in plasma.

#### Methylglyoxal

In contrast to 3-DG and its metabolites, the plasma concentration of MGO did not change significantly during the intervention (see Figure 63D). The MGO level of both subjects varied between 2.6 and 3.8  $\mu\text{mol/l}$ . Maessen et al. (2015) reported fasting state MGO concentration in plasma of 350 nmol/l, which increases to approx. 430 nmol/l after the consumption of 80 g glucose. During the study, no increase of plasma MGO neither due to glucose or dietary MGO was observed. In comparison to the published results, the MGO concentrations in this study were higher by factor 10. The sample preparation was the same as for 3-DG and its metabolites, for which the reported results matched with literature data. We assumed that a neoformation of MGO during the drying step of sample preparation may have occurred. Since this neoformation did not affect 3-DG, plasma glucose did not appear to be the cause. However, it might be that triose compounds like dihydroxyacetone phosphate (DHAP) or glyceraldehydes phosphate (GAP) formed MGO during drying of the plasma samples. To check whether the drying step caused the high MGO concentration, DHAP or GAP could be

added to the samples and the MGO concentration should be analysed. Although the absolute MGO concentrations should be considered with caution, the relative course of the MGO curve during the intervention did not show an increase, which confirmed the conclusion, that dietary MGO did not influence the “dicarbonyl load” in plasma.

#### Dihydroxyacetone phosphate

The study of the stability of DHA in the presence of simulated digestive fluids, showed that DHA was stable at different pH values over the incubation time of 8 h (see section 3.5.1). With the consumption of manuka honey, high amounts of up to 2700 mg/kg of DHA can be ingested (Atrott et al., 2012). Until now, there is no information available whether dietary DHA is resorbed during gastrointestinal digestion and how it is metabolized.

Figure 64 shows the development of the DHAP level in plasma after the consumption of manuka honey or artificial honey. Whereas the consumption of artificial honey did not lead to an increase of DHAP, the uptake of manuka honey increased the plasma DHAP concentration by 400 %. This indicated that dietary DHA was phosphorylated and quickly metabolized via glycolysis. There were no absolute concentrations of DHAP in plasma given, because the quantification of DHAP was achieved with [ $^{13}\text{C}_6$ ]3-DG as the internal standard. Absolute quantification requires the use of a more appropriate internal standard, with a similar chemical structure and close retention times to the derivative of DHAP. For the assessment of the dietary influence of DHA in manuka honey on the plasma DHAP level, the relative presentation of the results was sufficient.

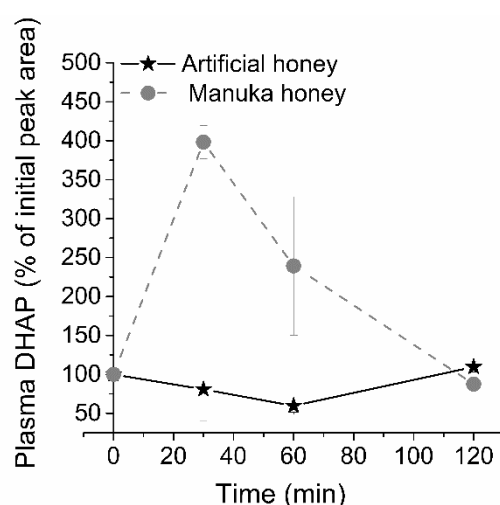


Figure 64: Progression of plasma DHAP level after the consumption of 125 g of manuka honey or artificial honey

The consumption of artificial honey, containing glucose which was metabolized via glycolysis, did not increase the DHAP concentration. This indicated that DHAP is a glycolytic intermediate, which was rapidly metabolized to pyruvate or lactate. However, when high amounts of dietary DHA were present, the concentration of DHAP could not be kept constant due to the formation of DHAP from DHA. On the one hand, dietary DHA was removed from the blood circulation through phosphorylation and therefore was not available for glycation reactions. On the other hand, high levels of DHAP can lead to the formation of MGO (Thornalley, 1996), which is even more prone to glycation reactions than DHA. The consequences of the metabolism of dietary DHA should be studied with further research.

### 3.5.3.3. Discussion of the metabolic transit of carbonyl compounds

According to the results, the uptake of dietary glucose led to a postprandial increase of 3-DG in blood plasma. The cellular location of this metabolic reaction is not clear yet. It was assumed that only intracellular compartments with direct contact to plasma glucose could be responsible for the rapid increase of dicarbonyl compounds after glucose consumption (Maessen et al., 2015). The ability of 3-DG to cross cell membranes was already shown by Fujii et al. (1995) and Sakiyama et al. (2006). However, the metabolite 3-DGA is too polar to cross cell membranes (Fujii et al., 1995), what raises the question where extracellular and urinary 3-DGA originated from. It might be that extracellular concentrations of 3-DG and its metabolite were actually only representing a minor part of dicarbonyl compounds and its metabolites, whereas the majority of these compounds was located intracellularly. Maessen et al. (2015) already proposed to study circulating cells and endothelial cells to get a more detailed understanding of dicarbonyl concentrations in the circulation. The conclusion that dietary 3-DG underwent a different metabolism compared to 3-DG, which was formed postprandial after glucose consumption, was backed up by the study of Bryland et al. (2010). The authors administered 3-DG intravenously to healthy volunteers and recovered 9.6 % of 3-DG in the urine. In the present study, only 0.3 to 4.5 % of the orally administered 3-DG was recovered as 3-DG in the urine. This indicated that 3-DG which reached the intestinal system, might be partially metabolised extracellularly to 3-DF by membrane-based enzymes and thus could not be recovered as 3-DG in the urine. In contrast, 3-DG which was directly administered to the circulation, bypassed this metabolic system. First evidence for the existence of these membrane-based, NADPH-dependent enzyme systems were also reported in the master thesis of Hoffmann (2012), who incubated Caco-2 cells with 3-DG and was able to recover 3-DF extracellularly. In the present study, a 3-DG to 3-DF ratio of 1: 30 was

found in the urine, whereas the ratio of 3-DG to 3-DF in blood was 1:2. These results showed that 3-DF underlined rapid renal clearance and we assumed that 3-DF elimination shifted the balance towards effective 3-DG metabolism. The relatively small increase of 3-DF compared to 3-DG in blood might also be an indicator for the extracellular metabolism of 3-DG to 3-DF and subsequent (slow) absorption processes. Besides the knowledge about the metabolizing enzyme systems, the transport pathways of dicarbonyl compounds and their metabolites are an important factor to understand the metabolic transit of dicarbonyl compounds. Fructose is transported into cells via passive diffusion with participation of the transport protein GLUT5. Due to the similar structure of fructose and 3-DF, it was assumed that 3-DF is mainly formed extracellularly and might cross cell membranes subsequently. The slow increase of 3-DF in contrast to the rapid increase of 3-DG after the consumption of dietary 3-DG, indicated slow resorption processes (see Figure 63). The same conclusion could be drawn for 3-DG: Due to its similar structure to glucose, its transport might be dependent on the transport proteins responsible for glucose resorption. However, Sakiyama et al. (2006) showed that cellular 3-DG uptake was not slowed down in the presence of glucose and therefore assumed that its transport was not dependent on the same transport protein. The findings of the present study and the current knowledge about the transport of glucose, 3-DG and its metabolites 3-DF and 3-DGA are presented in Figure 65. To summarize, dietary 3-DG can be metabolized rapidly and effectively in healthy subjects and it is not expected to pose a risk to human health. For MGO, no increase in the urine or in plasma was detected after dietary MGO administration, which suggested negligible bioavailability. The metabolic transit of DHA and its potential metabolism to DHAP should be addressed in further research. Based on the current information, the human gastrointestinal system detoxifies dietary dicarbonyl compounds rapidly.



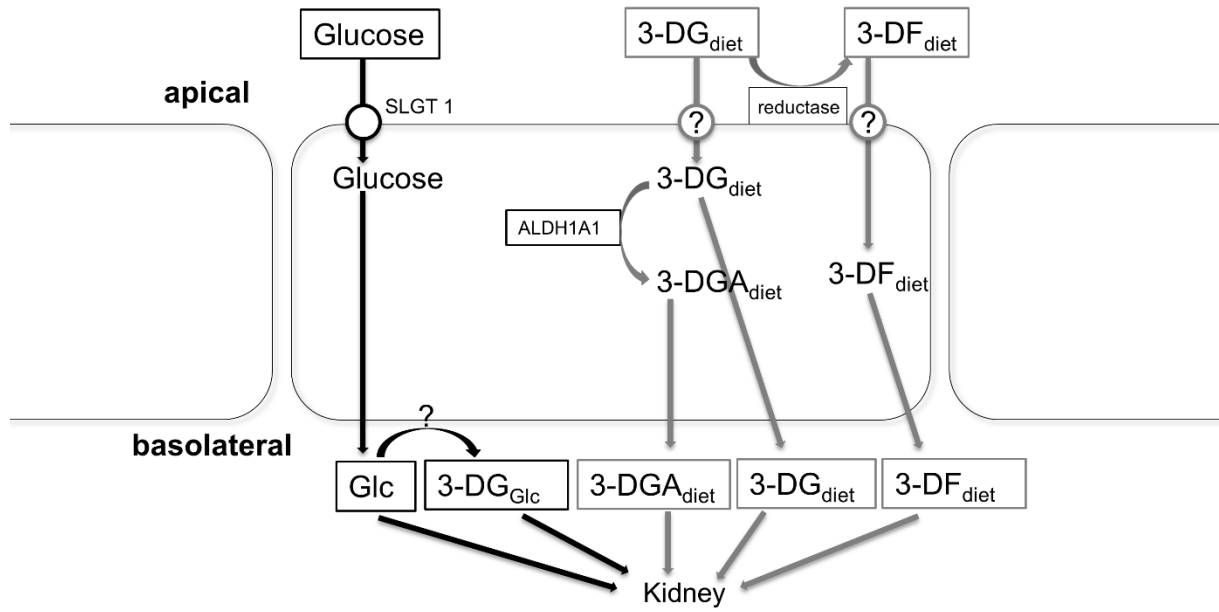


Figure 65: Schematic illustration of the metabolic routes for dietary glucose and 3-DG in cells

### 3.6. Summary of Chapter C - Metabolic transit of carbonyl compounds

Chapter C deals with the metabolic transit of dietary carbonyl compounds. Although dicarbonyl compounds are consumed in considerable amounts with the daily diet, little is known about their stability during gastrointestinal digestion and their resorption into the human body. Therefore, manuka honey containing methylglyoxal (MGO) and dihydroxyacetone (DHA) was incubated in simulated gastric and ileal fluids and the stability of the compounds was tested subsequently. Moreover, the influence of the fibre  $\alpha$ -cyclodextrin on their stability was examined. To gain more profound knowledge about potential resorption and metabolic reactions, an intervention study with 18 healthy volunteers was performed, whereby all subjects followed a nutrition protocol and collected their 24 h urine. Moreover, two subjects participated in a “sugar tolerance test”, whereby either 125 g manuka honey or artificial honey was consumed and blood samples were withdrawn prior to the intervention and 30, 60 and 120 min afterwards. The results of chapter C can be summarized as follows:

- 1 MGO in manuka honey was found to be stable during simulated digestion with human saliva and simulated gastric fluids. During simulated ileal digestion, the MGO concentration decreased to 9 % of the initial concentration. The main factor influencing the decrease of MGO was the change of pH value from 2 (gastric fluid) to 7-8 (ileal fluid). It was assumed that the acidic environment of the gastric fluids provides mainly protonized amino acid residues of protein side chains, which hindered MGO-derived protein modification. The honey matrix had no stabilising effect on MGO compared to a synthetic MGO solution. In contrast to MGO, the manuka honey compound DHA appeared to be stable during all simulated digestion steps. The consequences of gastrointestinal stability of DHA should be subject of further research.
- 2 The complexation of MGO with  $\alpha$ -cyclodextrin resulted in 5 % more stability compared to the uncomplexed dicarbonyl compound. However, the excess of reactions partners for MGO *in vivo* and the almost identical progression of the decrease in the uncomplexed versus complexed MGO, suggested no enhanced stability with  $\alpha$ -cyclodextrin.
- 3 The recovery of MGO by measuring protein glycation was not achieved due to low release of amino acids from the digestive enzymes during enzymatic hydrolysis. A dialysis step prior to enzymatic hydrolysis increased the yield of lysine and arginine from 12 to 42 % compared to previous work (Zeitz, 2013). The results of the amino acid analysis need to be questioned critically, since amino acids were not released properly.

Model experiments with casein instead of digestive enzymes should be performed to achieve better release rates after enzymatic hydrolysis.

- 4 It was shown that the urinary concentrations of 3-deoxyglucosone (3-DG), 3-deoxyfructose (3-DF) and 2-keto-3-deoxygluconic acid (3-DGA), but not MGO, were influenced by the diet. During intervention studies, up to 40 % of dietary 3-DG was recovered as the sum of 3-DG, 3-DF and 3-DGA. The metabolite 3-DGA had only a minor role in the metabolism of dietary 3-DG in comparison to 3-DF.
- 5 The complexation of manuka honey with  $\alpha$ -cyclodextrin in the commercial product “cyclopower” did not enhance the bioavailability of 3-DG or MGO. The urinary excretion of the compounds was not increased after consumption of 12 capsules (3 times the recommended daily dose).
- 6 The uptake of dietary glucose resulted in an increase of 3-DG in the plasma. No differences in the plasma 3-DG levels were observed when the subjects consumed a glucose/fructose mix with no 3-DG or manuka honey, which naturally contains high amounts of 3-DG.
- 7 The concentrations of 3-DF and 3-DGA in plasma increased only after the consumption of dietary 3-DG. This led to the conclusion that dietary 3-DG and 3-DG, which is formed postprandial from glucose, have different metabolic routes.
- 8 The concentration of MGO did not increase after the consumption of either a glucose/fructose mix without MGO or manuka honey with natural high MGO levels.
- 9 The plasma concentration of dihydroxyacetone phosphate (DHAP), a metabolite of glycolysis, increased after the consumption of manuka honey, which contained high concentrations of dihydroxyacetone (DHA). In contrast, the oral administration of a glucose/fructose mix did not influence the DHAP concentration. This is the first evidence that dietary DHA might be bioavailable and is metabolized via glycolytic routes.

---

## 4 Further studies and outlook

---

### 4.1. Antibacterial effect of manuka honey

#### 4.1.1. The inhibition of *Helicobacter pylori* with manuka honey

The studies were based on the hypothesis that manuka honey and its bioactive compounds MGO and DHA inhibit microbial urease and thus might inhibit *Helicobacter pylori* growth. The effect of manuka honey, MGO and DHA on jack bean urease *in vitro* was shown previously (see section 1.5.5). The antibacterial studies were performed at the German Institute of Human Nutrition (DIFE) in Potsdam, Germany. The methodological aspects of this section are described in chapter 1.4.11. During the beginning of the studies a contamination of the *H. pylori* cell culture (freeze-dried culture) with *B. subtilis* occurred. The contamination was confirmed by DNA sequencing and the study was started again with a new *H. pylori* culture (active culture), for which the identity was confirmed by a second DNA sequence test. The aim was to study the inhibitory effect of manuka honey, MGO and DHA on *H. pylori* by reading the optical density at 600 nm of the incubated cells. Unfortunately, it was not possible to observe a change of the optical density during the incubation of the cells neither in media alone (control) nor in the honey solutions (inhibition samples). This normally is a sign for absence of bacterial growth. It was described earlier, that *H. pylori* can change its morphology from a spiral to a coccoid form during incubation (Cellini, 2014). Stressing conditions, including antimicrobial agents in sub-inhibitory concentrations, facilitate entering the viable but non-culturable state in which bacterial cells acquire the coccoid form. Figure 66 shows *H. pylori* cells at the beginning of the incubation and after 48 h, respectively.

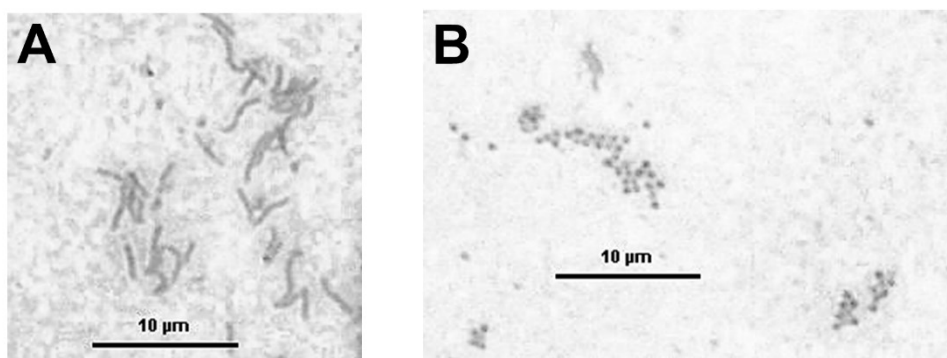


Figure 66: Microscopic picture of *H. pylori* cells prior to incubation (A) and after 48 h incubation (B)

The optical density or turbidity of the sample was measured at 600 nm and was an expression of light refraction in the sample. The morphological change from long, spiral cells to small coccoid cells led to a decrease of light refraction. Thus, there was no increase of the cell number detectable via the measurement of optical density. Due to the limited amount of time left at the German Institute of Human Nutrition after the microtiter plate experiment, it was not possible to try another approach to detect bacterial growth. Further studies should focus on counting the cell number at different time points during incubation.

Later on, a student at the German Institute of Human Nutrition in Potsdam, Germany, was able to continue this project under the supervision of the TU Dresden. This time, liquid media containing *H. pylori* was incubated with different concentrations of honey solutions and MGO or DHA for 0, 24 and 48 h. After incubation, the cells were cultured on fresh blood agar plates and cells were counted as a measure of bacterial growth. With this approach, the bactericidal effect of manuka honey, MGO and DHA was tested. According to the results, there was no permanent inhibition of *H. pylori* after incubation with manuka honey (max. conc. 30 %), MGO (max. conc. 1000 mg/l) or DHA (max. conc. 500 mg/l). All samples showed unhindered growth on fresh blood agar. However, the study provided no information about the bacteriostatic effect of manuka honey and its bioactive compounds. For most bacterial infections, a treatment with bacteriostatic agents might be sufficient, since the body is able to fight the infection with endogenous mechanisms after the immune system recovered (Pankey and Sabath, 2004). The results of the study did not allow quantifying the bacteriostatic effect of manuka honey on *H. pylori*, thus no final statement of its efficiency compared to conventional honeys can be made.

During the incubation experiments, two interesting observations were made. After the cells were incubated for 48 h in the media containing manuka honey (30 and 20 % (w/v)), MGO (1000 and 500 mg/l), the urease inhibitor acetohydroxamic acid (5 and 2.5 mg/l) or the antibiotics tetracycline hydrochloride or metronidazole, the cell suspension was centrifuged and the lactate concentration was measured enzymatically in the supernatant. Figure 67 shows the results of lactate analysis. Lactate represents the final product of the glyoxalase system, which degrades methylglyoxal *in vivo* (Racker, 1951). Moreover, lactate was found to be the final product of glycolysis, not only but preferentially when low amounts of oxygen are present (Rogatzki et al., 2015). The formation of lactate by *H. pylori* cells in the presence of MGO might indicate that the glyoxalase enzyme system is present in *H. pylori*. The detoxification of MGO via its reduction to lactate is crucial for bacteria to survive in the presence of high amounts of MGO. Even higher amounts of lactate were formed by *H. pylori*

in the presence of manuka honey, whereby the lactate production might be the sum of lactate produced from MGO via the glyoxalase pathway and lactate which is formed as the product of increased glycolytic activity. It is questionable whether the formation of lactate and thus the decrease of the pH in the incubation samples will influence *H. pylori* survival since the bacterium is known for its acid tolerance. However, the unbalanced triggering of on metabolic pathway might induce oxidative stress in the cells, which ultimately threatens their survival.

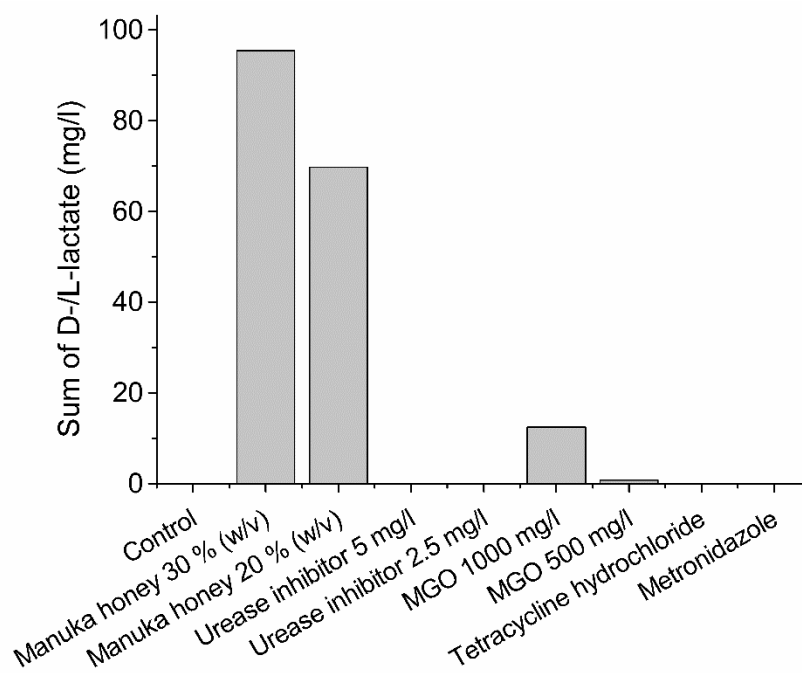


Figure 67: D- and L-Lactate concentration of cell supernatant. *H. pylori* cells were incubated for 48 h under microaerophilic conditions at pH 7 with the compounds mentioned above

The second observation during the incubation experiment was made when the cell supernatant was analysed for its MGO content. Originally, this analysis was performed to test the stability of MGO in the incubation media. It was shown during previous studies that the MGO concentration decreased by 50 % after 30 h incubation of manuka honey in bacterial media without bacterial cells (see section 1.5.2.3). A more drastic decrease was found in the incubation samples containing *H. pylori* cells, media and manuka honey or MGO and DHA. The added MGO could not be recovered, when media with manuka honey or MGO was mixed with *H. pylori* cells and a sample for MGO analysis was taken immediately after mixing. However, when the cells were incubated without MGO, with manuka honey or MGO for up to 24 h, MGO was formed or released from the cells in the media. This might be due to an increase of glycolysis activity and thus the formation of MGO as a by-product. The MGO concentration in the media never exceeded 2 mg/l, which is a non-toxic dose. Interestingly,

when the bacteria cells were incubated with DHA, higher amounts of up to 16 mg/l of MGO were formed. The highest amounts of up to 77 mg/l of MGO were formed when the cells were incubated with MGO and DHA. The increased formation of MGO in the presence of DHA might either be due to the non-enzymatic dehydration of DHA to MGO, as it occurs in honey, or DHA might be metabolized by the microorganisms to DHAP which is a potent precursor of MGO (Thornalley et al., 1999). Nevertheless, the formation of toxic amounts of MGO did only occur when DHA and MGO were present. This unbalanced metabolic state of the cells indicated that the detoxifying system for MGO was overloaded and thus MGO can accumulate in the cells and the media. Although manuka honey contains MGO and DHA, no MGO formation during the incubation with manuka honey was detected, which might be due to a low dosage. The results provide preliminary indications for the mechanism of bacterial inhibition with MGO and DHA, which needs further elucidation in the future. Some ideas for the inhibition mechanism are presented in the following section.

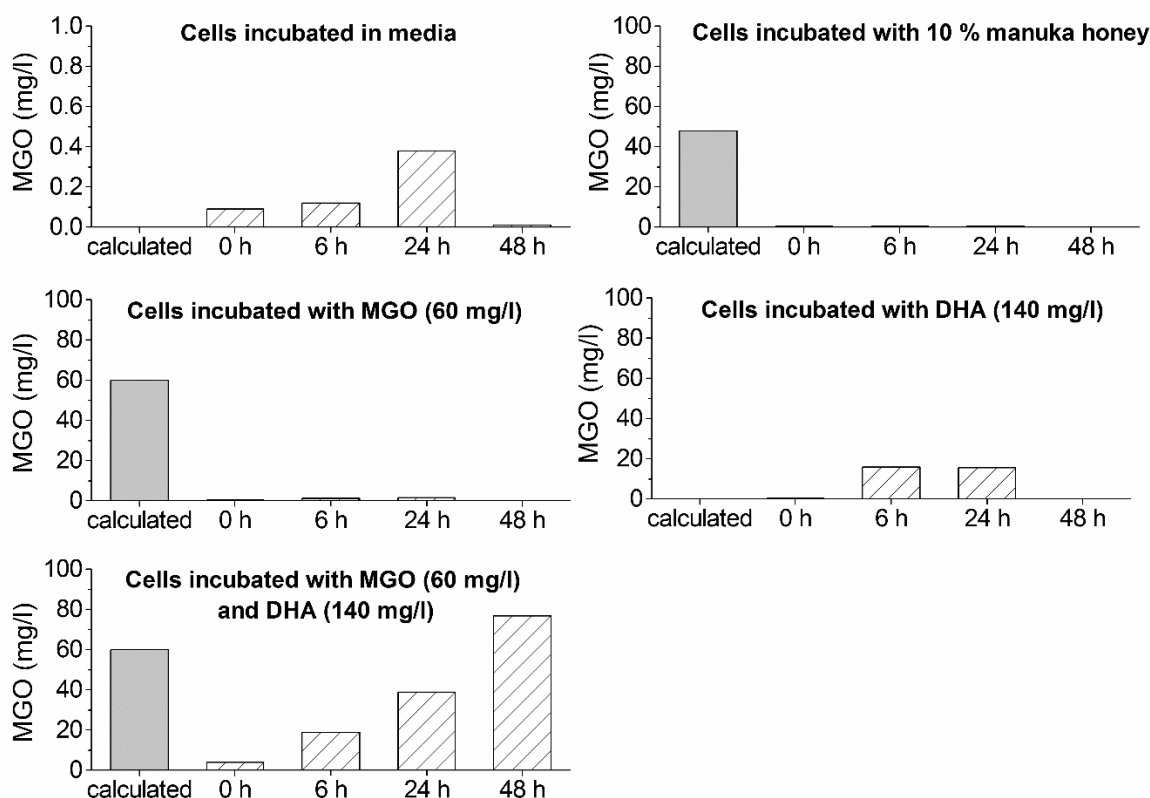


Figure 68: MGO concentration of cell supernatant. *H. pylori* cells were incubated for 48 h under microaerophilic conditions at pH 7 with the compounds mentioned in the diagram

#### 4.1.2. The mechanism of bacterial inhibition with manuka honey

Although there are several reports about the positive effect of manuka honey on bacterial infections, the mechanism by which manuka honeys kills bacteria is not fully elucidated yet. Rabie et al. (2016) performed an ultrastructural study on the bacterial inhibition caused by MGO. The authors showed that MGO effectively inhibited Gram positive (*B. subtilis* and *S. aureus*) and Gram negative (*P. aeruginosa* and *E. coli*) bacteria. At a concentration of 2 mM MGO, the authors observed the loss of fimbriae and flagella, the bacteria were rounded with shrinkage and lost their membrane integrity. The authors concluded that the morphologic changes led to limited bacterial adherence and motility. Henriques et al. (2010) suggested that the inhibition of *S. aureus* with manuka honey was due to hindered processes in the cell division machinery. The authors did not focus their study on the role of MGO. A possible reason for the signal cascade initiated by MGO might be the reaction of MGO with elements of the bacterial DNA. It was shown that MGO reacts with the DNA base guanine and forms guanine-adducts (Kalapos, 1999). Until now, these potential MGO-DNA adducts have not been studied in living cells. The analysis of cell material, which was incubated with MGO with the focus on DNA-adducts, could be an interesting new research topic. Moreover, it was recently discovered that manuka honey contains high amounts of up to 2000 mg/kg of 3-phenyllactic acid (3-PA) (Ministry for Primary Industries, 2017). Lactic acids are described as compounds with a broad antimicrobial spectrum (Mu et al., 2012; Axel et al., 2016). The role of 3-PA in the inhibitory mechanism of manuka honey needs further research.

## 4.2. Reactions of carbonyl compounds in honey

### 4.2.1 Reaction sites for carbonyl compounds in honey

The main focus of the present work was to study the reactivity of manuka honey MGO towards proteins and amino acids. It was shown, that modifications at the amino groups of proteins and amino acids occurred and assisted in distinguishing manuka honey from conventional honeys. Besides the reaction with proteins and amino acids, MGO may also react with other honey compounds to form unique reaction products. Recently, a method to distinguish manuka honey from other monofloral honeys was published by the Ministry of Primary Industries NZ (Ministry for Primary Industries, 2017). According to the MPI report, a “monofloral manuka honey” must contain the chemical markers phenyllactic acid (PLA) in



amounts above 400 mg/kg and the compounds 4-hydroxyphenyllactic acid (HPLA), 2-methoxybenzoic acid (2-MB) and 2'-methoxyacetophenone (MAP) at a minimum level of 1 mg/kg each and a certain level of DNA from manuka pollen. The structures of the chemical markers are shown in Figure 69.

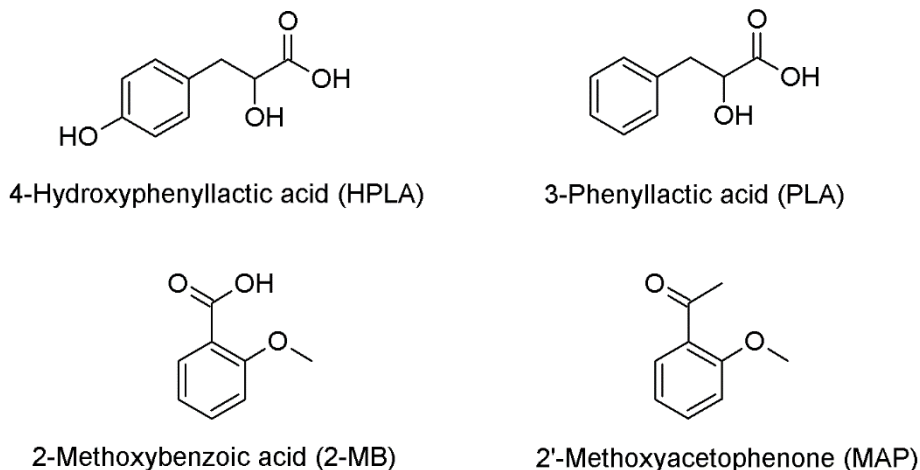


Figure 69: Chemical markers proposed by the Ministry of Primary Industries NZ for identifying manuka honey

Although the MPI claims that all chemical markers are stable during honey storage, other authors found a decrease of 2-MB and MAP during storage (Bong et al., 2017). Until now, little is known about the reactivity of MGO and DHA towards the four proposed chemical markers. Possible MGO-derived reaction products and thus the stability of the markers in the presence of MGO should be subject of further research. Moreover, according to oral reports from Manuka Health NZ Ltd. (Mandy Suddes, email conversation), the DNA test fails for genuine manuka honey. This might be due to the formation of DNA-MGO adducts, which are not accessible anymore for the polymerase reaction which leads to a hindered replication of DNA and ultimately to the failure of the test. Furthermore, MGO could directly react with the enzymes necessary for the test, e.g. polymerase, which also leads to an inhibition of the test. The role of MGO in the detection of manuka DNA should be elucidated further in the future.

#### 4.2.2 Functional consequences of carbonyl reactions with proteins

Honey contains 0.03-0.4 % proteins depending on the floral origin (Bogdanov, 1981). It is presumed that proteins can influence the flow behaviour of honey (Witczak et al., 2011). Especially high-molecular weight components might be responsible for the non-Newtonian flow behaviour of some honeys like heather, buckwheat or manuka honey. In chapter B,

section 2.5.2.1, it was shown that manuka honeys with significant amounts of MGO have higher amounts HMW fractions compared to non-manuka honeys. Moreover, the HMW fraction of manuka honey was stable against reducing agents like dithiothreitol, leading to the conclusion that HMW fractions in manuka honey are more likely caused by MGO-derived reactions than disulphide bonds. Preliminary rheological studies were performed to analyse the influence of MGO and cross-linked proteins on the flow behaviour of manuka honey. The methods used for the studies are described in section 2.4.18.

Newtonian fluids are characterized by their linear relationship between shear stress ( $T$ ) and the shear rate ( $D$ ). Its viscosity ( $\eta$ ) is independent of the applied shear rate. In contrast, non-Newtonian fluids show shear-thinning behaviour, which means that an increase of the applied shear rate leads to a decrease of its viscosity. It is presumed that certain intramolecular interactions are decreased during shearing and thus the fluid becomes less viscous. When the shear rate is slowly decreased again, some fluids can rebuild their intramolecular structures, resulting in the same shear stress as measured prior to shearing. However, when intramolecular structures are disrupted more severely and cannot be rebuilt quickly, this leads to a decreased shear stress compared to the initial value. This behaviour is called thixotropic or partially thixotropic. Concerning honey, the current knowledge about rheological behaviour appears to be diverse: Some Polish and Greek honeys are described as Newtonian fluids (Lazaridou et al., 2004; Juszczak and Fortuna, 2006), Brazilian honey samples are described as non-Newtonian fluids between 10-15 °C and Newtonian fluids from 20-30 °C (Silva et al., 2016) and heather honeys are consistently characterized as non-Newtonian fluids (Witczak et al., 2011; Osés et al., 2017). Manuka honey was also described to be a non-Newtonian fluid (Stephens, 2006). The reason for different rheological behaviours is either attributed to the crystallisation state of the honey (Smanalieva and Senge, 2009) or the presence of high-molecular weight components (Witczak et al., 2011).

The first attempt in our studies was to measure a thixotropy loop for some conventional and manuka honey samples. Therefore, the samples were sheared with an increasing shear rate for 3 min, kept at a constant shear rate for 3 min followed by a decrease of the shear rate to the initial value. Figure 70 and Figure 71 show the shear stress and viscosity curves of honeydew honey, polyfloral honey, heather honey and two manuka honeys with varying MGO content.

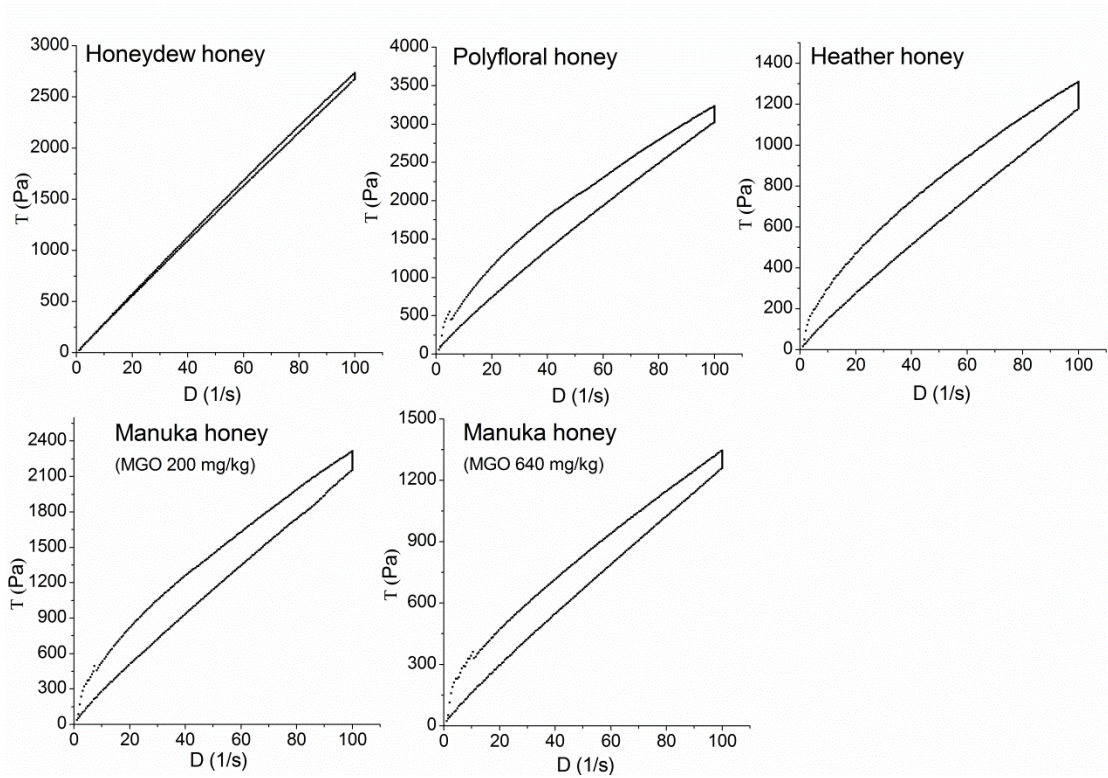


Figure 70: Shear stress curves (“thixotropy loop”) of honeydew, polyfloral, heather and manuka honey.

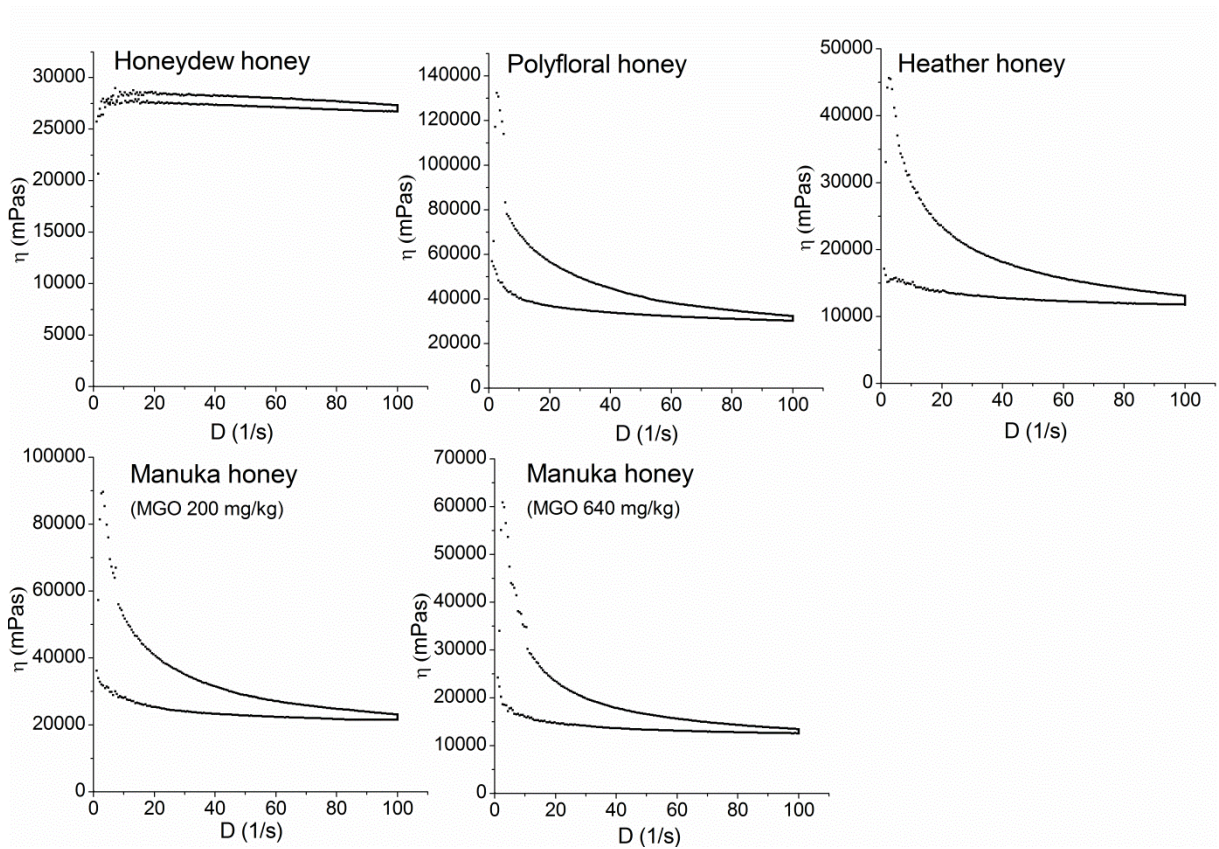


Figure 71: Viscosity curves of honeydew, polyfloral, heather and manuka honey.

It became visible that not only manuka and heather honey, but also the polyfloral honey displayed non-Newtonian behaviour. The measurement revealed two problems: First, the honey samples were measured in their original, commercial state, without prior harmonisation of the water content. The water content of the honeydew honey was 18.1 %, of the polyfloral honey 16.5 %, the heather honey 17.7 %, the manuka honey with MGO 200 mg/kg 16.7 % and of the manuka honey with MGO 640 mg/kg 18.2 %. The varying moisture contents of the honeys led to different initial viscosities, what can be seen in Figure 71. To compare the honeys and their rheological behaviour more fairly, the moisture of the sample should be equal. The second problem was that according to the rheology expert of Thermo Fisher Scientific Dr. Eberhard Pietsch, the thixotropy loop with shear rates up to  $100 \text{ s}^{-1}$  is not suitable to measure structural changes and their recovery, because the shear rate is quite high and might destroy internal structures irreversibly. Therefore another method, the “creep recovery” test was performed. For this method, one conventional honey, namely rewarewa honey and three manuka honeys with MGO 30, 250 and 550 mg/kg were stored for two weeks in desiccators with defined humidity, which was adjusted with saturated salt solutions. Ultimately, the honeys were stored at a humidity of 31 %, 54 % and 75 %. The “creep recovery” test was performed by applying a low shear rate of  $0.5 \text{ s}^{-1}$  for 60 s to receive a steady initial viscosity value. Afterwards, the sample was exposed to a shear rate of  $10 \text{ s}^{-1}$  for 30 s to strain intramolecular interactions. In the end, the shear rate was set back to  $0.5 \text{ s}^{-1}$  for 300 s so the sample can rebuild its intramolecular structure. Figure 72 shows the creep recovery measurement of a conventional honey without MGO, namely rewarewa honey, and of a manuka honey with approx. 550 mg MGO/kg. The initial viscosity, which was reached approximately after 60 s, was lower for the rewarewa honey than for the manuka honey. This might be due to different water contents of the honeys, since the samples were measured in their commercial conditions (without prior storage under controlled humidity).

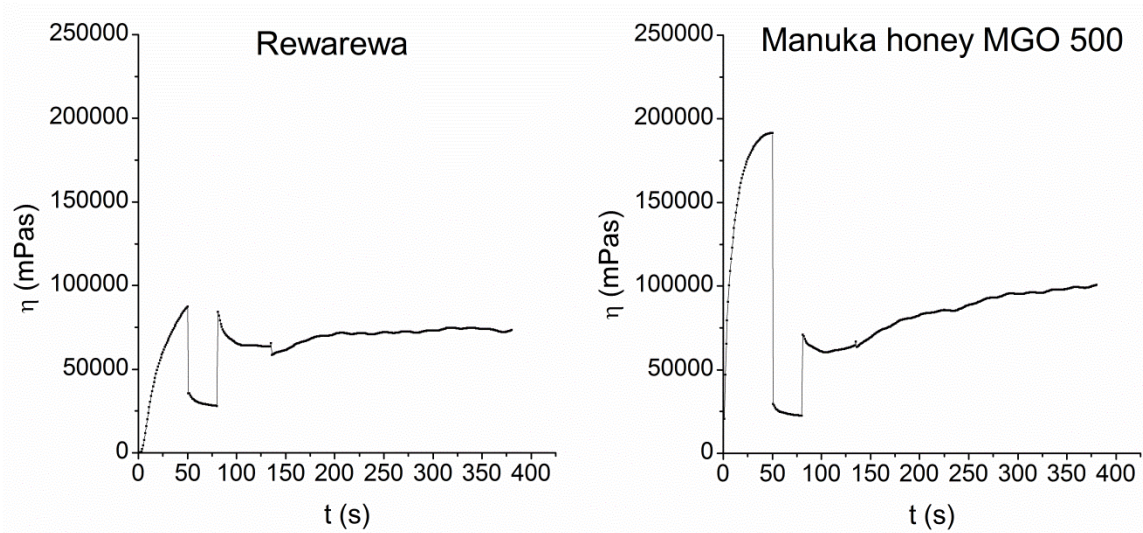


Figure 72: Creep recovery of rewarewa and manuka honey, samples were tested at 20 °C and under commercial conditions (no controlled humidity)

However, it is shown that although the viscosity of the rewarewa honey samples decreased during the increased shear rate, it recovered almost to the initial value after the stress is released. In contrast, the viscosity of the manuka honey sample decreased strongly when a higher shear rate is applied and only 50 % of the initial viscosity was recovered. The difference between initial viscosity after 60 s and the viscosity value of the end of the recovery phase was called  $\Delta\eta$  and is a measure of the stability of intramolecular structures. Figure 73 compares the  $\Delta\eta$  of the different honeys without moisture control or with moisture adjusted at 31, 54 and 75 %. Since the creep recovery appeared to depend on the moisture content, the sample which were not stored in controlled humid atmosphere cannot be compared since all honeys had different starting conditions. However, for the samples, which were stored at 31, 54 and 75 % moisture, equal starting conditions for moisture can be assumed and the rheological effects can be related to other molecular parameters.

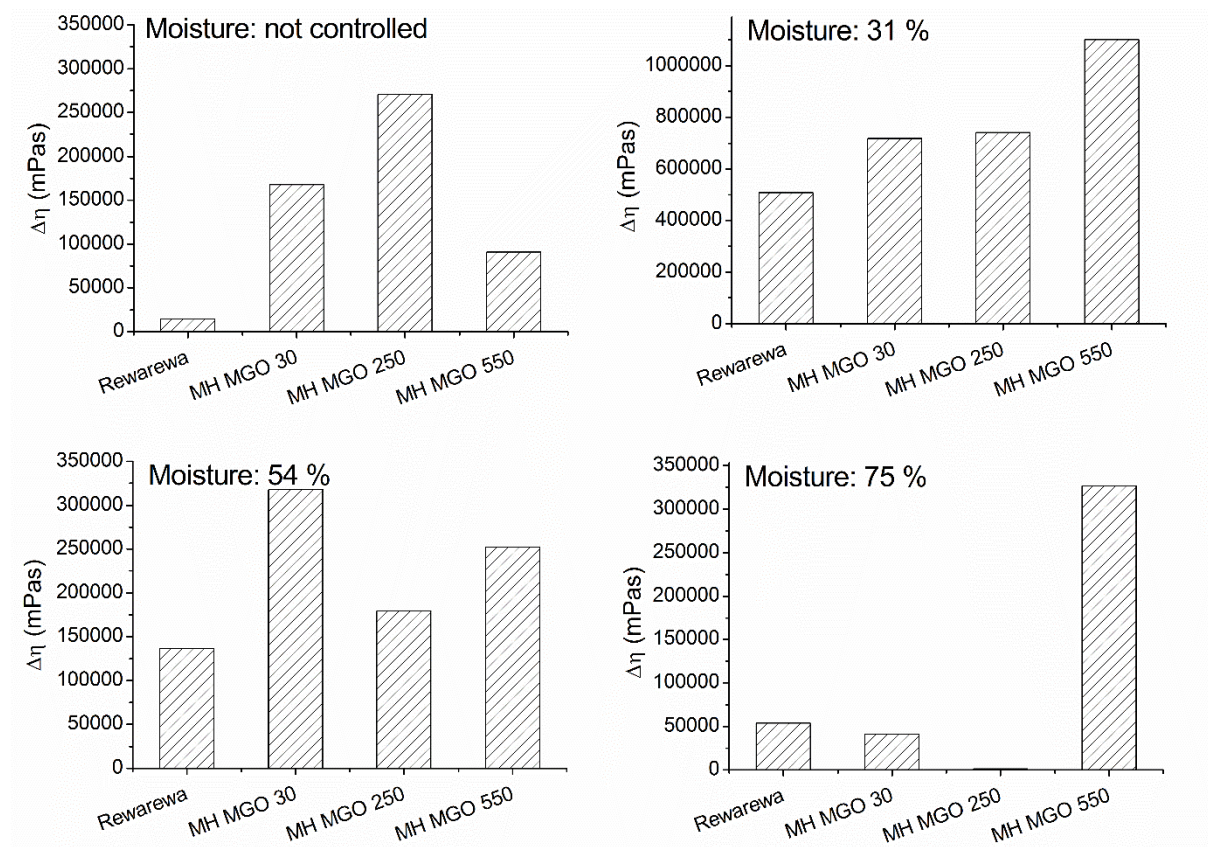


Figure 73: Difference of the initial viscosity and viscosity after shear stress ( $\Delta\eta$ ) of rewarewa and three manuka honey samples, which were stored at controlled humidity for two weeks

In general, the lower the moisture content of the samples, the higher was the initial viscosity and also the  $\Delta\eta$  value. Samples with higher initial viscosity values experienced higher shear stress. This might result in a more severe disruption of intramolecular networks, which were not easily rebuild during the release of shear stress. With increasing moisture of the samples, the  $\Delta\eta$  value decreased. Thus, lower moisture contents were apparently more suitable to measure the influence of shearing on intramolecular structures. To achieve a moisture content of 31 %, the honey samples were spread in thin layers on petri dishes and stored in a desiccator filled with  $\text{MgCl}_2 \cdot 6 \text{H}_2\text{O}$  for two weeks. However, it was not tested whether the moisture of 31 %, which was indicated by a hygrometer, was equally distributed in the samples as well. Moreover, the influence of the room humidity under which the sample were measured with the rheometer, was not tested. The analysis time was tried to be kept as short as possible, but since the sample needs to be placed on the geometry of the rheometer and is allowed to adopt to the temperature of the device (20 °C) for 5 min, the measurement took at least 10 min in total in which the sample was not kept under the controlled moisture.

Besides the imperfections of sample preparation and measurement, the rheological measurements pointed to the trend that the manuka honeys gave higher  $\Delta\eta$  values than the rewarewa honey. This might indicate that manuka honeys have different intramolecular structures than non-manuka honeys. Together with the results of the protein studies (see section 2.5.2.1), this led to the hypothesis that MGO-derived protein cross-links in manuka honey, might be responsible for the shear thinning behaviour of manuka honey. However, the results displayed in Figure 73, do not present clear evidence for a MGO-dependent effect, since only at 31 % moisture an increase of  $\Delta\eta$  with increasing MGO contents of the honeys was visible. Moreover, another possible cause for intramolecular interactions and a change of the viscosity of the samples might be the crystallisation state of sugars. Since the honeys do not always contain the same ratio of fructose and glucose, which profoundly influences the crystallisation process, no statements concerning its influence can be made. To test solely the effect of honey proteins on the rheological behaviour, honey proteins should be isolated via dialysis and resolubilised in a defined artificial honey matrix, stored at controlled moisture of 31 % and measured with the creep recovery test. Furthermore, additional commercial samples without MGO and also manuka honeys with varying MGO contents should be tested to prove the hypothesis that  $\Delta\eta$  is a suitable parameter to detect MGO-derived reactions in honey.

#### 4.2.3 The origin of dihydroxyacetone in manuka nectar

The reason for increased amounts of MGO in manuka honey was shown to be the high amounts of DHA in the nectar of the manuka plant. Although almost a decade has passed since this discovery, the origin of DHA in the manuka nectar is still unknown. The following prepositions made for the origin of DHA ought to be regarded as research ideas which are not yet proven.

##### 1.) Triose phosphate isomerase deficiency

The glycolytic enzyme triose phosphate isomerase (TPI) catalyzes the transition of dihydroxyacetone phosphate (DHAP) to glyceraldehyde phosphate (GAP). The enzyme is crucial for glycolysis, since only GAP can be further metabolized for energy metabolism. A deficiency of TPI may lead to an increase of DHAP in the cells. Ultimately, the dephosphorylation of DHAP might be due to enzymatic processes (e.g. kinases) or might be initiated by the pH value. The dephosphorylated compound DHA could be transported to the nectar via the plant phloem.

## 2.) Turn-on of pentose phosphate pathway

If glycolysis is hindered in manuka plants because of TPI deficiency, there need to be another way for energy metabolism. An alternative biochemical pathway might be the pentose phosphate pathway (PPP). Dorion et al. (2012) showed that transgenic potato roots with reduced cytosolic TPI have increased carbon metabolism through the PPP. The oxidative part of the PP produces ribulose-5-phosphate, which is transformed to various sugar phosphate intermediates during the non-oxidative part of the PPP. Finally, GAP is formed which can enter the rear part of glycolysis and serves energy gain. However, the turn-on of the PPP does not only explain the compensation of energy metabolism, but might also be responsible for the increase of other chemical compounds in manuka nectar compared to non-manuka plant varieties. For example, ribulose-5-phosphate, produced in the PPP, is the precursor molecule for the formation of lumazine derivatives like riboflavin. Daniels et al. (2016) reported the discovery of 3,6,7-trimethylumazine only in manuka nectar and honey, but not in any other NZ honey samples. An increase of lumazine derivatives might be due to increased amounts of ribulose-5-phosphate and the subsequent turn-on of certain metabolic pathways in the nectar and phloem of manuka plants. Moreover, another intermediate of the non-oxidative part of the PPP, erythrose-4-phosphate, plays an important role in the biosynthesis processes of plants. Erythrose-4-phosphate is one of the starting substrates of the Shikimate pathway, which is used for the biosynthesis of aromatic amino acids like phenylalanine and tyrosine and delivers starting material for phytochemical pathways. The recently proposed chemical markers by the NZ Ministry of Primary Industries, phenyllactic acid (PLA), 4-hydroxyphenyllactic acid (HPLA), 2-methoxybenzoic acid (2-MB) and 2'-methoxyacetophenone (MAP) might arise from the turn-on of this biochemical pathway.

## 3.) Biochemical reason

If the starting point of the unique biochemistry of the manuka plant is a TPI deficiency, there are some explanations for this mutation. The simplest explanation might be a genetic mutation in the manuka plant, which leads to unique reaction products, but does not affect the plants survival positively or negatively. However, some authors presumed that TPI deficiency might also have a positive effect on the life cycle of plants. According to Valancin et al. (2013) and Dorion et al. (2012), TPI deficiency is correlated with increased oxygen uptake and growth rate of the plants and Chen and Thelen (2010) speculated that plastidial TPI may have an essential role in the regulation of seedling establishment. This might be especially important



for manuka plants because of their short flowering season and thus limited amount of time for reproductive processes.

### 4.3. Metabolic transit of carbonyl compounds

#### 5.3.1 Impact of the diet on carbonyl compounds in saliva

In addition to the studies of the influence of dietary dicarbonyl compounds on urine and blood concentrations (see section 3), the influence of dietary carbonyl compounds on saliva was studied within the master thesis of Lisa-Marie Blasse (Blasse, 2017). The methods used for the analysis of carbonyl compounds in saliva are described in section 3.4.9.3. A GC-MS method for the simultaneous quantification of glucose, fructose, 3-DG, 3-DF, 3-DGA, MGO, DHA and DHAP was developed and applied to human saliva samples. Moreover the analytes lactate, pyruvate, glyoxal and glucose-6-phosphate were implemented in the method, but for their quantification further method improvement is necessary. Human saliva was collected from healthy individuals in fasting state and after intervention with a carbohydrate-rich meal (see 0). Saliva production was not stimulated and the samples were collected by the spitting method. In total, 34 subjects participated in the study.

The comparison of the fasting state saliva samples with the literature revealed that most of the analytes were present in higher concentrations in blood plasma, whereby the ratio between saliva to plasma was varying strongly between the analytes. For example, the median glucose excretion was  $24.52 \pm 15.83 \mu\text{mol/l}$  ( $n=35$ ), which was 180 times lower than the plasma concentration of 3900 - 5500  $\mu\text{mol/l}$  (World Health Organization, 2016). The median fructose concentration was  $1.03 \pm 0.65 \mu\text{mol/l}$  ( $n=38$ ), which was 100 times lower than the plasma concentration of 100  $\mu\text{mol/l}$  (Anderstam et al., 2013). This indicated that certain metabolites were transported differently from blood to saliva and that active or passive processes might be involved in the complex composition of saliva. More detailed information on the concentrations of carbonyl compounds in fasting saliva can be found in the thesis of Blasse (2017).

To study the dietary influence of carbonyl compounds on the saliva, five different intervention studies were performed. The subjects consumed either 75 g of glucose ( $n=10$ ), 40 g of fructose ( $n=6$ ), a glucose/fructose mix (34.7/30.3 g) ( $n=4$ ), 65 g of manuka honey MGO 550 ( $n=8$ ) or 65 g of rewarewa honey ( $n=9$ ). Saliva samples were collected prior to the

intervention (at 0 min) and 15, 30, 60 and 120 min after the intervention. Figure 74 shows the progression of salivary concentrations of glucose and fructose after the five different interventions. The uptake of dietary glucose mainly led to an increase of salivary glucose, whereas consumption of fructose led to an increase of salivary fructose. The food stuff which contained fructose or glucose also led to an increase of fructose and glucose, respectively.

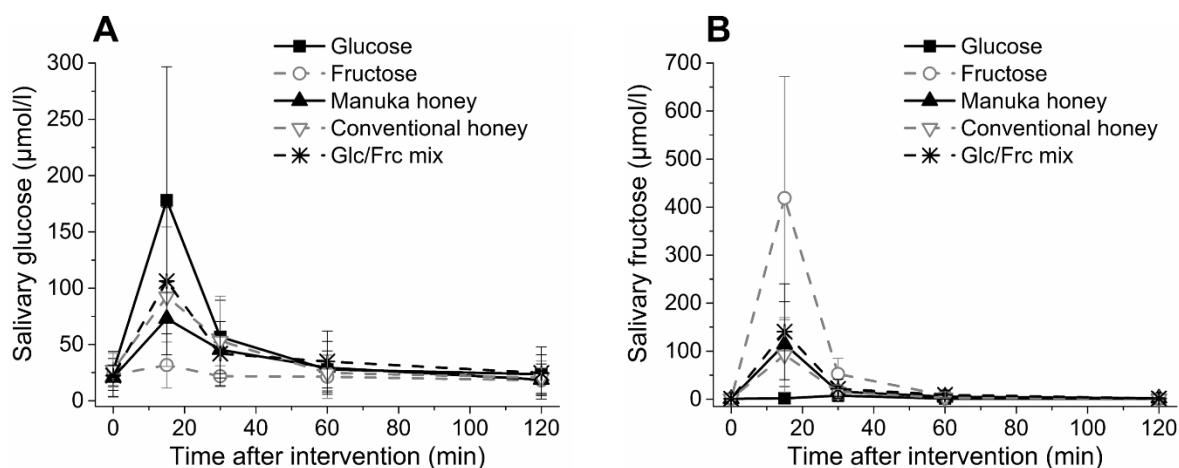


Figure 74: Salivary concentration of glucose (A) and fructose (B) prior (0 min) and after consumption of glucose, fructose, manuka honey, conventional honey or a glucose/fructose mix

Interestingly, the glucose concentration reached a maximum of approx. 170  $\mu\text{mol/l}$  at 15 min after the ingestion of 75 g glucose, whereby the fructose concentration reached a maximum also after 15 min, but at a concentration of 400  $\mu\text{mol/l}$ . Although only 40 g of fructose were consumed, the increase in salivary fructose was more pronounced compared to salivary glucose. This was probably due to the active resorption of glucose and immediate trapping of free glucose as glucose-6-phosphate in cells. In contrast, fructose is passively resorbed during gastrointestinal digestion, which leads to a less controlled level of fructose in the system. After its resorption, fructose is metabolized to fructose-1-phosphate or fructose-6-phosphate, which enters the glycolysis (Löffler et al., 2007). During the studies, it became clear that a part of the ingested sugar solutions stayed in the oral cavity even after swallowing, teeth brushing and mouth rinsing. Therefore, the results reflect the sum of the compounds, which remained in the oral cavity and flowed back into saliva and the compounds, which were transported via the gastrointestinal system to the blood and finally into saliva.

Figure 75 shows the postprandial concentration of 3-DG, 3-DF and 3-DGA in saliva. An increase of more than 400 % of the initial 3-DG concentration occurred after the consumption of manuka honey or conventional honey. After the consumption of fructose, the salivary

3-DG concentration was 3-times higher than the fasting 3-DG concentration, whereas the consumption of glucose did not increase the postprandial concentration of 3-DG.

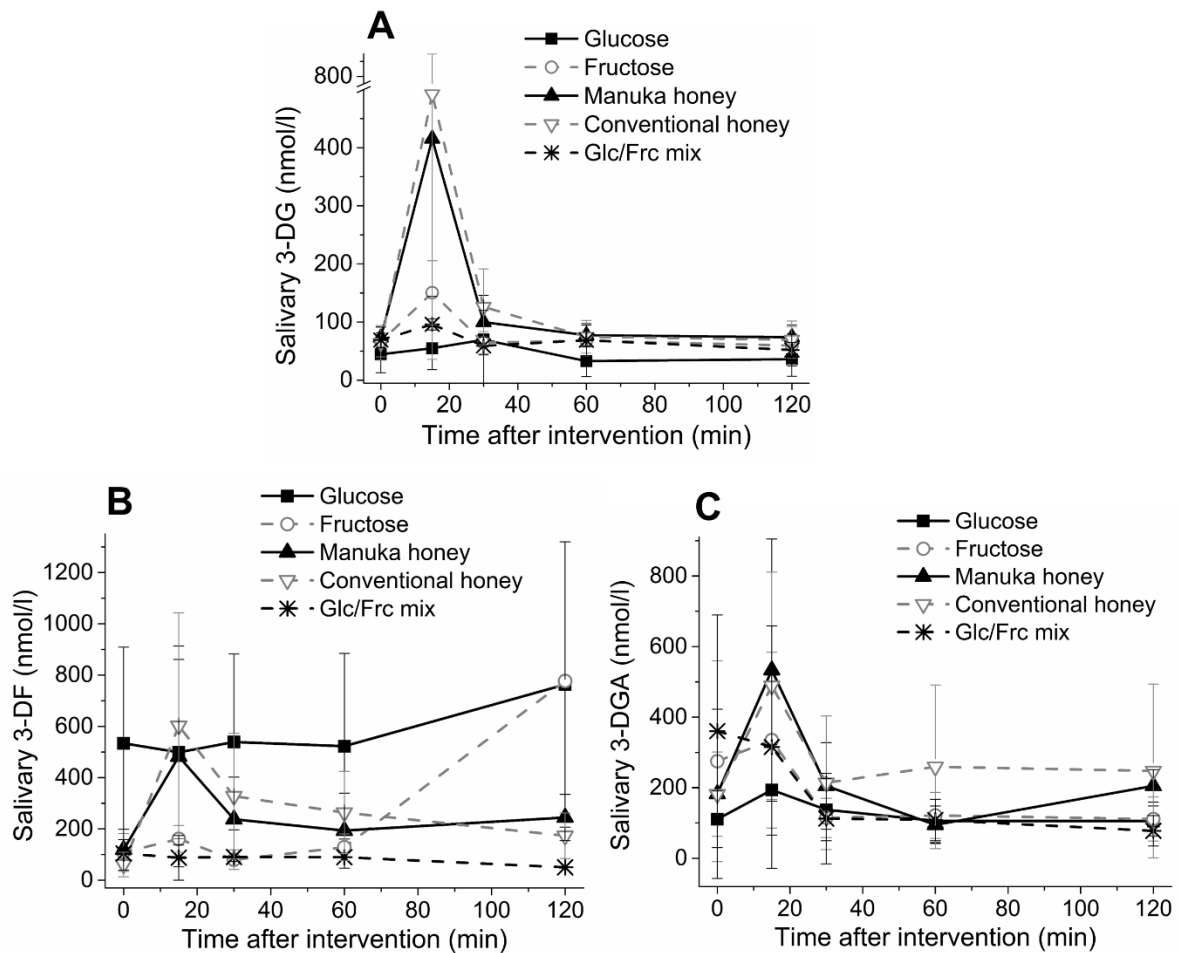


Figure 75: Salivary concentration of 3-DG (A), 3-DF (B) and 3-DGA (C) prior (0 min) and after consumption of glucose, fructose, manuka honey, conventional honey or a glucose/fructose mix

In section 3.5.3.2 it was shown that the consumption of artificial honey, containing glucose and fructose led to a postprandial increase of 3-DG. It was assumed that dietary glucose is responsible for this spike in 3-DG. However, the current results showed that the postprandial increase of 3-DG was even further enhanced by dietary fructose than glucose. The progression of the curves of the 3-DG metabolites 3-DF and 3-DGA confirmed our previous hypothesis: The ingestion of dietary 3-DG, in the form of manuka or conventional honey, led to an increase of 3-DF and 3-DGA. In contrast, 3-DG which is formed *in vivo* from fructose did not lead to a significant increase of 3-DF or 3-DGA. This again pointed to the fact that intestinal reductase or dehydrogenase enzymes on the apical side might exist, which metabolize dietary 3-DG in the moment it reaches the gut. This detoxifying mechanism for

the reactive dicarbonyl compound 3-DG might have evolved during human evolution as an adaptation to heated and carbohydrate rich food. Moreover, the ratio of 3-DG to 3-DF in fastened state saliva was with 1:2 very similar to the ratio, which was found in blood samples. This indicated that saliva is an appropriate body fluid to monitor biochemical processes and that dietary 3-DG, which was metabolized to 3-DF extracellularly was not rapidly transported into blood or saliva but is excreted with the urine (see section 3.5.3.3 for discussion).

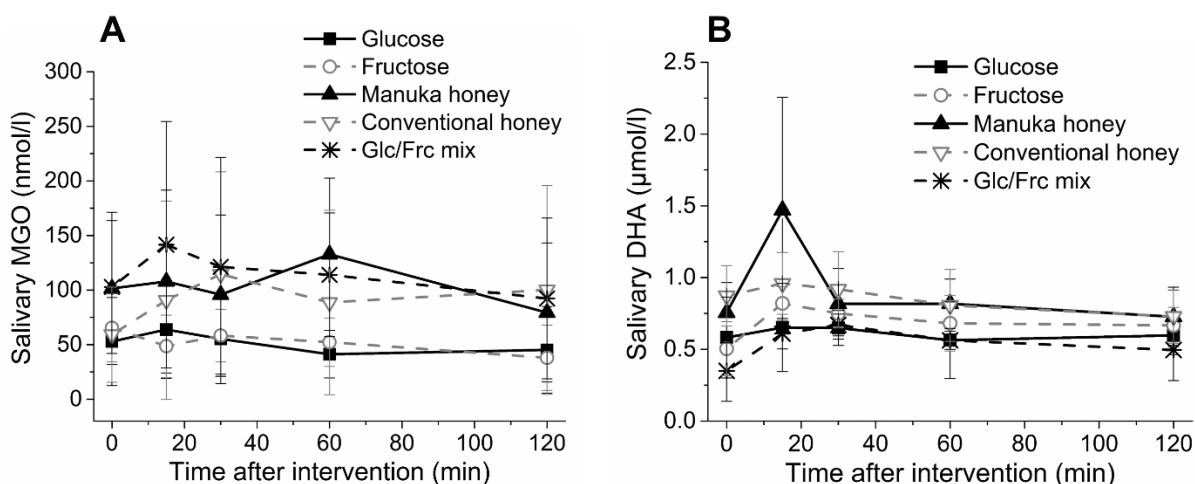


Figure 76: Salivary concentration of MGO (A) and DHA (B) prior (0 min) and after consumption of glucose, fructose, manuka honey, conventional honey or a glucose/fructose mix

Figure 76 shows the concentration of salivary MGO and DHA after the interventions. The level of MGO was not influenced by the dietary interventions, even though 560 μmol of MGO were consumed with the ingestion of manuka honey. These results were in accordance with the results of urine and blood samples after the consumption of MGO with manuka honey, which also showed no postprandial increase of MGO *in vivo*. Apparently MGO was either quickly degraded in the metabolic system or it reacted with gastrointestinal compounds, e.g. enzymes, during digestion and could not be recovered as MGO. The precursor compound for the formation of MGO in manuka honey is DHA. The fate of dietary DHA during digestion is only poorly studied. Figure 76B shows the increase of DHA in human saliva after the consumption of manuka honey containing natural DHA. The increase of less than 1 μmol/l is very low compared to the ingested dose of approx. 900 μmol DHA. In section 3.5.3.2 it was shown that the consumption of a DHA rich manuka honey by one subject led to an increase of the phosphorylated form of DHA, DHAP, in plasma by 400 %. In saliva, no significant increase of DHAP could be shown (data not displayed). The final fate of dietary

DHA and the role of DHAP could not be determined. An intervention study with at least five subjects, who consume manuka honey and subsequent analysis of DHA and DHAP in blood and saliva samples, should be performed to better understand DHA metabolism. However, neither MGO nor DHA in manuka honey seemed to significantly increase the MGO, DHA or DHAP level *in vivo*, respectively. MGO, and DHAP as a precursor of MGO formation, are discussed as risk factors for the formation of advanced glycation end-products (AGEs), which were correlated with diseases like diabetes. Based on the results of the current work, dietary MGO or DHA were not resorbed during digestion and therefore do not induce consecutive reactions.

Taken together, the biofluid saliva is a cheap, fast and convenient alternative to urine and blood and was suitable to study biochemical processes in humans. The dietary influence of certain metabolites could be monitored by collecting saliva during dietary interventions. However, it should be noted that the concentrations of most bioanalytes were lower in saliva compared to blood, which makes it less suitable for minor compounds. Moreover, the influence of incomplete elimination of the test meal from the oral cavity should be studied further and if necessary, the intervention procedure should be standardised (e.g. amount of swallows). In the interest of simplification, the collection of saliva was performed after unstimulated spitting in a glass vessel. The saliva was filtered and no further sample clean-up was applied. The sample collection could be improved with the use of salivettes and the sample clean-up could be enhanced with a protein precipitation prior to derivatisation.

---

## 5 Summary

---

The presented work deals with three key topics regarding manuka honey: The antibacterial activity of manuka honey in comparison to conventional honeys in chapter A, unique chemical reactions in the honey matrix, which might serve as quality control parameters for manuka honey in chapter B and the metabolic transit of dicarbonyl compounds during gastrointestinal digestion in chapter C.

The antibacterial studies in chapter A showed that bacterial species are affected differently by bioactive compounds present in honey. Methylglyoxal (MGO), which is solely present in manuka honeys and hydrogen peroxide, which is formed in most conventional honeys by glucose oxidase, are strong inhibitors of the growth of *S. aureus* and *E. coli*. The strain of *P. aeruginosa* used for this work was not inhibited by MGO, whereas *B. subtilis* was not inhibited by hydrogen peroxide. To compare and quantify the effect of MGO and hydrogen peroxide, a mathematic model was created. By comparing the slopes of the linearized dose-response curves, it was found that *S. aureus*, *E. coli* and *P. aeruginosa* were more sensitive to hydrogen peroxide than to MGO. However, the natural amounts of MGO in honey are higher than the formation of hydrogen peroxide. Although most bacteria are more sensitive to hydrogen peroxide, MGO is the predominantly antibacterial compound in honey, because of its higher concentrations compared to hydrogen peroxide formation. The inclusion of manuka honey in  $\alpha$ -cyclodextrin had only minor consequences on bioavailability and antibacterial activity. The commercial product cyclopower does not enhance the antibacterial activity of manuka honey on *S. aureus*, *E. coli* and *P. aeruginosa*. With the help of the newly developed quantitative model, it was shown that the growth of *B. subtilis* is synergistically inhibited with cyclopower compared to manuka honey and  $\alpha$ -cyclodextrin alone. The study of bacterial enzymes as possible targets for bacterial inhibition with manuka honey revealed that MGO and DHA inhibited jack bean urease, which was used as a model for *Helicobacter pylori* urease. The concentration of MGO and DHA in manuka honey positively correlated with its urease inhibition. Conventional honeys, which lack MGO and DHA, showed significantly less urease inhibition. Based on the unique presence of MGO, manuka honey has extraordinary effects on bacteria, which might lead to further application to fight the emerging crisis of antibacterial resistance to antibiotics.

Customers, who buy high-priced manuka honey with promised beneficial health effects, want to be sure that the product they are buying is genuine manuka honey. The NZ Ministry of Primary Industries is currently trying to establish a manuka honey definition, which confirms its origin with botanical marker compounds. In the present work, an approach based on unique chemical reactions in manuka honey was followed. It was shown that the exceptional high amounts of MGO induced the formation of 2-acetyl-1-pyrroline (2-AP). In manuka honey containing  $\geq 250$  mg/kg MGO, the 2-AP concentration was significantly increased compared to conventional honey. Moreover, honey proteins form MGO-derived reactions products, which were studied by measuring the molecular size of honey proteins. Manuka honey proteins significantly shifted to high molecular weights (HMW) with a size above 510 kDa. The amount of HMW protein in non-manuka honey was significantly lower. The cleavage of disulphide bonds led to a decrease of HMW fraction of conventional honeys but not of manuka honeys. It is hypothesized that MGO cross-linking of proteins is mainly responsible for the formation of HMW adducts in manuka honey. The formation of HMW adducts was also shown with fluorescence analysis, whereby manuka honey proteins had higher fluorescence intensities at  $\lambda_{\text{ex}}=350$  nm and  $\lambda_{\text{em}}=450$  nm compared to non-manuka honeys. The artificial addition of MGO and its precursor dihydroxyacetone (DHA) to a non-manuka honey did not lead to an increased fluorescence up to the level of commercial manuka honeys. The MGO-derived modifications of proteins were further studied by quantifying the protein-bound Maillard reaction products N- $\epsilon$ -carboxyethyllysine (CEL) and methylglyoxal-derived hydroimidazolone 1 (MG-H1) after enzymatic hydrolysis of honey proteins and LC-MS/MS analysis. Their amount was significantly higher in manuka compared to conventional honeys and correlated with the MGO content of the honey. Most of the MGO-derived reactions could be simulated by spiking a conventional honey or a low MGO manuka honey with artificial MGO and subsequent storage at elevated temperatures. Higher storage temperatures were associated with a quick increase of 5-hydroxymethylfurfuraldehyd (HMF). The HMF level in honey is used as a quality parameter and should not exceed 40 mg/kg (Codex Alimentarius Commission, 2001). High concentrations of HMF may point to a fraudulent addition of MGO and the production of artificial high-price manuka honey products. Taken together, the Maillard reaction in honey could be used to control the natural origin of MGO and DHA.

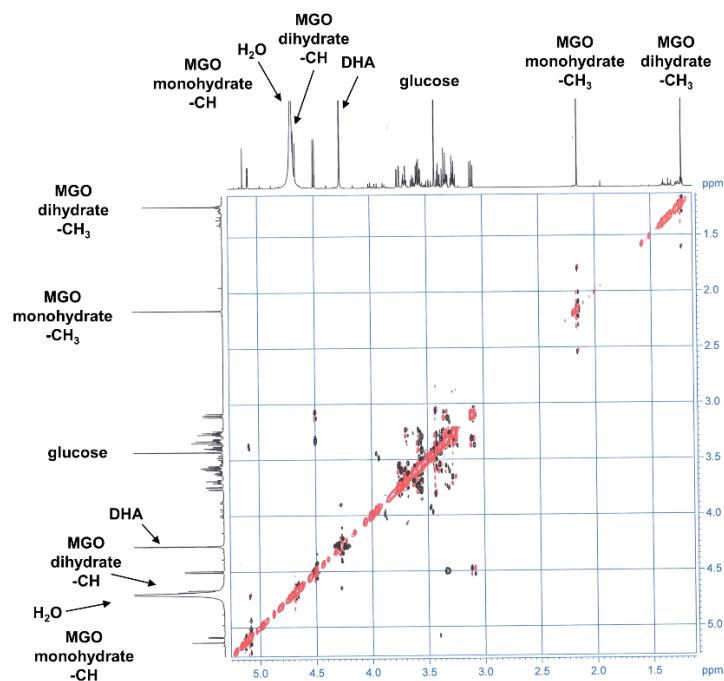
The consumption of honey and especially manuka honey exposes humans to high levels of dietary dicarbonyl compounds like MGO and 3-deoxyglucosone (3-DG). Both compounds are

discussed as potential risk factors for the development of age-related diseases. The present studies contribute to the understanding whether dietary dicarbonyl compounds increase the endogenous level of dicarbonyl compound and thus might be considered harmful. The simulated digestion of manuka honey in the presence of gastric and ileal fluids showed that only 9 % of the initial concentration could be recovered after 8 h. The honey matrix had no stabilising effect on MGO compared to a synthetic MGO solution. In contrast to MGO, the manuka honey compound DHA was stable during all simulated digestion steps. The consequences of gastrointestinal stability of DHA should be subject of further research. The complexation of MGO with  $\alpha$ -cyclodextrin did not enhance the stability of MGO. The metabolic transit of dietary MGO and 3-DG was further studied with an intervention study with healthy volunteers, who collected their daily urine. It was shown that the urinary concentrations of 3-DG and its less reactive metabolites 3-deoxyfructose (3-DF) and 2-keto-3-deoxygluconic acid (3-DGA), but not MGO, were influenced by the diet. Apparently, MGO was not resorbed into the blood circulation and therefore did not influence the endogenous MGO level. During the intervention studies, up to 40 % of dietary 3-DG was recovered as the sum of 3-DG, 3-DF and 3-DGA. The metabolite 3-DGA had only a minor role in the metabolism of dietary 3-DG in comparison to 3-DF. The complexation of manuka honey with  $\alpha$ -cyclodextrin in the commercial product “cyclopower” did not enhance the bioavailability of 3-DG or MGO. Neither of the compounds showed increased urinary excretion after consumption of 12 capsules, which is three times the recommended daily dose. The concentrations of 3-DF and 3-DGA in plasma only increased after the consumption of dietary 3-DG and not after the uptake of carbohydrate rich meals in general. This led to the conclusion that dietary 3-DG is effectively metabolized to 3-DF extracellularly on the apical site of the intestinal epithelium and is resorbed slowly into the circulation. In contrast, 3-DG, which is formed (intracellularly) postprandial from glucose, bypasses this metabolic system and cannot be metabolized as rapidly to 3-DF. Preliminary results obtained with saliva instead of urine as a bio fluid to study the dietary influence of dicarbonyl compounds confirmed the hypothesis. Based on the present results, dietary dicarbonyl compounds are effectively metabolized during digestion.

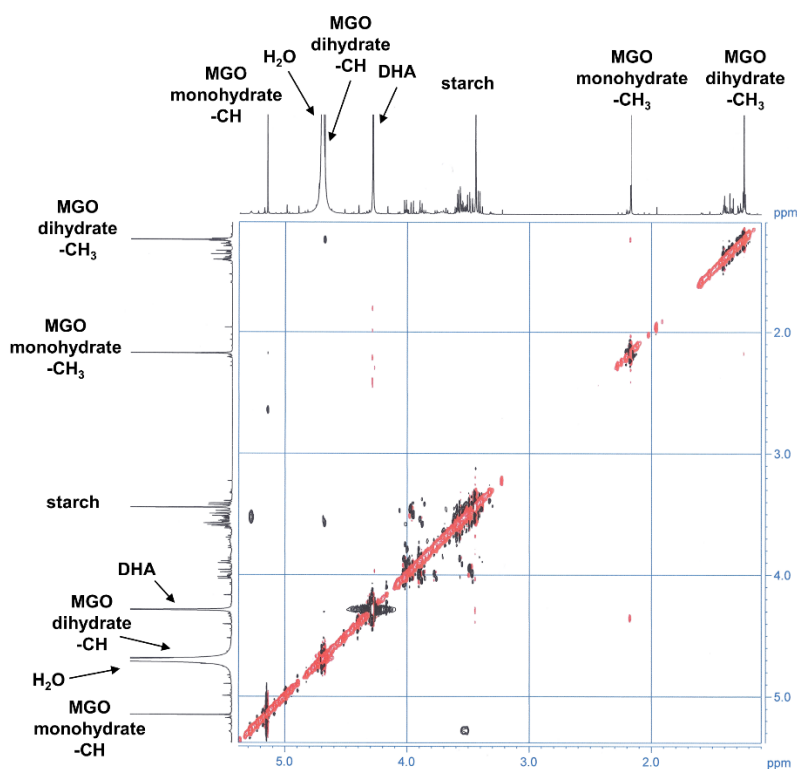


## 6 Annex

### ROESY-NMR data

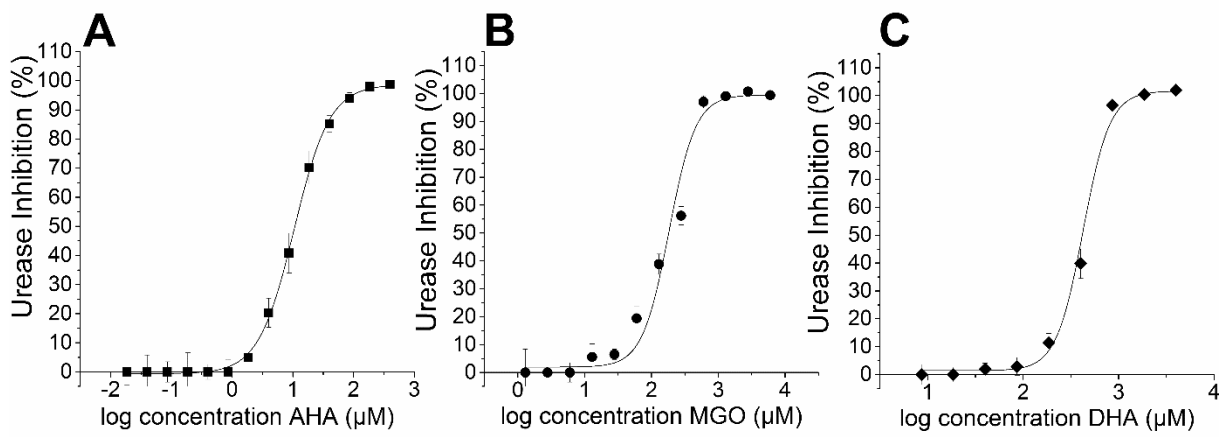


Annex-Figure 1: ROESY-NMR spectrum of glucose with DHA and MGO in equimolar ratio, protons are assigned to DHA, MGO and glucose



Annex-Figure 2: ROESY-NMR spectrum of starch with DHA and MGO in equimolar ratio, protons are assigned to DHA, MGO and starch

## Dose-response curves



Annex-Figure 3: Dose-response curves of urease inhibition by acetohydroxamic acid (A), MGO (B) and DHA (C).

---

## 7 References

---

- Abordo, E. a, Minhas, H. S. and Thornalley, P. J. (1999) Accumulation of alpha-oxoaldehydes during oxidative stress: a role in cytotoxicity., *Biochemical Pharmacology*, 58, 641–648.
- Adams, C. J., Boulton, C. H., Deadman, B. J., Farr, J. M., Grainger, M. N. C., et al. (2008) Isolation by HPLC and characterisation of the bioactive fraction of New Zealand manuka (*Leptospermum scoparium*) honey., *Carbohydrate Research*, 343, 651–9.
- Adams, C. J., Manley-Harris, M. and Molan, P. C. (2009) The origin of methylglyoxal in New Zealand manuka (*Leptospermum scoparium*) honey., *Carbohydrate Research*, 344, 1050–3.
- Adhikari, H. R. and Tappel, a L. (1973) Fluorescent products in a glucose-glycine browning reaction, *Journal Food Science*, 38, 486–488.
- Ahmad, S. I., Kirk, S. H. and Eisenstark, A. (1998) Thymine metabolism and thymineless death in prokaryotes and eukaryotes, *Annual Review of Microbiology*, 52, 591–625.
- Ahmed, N., Babaei-Jadidi, R., Howell, S. K., Thornalley, P. J. and Beisswenger, P. J. (2005) Glycated and oxidized protein degradation products are indicators of fasting and postprandial hyperglycemia in diabetes., *Diabetes Care*, 28, 2465–2471.
- Alanis, A. J. (2005) Resistance to antibiotics: Are we in the post-antibiotic era?, *Archives of Medical Research*, 36, 697–705.
- Allaman, I., Bélanger, M. and Magistretti, P. J. (2015) Methylglyoxal, the dark side of glycolysis, *Frontiers in Neuroscience*, 9, 1–12.
- Allen, H. K., Levine, U. Y., Looft, T., Bandrick, M. and Casey, T. A. (2013) Treatment, promotion, commotion: Antibiotic alternatives in food-producing animals, *Trends in Microbiology*, 21, 114–119.
- Allen, K. L., Molan, P. C. and Reid, G. M. (1991) A survey of the antibacterial activity of some New Zealand honeys, *Journal of Pharmacy and Pharmacology*, 43, 817–822.
- Alnaimat, S., Wainwright, M. and Al'Abri, K. (2012) Antibacterial potential of honey from different origins: A comparison with manuka honey, *Journal of Microbiology, Biotechnology and Food Sciences*, 1, 1328–1338.
- Amoroso, A., Maga, G. and Daglia, M. (2013) Cytotoxicity of  $\alpha$ -dicarbonyl compounds submitted to in vitro simulated digestion process, *Food Chemistry*, 140, 654–659.
- Anderstam, B., Bragfors-Helin, A.-C., Axelsson, J., Qureshi, A. R., Wibom, R., et al. (2013) Differences in acute metabolism of fructose between hemodialysis patients and healthy subjects., *Scandinavian Journal of Clinical and Laboratory Investigation*, 73, 154–160.
- Andreu, D. and Rivas, L. (1998) Peptides : An overview, *Biopolymers*, 47, 415–33.
- Anselmi, C., Centini, M., Maggiore, M., Gaggelli, N., Andreassi, M., et al. (2008) Non-covalent inclusion of ferulic acid with alpha-cyclodextrin improves photo-stability and delivery: NMR and modeling studies., *Journal of Pharmaceutical and Biomedical Analysis*, 46, 645–52.
- Arribas-Lorenzo, G. and Morales, F. J. (2010) Analysis, distribution, and dietary exposure of glyoxal and methylglyoxal in cookies and their relationship with other heat-induced

- contaminants, *Journal of Agricultural and Food Chemistry*, 58, 2966–2972.
- Atayoğlu, A. T., Soyulu, M., Silici, S. and İnanç, N. (2016) Glycemic index values of monofloral turkish honeys and the effect of their consumption on glucose metabolism, *Turkish Journal of Medical Sciences*, 46, 483–488.
- Atrott, J. (2013) Methylglyoxal in Manuka-Honig: Bildung, Wirkung, Konsequenzen, *Dissertation*, TU Dresden.
- Atrott, J., Haberlau, S. and Henle, T. (2012) Studies on the formation of methylglyoxal from dihydroxyacetone in Manuka (*Leptospermum scoparium*) honey., *Carbohydrate Research*, 361, 7–11.
- Axel, C., Brosnan, B., Zannini, E., Peyer, L. C., Furey, A., et al. (2016) Antifungal activities of three different *Lactobacillus* species and their production of antifungal carboxylic acids in wheat sourdough, *Applied Microbiology and Biotechnology*, 100, 1701–1711.
- Azeredo, L. D. C., Azeredo, M. a a, De Souza, S. R. and Dutra, V. M. L. (2003) Protein contents and physicochemical properties in honey samples of *Apis mellifera* of different floral origins, *Food Chemistry*, 80, 249–254.
- Bang, L. M., Bunting, C. and Molan, P. (2003) The effect of dilution on the rate of hydrogen peroxide production in honey and its implications for wound healing, *Journal of Alternative and Complementary Medicine*, 9, 267–273.
- Barski, O. A., Tipparaju, S. M. and Bhatnaga, A. (2008) The aldo-keto reductase superfamily and its role in drug metabolism and detoxification, *Drug Metabolism Reviews*, 40, 553–624.
- Barski, O. a, Papusha, V. Z., Ivanova, M. M., Rudman, D. M. and Finegold, M. J. (2005) Developmental expression and function of aldehyde reductase in proximal tubules of the kidney., *American Journal of Physiology. Renal Physiology*, 289, F200-7.
- Belitz H.-D., Grosch W., S. P. (2008) *Lehrbuch der Lebensmittelchemie*. 6th edn. Berlin: Springer.
- Benedé, S., López-Expósito, I., Giménez, G., Grishina, G., Bardina, L., et al. (2014) In vitro digestibility of bovine  $\beta$ -casein with simulated and human oral and gastrointestinal fluids. Identification and IgE-reactivity of the resultant peptides., *Food Chemistry*, 143, 514–21.
- Bernal, J. L., Nozal, M. J., Toribio, L., Diego, J. C. and Ruiz, A. (2005) A comparative study of several HPLC methods for determining free amino acid profiles in honey, *Journal of Separation Science*, 28, 1039–1047.
- Berrens, L. (1966) Fluorescent intermediates in the Maillard reaction, *Recueil des Travaux Chimiques des Pays-Bas*, 85, 1117–1128.
- Bilova, T., Lukasheva, E., Brauch, D., Greifenhagen, U., Paudel, G., et al. (2016) A snapshot of the plant glycated proteome structural, functional, and mechanistic aspects, *Journal of Biological Chemistry*, 291, 7621–7636.
- Blank, I., Fischer, K. and Grosch, W. (1989) Intensive neutral odourants of linden honey, *Zeitschrift für Lebensmittel-Untersuchung und Forschung*, 60, 426–433.
- Blasse, L. M. (2017) Untersuchung von Carbonylverbindungen in humanem Speichel, *Wissenschaftliche Abschlussarbeit*, TU Dresden.
- Bogdanov, S. (1981) Bestimmung von Honigprotein mit Coomassie Brilliantblau G 250, *Mitteilungen aus dem Gebiete der Lebensmitteluntersuchung und Hygiene*, 411–417.

- Bogdanov, S. (1997) Nature and origin of the antibacterial substances in honey, *LWT - Food Science and Technology*, 30, 748–753.
- Bong, J., Loomes, K. M., Lin, B. and Stephens, J. M. (2017) New approach: Chemical and fluorescence profiling of NZ honeys, *Food Chemistry*, In Press.
- Bong, J., Loomes, K. M., Schlothauer, R. C. and Stephens, J. M. (2016) Fluorescence markers in some New Zealand honeys, *Food Chemistry*, 192, 1006–1014.
- Bosch, L., Alegria, A., Farre, R. and Clemente, G. (2007) Fluorescence and color as markers for the Maillard reaction in milk–cereal based infant foods during storage, *Food Chemistry*, 105, 1135–1143.
- Bravo, A., Herrera, J. C., Scherer, E., Ju-Nam, Y., Rüksam, H., et al. (2008) Formation of alpha-dicarbonyl compounds in beer during storage of pilsner, *Journal of Agricultural and Food Chemistry*, 56, 4134–4144.
- Brown, E. D. and Wright, G. D. (2016) Antibacterial drug discovery in the resistance era, *Nature*, 529, 336–343.
- Brownlee, M., Vlassara, H. and Cerami, A. (1984) Nonenzymatic glycosylation and the pathogenesis of diabetic complications, *Annals of Internal Medicine*, 101, 527–537.
- Brudzynski, K., Abubaker, K., St-Martin, L. and Castle, A. (2011) Re-examining the role of hydrogen peroxide in bacteriostatic and bactericidal activities of honey, *Frontiers in Microbiology*, 2, 1–9.
- Brudzynski, K. and Miotto, D. (2011) Honey melanoidins: Analysis of the compositions of the high molecular weight melanoidins exhibiting radical-scavenging activity, *Food Chemistry*, 127, 1023–1030.
- Bryland, A., Broman, M., Erixon, M., Klarin, B., Lindén, T., et al. (2010) Infusion fluids contain harmful glucose degradation products, *Intensive Care Medicine*, 36, 1213–1220.
- Buchholz, K. and Goedelmann, B. (1978) Macrokinetics and operational stability of immobilized glucose oxidase and catalase, *Biotechnology and Bioengineering*, 20, 1201–1220.
- Burtis, C. A., Ashwood, E. R. and Bruns, D. E. (2013) *Tietz Textbook of Clinical Chemistry and Molecular Diagnostics*. 5th edn. Elsevier.
- van Bussel, B. C. T., van de Poll, M. C. G., Schalkwijk, C. G. and Bergmans, D. C. J. J. (2017) Increased dicarbonyl stress as a novel mechanism of multi-organ failure in critical illness., *International Journal of Molecular Sciences*, 18, 1–9.
- Buttery, R. G., Ling, L. C. and Mon, T. R. (1986) Quantitative analysis of 2-acetyl- 1 - pyrroline in rice, *Journal of Agricultural and Food Chemistry*, 34, 112–114.
- Buvari, A., Szejtli, J. and Barcza, L. (1983) Complexes of short-chain alcohols with beta-cyclodextrin, *Journal of Inclusion Phenomena*, 1, 151–157.
- Cao, D., Fan, S. T. and Chung, S. S. (1998) Identification and characterization of a novel human aldose reductase-like gene., *The Journal of Biological Chemistry*, 273, 11429–11435.
- Cellini, L. (2014) Helicobacter pylori: A chameleon-like approach to life, *World Journal of Gastroenterology*, 20, 5575–5582.
- Cerami, A. (1986) Aging of proteins and nucleic acids: what is the role of glucose?, *Trends in Biochemical Sciences*, 11, 311–314.

- Chakraborty, S., Karmakar, K. and Chakravorty, D. (2014) Cells producing their own nemesis: Understanding methylglyoxal metabolism, *IUBMB Life*, 66, 667–678.
- Chen, C., Campbell, L. T., Blair, S. E. and Carter, D. a (2012) The effect of standard heat and filtration processing procedures on antimicrobial activity and hydrogen peroxide levels in honey., *Frontiers in Microbiology*, 3, 265.
- Chen, M. and Thelen, J. J. (2010) The essential role of plastidial triose phosphate isomerase in the integration of seed reserve mobilization and seedling establishment., *Plant Signaling & Behavior*, 5, 583–5.
- Chepulis, L. M. and Francis, E. (2012) An initial investigation into the anti-inflammatory activity and antioxidant capacity of alpha-cyclodextrin-complexed Manuka honey., *Journal of Complementary & Integrative Medicine*, 9, 25.
- Codex Alimentarius Commission (2001) Codex Alimentarius Commission Standards, *Codex Stan 12-1981*, 1–8.
- Cokcetin, N. N., Pappalardo, M., Campbell, L. T., Brooks, P., Carter, A., et al. (2016) The antibacterial activity of Australian Leptospermum honey correlates with methylglyoxal levels, *PloS one*, 11, 1–13.
- Collard, F., Vertommen, D., Fortpied, J., Dueter, G. and Schaftingen, E. Van (2007) Identification of 3-deoxyglucosone dehydrogenase as aldehyde dehydrogenase 1A1 (Retinaldehyde dehydrogenase 1), *Biochimie.*, 89, 369–373.
- Collard, F., Wiame, E., Bergans, N., Fortpied, J., Vertommen, D., et al. (2004) Fructosamine 3-kinase-related protein and deglycation in human erythrocytes., *The Biochemical Journal*, 382, 137–143.
- Cooper, R. a, Jenkins, L., Henriques, a F. M., Duggan, R. S. and Burton, N. F. (2010) Absence of bacterial resistance to medical-grade manuka honey., *European Journal of Clinical Microbiology & Infectious Diseases : Official Publication of the European Society of Clinical Microbiology*, 29, 1237–41.
- Daglia, M., Amoroso, A., Rossi, D., Mascherpa, D. and Maga, G. (2013) Identification and quantification of  $\alpha$ -dicarbonyl compounds in balsamic and traditional balsamic vinegars and their cytotoxicity against human cells, *Journal of Food Composition and Analysis*, 31, 67–74.
- Daglia, M., Ferrari, D., Collina, S. and Curti, V. (2013) Influence of in vitro simulated gastroduodenal digestion on methylglyoxal concentration of manuka (*Leptospermum scoparium*) honey., *Journal of Agricultural and Food Chemistry*, 61, 2140–5.
- Daniels, B. J., Prijic, G., Meidinger, S., Loomes, K. M., Stephens, J. M., et al. (2016) Isolation, structural elucidation, and synthesis of lepteridine from mānuka (*Leptospermum scoparium*) honey, *Journal of Agricultural and Food Chemistry*, 64, 5079–5084.
- Davies, K. J. (1999) The broad spectrum of responses to oxidants in proliferating cells: a new paradigm for oxidative stress., *IUBMB life*, 48, 41–47.
- Degen, J. (2013) Vorkommen und metabolischer Transit alimentärer 1,2-Dicarbonylverbindungen, *Dissertation*, TU Dresden.
- Degen, J., Beyer, H., Heymann, B., Hellwig, M. and Henle, T. (2014) Dietary influence on urinary excretion of 3-deoxyglucosone and its metabolite 3-deoxyfructose, *Journal of Agricultural and Food Chemistry*, 62, 2449–2456.
- Degen, J., Hellwig, M. and Henle, T. (2012) 1,2-Dicarbonyl compounds in commonly

- consumed foods., *Journal of Agricultural and Food Chemistry*, 60, 7071–9.
- Degen, J., Vogel, M., Richter, D., Hellwig, M. and Henle, T. (2013) Metabolic transit of dietary methylglyoxal., *Journal of agricultural and food chemistry*, 61, 10253–10260.
- Degen, J., Vogel, M., Richter, D., Hellwig, M. and Henle, T. (2013) Metabolic transit of dietary methylglyoxal., *Journal of Agricultural and Food Chemistry*, 61, 10253–10260.
- Delgado-Andrade, C. and Morales, F. J. (2005) Unraveling the contribution of melanoidins to the antioxidant activity of coffee brews, *Journal of Agricultural and Food Chemistry*, 53, 1403–1407.
- Delpierre, G., Collard, F., Fortpied, J. and Van Schaftingen, E. (2002) Fructosamine 3-kinase is involved in an intracellular deglycation pathway in human erythrocytes., *The Biochemical Journal*, 365, 801–808.
- Delpierre, G., Vanstapel, F., Stroobant, V. and Van Schaftingen, E. (2000) Conversion of a synthetic fructosamine into its 3-phospho derivative in human erythrocytes., *The Biochemical Journal*, 352, 835–839.
- Delpierre, G., Veiga-da-Cunha, M., Vertommen, D., Buyschaert, M. and Van Schaftingen, E. (2006) Variability in erythrocyte fructosamine 3-kinase activity in humans correlates with polymorphisms in the FN3K gene and impacts on haemoglobin glycation at specific sites, *Diabetes and Metabolism*, 32, 31–39.
- Dorion, S., Clendenning, A., Jeukens, J., Salas, J. J., Parveen, N., et al. (2012) A large decrease of cytosolic triosephosphate isomerase in transgenic potato roots affects the distribution of carbon in primary metabolism, *Planta*, 236, 1177–1190.
- Elshafie, H. S., Sakr, S., Mang, S. M., Belviso, S., De Feo, V., et al. (2016) Antimicrobial activity and chemical composition of three essential oils extracted from mediterranean aromatic plants, *Journal of Medicinal Food*, 19, 1096–1103.
- Eteraf-Oskouei, T. and Najafi, M. (2013) Traditional and modern uses of natural honey in human diseases: A review, *Iranian Journal of Basic Medical Sciences*, 16, 731–742.
- Ewaschuk, J. B., Naylor, J. M. and Zello, G. A. (2005) D-lactate in human and ruminant metabolism, *The Journal of Nutrition*, 135, 1619–25.
- Ferguson, G. P., Töttemeyer, S., MacLean, M. J. and Booth, I. R. (1998) Methylglyoxal production in bacteria: suicide or survival?, *Archives of Microbiology*, 170, 209–18.
- Fiedler, T., Moritz, T. and Kroh, L. W. (2006) Influence of  $\alpha$ -dicarbonyl compounds to the molecular weight distribution of melanoidins in sucrose solutions: part 1, *European Food Research and Technology*, 223, 837–842.
- Finnegan, M., Linley, E., Denyer, S. P., McDonnell, G., Simons, C., et al. (2010) Mode of action of hydrogen peroxide and other oxidizing agents: Differences between liquid and gas forms, *Journal of Antimicrobial Chemotherapy*, 65, 2108–2115.
- Finot, A. (1982) Nonenzymatic browning products: physiologic effects and metabolic transit in relation to chemical structure. A review, *Diabetes*, 31, 22–28.
- Förster, A. (2006) Quantitative Studien zu Vorkommen und metabolischem Transit alimentärer Maillard-Reaktions-Produkte, *Dissertation*, TU Dresden.
- Fujii, E., Iwase, H., Ishii-Karakasa, I., Yajima, Y. and Hotta, K. (1995) The presence of 2-keto-3-deoxygluconic acid and oxoaldehyde dehydrogenase activity in human erythrocytes., *Biochemical and Biophysical Research Communications*, 852–857.

- Funasaki, N., Ishikawa, S. and Neya, S. (2002) Solution structures of  $\alpha$ -cyclodextrin complexes with propanol and propanesulfonate estimated from NMR and molecular surface area, *The Journal of Physical Chemistry B*, 106, 6431–6436.
- Gentilcore, D., Vanis, L., Teng, J. C., Wishart, J. M., Buckley, J. D., et al. (2011) The oligosaccharide  $\alpha$ -cyclodextrin has modest effects to slow gastric emptying and modify the glycaemic response to sucrose in healthy older adults., *The British Journal of Nutrition*, 106, 583–7.
- Gibson, Q. H., Swoboda, B. E. P. and Massey, V. (1964) Kinetics and mechanism of action of glucose oxidase, *The Journal of Biological Chemistry*, 239, 3927–3934.
- Gleiter, R. A., Horn, H. and Isengard, H. D. (2006) Influence of type and state of crystallisation on the water activity of honey, *Food Chemistry*, 96, 441–445.
- Gobert, J. and Glomb, M. A. (2009) Degradation of glucose: reinvestigation of reactive alpha-dicarbonyl compounds, *Journal of Agricultural and Food Chemistry*, 57, 8591–8597.
- Grainger, M. N. C., Manley-Harris, M., Lane, J. R. and Field, R. J. (2016a) Kinetics of conversion of dihydroxyacetone to methylglyoxal in New Zealand mānuka honey: Part I, *Food Chemistry*, 202, 484–91.
- Grainger, M. N. C., Manley-Harris, M., Lane, J. R. and Field, R. J. (2016b) Kinetics of conversion of dihydroxyacetone to methylglyoxal in New Zealand mānuka honey: Part II, *Food Chemistry*.
- Grimm, C. C., Champagne, E. T., Lloyd, I. S. W. and Easson, I. M. (2011) Analysis of 2-acetyl-1-pyrroline in rice by HSSE/GC/MS, *Cereal Chemistry Journal*, 88, 271–277.
- Guo, X., Li, H., Xu, H., Woo, S., Dong, H., et al. (2012) Glycolysis in the control of blood glucose homeostasis, *Acta Pharmaceutica Sinica B*, 2, 358–367.
- Hahne, F. (2014) 3-Desoxy-2-ketogluconsäure als Metabolit von 3-Desoxyglucoson in Erythrozyten: Synthese, Analyse und Rolle bei Diabetes, *Wissenschaftliche Abschlussarbeit*, TU Dresden.
- Hansell, N. K., Pang, D., Heath, A. C., Martin, N. G. and Whitfield, J. B. (2005) Erythrocyte aldehyde dehydrogenase activity: Lack of association with alcohol use and dependence or alcohol reactions in Australian twins, *Alcohol and Alcoholism*, 40, 343–348.
- Harrington, C. R. (1990) Lowry protein assay containing sodium dodecyl sulfate in microtiter plates for protein determinations on fractions from brain tissue, *Analytical Biochemistry*, 186, 285–287.
- Hartford, O. M. and Dowds, B. C. . (1994) Isolation and characterization of a hydrogen peroxide resistant mutant of *Bacillus subtilis*, *Microbiology*, 140, 297–304.
- Hayase, F., Liang, Z., Suzuki, Y. and Chuyen, N. (1991) Enzymatic metabolism of 3-deoxyglucosone, a Maillard intermediate, *Amino Acids*, 1, 307–318.
- Hayashi, K., Fukushima, A., Hayashi-Nishino, M. and Nishino, K. (2014) Effect of methylglyoxal on multidrug-resistant *Pseudomonas aeruginosa*., *Frontiers in Microbiology*, 5, 180.
- Hayashi, T. and Shibamoto, T. (1985) Analysis of methylglyoxal in foods and beverages., *Journal of Agricultural and Food Chemistry*, 33, 1090–1093.
- He, J., Zeng, M., Zheng, Z., He, Z. and Chen, J. (2014) Simultaneous determination of N  $\epsilon$ -(carboxymethyl) lysine and N  $\epsilon$ -(carboxyethyl) lysine in cereal foods by LC–MS/MS,



- European Food Research and Technology*, 238, 367–374.
- Heil, M. (2011) Nectar: Generation, regulation and ecological functions, *Trends in Plant Science*, 16, 191–200.
- Hellwig, M. (2011) Proteolytische Freisetzung und epithelialer Transport von Maillard-Reaktionsprodukten und Crosslink-Aminosäuren, *Dissertation*, TU Dresden.
- Hellwig, M., Bunzel, D., Huch, M., Franz, C. M. a P., Kulling, S. E., et al. (2015) Stability of individual Maillard reaction products in the presence of the human colonic microbiota., *Journal of Agricultural and Food Chemistry*, 63, 6723–30.
- Hellwig, M., Degen, J. and Henle, T. (2010) 3-Deoxygalactosone, a ‘new’ 1,2-dicarbonyl compound in milk products., *Journal of Agricultural and Food Chemistry*, 58, 10752–60.
- Hellwig, M. and Henle, T. (2014) Baking, ageing, diabetes: a short history of the Maillard reaction., *Angewandte Chemie (International ed. in English)*, 53, 10316–29.
- Hellwig, M., Kiessling, M., Rother, S. and Henle, T. (2015) Quantification of the glycation compound 6-(3-hydroxy-4-oxo-2-methyl-4(1H)-pyridin-1-yl)-l-norleucine (maltosine) in model systems and food samples, *European Food Research and Technology*, 4, 547–557.
- Hellwig, M., Matthes, R., Peto, A., Löbner, J. and Henle, T. (2014) N-ε-fructosyllysine and N-ε-carboxymethyllysine, but not lysinoalanine, are available for absorption after simulated gastrointestinal digestion, *Amino Acids*, 46, 289–299.
- Hellwig, M., Rückriemen, J., Sandner, D. and Henle, T. (2017) Unique pattern of protein-bound Maillard reaction products in manuka (*Leptospermum scoparium*) honey, *Journal of Agricultural and Food Chemistry*, 65.
- Hellwig, M., Witte, S. and Henle, T. (2016) Free and protein-bound Maillard reaction products in beer: method development and a survey of different beer types, *Journal of Agricultural and Food Chemistry*, 64, 7234–7243.
- Helou, C., Jacolot, P., Niquet-Léridon, C., Gadonna-Widehem, P. and Tessier, F. J. (2016) Maillard reaction products in bread: A novel semi-quantitative method for evaluating melanoidins in bread, *Food Chemistry*, 190, 904–911.
- Henle, T. (2005) Protein-bound advanced glycation endproducts (AGEs) as bioactive amino acid derivatives in foods, *Amino Acids*, 29, 313–322.
- Henle, T. (2007) Dietary advanced glycation end products--a risk to human health? A call for an interdisciplinary debate., *Molecular Nutrition & Food Research*, 51, 1075–8.
- Henle, T. (2008) Maillard reaction of proteins and advanced glycation end products (AGEs) in food, in *Process-Induced Food Toxicants*. John Wiley & Sons, Inc., 215–242.
- Henriques, a F., Jenkins, R. E., Burton, N. F. and Cooper, R. a (2010) The intracellular effects of manuka honey on *Staphylococcus aureus*., *European Journal of Clinical Microbiology & Infectious Diseases: Official Publication of the European Society of Clinical Microbiology*, 29, 45–50.
- Hodge, J. E. (1953) Browning reactions in model systems., *Journal of Agricultural and Food Chemistry*, 1, 928–943.
- Hoffmann, W. (2012) In vitro-Studien zur Untersuchung der Metabolisierung von 1,2-Dicarbonylverbindungen, *Wissenschaftliche Abschlussarbeit*, TU Dresden.
- Hofmann, T. (1998) Studies on the relationship between molecular weight and the color potency of fractions obtained by thermal treatment of Glucose / Amino Acid and glucose /

- protein solutions by Using ultracentrifugation and color dilution techniques, *Journal of Agricultural and Food Chemistry*, 46, 3891–3895.
- Hofmann, T. and Schieberle, P. (1998) 2-Oxopropanal, hydroxy-2-propanone, and 1-pyrrolines important intermediates in the generation of the roast-smelling food flavor compounds 2-acetyl-1-pyrroline and 2-acetyltetrahydropyridine, *Journal of Agricultural and Food Chemistry*, 46, 2270–2277.
- Hohmann, C. (2015) Reaktionen von Methylglyoxal in Manukahonig, *Wissenschaftliche Abschlussarbeit*, TU Dresden.
- Hu, J.-L., Nie, S.-P., Min, F.-F. and Xie, M.-Y. (2013) Artificial simulated saliva, gastric and intestinal digestion of polysaccharide from the seeds of *Plantago asiatica* L., *Carbohydrate Polymers*, 92, 1143–50.
- Vander Jagt, D. L. and Hunsaker, L. a. (2003) Methylglyoxal metabolism and diabetic complications: Roles of aldose reductase, glyoxalase-I, betaine aldehyde dehydrogenase and 2-oxoaldehyde dehydrogenase, *Chemico-Biological Interactions*, 143–144, 341–351.
- Jenkins, R., Burton, N. and Cooper, R. (2011) Manuka honey inhibits cell division in methicillin-resistant *Staphylococcus aureus*., *The Journal of antimicrobial chemotherapy*, 66, 2536–42.
- Jeuring, H. J. and Koppers, F. J. (1980) High performance liquid chromatography of furfural and hydroxymethylfurfural in spirits and honey., *Journal - Association of Official Analytical Chemists*, 63, 1215–1218.
- Johner, S., Libuda, L., Shi, L., Retzlaff, A., Joslowski, G., et al. (2010) Urinary fructose: a potential biomarker for dietary fructose intake in children, *European Journal of Clinical Nutrition*, 64, 1365–1370.
- Johnson, R. D., Bahnisch, J., Stewart, B., Shearman, D. J. C. and Edwards, J. B. (1992) Optimized spectrophotometric determination of aldehyde dehydrogenase activity in erythrocytes, *Clinical Chemistry*, 38, 584–588.
- Jurysta, C., Sener, A., Bulur, N., Oguzhan, B., Satman, I., et al. (2009) Salivary glucose concentration and excretion in normal and diabetic subjects, *Journal of Biomedicine and Biotechnology*, 2009, 1–6.
- Juszczak, L. and Fortuna, T. (2006) Rheology of selected Polish honeys, *Journal of Food Engineering*, 75, 43–49.
- Kalapos, M. P. (1999) Methylglyoxal in living organisms: chemistry, biochemistry, toxicology and biological implications., *Toxicology Letters*, 110, 145–75.
- Karabournioti, S. and Zervalaki, P. (2001) The effect of heating on honey hmf HMF and invertase, *Apiacta*, 4, 1977–1979.
- Kato, H., van Chuyen, N., Shinoda, T., Sekiya, F. and Hayase, F. (1990) Metabolism of 3-deoxyglucosone, an intermediate compound in the Maillard reaction, administered orally or intravenously to rats., *Biochimica et Biophysica Acta*, 1035, 71–6.
- Kato, H., Shin, D. B. and Hayase, F. (1987) 3-Deoxyglucosone crosslinks proteins under physiological conditions, *Agricultural and Biological Chemistry*, 51, 2009–2011.
- Kawasaki, T., Akanuma, H. and Yamanouchi, T. (2002) Increased fructose concentrations in blood and urine in patients with diabetes, *Diabetes Care*, 25, 353–357.
- Keenan, J. I., Salm, N., Hampton, M. B. and Wallace, A. J. (2010) Individual and combined

- effects of foods on *Helicobacter pylori* growth, *Phytotherapy Research*, 24, 1229–1233.
- Keenan, J. I., Salm, N., Wallace, A. J. and Hampton, M. B. (2012) Using food to reduce *H. pylori*-associated inflammation., *Phytotherapy Research*, 26, 1620–5.
- Klemm, O. (2016) Charakterisierung der Hemmwirkung von Manuka Honig auf Urease Inhaltsverzeichnis, *Wissenschaftliche Abschlussarbeit*, TU Dresden.
- Kleppe, K. (1966) The effect of hydrogen peroxide on glucose oxidase from *Aspergillus niger*, *Biochemistry*, 5, 2007.
- Knecht, K. J., Feather, M. S. and Baynes, J. W. (1992) Detection of 3-deoxyfructose and 3-deoxyglucosone in human urine and plasma: Evidence for intermediate stages of the Maillard reaction in vivo, *Archives of Biochemistry and Biophysics*, 294, 130–137.
- Ko, J., Kim, I., Yoo, S., Min, B., Kim, K., et al. (2005) Conversion of methylglyoxal to acetol by *Escherichia coli* aldo-keto reductases, *Journal of Bacteriology*, 187, 5782–5789.
- Kohanski, M. A., Dwyer, D. J. and Collins, J. J. (2009) How antibiotics kill bacteria : from targets to networks, *Nature Reviews Microbiology*, 8, 423–435.
- Krajewska, B. (2011) Hydrogen peroxide-induced inactivation of urease: Mechanism, kinetics and inhibitory potency, *Journal of Molecular Catalysis B: Enzymatic*, 68, 262–269.
- Krause, R., Knoll, K. and Henle, T. (2003) Studies on the formation of furosine and pyridosine during acid hydrolysis of different Amadori products of lysine, *European Food Research and Technology*, 216, 277–283.
- Krauze-Baranowska, M., Majdan, M., Halasa, R., Glod, D., Kula, M., et al. (2014) The antimicrobial activity of fruits from some cultivar varieties of *Rubus idaeus* and *Rubus occidentalis*., *Food & Function*, 5, 2536–2541.
- Kroh, L. W. (1994) Caramelisation in food and beverages, *Food Chemistry*, 51, 373–379.
- Kroh, L. W., Fiedler, T. and Wagner, J. (2008) alpha-Dicarbonyl compounds-key intermediates for the formation of carbohydrate-based melanoidins., *Annals of the New York Academy of Sciences*, 1126, 210–5.
- Kunze, S. (2009) Untersuchungen zur Aminosäure- und Proteinzusammensetzung von Manuka-Honigen, *Wissenschaftliche Abschlussarbeit*, TU Dresden.
- Kwakman, P. H. S., de Boer, L., Ruyter-Spira, C. P., Creemers-Molenaar, T., Helsper, J. P. F. G., et al. (2011b) Medical-grade honey enriched with antimicrobial peptides has enhanced activity against antibiotic-resistant pathogens., *European Journal of Clinical Microbiology & Infectious Diseases : Official Publication of the European Society of Clinical Microbiology*, 30, 251–7.
- Kwakman, P. H. S., Te Velde, A. a, de Boer, L., Vandenbroucke-Grauls, C. M. J. E. and Zaat, S. a J. (2011a) Two major medicinal honeys have different mechanisms of bactericidal activity., *PloS one*, 6, e17709.
- Lal, S., B.S. Szwergold, Taylor, A. H., Randall, W. C., Kappler, F., et al. (1995) Metabolism of fructose-3-phosphate in the diabetic rat lens, *Archives of Biochemistry and Biophysics*, 318, 191–199.
- Lal, S., Szwergold, B. S., Kappler, F. and Brown, T. (1993) Detection of fructose-3-phosphokinase activity in intact mammalian lenses by <sup>31</sup>P NMR spectroscopy, *Journal of Biological Chemistry*, 268, 7763–7767.
- Lazaridou, A., Biliaderis, C. G., Bacandritsos, N. and Sabatini, A. G. (2004) Composition,

- thermal and rheological behaviour of selected Greek honeys, *Journal of Food Engineering*, 64, 9–21.
- Ledl, F. and Schleicher, E. (1990) New aspects of the Maillard reaction in foods and in the human body, *Angewandte Chemie-International Edition*, 29, 565–594.
- Lee, H. K., Seo, I. A., Suh, D. J., Lee, H. J. and Park, H. T. (2009) A novel mechanism of methylglyoxal cytotoxicity in neuroglial cells., *Journal of Neurochemistry*, 108, 273–84.
- Leiterer, M. (2008) Validierung von Untersuchungsmethoden in der analytischen Praxis, *Thüringer Ministerium für Landwirtschaft, Naturschutz und Umwelt*, 21. (Accessed: 4 February 2017).
- Li, Y., Cohenford, M. a., Dutta, U. and Dain, J. a. (2008) In vitro nonenzymatic glycation of guanosine 5'-triphosphate by dihydroxyacetone phosphate, *Analytical and Bioanalytical Chemistry*, 392, 1189–1196.
- Lin, B., Loomes, K. M., Prijic, G., Schlothauer, R. and Stephens, J. M. (2017) Lepteridine as a unique fluorescent marker for the authentication of manuka honey, *Food Chemistry*, 225, 175–180.
- Lin, S. M., Molan, P. C. and Cursons, R. T. (2011) The controlled in vitro susceptibility of gastrointestinal pathogens to the antibacterial effect of manuka honey., *European Journal of Clinical Microbiology & Infectious Diseases : Official Publication of the European Society of Clinical Microbiology*, 30, 569–74.
- Lin, Y. T., Kwon, Y. I., Labbe, R. G. and Shetty, K. (2005) Inhibition of *Helicobacter pylori* and associated urease by oregano and cranberry phytochemical synergies, *Applied and Environmental Microbiology*, 71, 8558–8564.
- Lo, C.-Y., Hsiao, W.-T. and Chen, X.-Y. (2011) Efficiency of trapping methylglyoxal by phenols and phenolic acids., *Journal of Food Science*, 76, H90-6.
- Lo, C., Li, S., Wang, Y., Tan, D., Pan, M., et al. (2008) Reactive dicarbonyl compounds and 5-(hydroxymethyl)-2-furfural in carbonated beverages containing high fructose corn syrup, *Food Chemistry*, 107, 1099–1105.
- Lo, T. W. C., Westwood, M. E., Mclellan, A. C., Selwood, T. and Thornalleys, P. J. (1994) Binding and modification of proteins by methylglyoxal under physiological conditions, *The Journal of Biological Chemistry*, 269, 32299–32305.
- Löbner, J., Degen, J. and Henle, T. (2015) Creatine is a scavenger for methylglyoxal under physiological conditions via formation of N-(4-methyl-5-oxo-1-imidazolin-2-yl)sarcosine (MG-HCr)., *Journal of Agricultural and Food Chemistry*, 63, 2249–56.
- Löffler, G., Petrides, P. E. and Heinrich, P. C. (2007) *Biochemie und Pathobiochemie*. 8th edn. Heidelberg: Springer Medizin Verlag.
- Lowry, O. H., Rosebrough, N. J., Farr, A. L. and Randall, R. J. (1951) Protein measurement with the folin phenol reagent, *Analytical Biochemistry*, 217, 220–230.
- Lu, J., Carter, D. a, Turnbull, L., Rosendale, D., Hedderley, D., et al. (2013) The effect of New Zealand kanuka, manuka and clover honeys on bacterial growth dynamics and cellular morphology varies according to the species., *PloS one*, 8, e55898.
- Ludwig, E. (1979) Untersuchungen zur Maillard-Reaktion zwischen gamma-Lactoglobulin und Lactose, 3. Mitt. Der Einfluss intermolekularer Disulfidbrücken auf die Blockierung von Lysin, *Die Nahrung*, 23, 707–714.

- Luke, G. A., Gough, H., Beeley, J. A. and Geddes, D. A. M. (1999) Human salivary sugar clearance after sugar rinses and intake of foodstuffs, *Caries Research*, 33, 123–129.
- Lunow, D., Kaiser, S., Rückriemen, J., Pohl, C. and Henle, T. (2015) Tryptophan-containing dipeptides are C-domain selective inhibitors of angiotensin converting enzyme, *Food Chemistry*, 166, 596–602.
- Lusby, P. E., Coombes, A. L. and Wilkinson, J. M. (2005) Bactericidal activity of different honeys against pathogenic bacteria., *Archives of Medical Research*, 36, 464–7.
- Lyons, T. J., Silvestri, G., Dunn, J. A., Dyer, D. G. and Baynes, J. W. (1991) Role of glycation in modification of lens crystallins in diabetic and nondiabetic senile cataracts, *Diabetes*, 40, 1010–1015.
- Maessen, D. E., Hanssen, N. M., Scheijen, J. L., van der Kallen, C. J., van Greevenbroek, M. M., et al. (2015) Post-glucose load plasma  $\alpha$ -dicarbonyl concentrations are increased in individuals with impaired glucose metabolism and type 2 diabetes: The CODAM study, *Diabetes Care*, 38, 913–920.
- Maessen, M. F. H., Schalkwijk, C. G., Verheggen, R. J. H. M., Aengevaeren, V. L., Hopman, M. T. E., et al. (2017) A comparison of dicarbonyl stress and advanced glycation endproducts in lifelong endurance athletes vs. sedentary controls, *Journal of Science and Medicine in Sport*, S1440-2440, 30341–9.
- Maillard, L.-C. (1912) Action des acides amines sur les sucres: formation des melanoidines par voi methodique, *C. R. Hebd. Seances Acad. Sci.*, 154, 66–68.
- Majtan, J., Bohova, J., Prochazka, E. and Kludiny, J. (2013) Methylglyoxal may affect hydrogen peroxide accumulation in manuka honey through the inhibition of glucose oxidase., *Journal of Medicinal Food*, 17, 290–293.
- Majtan, J., Kludiny, J., Bohova, J., Kohutova, L., Dzurova, M., et al. (2012) Methylglyoxal-induced modifications of significant honeybee proteinous components in manuka honey: Possible therapeutic implications., *Fitoterapia*, 83, 671–7.
- Mandal, M. D. and Mandal, S. (2011) Honey: its medicinal property and antibacterial activity, *Asian Pacific Journal of Tropical Biomedicine*, 1, 154–160.
- Mannina, L., Sobolev, A. P., Coppo, E., Di Lorenzo, A., Nabavi, S. M., et al. (2016) Antistaphylococcal activity and metabolite profiling of manuka honey (*Leptospermum scoparium* L.) after in vitro simulated digestion, *Food Funct.* Royal Society of Chemistry, 7, 1664–1670.
- Manuka Health NZ Ltd. (2013) Process for the pilot scale production of MGO <sup>TM</sup>400+ Manuka Honey with CycloPower, 1–7.
- De Marco, L. M., Fischer, S. and Henle, T. (2011) High molecular weight coffee melanoidins are inhibitors for matrix metalloproteases., *Journal of Agricultural and Food Chemistry*, 59, 11417–23.
- Marriott, B. P., Cole, N. and Lee, E. (2009) National estimates of dietary fructose intake increased from 1977 to 2004 in the United States., *The Journal of Nutrition*, 139, 1228S–1235S.
- Marshall, B. J., Warren, J. R., Francis, G. J., Langton, S. R., Goodwin, C. S., et al. (1987) Rapid urease test in the management of *Campylobacter pyloridis*-associated gastritis., *American Journal of Gastroenterology*, 82, 200–210.
- Matiacevich, S. B. and Pilar Buera, M. (2006) A critical evaluation of fluorescence as a

- potential marker for the Maillard reaction, *Food Chemistry*, 95, 423–430.
- Matongo, F. and Nwodo, U. U. (2014) In vitro assessment of *Helicobacter pylori* ureases inhibition by honey fractions, *Archives of Medical Research*, 45, 540–546.
- Matsubara, S., Shibata, H., Ishikawa, F., Yokokura, T., Takahashi, M., et al. (2003) Suppression of *Helicobacter pylori*-induced gastritis by green tea extract in Mongolian gerbils, *Biochemical and Biophysical Research Communications*, 310, 715–719.
- Mavric, E., Wittmann, S., Barth, G. and Henle, T. (2008) Identification and quantification of methylglyoxal as the dominant antibacterial constituent of Manuka (*Leptospermum scoparium*) honeys from New Zealand., *Molecular nutrition & food research*, 52, 483–9.
- McCance, D. R., Dyer, D. G., Dunn, J. a, Bailie, K. E., Thorpe, S. R., et al. (1993) Maillard reaction products and their relation to complications in insulin-dependent diabetes mellitus., *The Journal of Clinical Investigation*, 91, 2470–2478.
- Mesana, M. I., Hilbig, A., Androutsos, O., Cuenca-García, M., Dallongeville, J., et al. (2016) Dietary sources of sugars in adolescents' diet: the HELENA study, *European Journal of Nutrition*, 1–13.
- Minekus, M., Alminger, M., Alvito, P., Ballance, S., Bohn, T., et al. (2014) A standardised static in vitro digestion method suitable for food – an international consensus, *Food & Function*, 5, 1113–1124.
- Ministry for Primary Industries (2015) *Apiculture Monitoring Report*.
- Ministry for Primary Industries (2017) *Criteria for identifying mānuka honey: A summary of the mānuka honey science programme*.
- Molan, P. C. (1992a) The Antibacterial Activity of Honey, *Bee World*, 73, 5–28.
- Molan, P. C. (1992b) The Antibacterial Activity of Honey 2 . Variation in the potency of the antibacterial activity, *Bee World*, 73, 59–76.
- Molan, P. C. (2006) The evidence supporting the use of honey as a wound dressing., *The international journal of lower extremity wounds*, 5, 40–54.
- Molan, P. C. and Russell, K. M. (1988) Non-peroxide antibacterial activity in some New Zealand honeys, *Journal of Apicultural Research*, 27, 62–67.
- Molin, M., Pilon, M. and Blomberg, A. (2007) Dihydroxyacetone-induced death is accompanied by advanced glycation endproduct formation in selected proteins of *Saccharomyces cerevisiae* and *Caenorhabditis elegans*, *Proteomics*, 7, 3764–3774.
- Moore, O. A., Smith, L. A., Campbell, F., Seers, K., McQuay, H. J., et al. (2001) Systematic review of the use of honey as a wound dressing, *BMC Complementary and Alternative Medicine*, 1, 1–6.
- Morales, F. J. and Boekel, M. a J. S. Van (1997) A study on advanced Maillard reaction in heated casein/sugar solutions: fluorescence accumulation, *International Dairy Journal*, 7, 675–683.
- Morales, F. J. and Jiménez-Pérez, S. (2001) Free radical scavenging capacity of Maillard reaction products as related to colour and fluorescence, *Food Chemistry*, 72, 119–125.
- Morales, F. J. and Jiménez-Pérez, S. (2001) Free radical scavenging capacity of Maillard reaction products as related to colour and Fluorescence, 72, 119–125.
- Morales, F. J., Romero, C. and Jiménez-Pérez, S. (1996) Fluorescence associated with

- Maillard reaction in milk and milk-resembling systems, *Food Chemistry*, 57, 423–428.
- Mu, W., Yu, S., Zhu, L., Zhang, T. and Jiang, B. (2012) Recent research on 3-phenyllactic acid, a broad-spectrum antimicrobial compound, *Applied Microbiology and Biotechnology*, 95, 1155–1163.
- Müller, D. (2013) Untersuchung zur antibakteriellen Aktivität von Manuka-Honig, *Wissenschaftliche Abschlussarbeit*, TU Dresden.
- Münch, G., Keis, R., Wessels, A., Riederer, P., Bahner, U., et al. (1997) Determination of advanced glycation end products in serum by fluorescence spectroscopy and competitive ELISA., *European Journal of Clinical Chemistry and Clinical Biochemistry*, 35, 669–677.
- Nagao, M., Fujita, Y. and Wakabayashi, K. (1986) Mutagens in coffee and other beverages, *Environmental Health Perspectives*, 67, 89–91.
- Nakamura, T. and Ogura, Y. (1962) Studies on the action of glucose oxidase, *The Journal of Biochemistry*, 52, 214–220.
- Nemet, I., Varga-Defterdarović, L. and Turk, Z. (2006) Methylglyoxal in food and living organisms., *Molecular Nutrition & Food Research*, 50, 1105–17.
- Nicolson, S. W., Nepi, M. and Pacini, E. (2007) *Nectaries and Nectar*. 1st edn. Springer Netherlands.
- Nishimura, C., Matsuura, Y., Kokai, Y., Akera, T., Carper, D., et al. (1990) Cloning and expression of human aldose reductase, *Journal of Biological Chemistry*, 265, 9788–9792.
- Niwa, T. (1999) 3-Deoxyglucosone: metabolism, analysis, biological activity, and clinical implication., *Journal of Chromatography. B, Biomedical Sciences and Applications*, 731, 23–36.
- Norton, A. M., Mckenzie, L. N., Brooks, P. R. and Pappalardo, L. J. (2015) Quantitation of dihydroxyacetone in Australian *Leptospermum* nectar via high-performance liquid chromatography, *Journal of Agricultural and Food Chemistry*, 63, 6513–6517.
- Novick, A. (1955) Growth of Bacteria, *Annual Review of Microbiology*, 9, 97–110.
- Ohta, T., Shibata, H., Kawamori, T., Iimuro, M., Sugimura, T., et al. (2001) Marked reduction of *Helicobacter pylori*-induced gastritis by urease inhibitors, acetohydroxamic acid and flurofamide, in Mongolian gerbils., *Biochemical and Biophysical Research Communications*, 285, 728–33.
- Olech, Z., Zaborska, W. and Kot, M. (2014) Jack bean urease inhibition by crude juices of *Allium* and *Brassica* plants. Determination of thiosulfates, *Food Chemistry*, 145, 154–160.
- Osés, S. M., Ruiz, M. O., Pascual-Maté, A., Bocos, A., Fernández-Muiño, M. Á., et al. (2017) Ling heather honey authentication by thixotropic parameters, *Food and Bioprocess Technology*, 10, 973–979.
- Pankey, G. a and Sabath, L. D. (2004) Clinical relevance of bacteriostatic versus bactericidal mechanisms of action in the treatment of Gram-positive bacterial infections., *Clinical Infectious Diseases: An Official Publication of the Infectious Diseases Society of America*, 38, 864–870.
- Pappalardo, M., Pappalardo, L. and Brooks, P. (2016) Rapid and reliable HPLC method for the simultaneous determination of dihydroxyacetone, methylglyoxal and 5-hydroxymethylfurfural in *Leptospermum* honeys, *Plos One*, 11, e0167006.
- Parkar, S. G., Jobsis, C. M. H., Herath, T. D., Stoklosinski, H. M., van Klink, J. W., et al.

- (2017) Metabolic and microbial responses to the complexation of manuka honey with  $\alpha$ -cyclodextrin after simulated gastrointestinal digestion and fermentation, *Journal of Functional Foods*, 31, 266–273.
- Penndorf, I., Biedermann, D., Maurer, S. V. and Henle, T. (2007) Studies on N-terminal glycation of peptides in hypoallergenic infant formulas: Quantification of  $\alpha$ -N-(2-furoylmethyl) amino acids, *Journal of Agricultural and Food Chemistry*, 55, 723–727.
- Phillips, S. A. and Thornalley, P. J. (1993) The formation of methylglyoxal from triose phosphates. Investigation using a specific assay for methylglyoxal., *European Journal of Biochemistry*, 212, 101–105.
- Polster, C. (2015) Stabilität und Wirkung von Methylglyoxal in Manukahonig und in dessen Cyclodextrinkomplexen, *Wissenschaftliche Abschlussarbeit*, TU Dresden.
- Pompei, C. and Spagnoello, A. (1997) Furosine as an index of heat treatment intensity in meat products: Its application to cooked ham, *Meat Science*, 46, 139–146.
- Poulsen, M. W., Hedegaard, R. V., Andersen, J. M., de Courten, B., Bügel, S., et al. (2013) Advanced glycation endproducts in food and their effects on health., *Food and Chemical Toxicology: An International Journal Published for the British Industrial Biological Research Association*, 60, 10–37.
- Powers, J. H. (2004) Antimicrobial drug development-the past, the present, and the future., *Clinical Microbiology and Infection: The Official Publication of the European Society of Clinical Microbiology and Infectious Diseases*, 10, 23–31.
- Raatz, S. K., Johnson, L. K. and Picklo, M. J. (2015) Consumption of honey, sucrose, and high-fructose corn syrup produces similar metabolic effects in glucose-tolerant and -intolerant individuals, *Journal of Nutrition*, 145, 2265–72.
- Rabbani, N. and Thornalley, P. J. (2008) The dicarbonyl proteome: Proteins susceptible to dicarbonyl glycation at functional sites in health, aging, and disease, *Annals of the New York Academy of Sciences*, 1126, 124–127.
- Rabie, E., Serem, J. C., Oberholzer, H. M., Gaspar, A. R. M. and Bester, M. J. (2016) How methylglyoxal kills bacteria: An ultrastructural study, *Ultrastructural Pathology*, 40, 107–111.
- Racker, E. (1951) The Mechanism of Action of Glyoxalase, *Journal of Biological Chemistry*, 190, 685–696.
- Rajalingam, D., Loftis, C., Xu, J. J. and Kumar, T. K. S. (2009) Trichloroacetic acid-induced protein precipitation involves the reversible association of a stable partially structured intermediate., *Protein Science: A Publication of the Protein Society*, 18, 980–993.
- Ray, S. and Ray, M. (1981) Isolation of methylglyoxal synthase from goat liver., *The Journal of Biological Chemistry*, 256, 6230–6233.
- Richard, J. P. (1991) Kinetic parameters for the elimination reaction catalyzed by triosephosphate isomerase and an estimation of the reaction's physiological significance, *Biochemistry*, 30, 4581–4585.
- Richard, J. P. (1993) Mechanism for the formation of methylglyoxal from triosephosphates., *Biochemical Society Transactions*, 21, 549–553.
- Richter, D. (2012) 1,2-Dicarbonylverbindungen in biologischen Matrices: Analytik, Metabolismus, Folgereaktionen, *Wissenschaftliche Abschlussarbeit*, TU Dresden.
- Riley, M. L. and Harding, J. J. (1995) The reaction of methylglyoxal with human and bovine



- lens proteins, *Biochimica et Biophysica Acta - Molecular Basis of Disease*, 1270, 36–43.
- Rogatzi, M. J., Ferguson, B. S., Goodwin, M. L. and Gladden, L. B. (2015) Lactate is always the end product of glycolysis, *Frontiers in Neuroscience*, 9, 1–7.
- Romano, A. H. and Conway, T. (1996) Evolution of carbohydrate metabolic pathways, *Research in Microbiology*, 147, 448–455.
- Rückriemen, J., Hohmann, C., Hellwig, M. and Henle, T. (2017) Unique fluorescence and high-molecular weight characteristics of protein isolates from manuka honey (*Leptospermum scoparium*), *Food Research International*, 99, 469–475.
- Rückriemen, J., Klemm, O. and Henle, T. (2017) Manuka honey (*Leptospermum scoparium*) inhibits Jack bean urease activity due to methylglyoxal and dihydroxyacetone, *Food Chemistry*, 230, 540–546.
- Rückriemen, J., Schwarzenbolz, U., Adam, S. and Henle, T. (2015) Identification and quantitation of 2-acetyl-1-pyrroline in manuka honey (*Leptospermum scoparium*), *Journal of Agricultural and Food Chemistry*, 63, 8488–8492.
- Ruhemann, S. (1910) Triketohydrindene Hydrate, *Journal of the Chemical Society, Transactions*, 97, 2025–2031.
- Sahin, H. (2015) Honey as an apitherapeutic product: its inhibitory effect on urease and xanthine oxidase, *Journal of Enzyme Inhibition and Medicinal Chemistry*, 31, 490–494.
- Sajithlal, G. B., Chithra, P. and Chandrakasan, G. (1998) Advanced glycation end products induce crosslinking of collagen in vitro, *Biochimica et Biophysica Acta - Molecular Basis of Disease*, 1407, 215–224.
- Sakiyama, H., Takahashi, M., Yamamoto, T., Teshima, T., Lee, S. H., et al. (2006) The internalization and metabolism of 3-deoxyglucosone in human umbilical vein endothelial cells, *Journal of Biochemistry*, 139, 245–253.
- Salústio, P. J., Feio, G., Figueirinhas, J. L., Pinto, J. F. and Marques, H. M. C. (2009) European Journal of Pharmaceutics and Biopharmaceutics The influence of the preparation methods on the inclusion of model drugs in a b-cyclodextrin cavity, *European Journal of Pharmaceutics and Biopharmaceutics*, 71, 377–386.
- Van Schaftingen, E., Collard, F., Wiame, E. and Veiga-Da-Cunha, M. (2012) Enzymatic repair of Amadori products, *Amino Acids*, 42, 1143–1150.
- Schalkwijk, C. G., Stehouwer, C. D. A. and van Hinsbergh, V. W. M. (2004) Fructose-mediated non-enzymatic glycation: Sweet coupling or bad modification, *Diabetes/Metabolism Research and Reviews*, 20, 369–382.
- Scheijen, J. L. J. M., Clevers, E., Engelen, L., Dagnelie, P. C., Brouns, F., et al. (2016) Analysis of advanced glycation endproducts in selected food items by ultra-performance liquid chromatography tandem mass spectrometry: Presentation of a dietary AGE database, *Food Chemistry*, 190, 1145–1150.
- Schieberle, P. and Grosch, W. (1987) Quantitative analysis of aroma compounds in wheat and rye bread crusts using a stable isotope dilution assay, *Journal of Agricultural and Food Chemistry*, 35, 252–257.
- Schmitt, A., Schmitt, J., Münch, G. and Gasic-Milencovic, J. (2005) Characterization of advanced glycation end products for biochemical studies: Side chain modifications and fluorescence characteristics, *Analytical Biochemistry*, 338, 201–215.

- Schmitt, C. P., von Heyl, D., Rieger, S., Arbeiter, K., Bonzel, K. E., et al. (2007) Reduced systemic advanced glycation end products in children receiving peritoneal dialysis with low glucose degradation product content., *Nephrology, Dialysis, Transplantation: Official Publication of the European Dialysis and Transplant Association - European Renal Association*, 22, 2038–44.
- Schopfer, P. and Brennicke, A. (2005) *Pflanzenphysiologie*. 6th edn. Spektrum Akademischer Verlag GmbH.
- Schultes, S. C. (2016) Untersuchungen zum metabolischen Transit alimentärer Carbonylverbindungen, *Wissenschaftliche Abschlussarbeit*, TU Dresden.
- Sell, D. R., Lane, M. a, Johnson, W. a, Masoro, E. J., Mock, O. B., et al. (1996) Longevity and the genetic determination of collagen glycoxidation kinetics in mammalian senescence., *Proceedings of the National Academy of Sciences of the United States of America*, 93, 485–490.
- Semkiw, P., Skowronek, W. and Skubida, P. (2008) Changes in water content of honey during ripening under controlled condition, *Journal of Apicultural Science*, 52, 57–64.
- Seneviratne, C., Dombi, G. W., Liu, W. and Dain, J. A. (2012) In vitro glycation of human serum albumin by dihydroxyacetone and dihydroxyacetone phosphate., *Biochemical and Biophysical Research Communications*, 417, 817–23.
- Severin, T., Hiebl, J. and Popp-Ginsbach, H. (1984) Untersuchungen zur Maillard-Reaktion XX. Nachweis von Glycerinaldehyd, Dihydroxyaceton und anderen hydrophilen Zuckerabbauprodukten in Caramellisierungsgemischen, *Zeitschrift für Lebensmittel-Untersuchung und -Forschung*, 178, 284–287.
- Shipanova, I. N., Glomb, M. a and Nagaraj, R. H. (1997) Protein modification by methylglyoxal: chemical nature and synthetic mechanism of a major fluorescent adduct., *Archives of biochemistry and biophysics*, 344, 29–36.
- Silva, V. M. Da, Carvalho, L. A. De, Oliveira, N. L. De, Torres Filho, R. D. A. and Resende, J. V. De (2016) Rheological and thermal properties of selected Brazilian honeys from various floral origins, *Journal of Texture Studies*, 47, 208–219.
- Singh, M., Sharma, R. and Banerjee, U. C. (2002) Biotechnological applications of cyclodextrins., *Biotechnology Advances*, 20, 341–59.
- Singh, N. and Bath, P. K. (1998) Relationship between heating and hydroxymethylfurfural formation in different honey types, *Journal of Food Science and Technology*, 35, 154–156.
- Smanalieva, J. and Senge, B. (2009) Analytical and rheological investigations into selected unifloral German honey, *European Food Research and Technology*, 229, 107–113.
- Al Somal, N., Coley, K. E., Molan, P. C. and Hancock, B. M. (1994) Susceptibility of *Helicobacter pylori* to the antibacterial activity of manuka honey., *Journal of the Royal Society of Medicine*, 87, 9–12.
- Stephens, J. M. C. (2006) The factors responsible for the varying levels of UMF ® in mānuka (*Leptospermum scoparium*) honey, *PhD Thesis*, University.
- Stetten, M. R. and Stetten, D. J. (1950) The metabolism of gluconic acid, *Journal of Biological Chemistry*, 187, 241–252.
- Sugimoto, K., Hosotani, T., Kawasaki, T., Nakagawa, K., Hayashi, S., et al. (2010) Eucalyptus leaf extract suppresses the postprandial elevation of portal, cardiac and peripheral

- fructose concentrations after sucrose ingestion in rats., *Journal of Clinical Biochemistry and Nutrition*, 46, 205–211.
- Sukdeo, N. and Honek, J. F. (2007) Pseudomonas aeruginosa contains multiple glyoxalase I-encoding genes from both metal activation classes, *Biochimica et Biophysica Acta - Proteins and Proteomics*, 1774, 756–763.
- Swift, S., Chepulis, L. M., Uy, B. and Radcliff, F. J. (2014) Enhanced antibacterial activity of MGO manuka honey complexed with alpha - cyclodextrin (manuka Honey with CycloPower TM), *Functional Foods in Health and Disease*, 4, 172–181.
- Szejtli, J. (1998) Introduction and general overview of cyclodextrin chemistry, *Chemical Reviews*, 98, 1743–1753.
- Takagi, D., Inoue, H., Odawara, M., Shimakawa, G. and Miyake, C. (2014) The calvin cycle inevitably produces sugar-derived reactive carbonyl methylglyoxal during photosynthesis: A potential cause of plant diabetes, *Plant and Cell Physiology*, 55, 333–340.
- Tanaka, T., Kawase, M. and Tani, S. (2004) Alpha-Hydroxyketones as inhibitors of urease, *Bioorganic and Medicinal Chemistry*, 12, 501–505.
- Tasevska, N., Runswick, S. A., McTaggart, A. and Bingham, S. A. (2005) Urinary sucrose and fructose as biomarkers for sugar consumption, *Cancer Epidemiology Biomarkers and Prevention*, 14, 1287–1294.
- Tasevska, N., Runswick, S. a, Welch, a a, McTaggart, A. and Bingham, S. a (2009) Urinary sugars biomarker relates better to extrinsic than to intrinsic sugars intake in a metabolic study with volunteers consuming their normal diet., *European Journal of Clinical Nutrition*, 63, 653–9.
- Teichert, T., Hellwig, A., Peßler, A., Hellwig, M., Vossoughi, M., et al. (2015) Association between advanced glycation end products and impaired fasting glucose: Results from the SALIA Study, *Plos One*, 10, e0128293.
- Tessier, F. J. (2010) The Maillard reaction in the human body. The main discoveries and factors that affect glycation, *Pathologie Biologie*, 58, 214–219.
- Thompson, D. O. (1997) Cyclodextrins-enabling excipients : Their present and future use in pharmaceuticals, *Critical Reviews in Therapeutic Drug Carrier Systems*, 14, 1–104.
- Thornalley, P., Battah, S., Ahmed, N., Karachalias, N., Agalou, S., et al. (2003) Quantitative screening of advanced glycation endproducts in cellular and extracellular proteins by tandem mass spectrometry, *Biochemical Journal*, 375, 581–592.
- Thornalley, P. J. (1993) The glyoxalase system in health and disease., *Molecular Aspects of Medicine*, 14, 287–371.
- Thornalley, P. J. (1996) Pharmacology of methylglyoxal: formation, modification of proteins and nucleic acids, and enzymatic detoxification-a role in pathogenesis and antiproliferative chemotherapy., *General Pharmacology*, 27, 565–73.
- Thornalley, P. J. (2005) Dicarbonyl intermediates in the maillard reaction., *Annals of the New York Academy of Sciences*, 1043, 111–117.
- Thornalley, P. J., Langborg, A. and Minhas, H. S. (1999) Formation of glyoxal, methylglyoxal and 3-deoxyglucosone in the glycation of proteins by glucose, *Biochemical Journal*, 344, 109–116.
- Thornalley, P. J. and Rabbani, N. (2014) Detection of oxidized and glycated proteins in

- clinical samples using mass spectrometry-a user's perspective., *Biochimica et Biophysica Acta*, 1840, 818–29.
- Valancin, A., Srinivasan, B., Rivoal, J. and Jolicoeur, M. (2013) Analyzing the effect of decreasing cytosolic triosephosphate isomerase on *Solanum tuberosum* hairy root cells using a kinetic-metabolic model, *Biotechnology and Bioengineering*, 110, 924–935.
- Villamiel, M., Arias, M., Corzo, N. and Olano, A. (2000) Survey of the furosine content in cheeses marketed in Spain, *Journal of Food Protection*, 63, 974–975.
- Vitek, M. P., Bhattacharya, K., Glendening, J. M., Stopa, E., Vlassara, H., et al. (1994) Advanced glycation end products contribute to amyloidosis in Alzheimer disease., *Proceedings of the National Academy of Sciences of the United States of America*, 91, 4766–4770.
- Vlamakis, H., Chai, Y., Beaugregard, P., Losick, R. and Kolter, R. (2013) Sticking together: building a biofilm the *Bacillus subtilis* way, *Nature Reviews Microbiology*, 11, 157–168.
- Vreugdenhil, D. and Koot-Gronsveld, E. A. M. (1989) Measurements of pH, sucrose and potassium ions in the phloem sap of castor bean (*Ricinus communis*) plants, *Physiologia Plantarum*, 77, 385–388.
- Wahdan, H. A. L. (1997) Causes of the antimicrobial activity of honey., *Infection*, 26, 26–31.
- Wang, Y. and Ho, C.-T. (2012) Flavour chemistry of methylglyoxal and glyoxal., *Chemical Society Reviews*, 41, 4140–9.
- Wang, Y. and Ho, C. T. (2008) Formation of 2,5-dimethyl-4-hydroxy-3(2H)-furanone through methylglyoxal: A maillard reaction intermediate, *Journal of Agricultural and Food Chemistry*, 56, 7405–7409.
- Weigel, K. U., Opitz, T. and Henle, T. (2004) Studies on the occurrence and formation of 1,2-dicarbonyls in honey, *European Food Research and Technology*, 218, 147–151.
- Weston, R. J. (2000) The contribution of catalase and other natural products to the antibacterial activity of honey: a review, *Food Chemistry*, 71, 235–239.
- White, J. W., Subers, M. H. and Schepartz, A. I. (1963) The Identification of Inhibine, the Antibacterial Factor in Honey, as Hydrogen Peroxide and its Origin in a Honey Glucose-Oxidase System, *Biochimica et Biophysica Acta*, 73, 57–70.
- Williams, P. M. E. (2008) *Te Rongoa Maori Medicine*. Raupo Publishing (NZ) Ltd.
- Williams, S., King, J., Revell, M., Manley-harris, M., Balks, M., et al. (2014) Regional, annual, and individual variations in the dihydroxyacetone content of the nectar of mānuka (*Leptospermum scoparium*) in New Zealand, *Journal of Agricultural and Food Chemistry*, 62, 10332–40.
- Windsor, S., Kavazos, K. and Brooks, P. (2013) The quantitation of hydroxymethylfurfural in Australian *Leptospermum* honeys, *Journal of Pharmacognosy and Phytotherapy*, 5, 21–25.
- Windsor, S., Pappalardo, M., Brooks, P., Williams, S. and Manley-Harris, M. (2012) A convenient new analysis of dihydroxyacetone and methylglyoxal applied to Australian *Leptospermum* honeys, *Journal of Pharmacognosy and Phytotherapy*, 4, 6–11.
- Witczak, M., Juszczak, L. and Galkowska, D. (2011) Non-Newtonian behaviour of heather honey, *Journal of Food Engineering*, 104, 532–537.
- Won, S.-R., Lee, D.-C., Ko, S. H., Kim, J.-W. and Rhee, H.-I. (2008) Honey major protein

characterization and its application to adulteration detection, *Food Research International*, 41, 952–956.

World Health Organization (2015) *Guideline: Sugars intake for adults and children*.

World Health Organization (2016) *Global Report on Diabetes*.

Wu, D. W., Yu, X. D., Xie, J. H., Su, Z. Q., Su, J. Y., et al. (2013) Inactivation of jack bean urease by scutellarin: Elucidation of inhibitory efficacy, kinetics and mechanism, *Fitoterapia*, 91, 60–67.

Wu, M.-L., Chou, K.-L., Wu, C.-R., Chen, J.-K. and Huang, T.-C. (2009) Characterization and the possible formation mechanism of 2-acetyl-1-pyrroline in aromatic vegetable soybean (*Glycine max* L.), *Journal of Food Science*, 74, S192-7.

Yadav, S. K., Singla-Pareek, S. L., Ray, M., Reddy, M. K. and Sopory, S. K. (2005) Methylglyoxal levels in plants under salinity stress are dependent on glyoxalase I and glutathione, *Biochemical and Biophysical Research Communications*, 337, 61–67.

Yamaguchi, M., Ishida, J., Xuan, Z. X., Nakamura, A. and Yoshitake, T. (1994) Determination of glyoxal, methylglyoxal, diacetyl, and 2, 3-pentanedione in fermented foods by high-performance liquid chromatography with fluorescence detection, *Journal of Liquid Chromatography*, 17, 203–211.

Zeitz, L. (2013) Reaktionen von Methylglyoxal im Verdauungstrakt -Untersuchungen am in vitro Modell, *Wissenschaftliche Abschlussarbeit*, TU Dresden.

Zhang, H.-M., Li, Z., Uematsu, K., Kobayashi, T. and Horikoshi, K. (2008) Antibacterial activity of cyclodextrins against *Bacillus* strains., *Archives of Microbiology*, 190, 605–9.

Zhong, L., Liu, Z., Yan, R., Johnson, S., Fang, X., et al. (2009) Aldo-keto reductase family 1 B10 protein detoxifies dietary and lipid-derived alpha, beta-unsaturated carbonyls at physiological levels, *Biochemical and Biophysical Research Communications*, 387, 245–250.

Zwietering, M. H., Jongenburger, I., Rombouts, F. M. and Van't Riet, K. (1990) Modeling of the bacterial growth curve, *Applied and Environmental Microbiology*, 56, 1875–1881.

---

## List of publications, posters and presentations

---

### Original Publications

- 1 Lunow D, Kaiser S, Rückriemen J, Pohl C, Henle T: Tryptophan-containing dipeptides are C-domain selective inhibitors of angiotensin converting enzyme. *Food Chemistry*, **166**, 596-602, **2015**
- 2 Rückriemen J, Schwarzenbolz U, Adam S, Henle T: Identification and quantitation of 2-acetyl-1-pyrroline in manuka honey (*Leptospermum scoparium*). *Journal of Agricultural and Food Chemistry*, **63**, 8488-8492, **2015**
- 3 Rückriemen J, Klemm O, Henle T: Manuka honey (*Leptospermum scoparium*) inhibits jack bean urease activity due to methylglyoxal and dihydroxyacetone. *Food Chemistry*, **230**, 540-546, **2017**
- 4 Hellwig M, Rückriemen J, Sandner D, Henle T: Unique pattern of protein-bound Maillard reaction products in manuka (*Leptospermum scoparium*) honey. *Journal of Agricultural and Food Chemistry*, **65**, 3532-3540, **2017**
- 5 Rückriemen J, Hohmann C, Hellwig M, Henle T: Unique fluorescence and high-molecular weight characteristics of protein isolates from manuka honey (*Leptospermum scoparium*). *Food Research International*, **99**(Pt 1), 469-475, **2017**
- 6 Rückriemen J, Schultes S, Hahne F, Hellwig A, Hellwig M, Henle T: The urinary excretion of 2-keto-3-deoxygluconic acid is influenced by the diet. **2017**, *in preparation*

### Published abstracts

- 1 Rückriemen J, Müller D, Henle T: Untersuchungen zur antibakteriellen Aktivität von Manuka-Honig. *Lebensmittelchemie*, **67**, 32, **2013**
- 2 Rückriemen J, Hellwig M, Hohmann C, Sandner D, Henle T: Reaktionen von Methylglyoxal in Manukahonig. *Lebensmittelchemie*, **70**, 128, **2016**
- 3 Rückriemen J, Klemm O, Henle T: Methylglyoxal und Dihydroxyaceton in Manuka-Honig sind Ureaseinhibitoren. *Lebensmittelchemie*, **71**, 82, **2017**

## Poster Presentations

- 1 Rückriemen J, Müller D, Henle T: Untersuchungen zur antibakteriellen Aktivität von Manuka-Honig. 42. Deutscher Lebensmittelchemikertag, Braunschweig, 16.-18.09.2013.
- 2 Rückriemen J, Henle T: Struktur von Manuka-Honig/ $\alpha$ -Cyclodextrin Komplexen. 43. Deutscher Lebensmittelchemikertag, Gießen, 22.-24.09.2014
- 3 Rückriemen J, Schwarzenbolz U, Adam S, Henle T: Identification and quantification of 2-actyl-1-pyrroline in manuka honey (*Leptospermum scoparium*). Euro Food Chem XVIII, Madrid, 13.-16.10.2015
- 4 Rückriemen J, Hellwig M, Hohmann C, Sandner D, Henle T: The unique chemistry of manuka honey (*Leptospermum scoparium*). Euro Food Chem XVIII, Madrid, 13.-16.10.2015
- 5 Rückriemen J, Klemm O, Henle T: Methylglyoxal and dihydroxyacetone present in manuka honey (*Leptospermum scoparium*) are inhibitors of urease. 45. Deutscher Lebensmittelchemikertag, Freising, 12.-14.09.2016
- 6 Rückriemen J, Klemm O, Henle T: Methylglyoxal and dihydroxyacetone present in manuka honey (*Leptospermum scoparium*) are inhibitors of urease. 13<sup>th</sup> International Conference on Chemical Reactions in Food, Prague, 15.-17.02.2017
- 7 Rückriemen J, Hellwig M, Hohmann C, Sandner D, Henle T: Die Maillard-Reaktion in Manuka-Honig. 46. Deutscher Lebensmittelchemikertag, Würzburg, 25.-27.09.2016

## Oral Presentations

- 1 Rückriemen J, Henle T: Zusammensetzung und Bioaktivität von Manuka-Honig. ZINT-Doktorandenforum, Dresden, 1.10.2013.
- 2 Rückriemen J, Hellwig M, Hohmann C, Sandner D, Henle T: Reaktionen von Methylglyoxal in Manuka-Honig. 26. Arbeitstagung des Regionalverbandes Süd-Ost der Lebensmittelchemischen Gesellschaft, Dresden, 18.03.2016.
- 3 Rückriemen J, Hellwig M, Schwarzenbolz U, Hohmann C, Sandner D, Henle T: The unique chemistry of manuka honey. 13<sup>th</sup> International Conference on Chemical Reactions in Food, Prague, 17.02.2017.

## Supervised master theses

**1** Polster, Constanze:

Stabilität und Wirkung von Methylglyoxal in Manukahonig und in dessen Cyclodextrinkomplexen. Dresden, Technische Universität, master thesis, 2015

**2** Hohmann, Christoph

Reaktionen von Methylglyoxal in Manukahonig. Dresden, Technische Universität, master thesis, 2015

**3** Schultes, Stephanie

Untersuchungen zum metabolischen Transit alimentärer Carbonylverbindungen. Dresden, Technische Universität, master thesis, 2016

**4** Klemm, Oliver

Charakterisierung der Hemmwirkung von Manuka Honig auf Urease. Dresden, Technische Universität, master thesis, 2016

**5** Blasse, Lisa-Marie

Untersuchung von Carbonylverbindungen in humanem Speichel. Dresden, Technische Universität, master thesis, 2017



---

## Acknowledgment

---

Ich danke meinem Doktorvater Prof. Thomas Henle für die Bereitstellung des interessanten Themas und die exzellente wissenschaftliche Betreuung. Das freundschaftliche Miteinander hat die Arbeit an der Dissertation enorm erleichtert und gemeinsame Besprechungen empfand ich immer als sehr motivierend. Danke Thomas, es wird eine Herausforderung, nochmal auf einen ähnlich guten Mentor zu treffen!

Des Weiteren danke ich Michael Hellwig für viele, sehr hilfreiche Ratschläge und die kontinuierliche Unterstützung. Der gleiche Dank geht auch an Anne Hellwig, deren Input zur Thematik 3-DG Metabolismus äußerst wertvoll war. In den Reigen der „Postdocs“ gehört natürlich auch Anke – mit dir habe ich nicht nur eine hilfbereite Kollegin sondern auch eine Freundin gewonnen.

Ohne die Hilfe von Uwe Schwarzenbolz wäre Vieles im Rahmen der Anfertigung der Arbeit nicht möglich gewesen. Ich danke für die stetige Unterstützung bei allerhand Computerfragen, Softwareproblemen und allgemein Geräteschwierigkeiten, aber vor allem für die fachlichen Diskussionen. Die LC ohne Uwe ist für mich nicht vorstellbar.

Gleiches gilt natürlich auch für die beiden Institutionen Frau Paul und Frau Schlosser. Vielen Dank für die unzähligen Male, die ich von Ihnen beiden unterstützt wurde!

Des Weiteren möchte ich mich auch bei allen anderen Mitarbeitern und Doktoranden der LC bedanken. Ein paar seien namentlich erwähnt: Seppa und Erik – vielen Dank für eure Freundschaft und die 1a Mittagspartnerschaft, Thomas Ho. – der beste Quizgegner überhaupt, Sophia – trinkfeste Bierexpertin, ich wünsche dir viel Erfolg bei eurem Projekt, Diana – ohne dich hätte ich wahrscheinlich gar nicht erst promoviert, Steffi – für Höhen und Tiefen, Julia D. – Young AGers forever ;) und Anja – danke für die äußerst angenehme Büropartnerschaft.

Zu guter Letzt danke ich meiner Familie. Mutschi, Pepe, Uwe, den beiden Opas und vor allem Omas gilt nicht nur Dank für die finanzielle Unterstützung sondern auch für das unerschütterliche Vertrauen. Meiner Schwester Tini und ihrer Familie danke ich für den emotionalen Support, vor allem bei Dingen, die Eltern eben nicht verstehen.

Meinem Fels in der Brandung, Armin, danke ich für alles was schon war und noch kommen wird.

---

## Affidavit

---

Hiermit versichere ich, dass ich die vorliegende Arbeit ohne unzulässige Hilfe Dritter und ohne Benutzung anderer als der angegebenen Hilfsmittel angefertigt habe; die aus fremden Quellen direkt oder indirekt übernommenen Gedanken sind als solche kenntlich gemacht. Die Arbeit wurde bisher weder im Inland noch im Ausland in gleicher oder ähnlicher Form einer anderen Prüfungsbehörde vorgelegt.

Die vorliegende Arbeit wurde an der Technischen Universität Dresden an der Professur für Lebensmittelchemie unter der Betreuung von Herrn Prof. Dr. rer. nat. Dr.-Ing. habil. Thomas Henle angefertigt.

Weiterhin versichere ich, dass bisher kein früheres erfolgloses Promotionsverfahren stattgefunden hat. Ich erkenne die Promotionsordnung der Technischen Universität Dresden, Fakultät Mathematik und Naturwissenschaften vom 23.02.2011, zuletzt geändert durch Beschlüsse des Fakultätsrates vom 15.06.2011 und 18.06.2014, in allen Teilen an.

---

Ort, Datum

---

Unterschrift